Graduate School ETD Form 9
(Revised 12/07)

PURDUE UNIVERSITY
GRADUATE SCHOOL
Thesis/Dissertation Acceptance

This is to certify that the thesis/dissertation prepared

By Gina Dembinski

Entitled
Evaluation of the IrisPlex DNA-based eye color prediction tool in the United States

For the degree of Master of Science

Is approved by the final examining committee:

Christine Picard
Chair

Stephen Randall

John Goodpaster

To the best of my knowledge and as understood by the student in the *Research Integrity and Copyright Disclaimer (Graduate School Form 20)*, this thesis/dissertation adheres to the provisions of Purdue University's "Policy on Integrity in Research" and the use of copyrighted material.

Approved by Major Professor(s): Christine Picard

Approved by: Christine Picard 06/13/2013
Head of the Graduate Program Date

EVALUATION OF THE IRISPLEX DNA-BASED EYE COLOR PREDICTION TOOL IN THE UNITED STATES

A Thesis

Submitted to the Faculty

of

Purdue University

by

Gina M. Dembinski

In Partial Fulfillment of the

Requirements for the Degree

of

Master of Science

August 2013

Purdue University

Indianapolis, Indiana

ACKNOWLEDGMENTS

I am grateful to have had the opportunity to work on this project, and to the School of Science start-up funds for allowing it to be possible. Dr. Picard, I really cannot begin to express the appreciation for all the challenges and supportive criticism in helping me pursue to my goals and to become a better scientist. I am very fortunate to have you as a mentor. Thank you for also allowing me to stick around for the next years and continue developing this project.

I also want to extend thanks to all others who helped me during this research process, some may not even know the extent to which they did; you have my sincerest gratitude.

TABLE OF CONTENTS

LIST OF TABLES

LIST OF FIGURES

LIST OF ABBREVIATIONS

®	registered
°C	degrees Celsius
α	alpha
α-MSH	alpha-melanocyte stimulating hormone
β	beta
µL	microliter
µM	micromolar
χ^2	chi-squared test
ALFRED	allele frequency database
ASIP	agouti signaling protein
ATP	adenosine triphosphate
AUC	area under receiver operating characteristic curve
BMV	bureau of motor vehicles
BN	Bayesian network
cAMP	cyclic adenosine monophosphate
CIELAB	International Commission on Illumination L*a*b* color space
CODIS	Combined DNA index system
CV	canonical variate
DA	discriminant analysis
DCT	dopachrome tautomerase
ddNTP	dideoxynucleotide
df	degrees of freedom
DNA	deoxyribonucleic acid
dNTP	deoxynucleotide
DOPA	3,4,-dihydroxylphenylalanine
EM	eumelanin
EVC	externally visible characteristic
FBI	Federal Bureau of Investigation
GWAS	genome-wide association study
HERC2	HECT and RLD domain containing E3 ubiquitin protein ligase 2
HGDP-CEPH	human genome diversity panel-center for the study of human polymorphisms

hr	hour
IMI	iris melanin index
IRF4	interferon regulatory factor 4
MATP	membrane associated transporter protein
MC1R	melanocortin 1 receptor
MITF	microphthalmia transcription factor
mL	milliliter
MLR	multinomial logistic regression
ng	nanogram
NPV	negative predictive value
OCA2	oculocutaneous albinism II gene
P	human homologue of mouse pink eyed dilution gene
PCR	polymerase chain reaction
PHR	peak height ratio
PKA	protein kinase A
PM	pheomelanin
PPV	positive predictive value
rfu	relative fluorescent units
RGB	red green blue
ROC	receiver operating characteristic curve
rpm	revolutions per minute
SAP	shrimp alkaline phosphatase
SBE	single base extension
SLC24A5	solute carrier family 24 member 5
SLC24A5	solute carrier family 24 member 5
SLC45A2	solute carrier family 45 member 2
SNP	single nucleotide polymorphism
STR	short tandem repeat
TYR	tyrosinase gene
TYRP1	tyrosinase related protein 1
™	trademark
UV	ultraviolet radiation

ABSTRACT

Dembinski, Gina M. M.S., Purdue University, August 2013. Evaluation of the IrisPlex DNA-Based Eye Color Prediction Tool in the United States. Major Professor: Christine J. Picard.

DNA phenotyping is a rapidly developing area of research in forensic biology. Externally visible characteristics (EVCs) can be determined based on genotype data, specifically from single nucleotide polymorphisms (SNPs). These SNPs are chosen based on their association with genes related to the phenotypic expression of interest, with known examples in eye, hair, and skin color traits. DNA phenotyping has forensic importance when unknown biological samples at a crime scene do not result in a criminal database hit; a phenotype profile of the sample can therefore be used to develop investigational leads. IrisPlex, an eye color prediction assay, has previously shown high prediction rates for blue and brown eye color in a European population. The objective of this work was to evaluate its utility in a North American population. We evaluated the six SNPs included in the IrisPlex assay in an admixed population sample collected from a U.S.A. college campus. We used a quantitative method of eye color classification based on (RGB) color components of digital photographs of the eye taken from each study volunteer and placed in one of three eye color categories: brown, intermediate, and blue. Objective color classification was shown to correlate with basic human visual

determination making it a feasible option for use in future prediction assay development. In the original IrisPlex study with the Dutch samples, they correct prediction rates achieved were 91.6% for blue eye color and 87.5% for brown eye color. No intermediate eyes were tested. Using these samples and various models, the maximum prediction accuracies of the IrisPlex system achieved was 93% and 33% correct brown and blue eye color predictions, respectively, and 11% for intermediate eye colors. The differences in prediction accuracies is attributed to the genetic differences in allele frequencies within the sample populations tested. Future developments should include incorporation of additional informative SNPs, specifically related to the intermediate eye color, and we recommend the use of a Bayesian approach as a prediction model as likelihood ratios can be determined for reporting purposes.

CHAPTER 1. INTRODUCTION

When biological material is left at a crime scene, ultimately the purpose of the forensic analysis of that evidence is to obtain a DNA profile. DNA profiling is considered the gold standard of forensic science because it allows for reliable individual identification with statistical support [3]. DNA profiling is currently based on the exploitations of the genetic variations within each individual's DNA, known as short tandem repeats (STR). Once generated from the biological material, the STR profiles from crime scene samples can then be used for comparison between putative individuals. One method is through searching DNA databases for possible lists of suspects. Currently, the main database is maintained by the Federal Bureau of Investigation (FBI), a database called the Combined DNA Index System (CODIS). There are also databases at local and state levels, but these feed into the national database. The profiles are currently based on 13 core STR loci (markers) [4]. There are close to 11 million profiles that exist in the national database (C. Sobieralski, Indiana State Police, personal communication).

There have been improvements in the sensitivity of STR testing where DNA profiles are now routinely obtained from minute quantities of biological material not visible to the naked eye [5]. However, the limitation of DNA evidence is when a DNA profile from a crime scene fails to match any one individual from a DNA database. FBI CODIS

statistics showed that DNA profiles increased exponentially from 2001-2006, yet hits increased linearly which leads to an increasing discrepancy between unmatched DNA profiles and hits [6]. At this time, a DNA profile does not provide any informative characteristics of the contributor other than the sex of the individual. Therefore, an unknown suspect(s) can never be identified using the current genetic markers in forensic DNA profiling [7]. One way to overcome this limitation is to obtain additional genetic information from the biological material to complement the STR profile. One of the rapidly developing areas in forensic biology is the ability to predict externally visible characteristics (EVC) of an individual based on DNA-based genetic information, known as DNA phenotyping [8]. In DNA phenotyping, single nucleotide polymorphism (SNP) markers, as opposed to STR markers, are found associated with EVC genes, and can be typed for the prediction of a particular phenotype prediction purposes [7]. Human sex determination is an accurately predicting EVC that is currently in use with existing DNA profiles [7]. In 2001, Grimes et al. [6] published the first example of a phenotype prediction test showing that variants in the *MC1R* gene was indicative of the red hair phenotype [2]. EVCs that show the most promise for the successful development of forensic prediction tests in the near future are skin, hair, and eye color; they are among the most visible phenotypic traits [9] and have a small number of markers that account for a large proportion of the variation [6].

As a complement to conventional STR profiling, DNA phenotyping can be used as an investigational tool, not just for criminal casework, but also those pertaining to missing persons or mass disasters [8]. For example, the information from a DNA phenotype profile will either corroborate or negate eye witness statements [8]. This has been

demonstrated in a criminal investigation to aid in a Louisiana serial killer case in 2003. DNAPrint Genomics, a genetic testing company, had developed an ancestry phenotype test called DNAWitness 1.0, which included 71 informative ancestry informative markers (AIMs) [10]. Eyewitness testimony had suggested a Caucasian assailant, and after finding no leads, the task force commissioned the DNAWitness testing, where the results suggested the contributor was predominantly African. A month later, the suspect, Derrick Todd Lee, an African-American male, was arrested and has since been convicted in two murders [10]. Once developed fully for forensic applications, the information possible from these predictions may help in developing plausible leads for investigations, especially in cases when they are limited.

The full genetic determination of externally visible traits is still being explored; however, many studies have identified genes and SNPs of interest that contribute to variation in pigmentation, such as eye, hair, or skin color, which results in differences of the expressed traits [2, 9, 11-19]. Melanin production and distribution is especially found to affect the expression of these phenotypes, thus the SNPs associated with pigmentation gene loci can be useful for the development of prediction models.

The objective of this work was to evaluate a previously developed DNA-based phenotyping assay that predicts eye color, called IrisPlex, as an informative forensic tool to be used within the United States. IrisPlex includes an assay of six eye color informative SNPs and a statistical model for predicting iris color. IrisPlex has been validated for several European populations [20, 21] in predicting blue and brown eye color, but still lacked evaluation with more admixed individuals, such as those in the U.S. population. In this current study, adjusted and alternative prediction models were also

tested, and quantitative color measurement for determining iris color was also applied as an objective color classification method.

1.1 Iris Structure

Human eye color expression is based on genetic, developmental, molecular, and morphological features of the iris [1]. The stroma and anterior layer of the iris have been shown to be the most important structural cell layers for eye color appearance and contain pigment cells (see Figure 1.1) [1]. Pigment cells are called melanocytes. Stromal melanocytes have the same embryological origin as dermal melanocytes, and they migrate through the uveal tract during development [1]. The iris pigmented epithelium (IPE), the posterior layer, is always pigmented regardless of eye color, except in individuals who exhibit albinism [1]. The stromal layer consists of loose connective tissue made of fibroblasts, melanocytes, and several collagen fibril proteins [1]. It has been shown that approximately 66% of the stromal composition is made of melanocytes, regardless of eye color; no statistical significance is seen in the total mean melanocyte number (the same cell density among different color groups) [22]. Unlike hair and skin where melanin (pigment) is continuously produced and secreted, melanosomes in the iris are retained in the iris (stroma) [1]. Three factors considered the major determining factors of the appearance of iris color are: pigment granules in the iris pigment epithelium (IPE), concentration of pigment in stromal melanocytes, and light scattering and absorptive properties of extracellular components [23].

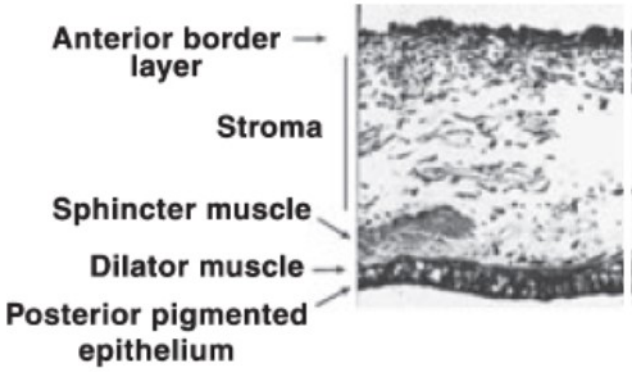

Figure 1.1. Transverse view of the human iris [1]. The five structural layers of the iris can be seen. Reproduced with permission from Springer Science and Business Media.

1.2 Pigmentation and Melanogenesis

Melanin is a indole derivative of 3,4 di-hydroxy-phenylalanine (DOPA) and is formed from tyrosine in a series of oxidative steps [24]. The major known function of melanin is protection against UV-induced DNA damage as it absorbs and scatters the UV radiation [24]. Variation in the expression of human pigmentation is described by differences in the type of melanin, the amount of melanin synthesized in melanosomes (specialized vesicles) and the size, shape, and export of melanosomes to the hair, skin, and iris [6]. There are two types of melanin, eumelanin (EM) and pheomelanin (PM) which differ mainly in sulfur content [6]. Most melanin pigments present in hair, skin, and eyes are complex heteropolymers made up of both EM and PM building blocks, not a homopolymer of one or the other [25]. Eumelanin is a brown/black pigment and pheomelanin is a yellow/red pigment. A study on cultured uveal melanocytes demonstrated a trend in the type of melanin and eye color. Dark iris colors have a greater amount of EM, intermediate iris colors (i.e., green) have more PM and the lighter eye

colors, such as blue, have very little of either pigment [23]. The formation of pupillary rings (brown around blue, brown around green) are not yet genetically understood [26].

Melanogenesis is illustrated in Figure 1.2. The first step in melanin formation is oxidation of tyrosine to L-DOPA, this is known as the Raper-Mason pathway [24]. L-DOPA activates the enzyme tyrosinase. Mutations of tyrosinase affecting its function lead to forms of oculocutaneous albinism, hereditary disorders resulting in melanin deficiency (or absence) [24]. The pathway begins with the α-melanocyte stimulating hormone (α-MSH) binding to the melanocortin 1 receptor (MC1R). Melanocortin receptors have seven transmembrane domains and are a group belonging to the G-protein coupled receptor superfamily; MC1R is expressed in melanocytes [24]. This binding of α-MSH leads to a G-protein dependent activation of adenylate cyclase and increases cAMP levels to activate protein kinase A (PKA) [24]. PKA induces the microphthalmia transcription factor (MITF) [24]. The MITF regulates transcription of tyrosinase and of Rab27a, which is an important protein in melanosome transport [24]. Tyrosinase, once activated, acts on tyrosine to make dopaquinone and addition of cysteine if present [2]. When cAMP is limited, pheomelanin formation is favored [2]. Tyrosine related protein I (TYRP1) is stimulated by MITF along with dopachrome tautomerase (DCT) which will lead to eumelanin production as long as the following required proteins Pmel17, MATP, P, and SLC24A5 are present, all which are important to transport and maturation of the melanosome structure [2].

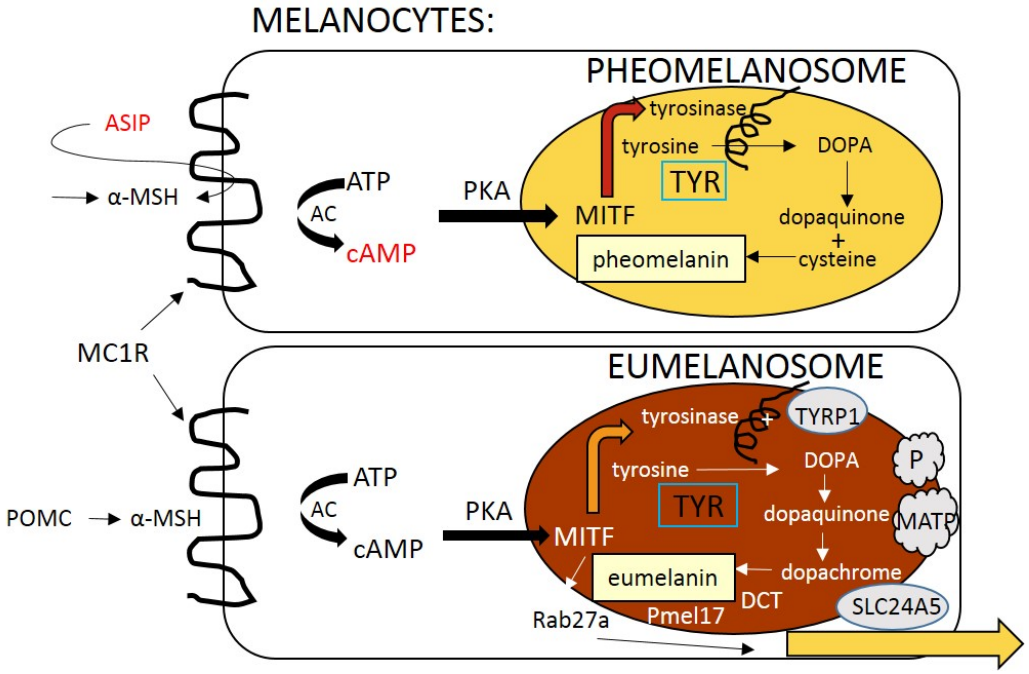

Figure 1.2. Illustration of melanogenesis. Shown is the melanogenesis pathway leading to the production of eumelanin and/or pheomelanin. Genes boxed in blue are included in IrisPlex. Adapted from Tully [2].

1.3 Pigmentation Genes and Informative SNPs

Common variants associated with normal pigmentation in humans have thus far been identified currently by genome-wide association studies (GWAS) in six genes: *MC1R*, *OCA2*, *SLC24A5*, *MATP* (*SLC45A2*), *ASIP*, and *TYR* [9]. The *MC1R* gene relates to the MC1R receptor in the melanogenesis pathway. The *OCA2* gene encodes the P protein involved in melanogenesis, as well as the *MATP* gene. The *ASIP* gene encodes the agouti signaling protein which interacts with the MC1R receptor and competes with binding of α-MSH to the MC1R receptor in melanogenesis, this can lead to higher production of pheomelanin [27]. It has also been shown to lead to expression of yellow coat color in mice, therefore it influences the expression of lighter pigmentation [27]. Specifically for

eye color, three SNPs in these pigment associated genes are shown to have significant reduced melanin effects in human melanocytes to further support their involvement in pigmentation: rs12913832 (*HERC2*), rs16891982 (*SLC24A4*), and rs1426654 (*SLC24A5*) [28]. *SLC24A4* and *SLC24A5* have already been discussed as being involved in melanin production. The function of the *HERC2* gene is unknown, and will be discussed further below.

Though these phenotype informative SNPs are expected to be used in future forensic investigations, more research is necessary as the traits of focus indicated by these SNPs are highly polymorphic and complex, involving several genes and contributions from various gene-gene interactions [13]. Complex traits do not exhibit Mendelian inheritance, attributed to a single gene locus with one dominant and one recessive allele. Complex traits could mean that the same genotype can result in more than one phenotype, and conversely, more than one genotype results in the same phenotype [29]. It is nearly impossible to find a genetic marker that shows perfect co-segregation with a complex trait because of incomplete penetrance (has allele but phenotype not expressed), phenocopy (doesn't have allele but due to environmental factors expresses the phenotype), genetic heterogeneity, or polygenic inheritance (more than one type of variant allele is required for a certain phenotype to be expressed) [29].

The human iris color phenotype is under strong genetic control and highly polymorphic in individuals especially of European descent, which is where eye color variation originates [8]. The ancestral expressed eye color is brown, which agrees with the Out-of-Africa theory of evolution stating that the modern human population is descendant from a small group of *Homo sapiens* from Africa that emigrated [7]. Genetic

adaptation, especially considering the geographic adaptation of the UV response between Africa and Europe, is the most probable cause of pigment variation [7]. The UV response is more active and advantageous for Africans and individuals who live in regions closer to the equator as they receive higher levels of UV sun exposure and therefore require higher levels of melanin production than individuals who live further away from the equator, such as in northern regions of Europe e.g., Scandinavia.

The SNP rs12913832 is in the highly conserved intronic region of the *HERC2* gene, and is located upstream from the *OCA2* promoter on chromosome 15 [19]. This SNP, in conjunction with *OCA2*, has the highest association to iris color, especially in predicting blue eye color [19]. However, no single gene could be used to make a reliable iris color inference which suggests intergenic complexity for iris color determination [12]. There have been several studies looking to identify the SNP loci that best associate with iris color and therefore might be used for accurate predictions. In 2011, Walsh et al. [8] developed the IrisPlex assay that incorporated the six most informative eye color SNPs known at the time [8, 30].

The most significantly associated SNP involved in eye color expression is rs12913832. The functionality of the *HERC2* gene is still not understood [19], though in one study it was found to have a very significant association ($p < 1.0 \times 10^{-300}$) to blue and brown eye color [30] . This SNP is found in the conserved region of intron 86 on chromosome 15 of the *HERC2* gene [31]. It is found upstream of the oculocutaneous albinisim II (*OCA2*) gene. It has been suggested that the *HERC2* gene acts as a silencer sequence on the *OCA2* gene promoter (see Figure 1.3) [19]. Therefore if *OCA2* is

silenced by *HERC2* (C allele), blue eye color is expressed. The T allele of rs12913832 (*HERC2*) acts as an enhancer for melanin production.[32].

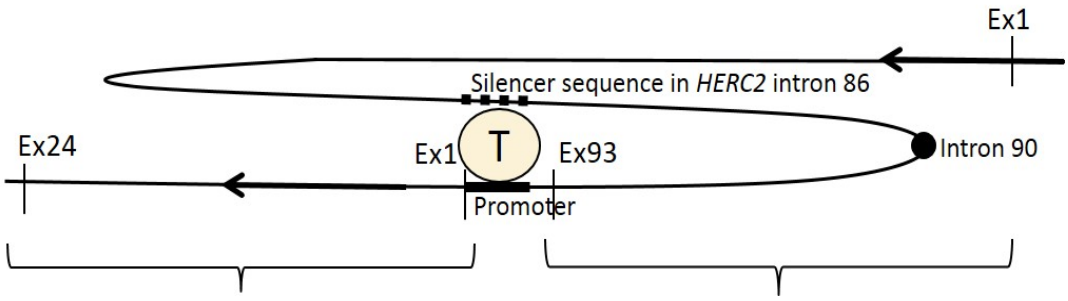

Figure 1.3. *HERC2-OCA2* interaction. The silencer sequence in *HERC2* acts on the promoter region of *OCA2* which will lead to blue eye color expression. Adapted from Eiberg et al. [19].

Before the discovery of the *HERC2* dominant association, *OCA2* was shown to have the most SNPs associated with eye color. It is located downstream of the *HERC2* gene on chromosome 15. One SNP (rs1800407) of *OCA2* shown with second highest association to eye color ($p = 1.7 \times 10^{-28}$) by Liu et al. [30] which is located within exon 13 of the *OCA2* gene. There are many other SNPs linked to the *OCA2* gene region that have been shown to have high heritability association on eye color, however the OCA2 association to eye color is severely reduced when adjusted with the effect of rs12913832 [30].

The *HERC2-OCA2* region on chromosome 15 has shown highest heritable association with pigmentation expression, but as eye color is a complex polymorphic trait, many genes have additive effects to these SNPs to improve upon iris color determination. Another SNP is rs1393350, which is located within an intronic region of the tyrosinase

(*TYR*) gene on chromosome 11 [33]. Tyrosinase as mentioned, is a protein involved in melanin production. The SNP rs12203592 is found in intron 4 of the interferon regulatory factor 4 (*IRF4*) gene on chromosome 6. Its polymorphism has additive effects related to blue eye color, though it does not seem to be directly involved in the pigmentation pathway [34]. SNP rs12896399 is located within an intronic region of the *SLC24A4* gene on chromosome 14. The gene is in the same family as *SLC45A5* which was found to be the human ortholog of the zebrafish *golden* gene, which influences expression of lighter pigmentation such as blonde hair and blue eyes [6]. SNP rs16891982 is a non-synonymous variant within exon 5 of the *SLC45A2* gene, also known as the membrane associated transporter protein (*MATP*) gene, on chromosome 5. This gene is thought to be involved in the intracellular processing and trafficking of melanosomal proteins, e.g. tyrosinase [2].

As these eye color informative SNPs are being discovered, there have been several studies in developing assays that range in differing combination of SNP markers for eye color prediction [6, 8, 35, 36]. One of the first highly successful eye color prediction assays designed is IrisPlex. Developed in the Netherlands and based on a Dutch population, the IrisPlex assay detects six SNPs: rs12913832, rs1800407, rs1393350, rs12203592, rs12896399, and rs16891982 associated with the following genes, respectively: *HERC2*, *OCA2*, *SLC45A2*, *SLC24A4*, *IRF4*, and *TYR* [8]. These markers were found at the time to be the six highest associated SNPs to eye color expression [8]. Eye color predictions were made in three eye color categories: brown, blue, or intermediate. In the original published work [8], the predictive ability is high for blue and brown eye color (91.6% blue and 87.5% brown) using a prediction model based from

multinomial logistic regression which has parameters derived from minor allele frequencies [8]. This particular model, though accurate at predicting blue and brown eye color, used a homogenous population in which no intermediate eye colored individuals were tested.

The objective of this work was to test the IrisPlex model (under the described parameters, [8]) in an admixed North American population. When it was determined that the predictive power of the model did not give similar accuracy as the original study of Dutch individuals, we developed additional models for the use of eye color prediction and also incorporated a method for objective quantification of color based on the color components obtained from digital photographs.

CHAPTER 2. METHODOLOGY

2.1 Sample Collection

Buccal swabs were collected from 200 anonymous volunteers (Indiana University IRB Approval Protocol #1111007371). At the time of buccal swab collection, a digital photograph was also taken of each volunteer's right eye (with care for volunteers to remove any corrective lenses). A Canon PowerShot digital camera (Canon Inc., Tokyo, Japan) was used with macro mode, ISO80, and flash settings. A light box was built for photo collection to ensure equal distance and lighting conditions for all photos.

2.2 DNA Extraction and Quantitation

DNA was extracted by a modified organic extraction. Briefly, swabs were incubated in 1.5 mL tubes at 65 °C for a minimum of 8 hrs in 500 µL lysis buffer (Invitrogen, Carlsbad, CA) with 50 µL proteinase K (Qiagen, Hilden, Germany). Following lysis, the swabs were spun dry into tubes with the use of DNA IQ™ spin baskets (Promega Corporation, Madison, WI) and discarded. Then, 500 µL phenol (Thermo Fisher Scientific Inc., Waltham, MA) was added and centrifuged at 13,000 rpm for 1 minute. The aqueous layer was removed to a new tube and 500 µL phenol: chloroform: isoamyl alcohol (25:24:1) (Thermo Fisher Scientific Inc.) was added and centrifuged at 13,000 rpm for 1 minute. The aqueous layer was removed and placed into a new tube to which

500 µL of cold 95% ethanol (Thermo Fisher Scientific Inc.) and 25 µL of cold 0.2M NaCl (Thermo Fisher Scientific Inc.) was added. The tubes centrifuged at 4 °C at 13,000 rpm for 15 minutes. The supernatant was discarded and the pellet was washed with 500 µL of cold 70% ethanol (Thermo Fisher Scientific Inc.) followed by centrifugation at 4 °C at 13,000 rpm for 5 minutes. The supernatant was removed and the sample was allowed to air dry. The sample was re-suspended in 50 µL of TE buffer (Thermo Fisher Scientific Inc.) and stored at -20 °C until further use. DNA quantitation was performed according to the manufacturer's specifications using the Quantifiler® Human DNA Quantification kit (Applied Biosystems Inc.) on a 7300 Real Time PCR System (Applied Biosystems Inc.).

2.3 SNP Amplification and Genotyping

SNP amplification was performed via single base extension (SBE). SBE utilizes fluorescently labeled dideoxynucleotides (ddNTPs) to extend the primer by one base, which is the SNP of interest (Figure 2.1). This SNP is what is detected during capillary electrophoresis and the output is shown as discretely spaced, peaks which color indicates which base variant is at the targeted site of the DNA. Two purification steps are required in between the PCR reactions to inactivate unincorporated primers, dNTPs and ddNTPs.

The same six SNPs were amplified using the same primer sequences described in Walsh et al. [8] where the only difference was in primer concentrations (Table 2.1). However, a single multiplex reaction of all six SNPs was never successfully amplified.

Instead, two multiplex reactions, one of four IrisPlex SNP primers (*HERC2*, *SLC45A2*, *TYR*, *IRF4*) and one of the remaining two IrisPlex SNP primers (*SLC24A4* and *OCA2*) were amplified.

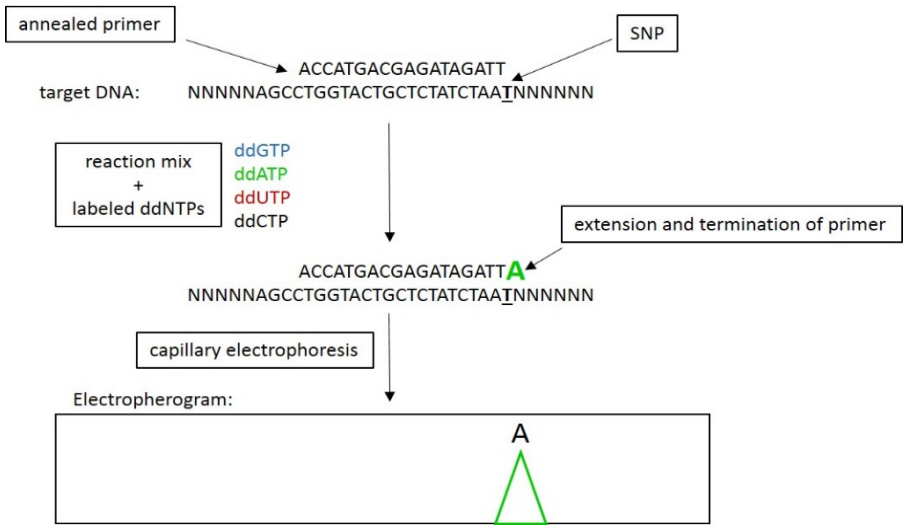

Figure 2.1. Outline of single base extension (SBE). Initial PCR product with primer sequence is then extended by base variant (target SNP) with ddNTP. Adapted from SNaPshot Multiplex kit manual (Applied Biosystems Inc.).

For each multiplex reaction, 1 ng of DNA was amplified in a 12uL reaction with 6uL of AmpliTaq Gold 360 Master Mix (Applied Biosystems) including 0.5 uL GC Enhancer, and a final concentration of each primer of 5.0 μM. PCR was performed using the same parameters as in Walsh et al [8] on a Mastercycler Pro thermal cycler (Eppendorf, Hamburg, Germany).

The PCR products were purified using USB ExoSAP-IT® (Affymetrix, Santa Clara, CA). The purified PCR products were pooled for a multiplex single base extension (SBE) reaction, using the same SBE primers designed by Walsh et al [8]. The SBE reaction used 1 μL of total pooled PCR product (0.5 μL of each previously purified

product) and 2 μL of SnaPshot reaction mix in a reaction volume of 5 μL using the SNaPshot® Multiplex kit (Applied Biosystems). PCR was performed on a Mastercycler Pro (Eppendorf) following the same SBE conditions as Walsh et al. [8]. SBE products were then purified using shrimp alkaline phosphatase (SAP, Takara, Kyoto, Japan).

Table 2.1. Modified IrisPlex SNP primer concentrations. Primer concentrations were the only differing property from the primers designed for use in the original IrisPlex study [8]. All other primer properties can been found in Walsh et al. [8].

SNP	Primer concentration (μM)	Extension primer concentration (μM)
rs12913832	2.5	1.0
rs1800407	2.5	1.0
rs12896399	2.5	1.0
rs16891982	2.5	1.0
rs1393350	2.5	1.5
rs12203592	2.5	1.0

Capillary electrophoresis was performed where 1 uL of purified SNaPshot products was analyzedon an ABI 3500 Genetic Analyzer (Applied Biosystems) following standard protocol of the SNaPshot® Multiplex kit. Data analysis was performed using GeneMarker v2.20 software (SoftGenetics, State College, PA). For sensitivity, a threshold of 200 rfu was set for peak intensities, and a minimum heterozygote peak height ratio (PHR) of 0.40 was used for genotyping, however, for *IRF4* and *SLC45A2*, a PHR of 0.20 was used for genotyping due to overall low peak imbalance.

2.4 Iris Color Determination and Measurement

An objective color classification method was applied in addition to basic human visualization for classifying the eye color of each sample into the same three categories: brown, blue, or intermediate.

Eye color was determined both subjectively and objectively. The first subjective manner was basic human visual identification, in which every digital photo was evaluated by 5 individuals to classify eye color as brown, intermediate, or blue. Intermediate color was defined as any color that was not brown or blue. The consensus rating of the individual examinations was used as the visual determined color.

2.4.1 Color Components

There are several generic color space models that can describe color quantitatively, with the intent of measuring similarly to human perception while standardizing color between instrumentation used to obtain the color of a given sample: RGB, HSV, CIEXYZ, and CIELAB. Measuring digital color for iris color in terms of the hue and saturation color space has been described [14] as well as by red, blue, green (RGB) components [16], and by the Commission Internationale de L'Eclairage L*a*b* (CIELAB) color space [10, 37]. All color component values can be converted between each color model and therefore a color can be described within each color space. The CIEXYZ color space can be considered as just xy coordinates and plotted on a two dimensional axis to show color chromaticity (no luminosity considered). CIELAB components are thought to be perceptually uniform to that of human vision [37]. L*

describes the brightness dimension, a* describes the green/red dimension, and b* describes the blue/yellow dimension [37]. There are trends within these quantitative color spaces for the three eye color categories of focus here (blue, brown, intermediate), for example, for CIELAB colors, blue irides tend to have a high L* value, and negative a* and b* values; green have a high L*, a negative a*, and a b* value around zero, and brown irides tend to have a low L* and positive a* and b* [37]. In terms of RGB components, darker irises, e.g. brown, have lower RGB values than blue and intermediate colors. In any of the above models, the color is a condensed value, meaning it is measured homogenously as a single color, therefore not capturing the complex color pattern that may be present, e.g. green or blue iris with a brown peripupillary ring (Figure 2.2) [10, 37]. The color spaces applied in this study are RGB and xy coordinates to highlight the objective differences between the brown, intermediate, and blue eye color categories used for sample color classification from digital photographs.

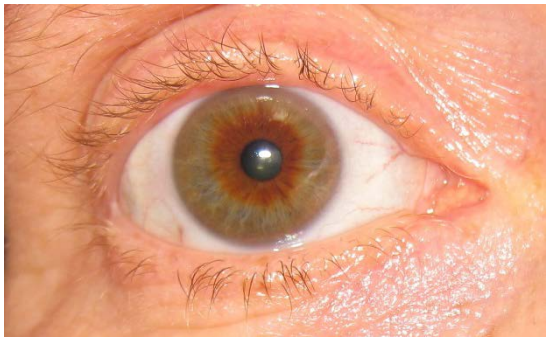

Figure 2.2. Iris digital photo sample. Example of an iris with a peripupillary ring.

2.4.2 Objective Color Classification

A second, quantitative eye color determination was made using a numerical value known as the iris melanin index (IMI) [10]. This method involves determining the red, green, and blue (RGB) color components of the iris from each digital photo. The iris was digitally extracted to determine the RGB components and luminosity value using Adobe Photoshop® Elements 10 (Adobe Systems Inc., San Jose, CA). A ratio of these components as determined by the histogram function measures the color as a single numerical value, the iris melanin index (IMI) (see Figure 2.3) [10].

$$\textbf{Color Scale:}\ \frac{\text{Red}}{\text{Green}} + \frac{\text{Red}}{\text{Blue}} + \frac{\text{Green}}{\text{Blue}}$$

$$\textbf{IMI:}\ \frac{\text{luminosity}}{\text{avg. luminosity}} + \frac{\text{avg. color scale}}{\text{color scale value}}$$

Figure 2.3. The IMI formula. Using a ratio of the average RGB color components and the luminosity (brightness) values as collected from the histogram function from the extracted iris digital photo calculates the IMI as a single value.

In this work, the RGB components were converted to xy color coordinates using the OpenRGB software program (Logicol, Trieste, Italy), with F7 fluorescent illuminant and 10° observation angle used in the conversion factors, allowing for two point comparison and graphical representations of each color category. CIELAB color components were also determined through conversion. The xy coordinates were separated statistically by discriminant analysis (DA) using XLSTAT 2010 (Addinsoft, Paris, France) within Microsoft Excel (Microsoft, Redmond, WA). To determine that our sample population

was representative of the larger U.S. population, a chi-square test was done to determine any statistically significant deviations in population eye color frequency when compared to a larger U.S. sample population (State of Indiana).

2.5 Statistical Phenotype Prediction Models

Phenotype inferences, such as eye color, are determined from a statistical model. Models are used to produce information on the basis of valid input information; this is the inference process [38]. Traditional statistical models require large sample sizes, experimental and control samples that are distinctly different enough in terms of the phenotype of interest to convey significant probability power [38]. The goal of any model-building technique is to find the best fitting yet biologically reasonable model to describe the relationship between an outcome (dependent variable) and set of predictors (independent variables) [39].

2.5.1 Multinomial Logistic Regression Model

Logistic regression modelling evolved from the binary based maximum likelihood method of estimation [40]. A logistic regression model is distinguished from a linear regression model in that the dependent variable is binary [39]. Multinomial models apply to scenarios with more than two variables assume that the categories are not ordered and are independent of each other [40]. The regression model gives a set of coefficients for each independent variable as it relates to the predictor category. The coefficients represent the rate of change of a function of the dependent variable per unit of change in

the independent variable [39]. Multivariate statistical models, such as logistic regression, examines overall dependency structure between genotypes, phenotype, and environmental variables [38]. Model validation is important when the fitted model is used to predict outcome of future subjects, to assess the goodness-of-fit of the developed model [39].

Eye color prediction was done using the multinomial logistic regression model as used by Walsh et al. [8]. In the three category model there are two logit functions, i.e. two sets of coefficients per independent variable (SNP), in this case the two functions correspond to blue vs. brown eye color and intermediate vs. brown eye color. The difference between the two gives the third logit (blue vs. brown). This model uses categorical classification of subjects (eye color) based on a set of predictor variables (population minor allele frequencies), and calculated probabilities of each individual for each color category: brown, intermediate, or blue [30]. The color category with the highest probability is the predicted color. The three logit functions used are as those as established by Liu et al. [30]

The α and β values in the logit functions are the logistic regression intercepts and coefficients, respectively. The x values are the minor allele frequencies of each SNP. The original model was built on data from a Dutch population that included 3804 individuals [30] and was tested using a second sample set of 40 individuals [8]. Given the poor results using the model with the same parameters, minor allele frequencies were calculated from 100 random samples (training set) and an adjusted multinomial regression model was developed and tested with the remaining 100 samples (verification

set) using MATLAB® 2012a (The MathWorks Inc., Natick, MA). Table 2.2 shows the regression coefficients of both the IrisPlex and our adjusted population.

2.5.2 Bayesian Network Model

An alternative prediction model was developed based on Bayesian network (BN) analysis, based on minor allele frequencies as described by Pośpiech et al. [41] using the Hugin Lite 7.6 software program (Hugin Expert A/S, Aalborg, Denmark) (Figure 2.4). A BN gives a graphical representation of relationships between observed data and allow inference of an individual phenotype (e.g. eye color) based on known genotypes of an individual in the range of analyzed multiple SNP loci [41].

Table 2.2. The regression parameters for the multinomial logistic regression of the original IrisPlex model and our adjusted frequency model. A) The alpha intercept values. B) The beta coefficients for each SNP.

A)

Intercept	**IrisPlex [21]**	**Adjusted**
α1	3.94	12.51
α2	0.65	5.45

B)

SNP	**IrisPlex [21]**		**Adjusted**		**Minor Allele**
	β1	**β2**	**β1**	**β2**	
rs12913832	-4.81	-1.79	-13.08	-7.29	T
rs1800407	1.40	0.87	0.54	1.89	T
rs12896399	-0.58	-0.03	-0.27	0.91	G
rs16891982	-1.30	-0.50	-8.43	-2.54	C
rs1393350	0.47	0.27	0.99	-0.18	T
rs12203592	0.70	0.73	2.31	0.64	A

Each node represents an uncertain variable and arrows between nodes represent links among the different variables [42]. The output is a conditional probability that represents the likelihood based on prior information [42]. They can accommodate complex structure of gene environment interactions with phenotypes defined by multiple variables (e.g. SNPs) [43].

The BN model gives a probability for each eye color category based on *a priori* odds of each eye color frequency. Two *a priori* odds were tested: equal odd for all three color categories, as well as odds based on the known eye color distribution determined from the Indiana Bureau of Motor Vehicles database. In addition to probabilities, likelihood ratios are also able to be calculated from the BN analysis model [41].

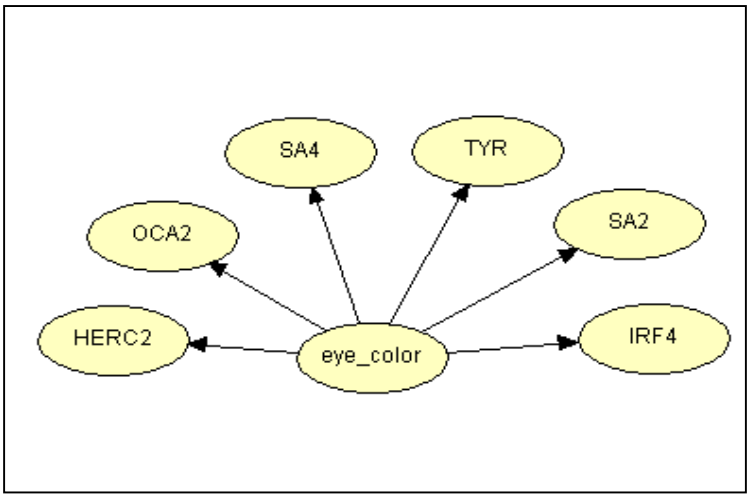

Figure 2.4. Outline of the Bayesian network nodal relationship.

2.5.3 Linear Discriminant Analysis

Linear discriminant analysis, or just discriminant analysis (DA), is a multivariate statistic technique used to visualize group differences. There are two sources of

variation, within source and between source [44]. Discriminant analysis constructs a set of axes to separate data into groups by maximizing between group variance and minimizing within group variance [45]. This is a supervised technique, meaning knowledge of group membership (e.g. eye color category) for each sample before analysis is required [45]. Classification of an unknown sample to a group also requires quantitative measurement of pattern similarity, in this case, RGB color components [45]. One option with DA is to conduct a cross validation, which produces a confusion matrix showing the number of true positives, true negatives, false positives, and false negatives of the samples analyzed and overall classification rate. This matrix is calculated by the leave-one-out cross validation method, where a sample is temporarily removed from the data set, the classifier adjusts for the remaining samples, and then used to predict the group classification of the removed sample [45]. The DA function in XLSTAT (Addinsoft) also calculates the receiver characteristic operative curve (ROC). An ROC curve is a graphical plot with the false positive rate on the x axis and true positive rate on the y axis or, the inverse specificity vs. the sensitivity, respectively [40]. The six SNPs used in the IrisPlex assay were initially evaluated by Liu et al. [30] where area under the receiver characteristic operative curve (AUC) was used to evaluate the overall prediction model performance. To compare model performance to that of the original IrisPlex model (e.g. ability to classify correctly), the area (AUC), sensitivity, specificity, positive predictive value (PPV) and negative predictive value (NPV) were determined for our multinomial regression and Bayesian prediction models.

In evaluating ROC curves an AUC value of 0.5 indicates a lack of prediction ability and an AUC close to 1 indicates near perfect prediction accuracy. One important note for

evaluating an AUC value, it reflects both true positive values (e.g. correctly predicting blue for blue samples) and true negative values (e.g. correctly predicting non-blue for non-blue samples). Sensitivity is the true positive rate, the number of true positives out of the total number of positives (total number accounts for false negatives) and specificity is the true negative rate, the number of true negatives out of the total number of negatives (total number accounts for false positives). An ideal model will give a high rate of both specificity and sensitivity i.e. will be accurate in predicting the true positives and negatives while minimizing false positives and negatives. The PPV is the number of true positives out of the total number of true and false positive predictions, and the NPV is the number of true negatives out of the total number of true and false negative predictions.

CHAPTER 3. IRISPLEX EVALUATION: RESULTS AND DISCUSSION

3.1 Eye Color Determination

The digital photo's iris color was subjectively and objectively determined for all 200 samples. An IMI scale was determined after digital analysis and set with highest agreement to the visual determinations (Table 3.1). Values were classified as brown if they fell in the range 1.25-1.65, intermediate in the range of 1.66-2.32, and blue in the range of 2.33-3.20. There were 22 (out of the 200 samples, Appendix A) which did not identify in the same color category between the objective IMI classification and subjective human visual determination. All mistaken classifications were between intermediate and either brown or blue.

To determine if the 200 samples were a representative sample of the Indiana population, data from the Indiana Bureau of Motor Vehicles (D. Rosebrough, Indiana BMV, personal communication) was used as a comparison to a larger sample population. There was no significant difference between the frequency distributions of our collected sample (N=200) and that collected by the BMV (N=7,115,106, Table 3.2), although there were a higher number of observed blue-eyed individuals in the collected samples ($\chi 2$ test, df=2, $p > 0.10$).

Table 3.1. Percentage (%) of samples determined for each eye color category. The IMI values calculated for each sample and the IMI ranges based on least number of misclassifications when compared with the visual determinations.

Eye Color	Visually determined (%)	IMI Value	IMI determined (%)
Brown	34.0	1.25-1.65	36.5
Intermediate	26.0	1.66-2.32	22.0
Blue	40.0	2.33-3.20	41.5

Important to note, eye color is self-reported for driving records, therefore some subjective discrepancy might be present. Visual determinations cannot be disregarded however as they are the basis for eye witness testimonies and the practical manner of classification for forensic investigations; therefore, it is essential that objective eye color classification correlates with visual determinations. The data illustrates that there is no statistical difference between the visual and quantitative eye color measurements and therefore the quantitative measurement (IMI) was used in further analyses.

Quantitative color classification has led to more accurate predictions in model development. One recent study used hue and saturation values in a GWAS study for quantifying eye color and as actual quantitation is a more systematic, objective approach compared to categorical classification, additional candidate eye color SNPs were discovered as a result [14].

Table 3.2. Eye color distribution (%) among sample population and larger scale United States sample population and statistical significance (χ^2) between them.

	Collected Samples (%)	**State of Indiana (%)**	**χ2 values (df=2)**
Brown	34	43	1.88
Blue	40	34	1.06
Intermediate	26	23	0.39
Sample Size (N)	200	7,115,106	$p > 0.10$

Additional statistical analysis of the quantitative color components was done to determine if the quantitative measurements exhibit sufficient discrimination between color categories. Sample color components were converted to xy color coordinates and demonstrates statistical separation by DA (Figure 3.1). The ellipses shown for each color category in Figure 3.1 show the 95% confidence interval of a sample belonging to that particular group. There is overlap seen between the ellipses only between the blue or brown and intermediate groups, with most occurring between brown and intermediate; there is no overlap of the brown and blue groups. This is expected as most conflicting predictions were between either brown or blue and intermediate for the visual determinations.

3.2 Multinomial Logistic Regression Analysis

The six IrisPlex SNP genotypes for all individuals were determined (Appendix A) and used as the basis for the prediction models. The prediction model used by Walsh et al. [8] calculates probabilities in each of the three color categories based on multinomial logistic regression using previously published formulas [30].

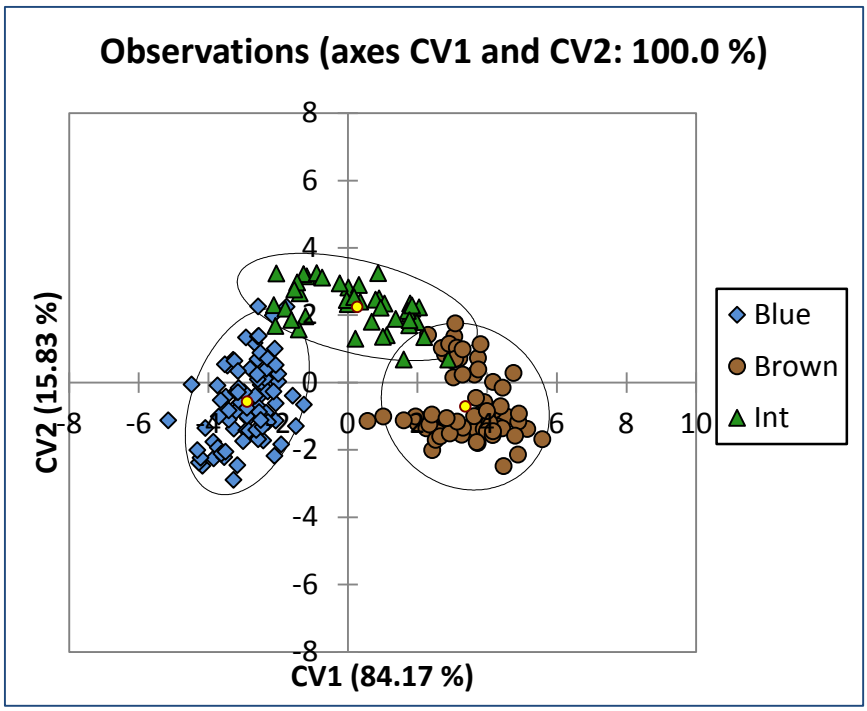

Figure 3.1. DA scatterplot of xy color coordinates. Separation of each eye color category with 100% of the discrimination captured by the first two canonical variates. The x color coordinate contributes to CV1 and the y color coordinate contributes to CV2.

Two different parameter sets were used for prediction evaluation: the Walsh et al. parameters [8] and an adjusted set based on our sample allele frequency data. Two cut-off probability thresholds were chosen as discussed by Walsh et al. [8] in evaluating accuracy of prediction, 0.5 and 0.7. The IMI classifications, not the visual determinations, were used as the true eye color for each sample.

In the Dutch study, Walsh et al. had reasonable prediction accuracies 91.6% and 56% for blue and brown eye colors, respectively, at the 0.7 threshold; and 91.6% and 87.5% for blue and brown eye colors, respectively, at the 0.5 threshold [8]. It is imperative to note that their sample set did not contain any individuals with an intermediate eye color.

Using the Walsh et al. frequencies [8], the predicted eye color rates were 5% and 52% for blue and brown eye colors, respectively, at the 0.7 threshold and 8% and 93% for blue and brown eye colors, respectively, at the 0.5 threshold (Table 3.3). The intermediate color at both thresholds did not yield any true positive predictions. Using the adjusted parameters (based on our training set), the predicted eye colors of the verification set (N = 100) were 33% and 48% for blue and brown eye colors at the 0.7 threshold, respectively, and 28% and 3% for blue and brown eye color at the 0.5 threshold, respectively. For the intermediate color the rate of prediction was 4% at the 0.7 threshold and 11% at the 0.5 threshold (Table 3.3). See Appendix B for the prediction probabilities for all samples.

Table 3.3. The correct prediction rates (%) by color category of all 200 samples evaluated for each prediction model. Only the verification set (N=100) was evaluated against the adjusted regression parameters; all 200 samples were evaluated using the Bayesian network correct predictions with either set of *a priori* odds.

Parameters	Threshold	Brown (%)	Intermediate (%)	Blue (%)
MLR: IrisPlex	0.5	93	0	8
	0.7	52	0	5
MLR: Adjusted	0.5	48	11	33
	0.7	3	4	28
Bayesian: Equal odds	0.5	40	20	57
	0.7	27	20	52
Bayesian: Adjusted	0.5	51	23	76
	0.7	32	2	57

Equal odds = 0.33 each eye color category, adjusted odds= 0.33 brown, 0.44 blue, 0.17 intermediate

The number of correct predictions decreased for the brown eye color and increased for blue and intermediate using the adjusted parameters. The adjusted parameters did not

measure more accurate predictions than those of Walsh et al., however, there were fewer number of incorrect predictions and an increase in inconclusive predictions in which the probabilities in either color category did not measure above the 0.5 threshold (Figure 3.2).

Receiver operating characteristics (ROC) were used to evaluate model performance, including the area under the ROC (AUC) which is a value that compares the specificity and sensitivity in a model's prediction ability. The AUC was determined for our samples using the IrisPlex and adjusted parameters (Table 3.4). Our samples evaluated with the IrisPlex parameters show an AUC of 0.78 for blue, 0.70 for intermediate, and 0.82 for brown. They were improved when our samples were evaluated with the adjusted frequency parameters with AUC of 0.87 for blue, 0.78 for intermediate, and 0.83 for brown. The positive predictive value (PPV) was more accurate with the adjusted frequency parameters with 80.5% for blue, 50% for intermediate, and 71% for brown (Table 3.5).

Table 3.4. AUC values of each prediction model. AUC reflects model performance (ability to make accurate predictions). Higher AUC value indicates better model performance. **Bold** indicates the most accurate model.

Prediction Model	Blue	Intermediate	Brown
Liu et al. [30]	0.91	0.73	0.93
IrisPlex parameters [8]	0.79	0.70	0.82
Adjusted parameters	0.87	0.78	0.83
Bayesian: Equal Odds	**0.90**	**0.82**	**0.86**
Bayesian: Adjusted	0.90	0.78	0.86

The adjusted frequency model showed more accurate negative predictive values than positive, and the AUC is relatively high because it considers both the true negative and true positive predictions. This is also demonstrated in the measure of sensitivity and specificity of the model (Table 3.5). With this model, the sensitivity is more accurate than the specificity. The specificity is overestimated as the true negative rate was higher than the true positive rate. True negative predictions are still important for exclusionary purposes in forensic investigations but true positive predictions for inferring an unknown individual's phenotype are what the goal is, and with this model, positive predictions are not yet sufficient for acceptably accurate inferences.

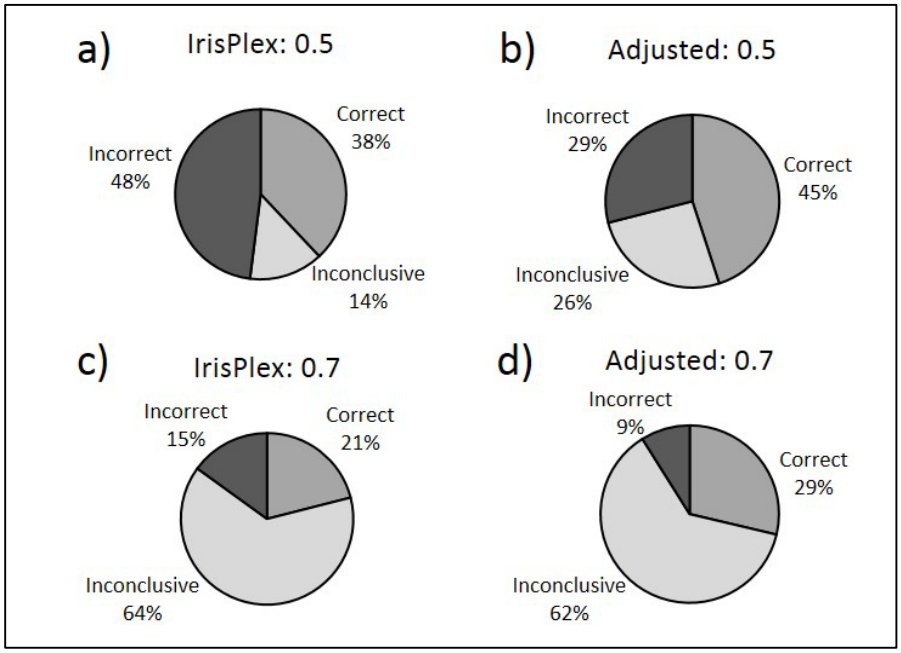

Figure 3.2. The frequency of overall correct, incorrect, and inconclusive eye color predictions using the MLR model. a) Predictions under IrisPlex parameters at the 0.5 threshold, b) predictions under adjusted parameters at the 0.5 threshold, c) predictions under IrisPlex parameters at the 0.7 threshold, and d) predictions under adjusted parameters at the 0.7 threshold.

3.3 Bayesian Network Analysis

Statistical analysis was performed using a Bayesian network prediction model as described by Pośpiech et al. [41]. The predictions were evaluated with two *a priori* probability scenarios. One scenario adjusted the prior probabilities to the eye color frequencies of our training set, and the other scenario assumed no previous knowledge of population frequencies thus equal odds for each color. Table 3.5 shows the positive prediction rates for each eye color category and Figure 3.3 shows a summary of the overall number of predictions for both prior probability sets. See Appendix C for prediction probabilities for all samples of each *a priori* set

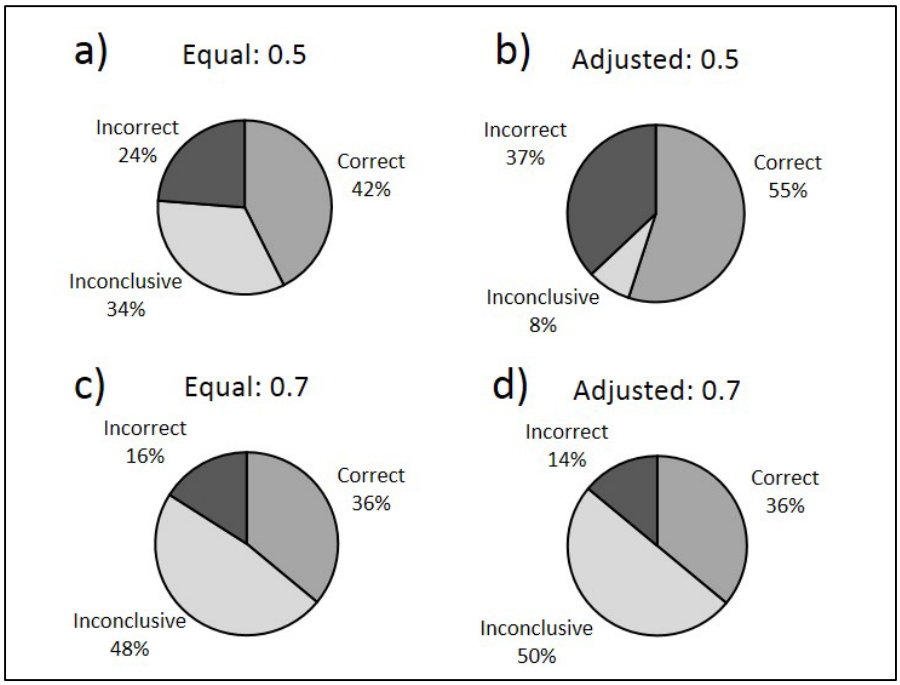

Figure 3.3. The frequency of overall correct, incorrect, and inconclusive eye color predictions using the BN model. a) Predictions under equal odds at the 0.5 threshold, b) predictions under adjusted frequency odds at the 0.5 threshold, c) predictions under equal odds at the 0.7 threshold, and d) predictions under adjusted frequency odds at the 0.7 threshold.

The AUC for the Bayesian model was also determined for its prediction accuracy (Table 3.4). The AUC with both *a priori* probabilities was 0.86 for brown eye color, and 0.90 for blue eye color. For the intermediate color, the AUC for *a priori* equal odds (equal probability) was 0.82, whereas with adjusted frequencies, it was slightly lower at 0.78 (Table 3.4). The positive predictive value was 82.5 for blue, 70.0 for brown, and 46.2 for intermediate (Table 3.5).

As previously mentioned, an advantage of a Bayesian model is the ability to calculate likelihood ratios. This is a ratio between the tested outcomes and prior odds. These ratios ranged between 0 and 498 (Appendix D). Likelihood ratios are used in forensic interpretations based on competing hypotheses and are suitable for reporting phenotype inference on genotypes. Likelihood ratios are comparisons between two probabilities of two possible scenarios, for example, that an individual has blue eyes, or has brown eyes. If the ratio (LR) between the two scenario probabilities is greater than 1, it generally indicates that one scenario is more likely than the other. This is calculated in a similar manner as likelihood ratios for paternity testing in which nationally recognized standards have been developed for evaluating the meaning of an LR obtained in such cases [46]. This could easily apply to DNA phenotyping cases.

3.4 Genetic Variation within the U.S. Population

The original IrisPlex study involved a collection of samples from a Dutch population [8]. Geographic and ancestral differences of subpopulations affect allele frequency distributions within the human population. This is especially important in forensic

testing, as it is an aim to design assays with loci that have little difference between populations so the testing can apply on a global platform. Table 3.6 shows the allele frequencies of each of the SNPs used in IrisPlex assay in the 200 collected samples herein, the 40 samples used in the original IrisPlex study, and also includes larger scale allele frequency distributions of the target population from the allele frequency database (ALFRED).

Table 3.5. Prediction model performance test characteristics (%) of both regression and Bayesian parameter sets after analysis of our 200 samples. These values were the same for both prior odd sets for the Bayesian model.

Model	Test Characteristics	Blue	Intermediate	Brown
IrisPlex	Sensitivity	65.9	0	85.3
Frequencies	Specificity	75.0	98.8	56.4
(MLR)	PPV	67.4	0	71
	NPV	73.7	100	75.3
Adjusted	Sensitivity	85.7	91.6	85.3
Frequencies	Specificity	75.0	41.2	56.4
(MLR)	PPV	80.5	50	71
	NPV	81.4	88.4	75.3
Bayesian	Sensitivity	75	35.3	53.9
Network	Specificity	87.5	91.6	85.3
(BN)	PPV	82.5	46.2	70
	NPV	81.7	87.4	74.3

PPV=positive prediction value (correctly predicted positives)
NPV= negative prediction value (correctly predicted negatives)

ALFRED compiles gene frequency data on human populations; at this point in time there is data on 719 populations in the database [33]. The target population used here is the European American population which consists of samples from across the United States of individuals with European descent. It should be noted that the allele frequency

distributions of the rs12913832 SNP, which is the highest associated eye color locus, vary greatly even within the same subpopulation (the United States, Table 3.6).

This high variation within the United States population is further demonstrated by the differences between the reported eye color distributions among individual states (Table 3.7). These distributions were determined from licensed driver databases (BMV databases, personal communications) and are percentages of eye colors reported in as many as 8 color categories and were combined into one of the three color categories evaluated here (Table 3.7).

Table 3.6. SNP nucleotide position and allele frequency comparison. Frequencies shown are ALFRED population data, the 200 collected samples in this study, and the 40 Dutch samples collected in the original IrisPlex study.

SNP position/ alleles	European American (ALFRED)	Collected Samples (N=200)	IrisPlex Samples (N=40)
rs12913832			
C	0.79	0.49	0.69
T	0.21	0.51	0.31
rs1800407			
C	0.92	0.93	0.96
T	0.08	0.07	0.04
rs12896399			
G	0.43	0.61	0.6
T	0.57	0.39	0.4
rs1393350			
C	0.77	0.71	0.9
T	0.23	0.29	0.1
rs16891982			
G	0.96	0.64	0.71
C	0.04	0.36	0.29
rs12203592			
G	0.84	0.91	0.93
A	0.16	0.09	0.07

ALFRED = ALlele FREquency Database [33]

Furthermore, the genotype data (Appendices A and F) demonstrated, in several cases, confusion between either brown or blue phenotypes with intermediate phenotype for identical genotypes. There were two SNP genotype profile groups that exhibited all three eye color phenotypes: HERC2 (C/T), OCA2 (C/C), SLC45A2 (G/G), SLC24A4 (G/G), TYR (C/C), IRF4 (G/G), and HERC2 (C/T), OCA2 (C/C), SLC45A2 (G/T), SLC24A4 (G/G), TYR (C/T), IRF4 (G/G). Knowledge of the admixed nature of the United States populations is further supported by the observation of increased heterozygosity and therefore should be considered an appropriate model population to test for validation of forensic assays that have only been tested on more homogeneous subpopulations.

Table 3.7. Eye color distribution among 11 states. These distributions show the high degree of variation within the U.S. population (approximate percentages (%), personal communications, BMV databases).

State	Blue	Intermediate	Brown
Indiana	34	23	43
Kentucky	34	25	39
Washington	33	23	44
New York	21	16	63
N. Dakota	41	28	31
Georgia	21	16	52
Illinois	28	21	51
Colorado	30	25	45
Idaho	38	27	35
N. Carolina	28	23	49
Wisconsin	33	21	36

3.5 Evaluation of Samples with Conflicting Eye Classification

As previously stated, there were 22 collected samples where the quantitative eye color measurements disagreed with the visually determined classifications (Appendix E for photos, Table 3.8). There are several possible reasons for the disagreement between visual and objective color classification of these samples. One, the presence of a brown peripupillary ring can be seen in many of the 22 samples (Appendix E). As the iris color was measured homogeneously from the digital photo, this could contribute to some differences. Also, if there was an iris pattern present, no instruction was given to the 5 subjective examiners as to how to consider it in their rating. In some cases, the sample could have been rated intermediate because it was not seen as homogeneous brown or blue, even if there was only very little of another color present within the iris. Furthermore, the IMI values of some the samples fall within 0.05 or less of the scale cut-off between categories (e.g., sample 279, IMI =1.70). As the IMI scale was user-set, adjusting it in either direction would categorize some samples into a different color category. However, as previously stated, these scale values were set where there was least disagreement between visual and objective classifications, and as color is not a discrete variable (i.e. many shades possible for any one color), the choosing a discrete value cut-off may not be ideal.

The predictions of those 22 samples were compared (Table 3.9) to evaluate any differences in the prediction accuracy. The quantitative values were more accurate at the 0.5 threshold. There were 4 and 2 more correct predictions for the MLR models, IrisPlex and adjusted frequency parameters, respectively. For the BN models at the 0.5 threshold, 0 and 2 more correct predictions, equal odds and adjusted frequencies, respectively. The

visual determinations were slightly more accurate at the 0.7 threshold. For the MLR models, 1 and 0 more correct predictions, IrisPlex and adjusted parameters, respectively; and 1 and 1 more correct predictions for the BN model with equal and adjusted odds, respectively. The majority of samples had the same eye color prediction regardless of being evaluated by its visual or quantitative classification and were determined to have no change on the prediction outcome (Table 3.9).

Table 3.8. The 22 samples with conflicting visual and objective color classifications. Visual determinations indicates the ratings from the subjective examiners (5 total). IMI indicates the IMI value and color. Br = brown, I = intermediate, Bl = blue.

Sample	**Visual Determinations**	**IMI**
124	4I , 1 Br	1.65 = Br
168	4I , 1 Bl	2.37 = Bl
170	5 Bl	2.26 = I
219	3 I , 2 Br	1.60 = Br
256	5 Bl	2.31 = I
273	4 I , 1 Br	1.58 = Br
279	3 Br , 2 I	1.70 = I
313	4 I , 1 Br	1.61 = Br
319	4 Br , 1 I	1.74 = Br
321	3 Br , 2 I	1.82 = I
348	4 I , 1 Bl	2.37 = Bl
367	5 I	1.60 = Br
419	4 I , 1 Bl	2.78 = Bl
421	3 I , 2 Bl	2.48 = Bl
487	5 Br	1.72 = I
652	4 I , 1 Bl	2.53 = Bl
653	4 Bl , 1 I	2.26 = I
726	3 I , 2 Br	1.50 = Br
847	4 I , 1 Bl	2.49 = Bl
853	4 I , 1 Br	1.62 = Br
916	3 I , 2 Br	2.61 = Bl
947	3 I , 2 Bl	2.71 = Bl

Table 3.9. Comparison of the number of correct predictions of the 22 samples that differed in visual and quantitative eye color classification. Visual indicates the number of samples where visual determination resulted in a correct prediction over the IMI classification. IMI indicates the number of samples where the IMI classification results in a correct prediction over the visual determination. No change indicates the number of samples where the difference in eye color classification did not result in a change in prediction.

Model	Threshold	Visual	IMI	No change
IrisPlex MLR	0.5	5	9	8
IrisPlex MLR	0.7	3	2	17
Adjusted MLR	0.5	4	6	12
Adjusted MLR	0.7	2	2	18
Equal BN	0.5	4	4	14
Equal BN	0.7	4	3	15
Adjusted BN	0.5	5	7	10
Adjusted BN	0.7	4	3	15

CHAPTER 4. CONCLUSIONS AND FUTURE CONSIDERATIONS

Eye color variation is a highly polygenic trait confirmed by GWAS studies in individuals of European descent [14] and the SNPs identified in the IrisPlex assay have proven to be useful for eye color predictions in European populations [8, 20, 30, 47]. However, the IrisPlex assay is shown to be only moderately predictive of eye color in a representative U.S. population due to the presumed population admixture compared to European population.

Our sample set had more inconclusive results as compared to the IrisPlex samples. This is likely due to the presence of intermediate samples. As previously mentioned, the rs12913832 SNP at the *HERC2* locus alone should explain most of the differences in phenotype expression between blue and brown eye color[19, 31]. At this SNP, in a homozygous allele state, TT is almost exclusively exhibited in brown eye phenotypes and CC exclusively in blue eye phenotypes. Most of our individuals (92%) were heterozygous (C/T) at the HERC2 SNP. Additional data support this hypothesis for the failure of prediction rates. For example, an additional study analyzed 60 samples of individuals with European-Asian background and the results showed that with higher levels of admixture, the predictions were less accurate [48]. Also, in evaluating IrisPlex across Europe, which included 3840 individuals from seven other European countries,

and with adjustments in the regression model parameters, blue-associated alleles were seen at some of the SNPs in brown-eyed Europeans [20].

In the developmental validation study of IrisPlex, subsets from the Human Genome Diversity Cell Line Panel (HGDP-CEPH), a large DNA database comprised of many populations, were used to show prediction accuracy applied to several populations [21], however, the eye color phenotypes were not available for genotyped samples. Therefore, even if a sample was determined to be 90% or greater for a certain eye color category, it may be a false positive as the actual phenotype is unknown. Our study looked at samples with known phenotypes, which offers strong empirical support that predictions are not always accurate given a high probability in any one color category.

Overall AUC measurements indicate the BN model of prediction performs better than the MLR model. Assessing the specificity and sensitivity, although the sensitivity is decreased, specificity is increased, so true negative predictions are more accurate. Also, likelihood ratios can be calculated from these Bayesian probabilities using the prior odds as described by Pośpiech [41]. Recently, Ruiz et al. reported success in using a modified online Bayesian classifier application, *Snipper*, to give such likelihood-based eye color predictions based on SNP allelic frequencies [35]. Still, as with the regression model, positive prediction inferences were not shown to be at an acceptable level for forensic application with a North American population, especially for the intermediate color category.

Objective color quantitation is comparably better to visual color determination which may be more effective in classification of eye color. One caveat of IMI is that the method depends on the specific sample set analyzed as the average luminosity and color

scale of all samples are used in deriving the single numerical value. Also, accounting for iris patterns could be further considered, especially the presence of a peripupillary ring. A study by Larsson et al. in 2011 describes SNP markers for identifying such patterns relating to variations in normal neuronal pattern development [49]. Incorporating these iris pattern SNPs may help reduce conflicting classifications. If using such a classification scheme, it may be possible to establish a reference database of group-specific SNP profiles associated with each eye color category with a large enough sample population. Using color components could also be further explored, possibly relating the SNP genotype with predicted color components instead of a discrete color category. Though considered in some studies without much success [41], further breakdown of color category discrimination of the intermediate colors should be explored (e.g., green and hazel instead of intermediate).

In order for the IrisPlex assay to be useful as a forensic tool in a North American population, additional SNPs must be developed and evaluated. Recently, three additional SNPs associated with the intermediate color especially were discovered and may be informative [14]. Eye color prediction is not the only forensically useful phenotype. Combining SNPs into one assay for inferring hair, skin, and eye color simultaneously would be ideal in developing a phenotypic profile of multiple traits based on DNA profiles. Recently Walsh et al. published a combined hair and eye color assay called HIrisPlex [50], however, its utility in a North American population should also be determined.

REFERENCES

REFERENCES

[1] R. Sturm, M. Larsson. Genetics of human iris colour and patterns. Pigment Cell Melanoma Research. 2009;22:544-62.

[2] G. Tully. Genotype versus phenotype: human pigmentation. Forensic Science International: Genetics. 2007;1:105-10.

[3] M. Kayser, P. de Knijff. Improving human forensics through advances in genetics, genomics and molecular biology. Nature Reviews Genetics. 2011;12:179-92.

[4] J.M. Butler. Genetics and genomics of core short tandem repeat loci used in human identity testing. Journal of Forensic Sciences. 2006;51:253-65.

[5] S. Aditya, A.K. Sharma, C.N. Bhattacharyya, K. Chaudhuri. Generating STR profile from “Touch DNA”. Journal of Forensic and Legal Medicine. 2011;18:295-8.

[6] R.K. Valenzuela, M.S. Henderson, M.H. Walsh, N.A. Garrison, J.T. Kelch, O. Cohen-Barak, D.T. Erickson, F. John Meaney, J. Bruce Walsh, K.C. Cheng, S. Ito, K. Wakamatsu, T. Frudakis, M. Thomas, M.H. Brilliant. Predicting phenotype from genotype: normal pigmentation. Journal of Forensic Sciences. 2010;55:315-22.

[7] M. Kayser, P. Schneider. DNA-based prediction of human externally visible characteristics in forensics: motivations, scientific challenges, and ethical considerations. Forensic Science International: Genetics. 2009;3:154-61.

[8] S. Walsh, F. Liu, K.N. Ballantyne, M. van Oven, O. Lao, M. Kayser. IrisPlex: a sensitive DNA tool for accurate prediction of blue and brown eye colour in the absence of ancestry information. Forensic Science International: Genetics. 2011;5:170-80.

[9] P. Sulem, D.F. Gudbjartsson, S.N. Stacey, A. Helgason, T. Rafnar, K.P. Magnusson, A. Manolescu, A. Karason, A. Palsson, G. Thorleifsson, M. Jakobsdottir, S. Steinberg, S. Pálsson, F. Jonasson, B. Sigurgeirsson, K. Thorisdottir, R. Ragnarsson, K.R. Benediktsdottir, K.K. Aben, L.A. Kiemeney, J.H. Olafsson, J. Gulcher, A. Kong, U. Thorsteinsdottir, K. Stefansson. Genetic determinants of hair, eye and skin pigmentation in Europeans. Nature Genetics. 2007;39:1443-52.

[10] T. Frudakis. Molecular Photofitting: Predicting Ancestry and Phenotype from DNA. 1 ed. Burlington, MA: Academic Press; 2008.

[11] R.A. Sturm. Molecular genetics of human pigmentation diversity. Human Molecular Genetics. 2009;18:R9-R17.

[12] T. Frudakis, M. Thomas, Z. Gaskin, K. Venkateswarlu, K.S. Chandra, S. Ginjupalli, S. Gunturi, S. Natrajan, V.K. Ponnuswamy, K.N. Ponnuswamy. Sequences associated with human iris pigmentation. Genetics. 2003;165:2071-83.

[13] E. Pośpiech, J. Draus-Barini, T. Kupiec, A. Wojas-Pelc, W. Branicki. Gene-gene interactions contribute to eye colour variation in humans. Journal of Human Genetics. 2011;56:447-55.

[14] F. Liu, A. Wollstein, P.G. Hysi, G.A. Ankra-Badu, T.D. Spector, D. Park, G. Zhu, M. Larsson, D.L. Duffy, G.W. Montgomery, D.A. Mackey, S. Walsh, O. Lao, A. Hofman, F. Rivadeneira, J.R. Vingerling, A.G. Uitterlinden, N.G. Martin, C.J. Hammond, M. Kayser. Digital quantification of human eye color highlights genetic association of three new loci. PLoS Genetics. 2010;6:e1000934.

[15] W. Branicki, U. Brudnik, A. Wojas-Pelc. Interactions between HERC2, OCA2 and MC1R may influence human pigmentation phenotype. Annals of Human Genetics. 2009;73:160-70.

[16] T. Frudakis, T. Terravainen, M. Thomas. Multilocus OCA2 genotypes specify human iris colors. Human Genetics. 2007;122:311-26.

[17] J.L. Han, P. Kraft, H. Nan, Q. Guo, C. Chen, A. Qureshi, S.E. Hankinson, F.B. Hu, D.L. Duffy, Z.Z. Zhao, N.G. Martin, G.W. Montgomery, N.K. Hayward, G. Thomas, R.N. Hoover, S. Chanock, D.J. Hunter. A genome-wide association study identifies novel alleles associated with hair color and skin pigmentation. PLoS Genetics. 2008;4:e1000074.

[18] J. Mengel-From, C. Børsting, J.J. Sanchez, H. Eiberg, N. Morling. Human eye colour and HERC2, OCA2, and MATP. Forensic Science International: Genetics. 2010;4:323-8.

[19] H. Eiberg, J. Troelsen, M. Nielsen, A. Mikkelsen, J. Mengel-From, K.W. Kjaer, L. Hansen. Blue eye color in humans may be caused by a perfectly associated founder mutation in a regulatory element located within the HERC2 gene inhibiting OCA2 expression. Human Genetics. 2008;123:177-87.

[20] S. Walsh, A. Wollstein, F. Liu, U. Chakravarthy, M. Rahu, J.H. Seland, G. Soubrane, L. Tomazzoli, F. Topouzis, J.R. Vingerling, J. Vioque, A.E. Fletcher, K.N. Ballantyne, M. Kayser. DNA-based eye colour prediction across Europe with the IrisPlex system. Forensic Science International: Genetics. 2012;6:330-40.

[21] S. Walsh, A. Lindenbergh, S. Zuniga S, T. Sijen, P. de Knijff, M. Kayser, K.N. Ballantyne. Developmental validation of the IrisPlex system: determination of blue and brown iris colour for forensic intelligence. Forensic Science International: Genetics. 2011;5:464-71.

[22] C.L. Wilkerson, N.A. Syed, M.R. Fisher, N.L. Robinson, I.H.L. Wallow, D.M. Albert. Melanocytes and Iris Color. Archives of Opthalmology. 1996;114:437-42.

[23] G. Prota, D.N. Hu, M.R. Vincensi, S.A. McCormick, A. Napolitano. Characterization of melanins in human irides and cultured uveal melanocytes from eyes of different colors. Experimental Eye Research. 1998;67:293-9.

[24] H.Y. Park, M. Kosmadaki, M. Yaar, B.A. Gilchrest. Cellular mechanisms regulating human melanogenesis. Cellular and Molecular Life Sciences. 2009;66:1493-506.

[25] K. Wakamatsu, R. Kavanagh, A.L. Kadekaro, S. Terzieva, R.A. Sturm, S. Leachman, Z. Abdel-Malek, S. Ito. Diversity of pigmentation in cultured human melanocytes is due to differences in the type as well as quantity of melanin. Pigment Cell Research. 2006;19:154-62.

[26] R.A. Sturm, T.N. Frudakis. Eye colour: portals into pigmentation genes and ancestry. Trends in Genetics. 2004;20:327-32.

[27] Z.A. Abdel-Malek, M.C. Scott, M. Furumura, M.L. Lamoreux, M. Ollmann, G.S. Barsh, V.J. Hearing. The melanocortin 1 receptor is the principal mediator of the effects of agouti signaling protein on mammalian melanocytes. Journal of Cell Science. 2001;114:1019-24.

[28] A. Pneuman, Z.M. Budimlija, T. Caragine, M. Prinz, E. Wurmbach. Verification of eye and skin color predictors in various populations. Legal Medicine. 2012;14:78-83.

[29] E. Lander, N.J. Schork. Genetic dissection of complex traits. Science. 1994;265:2037-48.

[30] F. Liu, FK. van Duijn, J. Vingerling, A. Hofman, A. Uitterlinden, A. Janssens, M. Kayser. Eye color and the prediction of complex phenotypes from genotypes. Current Biology. 2009;19:R192-R3.

[31] R.A. Sturm, D.L. Duffy, Z.Z. Zhao, F.P.N. Leite, M.S. Stark, N.K. Hayward, N.G. Martin, G.W. Montgomery. A single SNP in an evolutionary conserved region within intron 86 of the HERC2 gene determines human blue-brown eye color. The American Journal of Human Genetics. 2008;82:424-31.

[32] M. Visser, M. Kayser, R.J. Palstra. HERC2 rs12913832 modulates human pigmentation by attenuating chromatin-loop formation between a long-range enhancer and the OCA2 promoter. Genome Research. 2012;22:446-55.

[33] K. Kidd. ALFRED: The Allele Frequency Database. Yale University2012. http://alfred.med.yale.edu/. Date Accessed: August 2012

[34] D. Scherer, R. Kumar. Genetics of pigmentation in skin cancer--a review. Mutation Research. 2010;705:141-53.

[35] Y. Ruiz, C. Phillips, A. Gomez-Tato, J. Alvarez-Dios, M. Casares de Cal, R. Cruz, O. Maroñas, J. Söchtig, M. Fondevila, M.J. Rodriguez-Cid, Á. Carracedo, M.V. Lareu. Further development of forensic eye color predictive tests. Forensic Science International: Genetics. 2013;7:28-40.

[36] O. Spichenok, Z.M. Budimlija, A.A. Mitchell, A. Jenny, L. Kovacevic, D. Marjanovic, T. Caragine, M. Prinz, E. Wurmbach. Prediction of eye and skin color in diverse populations using seven SNPs. Forensic Science International: Genetics. 2011;5:472-8.

[37] M. Edwards, A. Gozdzik, K. Ross, J. Miles, E.J. Parra. Technical note: quantitative measures of iris color using high resolution photographs. American Journal of Physical Anthropology. 2012;147:141-9.

[38] O. Pourret, P. Naim, B. Marcot. Bayesian Networks: A Practical Guide to Applications. Hoboken, NJ: Wiley; 2008.

[39] D.W. Hosmer, S. Lemeshow. Applied Logistic Regression. 1st ed. New York: Wiley; 1989.

[40] J. M. Hilbe. Logistic Regression Models. Boca Raton, FL: Chapman & Hall/CRC Press; 2009.

[41] E. Pośpiech, J. Draus-Barini, T. Kupiec, A. Wojas-Pelc, W. Branicki. Prediction of eye color from genetic data using Bayesian approach. Journal of Forensic Sciences. 2012;57:880-6.

[42] G. Zadora, P. Wolańska-Nowak. Application of Bayesian networks in forensic genetics and criminalistics. Problems of Forensic Science. 2009;78:141-59.

[43] P. Sebastiani, T.T. Perls. Complex genetic models. Bayesian Networks: a practical guide to applications. Hoboken, NJ: Wiley; 2008.

[44] C. Aitken, F. Taroni. Statistics and the Evaluation of Evidence for Forensic Scientists. 2nd ed. Chichester, UK: Wiley; 2004.

[45] S.L. Morgan, E.G. Bartick. Discrimination of Forensic Analytical Chemical Data Using Multivariate Statistics. In: Blackledge RD, editor. Forensic Analysis on the Cutting Edge: New Methods for Trace Evidence Analysis. Hoboken, NJ: Wiley & Sons, Inc.; 2007.

[46] K. Hummel, J. Gerchow, E. Essen-Möller. Biomathematical evidence of paternity: Festschrift for Erik Essen-Möller. Berlin; New York, NY: Springer-Verlag; 1981.

[47] J. Purps, M. Geppert, M. Nagy, L. Roewer. Evaluation of the IrisPlex eye colour prediction tool in a German population sample. Forensic Science International: Genetics Supplement Series. 2011.

[48] P.R. Prestes, R.J. Mitchell, R. Daniel, K.N. Ballantyne, R.A.H. van Oorschot. Evaluation of the IrisPlex system in admixed individuals. Forensic Science International: Genetics Supplement Series. 2011;3:e283-e4.

[49] M. Larsson, D.L. Duffy, G. Zhu, J.Z. Liu, S. Macgregor, A.F. McRae, M.J. Wright, R.A. Sturm, D.A. Mackey, G.W. Montgomery, N.G. Martin, S.E. Medland. GWAS findings for human iris patterns: associations with variants in genes that influence normal neuronal pattern development. American Journal of Human Genetics. 2011;89:334-43.

[50] S. Walsh, F. Liu, A. Wollstein, L. Kovatsi, A. Ralf, A. Kosiniak-Kamysz, W. Branicki, M. Kayser. The HIrisPlex system for simultaneous prediction of hair and eye colour from DNA. Forensic Science International: Genetics. 2013;7:98-115.

PERMISSIONS

JOHN WILEY AND SONS LICENSE
TERMS AND CONDITIONS

This is a License Agreement between Gina Dembinski ("You") and John Wiley and Sons ("John Wiley and Sons") provided by Copyright Clearance Center ("CCC"). The license consists of your order details, the terms and conditions provided by John Wiley and Sons, and the payment terms and conditions.

All payments must be made in full to CCC. For payment instructions, please see information listed at the bottom of this form.

License Number	3120340750199
License date	Apr 01, 2013
Licensed content publisher	John Wiley and Sons
Licensed content publication	Pigment Cell & Melonoma Research
Licensed content title	Genetics of human iris colour and patterns
Licensed copyright line	Â© 2009 John Wiley & Sons A/S
Licensed content author	Richard A. Sturm,Mats Larsson
Licensed content date	Jul 8, 2009
Start page	544
End page	562
Type of use	Dissertation/Thesis
Requestor type	University/Academic
Format	Print and electronic
Portion	Figure/table
Number of figures/tables	1
Original Wiley figure/table number(s)	Figure 1. Human iris structure
Will you be translating?	No
Total	0.00 USD
Terms and Conditions	

TERMS AND CONDITIONS

This copyrighted material is owned by or exclusively licensed to John Wiley & Sons, Inc. or one of its group companies (each a "Wiley Company") or a society for whom a Wiley

Company has exclusive publishing rights in relation to a particular journal (collectively "WILEY"). By clicking "accept" in connection with completing this licensing transaction, you agree that the following terms and conditions apply to this transaction (along with the billing and payment terms and conditions established by the Copyright Clearance Center Inc., ("CCC's Billing and Payment terms and conditions"), at the time that you opened your RightsLink account (these are available at any time at http://myaccount.copyright.com).

Terms and Conditions

1. The materials you have requested permission to reproduce (the "Materials") are protected by copyright.

2. You are hereby granted a personal, non-exclusive, non-sublicensable, non-transferable, worldwide, limited license to reproduce the Materials for the purpose specified in the licensing process. This license is for a one-time use only with a maximum distribution equal to the number that you identified in the licensing process. Any form of republication granted by this license must be completed within two years of the date of the grant of this license (although copies prepared before may be distributed thereafter). The Materials shall not be used in any other manner or for any other purpose. Permission is granted subject to an appropriate acknowledgement given to the author, title of the material/book/journal and the publisher. You shall also duplicate the copyright notice that appears in the Wiley publication in your use of the Material. Permission is also granted on the understanding that nowhere in the text is a previously published source acknowledged for all or part of this Material. Any third party material is expressly excluded from this permission.

3. With respect to the Materials, all rights are reserved. Except as expressly granted by the terms of the license, no part of the Materials may be copied, modified, adapted (except for minor reformatting required by the new Publication), translated, reproduced, transferred or distributed, in any form or by any means, and no derivative works may be made based on the Materials without the prior permission of the respective copyright owner. You may not alter, remove or suppress in any manner any copyright, trademark or other notices displayed by the Materials. You may not license, rent, sell, loan, lease, pledge, offer as security, transfer or assign the Materials, or any of the rights granted to you hereunder to any other person.

4. The Materials and all of the intellectual property rights therein shall at all times remain the exclusive property of John Wiley & Sons Inc or one of its related companies (WILEY) or their respective licensors, and your interest therein is only that of having possession of and the right to reproduce the Materials pursuant to Section 2 herein during the continuance of this Agreement. You agree that you own no right, title or interest in or to the Materials or any of the intellectual property rights therein. You shall have no rights hereunder other than the license as provided for above in Section 2. No right, license or interest to any trademark, trade name, service mark or other branding ("Marks") of WILEY or its licensors is granted

hereunder, and you agree that you shall not assert any such right, license or interest with respect thereto.

5. NEITHER WILEY NOR ITS LICENSORS MAKES ANY WARRANTY OR REPRESENTATION OF ANY KIND TO YOU OR ANY THIRD PARTY, EXPRESS, IMPLIED OR STATUTORY, WITH RESPECT TO THE MATERIALS OR THE ACCURACY OF ANY INFORMATION CONTAINED IN THE MATERIALS, INCLUDING, WITHOUT LIMITATION, ANY IMPLIED WARRANTY OF MERCHANTABILITY, ACCURACY, SATISFACTORY QUALITY, FITNESS FOR A PARTICULAR PURPOSE, USABILITY, INTEGRATION OR NON-INFRINGEMENT AND ALL SUCH WARRANTIES ARE HEREBY EXCLUDED BY WILEY AND ITS LICENSORS AND WAIVED BY YOU.

6. WILEY shall have the right to terminate this Agreement immediately upon breach of this Agreement by you.

7. You shall indemnify, defend and hold harmless WILEY, its Licensors and their respective directors, officers, agents and employees, from and against any actual or threatened claims, demands, causes of action or proceedings arising from any breach of this Agreement by you.

8. IN NO EVENT SHALL WILEY OR ITS LICENSORS BE LIABLE TO YOU OR ANY OTHER PARTY OR ANY OTHER PERSON OR ENTITY FOR ANY SPECIAL, CONSEQUENTIAL, INCIDENTAL, INDIRECT, EXEMPLARY OR PUNITIVE DAMAGES, HOWEVER CAUSED, ARISING OUT OF OR IN CONNECTION WITH THE DOWNLOADING, PROVISIONING, VIEWING OR USE OF THE MATERIALS REGARDLESS OF THE FORM OF ACTION, WHETHER FOR BREACH OF CONTRACT, BREACH OF WARRANTY, TORT, NEGLIGENCE, INFRINGEMENT OR OTHERWISE (INCLUDING, WITHOUT LIMITATION, DAMAGES BASED ON LOSS OF PROFITS, DATA, FILES, USE, BUSINESS OPPORTUNITY OR CLAIMS OF THIRD PARTIES), AND WHETHER OR NOT THE PARTY HAS BEEN ADVISED OF THE POSSIBILITY OF SUCH DAMAGES. THIS LIMITATION SHALL APPLY NOTWITHSTANDING ANY FAILURE OF ESSENTIAL PURPOSE OF ANY LIMITED REMEDY PROVIDED HEREIN.

9. Should any provision of this Agreement be held by a court of competent jurisdiction to be illegal, invalid, or unenforceable, that provision shall be deemed amended to achieve as nearly as possible the same economic effect as the original provision, and the legality, validity and enforceability of the remaining provisions of this Agreement shall not be affected or impaired thereby.

10. The failure of either party to enforce any term or condition of this Agreement shall not constitute a waiver of either party's right to enforce each and every term and condition of this Agreement. No breach under this agreement shall be deemed waived or excused by either party unless such waiver or consent is in writing signed by the party granting such

waiver or consent. The waiver by or consent of a party to a breach of any provision of this Agreement shall not operate or be construed as a waiver of or consent to any other or subsequent breach by such other party.

11. This Agreement may not be assigned (including by operation of law or otherwise) by you without WILEY's prior written consent.

12. Any fee required for this permission shall be non-refundable after thirty (30) days from receipt

13. These terms and conditions together with CCC's Billing and Payment terms and conditions (which are incorporated herein) form the entire agreement between you and WILEY concerning this licensing transaction and (in the absence of fraud) supersedes all prior agreements and representations of the parties, oral or written. This Agreement may not be amended except in writing signed by both parties. This Agreement shall be binding upon and inure to the benefit of the parties' successors, legal representatives, and authorized assigns.

14. In the event of any conflict between your obligations established by these terms and conditions and those established by CCC's Billing and Payment terms and conditions, these terms and conditions shall prevail.

15. WILEY expressly reserves all rights not specifically granted in the combination of (i) the license details provided by you and accepted in the course of this licensing transaction, (ii) these terms and conditions and (iii) CCC's Billing and Payment terms and conditions.

16. This Agreement will be void if the Type of Use, Format, Circulation, or Requestor Type was misrepresented during the licensing process.

17. This Agreement shall be governed by and construed in accordance with the laws of the State of New York, USA, without regards to such state's conflict of law rules. Any legal action, suit or proceeding arising out of or relating to these Terms and Conditions or the breach thereof shall be instituted in a court of competent jurisdiction in New York County in the State of New York in the United States of America and each party hereby consents and submits to the personal jurisdiction of such court, waives any objection to venue in such court and consents to service of process by registered or certified mail, return receipt requested, at the last known address of such party.

Wiley Open Access Terms and Conditions

Wiley publishes Open Access articles in both its Wiley Open Access Journals program [http://www.wileyopenaccess.com/view/index.html] and as Online Open articles in its subscription journals. The majority of Wiley Open Access Journals have adopted the Creative Commons Attribution License (CC BY) which permits the unrestricted use, distribution, reproduction, adaptation and commercial exploitation of the article in any

medium. No permission is required to use the article in this way provided that the article is properly cited and other license terms are observed. A small number of Wiley Open Access journals have retained the Creative Commons Attribution Non Commercial License (CC BY-NC), which permits use, distribution and reproduction in any medium, provided the original work is properly cited and is not used for commercial purposes.

Online Open articles - Authors selecting Online Open are, unless particular exceptions apply, offered a choice of Creative Commons licenses. They may therefore select from the CC BY, the CC BY-NC and the Attribution-NoDerivatives (CC BY-NC-ND). The CC BY-NC-ND is more restrictive than the CC BY-NC as it does not permit adaptations or modifications without rights holder consent.

Wiley Open Access articles are protected by copyright and are posted to repositories and websites in accordance with the terms of the applicable Creative Commons license referenced on the article. At the time of deposit, Wiley Open Access articles include all changes made during peer review, copyediting, and publishing. Repositories and websites that host the article are responsible for incorporating any publisher-supplied amendments or retractions issued subsequently.
Wiley Open Access articles are also available without charge on Wiley's publishing platform, **Wiley Online Library** or any successor sites.

Conditions applicable to all Wiley Open Access articles:

- The authors' moral rights must not be compromised. These rights include the right of "paternity" (also known as "attribution" - the right for the author to be identified as such) and "integrity" (the right for the author not to have the work altered in such a way that the author's reputation or integrity may be damaged).

- Where content in the article is identified as belonging to a third party, it is the obligation of the user to ensure that any reuse complies with the copyright policies of the owner of that content.

- If article content is copied, downloaded or otherwise reused for research and other purposes as permitted, a link to the appropriate bibliographic citation (authors, journal, article title, volume, issue, page numbers, DOI and the link to the definitive published version on Wiley Online Library) should be maintained. Copyright notices and disclaimers must not be deleted.
    - Creative Commons licenses are copyright licenses and do not confer any other rights, including but not limited to trademark or patent rights.

- Any translations, for which a prior translation agreement with Wiley has not been agreed, must prominently display the statement: "This is an unofficial translation of

an article that appeared in a Wiley publication. The publisher has not endorsed this translation."

Conditions applicable to non-commercial licenses (CC BY-NC and CC BY-NC-ND)

For non-commercial and non-promotional purposes individual non-commercial users may access, download, copy, display and redistribute to colleagues Wiley Open Access articles. In addition, articles adopting the CC BY-NC may be adapted, translated, and text- and data-mined subject to the conditions above.

Use by commercial "for-profit" organizations

Use of non-commercial Wiley Open Access articles for commercial, promotional, or marketing purposes requires further explicit permission from Wiley and will be subject to a fee. Commercial purposes include:

- Copying or downloading of articles, or linking to such articles for further redistribution, sale or licensing;
- Copying, downloading or posting by a site or service that incorporates advertising with such content;
- The inclusion or incorporation of article content in other works or services (other than normal quotations with an appropriate citation) that is then available for sale or licensing, for a fee (for example, a compilation produced for marketing purposes, inclusion in a sales pack)
- Use of article content (other than normal quotations with appropriate citation) by for-profit organizations for promotional purposes
- Linking to article content in e-mails redistributed for promotional, marketing or educational purposes;
- Use for the purposes of monetary reward by means of sale, resale, license, loan, transfer or other form of commercial exploitation such as marketing products
- Print reprints of Wiley Open Access articles can be purchased from: corporatesales@wiley.com

  The modification or adaptation for any purpose of an article referencing the CC BY-NC-ND License requires consent which can be requested from RightsLink@wiley.com .

Other Terms and Conditions:

BY CLICKING ON THE "I AGREE..." BOX, YOU ACKNOWLEDGE THAT YOU HAVE READ AND FULLY UNDERSTAND EACH OF THE SECTIONS OF AND PROVISIONS SET FORTH IN THIS AGREEMENT AND THAT YOU ARE IN AGREEMENT WITH AND ARE WILLING TO ACCEPT ALL OF YOUR OBLIGATIONS AS SET FORTH IN THIS AGREEMENT.

v1.8

If you would like to pay for this license now, please remit this license along with your payment made payable to "COPYRIGHT CLEARANCE CENTER" otherwise you will be invoiced within 48 hours of the license date. Payment should be in the form of a check or money order referencing your account number and this invoice number 500989678. Once you receive your invoice for this order, you may pay your invoice by credit card. Please follow instructions provided at that time.

Make Payment To:
Copyright Clearance Center
Dept 001
P.O. Box 843006
Boston, MA 02284-3006

For suggestions or comments regarding this order, contact RightsLink Customer Support: customercare@copyright.com or +1-877-622-5543 (toll free in the US) or +1-978-646-2777.

Gratis licenses (referencing $0 in the Total field) are free. Please retain this printable license for your reference. No payment is required.

APPENDICES

Appendix A. SNP Genotype Profiles and Eye Color Classification

The shaded cells are the 22 samples that disagreed between visual and IMI color classification. The boxed samples are the 100 random samples used for the model building.

Sample	HE	OCA2	SLC24A4	SLC45A2	TYR	IR	Visual Color	IMI	IMI Color
719	CT	CC	GG	GC	CC	GG	Br	1.25	Br
264	CT	CC	GG	GG	CC	GG	Br	1.26	Br
983	CT	CC	GT	GG	CT	GG	Br	1.26	Br
194	CT	CC	GT	GG	TT	GG	Br	1.27	Br
283	CT	CC	GG	GC	CC	GG	Br	1.28	Br
639	CT	CC	GT	GC	CT	GG	Br	1.28	Br
185	CT	CC	GG	GG	CT	GG	Br	1.30	Br
193	CT	CT	TT	GG	CT	GG	Br	1.30	Br
281	CT	CC	GG	GG	CT	GG	Br	1.30	Br
571	CT	CC	GT	GG	CC	GG	Br	1.32	Br
720	CT	CC	GT	GG	CC	GG	Br	1.32	Br
930	CT	CC	GT	GG	CC	GG	Br	1.32	Br
516	CT	CC	GT	GG	CT	GG	Br	1.33	Br
202	CT	CT	GT	CC	CC	GG	Br	1.36	Br
296	TT	CC	GG	GC	CC	GG	Br	1.37	Br
271	CT	CC	GT	GG	CT	GG	Br	1.38	Br
812	CT	CC	GG	GC	CC	GG	Br	1.38	Br
785	CT	CC	GG	GG	CC	GG	Br	1.39	Br
965	CC	CC	TT	GG	CT	GG	Br	1.39	Br
125	CT	CC	GG	GC	CT	GG	Br	1.40	Br
578	TT	CC	GG	GG	CC	GG	Br	1.40	Br
957	TT	CC	GT	GC	CC	GG	Br	1.40	Br
161	TT	CC	GG	CC	CC	GG	Br	1.41	Br
163	CT	CC	GG	GG	CT	GG	Br	1.41	Br
519	CT	CC	TT	GG	CC	GG	Br	1.41	Br
756	CT	CC	GG	GG	CC	GG	Br	1.41	Br
529	CT	CC	GG	GG	CT	GG	Br	1.42	Br
143	CT	CT	GT	GG	CT	GG	Br	1.43	Br
584	CT	CC	GG	GG	CC	GG	Br	1.43	Br
742	CT	CC	GT	GG	CT	GG	Br	1.43	Br
269	CT	CC	GT	GG	CT	GG	Br	1.44	Br

372	CT	CC	GT	GG	CT	GG	Br	1.45	Br
528	CT	CC	GT	GG	CT	GG	Br	1.45	Br
634	CT	CC	GG	GG	TT	GG	Br	1.45	Br
751	CT	CC	GG	GG	CC	GG	Br	1.46	Br
791	CT	CC	GT	GG	CC	GG	Br	1.46	Br
286	CT	CC	GG	GC	CC	GG	Br	1.47	Br
300	CT	CC	GG	GC	CC	GG	Br	1.47	Br
328	CT	CC	GT	GG	CT	GG	Br	1.47	Br
378	CT	CC	GT	GC	CT	GG	Br	1.47	Br
120	CT	CC	GG	GG	CT	GG	Br	1.48	Br
217	CT	CC	GT	GG	CT	GG	Br	1.48	Br
265	CT	CC	GG	GG	CC	GG	Br	1.48	Br
741	CT	CC	GG	GG	CT	GG	Br	1.48	Br
692	CT	CC	GT	GG	CC	GG	Br	1.49	Br
752	CT	CC	GG	GC	CC	GG	Br	1.49	Br
181	CT	CT	GG	GC	CC	GG	Br	1.50	Br
726	CT	CC	GT	GG	CC	GA	I	1.50	Br
232	CT	CC	GT	GG	CT	GG	Br	1.51	Br
451	CT	CC	GT	GC	CC	GG	Br	1.51	Br
753	TT	CC	GG	CC	CC	GG	Br	1.53	Br
825	TT	CC	GG	GG	CC	GG	Br	1.54	Br
948	CT	CC	GG	GG	CT	GG	Br	1.54	Br
374	CT	CC	GT	GG	CT	GA	Br	1.55	Br
695	CT	CC	GT	GG	CC	GG	Br	1.55	Br
657	CT	CT	GT	GG	CT	GG	Br	1.56	Br
298	TT	CC	GG	GC	CC	GA	Br	1.57	Br
531	CT	CT	GG	GC	CC	GG	Br	1.57	Br
273	CT	CC	GT	GG	CC	GG	I	1.58	Br
975	CT	CC	GT	GG	CC	GA	Br	1.58	Br
219	CT	CC	GT	GG	TT	GG	I	1.60	Br
367	CT	CC	GG	GG	CC	GG	I	1.60	Br
492	CT	CT	GT	GG	CT	GG	Br	1.60	Br
932	CT	CC	TT	GG	CC	GG	Br	1.60	Br
313	CT	CC	TT	GG	CT	GG	I	1.61	Br
916	CT	CC	GG	GG	CC	GA	I	1.61	Br
853	CT	CC	GG	GG	CT	GG	I	1.62	Br

873	CT	CC	GT	GG	CC	GG	Br	1.62	Br
176	CT	CC	GG	GC	CC	GG	Br	1.63	Br
396	CT	CC	GG	GC	CC	GG	Br	1.63	Br
845	CT	CC	GT	GC	CT	GA	Br	1.64	Br
124	CT	CC	GT	GG	CT	GG	I	1.65	Br
231	CT	CC	GT	GG	CC	GG	I	1.67	I
200	CT	CC	TT	GG	CT	GG	I	1.68	I
233	CT	CC	GG	GG	CC	GG	I	1.68	I
412	CT	CC	GT	GG	CC	GG	I	1.68	I
943	CT	CC	GT	GG	CC	GG	I	1.69	I
279	CT	CC	GT	GG	TT	GG	Br	1.70	I
856	CT	CC	GG	GG	TT	GG	I	1.71	I
487	TT	CC	GG	CC	CC	GG	Br	1.72	I
672	TT	CT	GG	GG	CT	GG	I	1.72	I
700	CT	CC	GT	GG	CT	GG	I	1.72	I
197	CT	CC	GT	GG	CT	GG	I	1.74	I
319	CT	CC	GG	GG	CT	GG	Br	1.74	I
121	CT	CC	GG	GG	CC	GG	I	1.76	I
852	CT	CT	GT	GC	CT	GA	I	1.77	I
765	CT	CC	GG	GG	CC	GG	I	1.79	I
869	CT	CT	GT	GG	CC	GG	I	1.81	I
321	CT	CC	GT	GG	CC	GG	Br	1.82	I
368	CT	CC	GG	GG	CC	GG	I	1.85	I
862	CT	CT	GG	GG	CC	GA	I	1.85	I
354	CT	CT	GT	GG	CC	GG	I	1.87	I
186	CT	CT	GT	GG	CT	GG	I	1.89	I
259	CT	CC	GT	GG	CT	GG	I	1.91	I
537	CT	CC	GT	GG	TT	GG	I	1.91	I
135	CT	CC	GT	GG	CT	GG	I	1.95	I
254	CT	CC	GT	GG	CC	GA	I	1.96	I
658	CT	CT	GG	GG	CT	GG	I	1.96	I
538	CT	CC	GG	GG	TT	GG	I	2.00	I
388	CT	CT	GT	GG	CT	GG	I	2.01	I
839	CT	CT	GT	GG	CT	GG	I	2.06	I
823	CT	CC	GT	GG	CC	GA	I	2.09	I
297	CT	CC	GG	GG	CT	GA	I	2.10	I
512	CT	CT	GG	GG	CC	GG	I	2.10	I

182	CC	CC	GT	GC	CC	GG	I	2.12	I
991	CT	CC	GT	GG	TT	GG	I	2.18	I
645	CT	CC	GT	GC	CC	GG	I	2.19	I
536	CT	CC	GT	GG	TT	GG	I	2.23	I
758	CT	CC	GT	GG	CC	GG	I	2.23	I
735	CT	CC	GT	GG	CT	GA	I	2.24	I
170	CT	CC	TT	GG	CT	GG	Bl	2.26	I
653	CC	CC	GG	GG	CC	GG	Bl	2.26	I
196	CT	CC	TT	GG	CC	GG	I	2.28	I
763	CT	CC	GG	GG	CC	GG	I	2.30	I
256	CT	CC	TT	GG	CC	GG	Bl	2.31	I
518	CT	CC	GT	GG	CC	GG	I	2.31	I
327	CT	CC	GG	GG	CT	GG	Bl	2.33	Bl
369	CT	CC	GT	GG	CT	GG	Bl	2.33	Bl
362	CT	CC	GG	GG	CC	GG	Bl	2.36	Bl
968	CC	CC	GG	GG	CC	GG	Bl	2.36	Bl
168	CT	CC	TT	GG	CT	GG	I	2.37	Bl
348	CT	CC	GG	GG	CT	GG	I	2.37	Bl
917	CT	CC	GT	GG	CC	GG	Bl	2.39	Bl
678	CT	CT	TT	GG	CT	GA	Bl	2.41	Bl
306	CT	CC	GT	GG	CC	GA	Bl	2.42	Bl
951	CT	CC	TT	GG	CT	GG	Bl	2.43	Bl
187	CT	CC	GG	GG	CC	GG	Bl	2.46	Bl
586	CT	CC	GT	GG	CT	GG	Bl	2.46	Bl
421	CT	CC	GT	GG	TT	GG	I	2.48	Bl
724	CT	CC	GT	GG	CT	GG	Bl	2.48	Bl
893	CT	CC	GT	GG	CT	GG	Bl	2.48	Bl
133	CT	CC	TT	GG	CC	GA	Bl	2.49	Bl
847	CT	CC	GT	GG	CT	GG	I	2.49	Br
123	CT	CC	GT	GG	TT	GG	Bl	2.51	Bl
270	CT	CC	GT	GG	CT	GA	Bl	2.51	Bl
149	CT	CC	GT	GG	TT	GG	Bl	2.52	Bl
275	CT	CC	GG	GG	TT	GG	Bl	2.52	Bl
569	CT	CC	GT	GG	TT	GG	Bl	2.52	Bl
746	CT	CC	GG	GG	TT	GA	Bl	2.52	Bl
239	CT	CC	GT	GG	CT	GG	Bl	2.53	Bl
652	CT	CC	GG	GG	CC	GA	I	2.53	Bl

723	CC	CT	GG	GG	CT	AA	Bl	2.53	Bl
157	CT	CC	GT	GG	CC	GA	Bl	2.54	Bl
574	CT	CT	GG	GG	CC	GA	Bl	2.55	Bl
879	CT	CC	GT	GG	CC	GG	Bl	2.55	Bl
351	CT	CC	GG	GG	CT	GA	Bl	2.58	Bl
579	CT	CC	GT	GG	TT	GG	Bl	2.58	Bl
749	CT	CC	TT	GG	CT	GA	Bl	2.59	Bl
122	CT	CC	GT	GG	CC	GG	Bl	2.61	Bl
145	CT	CC	GT	GG	CT	GA	Bl	2.61	Bl
377	CT	CC	TT	GG	CC	GG	Bl	2.61	Bl
857	CT	CC	GT	GG	CC	GG	Bl	2.61	Bl
160	CT	CC	GT	GG	CT	GG	Bl	2.62	Bl
234	CT	CT	GT	GG	CT	GG	Bl	2.62	Bl
364	CT	CC	GT	GG	TT	GA	Bl	2.62	Bl
867	CT	CC	GT	GG	TT	GG	Bl	2.63	Bl
539	CT	CC	GT	GG	CT	GG	Bl	2.64	Bl
768	CT	CT	GG	GG	CT	GA	Bl	2.64	Bl
827	CT	CC	GT	GG	CT	GG	Bl	2.64	Bl
268	CT	CC	GT	GG	CT	GA	Bl	2.65	Bl
305	CT	CC	GT	GG	CC	GA	Bl	2.66	Bl
673	CT	CT	GG	GG	TT	GG	Bl	2.66	Bl
278	CT	CT	TT	GG	CT	GG	Bl	2.67	Bl
987	CT	CC	GT	GG	CC	GG	Bl	2.68	Bl
453	CT	CC	GT	GG	CT	GG	Bl	2.69	Bl
698	CT	CC	GG	GG	CC	GG	Bl	2.69	Bl
612	CT	CC	GT	GG	CT	GA	Bl	2.70	Bl
625	CT	CC	GT	GG	CC	GG	Bl	2.70	Bl
834	CT	CC	GT	GG	TT	GG	Bl	2.71	Bl
947	CT	CC	GT	GG	TT	GG	I	2.71	Bl
276	CT	CC	GT	GG	CT	GG	Bl	2.73	Bl
457	CT	CC	GT	GG	CC	GG	Bl	2.73	Bl
318	CT	CC	GT	GG	CC	GG	Bl	2.74	Bl
826	CC	CT	GT	GG	TT	GA	Bl	2.75	Bl
128	CC	CC	GG	GG	CT	GG	Bl	2.76	Bl
260	CT	CC	GG	GG	CT	GG	Bl	2.77	Bl
419	CT	CC	GT	GG	CC	GG	I	2.78	Bl

986	CT	CC	TT	GG	CC	GG	Bl	2.78	Bl
165	CT	CC	GG	GG	CT	GG	Bl	2.79	Bl
137	CT	CC	GT	GG	TT	GG	Bl	2.80	Bl
172	CT	CC	GT	GG	CT	GG	Bl	2.82	Bl
134	CT	CC	GT	GG	TT	GG	Bl	2.83	Bl
147	CT	CC	TT	GG	CT	GG	Bl	2.84	Bl
285	CT	CC	GT	GG	CT	GG	Bl	2.85	Bl
458	CT	CC	TT	GG	CT	GG	Bl	2.85	Bl
769	CT	CC	TT	GG	CC	GG	Bl	2.90	Bl
927	CT	CC	GG	GG	CC	GG	Bl	2.91	Bl
945	CT	CC	GT	GG	CT	GA	Bl	2.92	Bl
148	CT	CC	TT	GG	CT	GA	Bl	2.95	Bl
169	CT	CT	TT	GG	CT	GG	Bl	2.96	Bl
936	CT	CC	GG	GG	TT	GG	Bl	2.97	Bl
184	CT	CC	GT	GG	TT	GG	Bl	2.99	Bl
851	CT	CC	GT	GG	TT	GG	Bl	2.99	Bl
152	CT	CC	GT	GG	CT	GG	Bl	3.00	Bl
251	CT	CC	GT	GG	CT	GA	Bl	3.02	Bl
796	CT	CC	TT	GG	CC	GA	Bl	3.05	Bl
132	CT	CC	GT	GG	TT	GG	Bl	3.06	Bl
498	CT	CC	TT	GG	CT	GA	Bl	3.10	Bl
250	CT	CC	GG	GG	CT	GG	Bl	3.11	Bl
728	CT	CC	GT	GG	TT	GG	Bl	3.17	Bl

Appendix B. MLR Prediction Probabilities

			IrisPlex Predictions			Adjusted Predictions		
Sample	IMI	IMI Color	**Blue**	**Int**	**Brown**	Blue	Int	Brown
719	1.25	Br	0.024	0.083	0.892	0.000	0.130	0.870
264	1.26	Br	0.094	0.148	0.758	0.143	0.295	0.562
983	1.26	Br	0.207	0.161	0.632	0.467	0.120	0.413
194	1.27	Br	0.277	0.179	0.543	0.719	0.073	0.208
283	1.28	Br	0.024	0.083	0.892	0.000	0.130	0.870
639	1.28	Br	0.060	0.102	0.838	0.000	0.076	0.924
193	1.30	Br	0.503	0.211	0.286	0.579	0.205	0.217
185	1.30	Br	0.134	0.175	0.691	0.323	0.261	0.415
281	1.30	Br	0.134	0.175	0.691	0.323	0.261	0.415
571	1.32	Br	0.150	0.140	0.711	0.229	0.150	0.621
930	1.32	Br	0.150	0.140	0.711	0.229	0.150	0.621
720	1.32	Br	0.150	0.140	0.711	0.229	0.150	0.621
516	1.33	Br	0.207	0.161	0.632	0.467	0.120	0.413
202	1.36	Br	0.027	0.111	0.861	0.000	0.121	0.879
296	1.37	Br	0.000	0.013	0.987	0.000	0.174	0.826
271	1.38	Br	0.207	0.161	0.632	0.467	0.120	0.413
812	1.38	Br	0.024	0.083	0.892	0.000	0.130	0.870
965	1.39	Br	0.962	0.025	0.013	1.000	0.000	0.000
785	1.39	Br	0.094	0.148	0.758	0.143	0.295	0.562
957	1.40	Br	0.000	0.013	0.987	0.000	0.089	0.911
125	1.40	Br	0.036	0.104	0.860	0.000	0.152	0.848
578	1.40	Br	0.001	0.026	0.973	0.000	0.426	0.574
163	1.41	Br	0.134	0.175	0.691	0.323	0.261	0.415
519	1.41	Br	0.229	0.128	0.643	0.325	0.068	0.607
756	1.41	Br	0.094	0.148	0.758	0.143	0.295	0.562
161	1.41	Br	0.000	0.006	0.994	0.000	0.056	0.944
529	1.42	Br	0.134	0.175	0.691	0.323	0.261	0.415

742	1.43	Br	0.207	0.161	0.632	0.467	0.120	0.413
143	1.43	Br	0.375	0.264	0.361	0.376	0.419	0.205
584	1.43	Br	0.094	0.148	0.758	0.143	0.295	0.562
269	1.44	Br	0.207	0.161	0.632	0.467	0.120	0.413
634	1.45	Br	0.185	0.201	0.614	0.575	0.183	0.242
528	1.45	Br	0.207	0.161	0.632	0.467	0.120	0.413
372	1.45	Br	0.207	0.161	0.632	0.467	0.120	0.413
751	1.46	Br	0.094	0.148	0.758	0.143	0.295	0.562
791	1.46	Br	0.150	0.140	0.711	0.229	0.150	0.621
328	1.47	Br	0.207	0.161	0.632	0.467	0.120	0.413
286	1.47	Br	0.024	0.083	0.892	0.000	0.130	0.870
300	1.47	Br	0.024	0.083	0.892	0.000	0.130	0.870
378	1.47	Br	0.060	0.102	0.838	0.000	0.076	0.924
265	1.48	Br	0.094	0.148	0.758	0.143	0.295	0.562
120	1.48	Br	0.134	0.175	0.691	0.323	0.261	0.415
741	1.48	Br	0.134	0.175	0.691	0.323	0.261	0.415
217	1.48	Br	0.207	0.161	0.632	0.467	0.120	0.413
752	1.49	Br	0.024	0.083	0.892	0.000	0.130	0.870
692	1.49	Br	0.150	0.140	0.711	0.229	0.150	0.621
181	1.50	Br	0.063	0.198	0.739	0.000	0.512	0.488
726	1.50	Br	0.215	0.221	0.564	0.709	0.083	0.208
232	1.51	Br	0.207	0.161	0.632	0.467	0.120	0.413
451	1.51	Br	0.040	0.083	0.877	0.000	0.064	0.936
753	1.53	Br	0.000	0.006	0.994	0.000	0.056	0.944
825	1.54	Br	0.001	0.026	0.973	0.000	0.426	0.574
948	1.54	Br	0.134	0.175	0.691	0.323	0.261	0.415
374	1.55	Br	0.283	0.241	0.476	0.876	0.040	0.084
695	1.55	Br	0.150	0.140	0.711	0.229	0.150	0.621
657	1.56	Br	0.375	0.264	0.361	0.376	0.419	0.205
298	1.57	Br	0.000	0.025	0.975	0.000	0.260	0.740

531	1.57	Br	0.063	0.198	0.739	0.000	0.512	0.488
975	1.58	Br	0.215	0.221	0.564	0.709	0.083	0.208
273	1.58	Br	0.150	0.140	0.711	0.229	0.150	0.621
932	1.60	Br	0.229	0.128	0.643	0.325	0.068	0.607
219	1.60	Br	0.277	0.179	0.543	0.719	0.073	0.208
492	1.60	Br	0.375	0.264	0.361	0.376	0.419	0.205
367	1.60	Br	0.094	0.148	0.758	0.143	0.295	0.562
313	1.61	Br	0.306	0.142	0.552	0.591	0.048	0.361
916	1.61	Br	0.140	0.241	0.620	0.557	0.206	0.237
873	1.62	Br	0.150	0.140	0.711	0.229	0.150	0.621
853	1.62	Br	0.134	0.175	0.691	0.323	0.261	0.415
396	1.63	Br	0.024	0.083	0.892	0.000	0.130	0.870
176	1.63	Br	0.024	0.083	0.892	0.000	0.130	0.870
845	1.64	Br	0.094	0.177	0.729	0.000	0.121	0.879
124	1.65	Br	0.207	0.161	0.632	0.467	0.120	0.413
231	1.67	I	0.150	0.140	0.711	0.229	0.150	0.621
412	1.68	I	0.150	0.140	0.711	0.229	0.150	0.621
233	1.68	I	0.094	0.148	0.758	0.143	0.295	0.562
200	1.68	I	0.306	0.142	0.552	0.591	0.048	0.361
943	1.69	I	0.150	0.140	0.711	0.229	0.150	0.621
279	1.70	I	0.277	0.179	0.543	0.719	0.073	0.208
856	1.71	I	0.185	0.201	0.614	0.575	0.183	0.242
672	1.72	I	0.004	0.090	0.906	0.000	0.863	0.137
700	1.72	I	0.207	0.161	0.632	0.467	0.120	0.413
487	1.72	I	0.000	0.006	0.994	0.000	0.056	0.944
197	1.74	I	0.207	0.161	0.632	0.467	0.120	0.413
319	1.74	I	0.134	0.175	0.691	0.323	0.261	0.415
121	1.76	I	0.094	0.148	0.758	0.143	0.295	0.562
852	1.77	I	0.195	0.330	0.475	0.000	0.492	0.508
765	1.79	I	0.094	0.148	0.758	0.143	0.295	0.562

869	1.81	I	0.299	0.253	0.448	0.182	0.515	0.303
321	1.82	I	0.150	0.140	0.711	0.229	0.150	0.621
862	1.85	I	0.253	0.393	0.354	0.349	0.560	0.091
368	1.85	I	0.094	0.148	0.758	0.143	0.295	0.562
354	1.87	I	0.299	0.253	0.448	0.182	0.515	0.303
186	1.89	I	0.375	0.264	0.361	0.376	0.419	0.205
537	1.91	I	0.277	0.179	0.543	0.719	0.073	0.208
259	1.91	I	0.207	0.161	0.632	0.467	0.120	0.413
135	1.95	I	0.207	0.161	0.632	0.467	0.120	0.413
254	1.96	I	0.215	0.221	0.564	0.709	0.083	0.208
658	1.96	I	0.263	0.310	0.427	0.189	0.662	0.149
538	2.00	I	0.185	0.201	0.614	0.575	0.183	0.242
388	2.01	I	0.375	0.264	0.361	0.376	0.419	0.205
839	2.06	I	0.375	0.264	0.361	0.376	0.419	0.205
823	2.09	I	0.215	0.221	0.564	0.709	0.083	0.208
512	2.10	I	0.202	0.286	0.512	0.081	0.723	0.196
297	2.10	I	0.190	0.271	0.539	0.779	0.113	0.108
182	2.12	I	0.780	0.090	0.130	0.105	0.041	0.854
991	2.18	I	0.277	0.179	0.543	0.719	0.073	0.208
645	2.19	I	0.040	0.083	0.877	0.000	0.064	0.936
536	2.23	I	0.277	0.179	0.543	0.719	0.073	0.208
758	2.23	I	0.150	0.140	0.711	0.229	0.150	0.621
735	2.24	I	0.283	0.241	0.476	0.876	0.040	0.084
653	2.26	I	0.870	0.076	0.053	0.999	0.000	0.001
170	2.26	I	0.306	0.142	0.552	0.591	0.048	0.361
196	2.28	I	0.229	0.128	0.643	0.325	0.068	0.607
763	2.30	I	0.094	0.148	0.758	0.143	0.295	0.562
518	2.31	I	0.150	0.140	0.711	0.229	0.150	0.621
256	2.31	I	0.229	0.128	0.643	0.325	0.068	0.607
327	2.33	Bl	0.134	0.175	0.691	0.323	0.261	0.415

369	2.33	Bl	0.207	0.161	0.632	0.467	0.120	0.413
362	2.36	Bl	0.094	0.148	0.758	0.143	0.295	0.562
968	2.36	Bl	0.870	0.076	0.053	0.999	0.000	0.001
168	2.37	Bl	0.306	0.142	0.552	0.591	0.048	0.361
348	2.37	Bl	0.134	0.175	0.691	0.323	0.261	0.415
917	2.39	Bl	0.150	0.140	0.711	0.229	0.150	0.621
678	2.41	Bl	0.564	0.259	0.177	0.906	0.058	0.037
306	2.42	Bl	0.215	0.221	0.564	0.709	0.083	0.208
951	2.43	Bl	0.306	0.142	0.552	0.591	0.048	0.361
586	2.46	Bl	0.207	0.161	0.632	0.467	0.120	0.413
187	2.46	Bl	0.094	0.148	0.758	0.143	0.295	0.562
724	2.48	Bl	0.207	0.161	0.632	0.467	0.120	0.413
893	2.48	Bl	0.207	0.161	0.632	0.467	0.120	0.413
421	2.48	Bl	0.277	0.179	0.543	0.719	0.073	0.208
133	2.49	Bl	0.317	0.193	0.490	0.807	0.030	0.163
847	2.49	Bl	0.207	0.161	0.632	0.467	0.120	0.413
270	2.51	Bl	0.283	0.241	0.476	0.876	0.040	0.084
123	2.51	Bl	0.277	0.179	0.543	0.719	0.073	0.208
149	2.52	Bl	0.277	0.179	0.543	0.719	0.073	0.208
569	2.52	Bl	0.277	0.179	0.543	0.719	0.073	0.208
275	2.52	Bl	0.185	0.201	0.614	0.575	0.183	0.242
746	2.52	Bl	0.249	0.296	0.455	0.907	0.052	0.041
239	2.53	Bl	0.207	0.161	0.632	0.467	0.120	0.413
723	2.53	Bl	0.927	0.061	0.012	1.000	0.000	0.000
652	2.53	Bl	0.140	0.241	0.620	0.557	0.206	0.237
157	2.54	Bl	0.215	0.221	0.564	0.709	0.083	0.208
879	2.55	Bl	0.150	0.140	0.711	0.229	0.150	0.621
574	2.55	Bl	0.253	0.393	0.354	0.349	0.560	0.091
351	2.58	Bl	0.190	0.271	0.539	0.779	0.113	0.108
579	2.58	Bl	0.277	0.179	0.543	0.719	0.073	0.208

749	2.59	Bl	0.400	0.203	0.397	0.925	0.014	0.061
145	2.61	Bl	0.283	0.241	0.476	0.876	0.040	0.084
377	2.61	Bl	0.229	0.128	0.643	0.325	0.068	0.607
857	2.61	Bl	0.150	0.140	0.711	0.229	0.150	0.621
122	2.61	Bl	0.150	0.140	0.711	0.229	0.150	0.621
364	2.62	Bl	0.359	0.254	0.387	0.953	0.017	0.030
234	2.62	Bl	0.375	0.264	0.361	0.376	0.419	0.205
160	2.62	Bl	0.207	0.161	0.632	0.467	0.120	0.413
867	2.63	Bl	0.277	0.179	0.543	0.719	0.073	0.208
539	2.64	Bl	0.207	0.161	0.632	0.467	0.120	0.413
827	2.64	Bl	0.207	0.161	0.632	0.467	0.120	0.413
768	2.64	Bl	0.314	0.405	0.281	0.583	0.367	0.050
268	2.65	Bl	0.283	0.241	0.476	0.876	0.040	0.084
305	2.66	Bl	0.215	0.221	0.564	0.709	0.083	0.208
673	2.66	Bl	0.331	0.324	0.345	0.380	0.522	0.098
278	2.67	Bl	0.503	0.211	0.286	0.579	0.205	0.217
987	2.68	Bl	0.150	0.140	0.711	0.229	0.150	0.621
698	2.69	Bl	0.094	0.148	0.758	0.143	0.295	0.562
453	2.69	Bl	0.207	0.161	0.632	0.467	0.120	0.413
612	2.70	Bl	0.283	0.241	0.476	0.876	0.040	0.084
625	2.70	Bl	0.150	0.140	0.711	0.229	0.150	0.621
834	2.71	Bl	0.277	0.179	0.543	0.719	0.073	0.208
947	2.71	Bl	0.277	0.179	0.543	0.719	0.073	0.208
276	2.73	Bl	0.207	0.161	0.632	0.467	0.120	0.413
457	2.73	Bl	0.150	0.140	0.711	0.229	0.150	0.621
318	2.74	Bl	0.150	0.140	0.711	0.229	0.150	0.621
826	2.75	Bl	0.963	0.035	0.003	1.000	0.000	0.000
128	2.76	Bl	0.899	0.066	0.035	1.000	0.000	0.000
260	2.77	Bl	0.134	0.175	0.691	0.323	0.261	0.415
419	2.78	Bl	0.150	0.140	0.711	0.229	0.150	0.621

986	2.78	Bl	0.229	0.128	0.643	0.325	0.068	0.607
165	2.79	Bl	0.134	0.175	0.691	0.323	0.261	0.415
137	2.80	Bl	0.277	0.179	0.543	0.719	0.073	0.208
172	2.82	Bl	0.207	0.161	0.632	0.467	0.120	0.413
134	2.83	Bl	0.277	0.179	0.543	0.719	0.073	0.208
147	2.84	Bl	0.306	0.142	0.552	0.591	0.048	0.361
458	2.85	Bl	0.306	0.142	0.552	0.591	0.048	0.361
285	2.85	Bl	0.207	0.161	0.632	0.467	0.120	0.413
769	2.90	Bl	0.229	0.128	0.643	0.325	0.068	0.607
927	2.91	Bl	0.094	0.148	0.758	0.143	0.295	0.562
945	2.92	Bl	0.283	0.241	0.476	0.876	0.040	0.084
148	2.95	Bl	0.400	0.203	0.397	0.925	0.014	0.061
169	2.96	Bl	0.503	0.211	0.286	0.579	0.205	0.217
936	2.97	Bl	0.185	0.201	0.614	0.575	0.183	0.242
851	2.99	Bl	0.277	0.179	0.543	0.719	0.073	0.208
184	2.99	Bl	0.277	0.179	0.543	0.719	0.073	0.208
152	3.00	Bl	0.207	0.161	0.632	0.467	0.120	0.413
251	3.02	Bl	0.283	0.241	0.476	0.876	0.040	0.084
796	3.05	Bl	0.317	0.193	0.490	0.807	0.030	0.163
132	3.06	Bl	0.277	0.179	0.543	0.719	0.073	0.208
498	3.10	Bl	0.400	0.203	0.397	0.925	0.014	0.061
250	3.11	Bl	0.134	0.175	0.691	0.323	0.261	0.415
728	3.17	Bl	0.277	0.179	0.543	0.719	0.073	0.208

Appendix C. BN Prediction Probabilities

			EQUAL			FREQUENCY		
Sample	IMI	IMI Color	Bl	Br	Int	Bl	Br	Int
719	1.25	Br	0.0	94.6	5.4	0.0	97.6	2.4
264	1.26	Br	12.8	54.8	32.4	17.3	65.7	17.0
983	1.26	Br	41.6	31.6	26.8	52.0	36.1	12.9
194	1.27	Br	79.9	7.3	12.8	87.5	7.1	5.4
283	1.28	Br	0.0	94.6	5.4	0.0	97.6	2.4
639	1.28	Br	0.0	92.4	7.6	0.0	96.5	3.5
185	1.30	Br	26.5	42.0	31.5	34.9	49.0	16.1
193	1.30	Br	96.6	3.4	0.0	97.0	3.0	0.0
281	1.30	Br	26.5	42.0	31.5	34.9	49.0	16.1
571	1.32	Br	22.6	46.4	31.0	29.8	54.3	15.8
930	1.32	Br	22.6	46.4	31.0	29.8	54.3	15.8
720	1.32	Br	22.6	46.4	31.0	29.8	54.3	15.8
516	1.33	Br	41.6	31.6	26.8	52.0	36.1	12.9
202	1.36	Br	0.0	21.9	78.1	0.0	39.1	60.9
296	1.37	Br	0.0	96.6	3.4	0.0	98.5	1.5
271	1.38	Br	41.6	31.6	26.8	52.0	36.1	12.9
812	1.38	Br	0.0	94.6	5.4	0.0	97.6	2.4
965	1.39	Br	100.0	0.0	0.0	100.0	0.0	0.0
785	1.39	Br	12.8	54.8	32.4	17.3	65.7	17.0
957	1.40	Br	0.0	96.1	3.9	0.0	98.3	1.7
125	1.40	Br	0.0	93.2	6.8	0.0	96.9	3.1
578	1.40	Br	0.0	96.6	3.4	0.0	98.5	1.5
163	1.41	Br	26.5	42.0	31.5	34.9	49.0	16.1
519	1.41	Br	84.1	15.9	0.0	85.6	14.4	0.0
756	1.41	Br	12.8	54.8	32.4	17.3	65.7	17.0
161	1.41	Br	0.0	85.5	14.5	0.0	93.1	6.9
529	1.42	Br	26.5	42.0	31.5	34.9	49.0	16.1
143	1.43	Br	19.3	7.4	73.3	35.6	12.2	52.2
742	1.43	Br	41.6	31.6	26.8	52.0	36.1	12.9
584	1.43	Br	12.8	54.8	32.4	17.3	65.7	17.0
269	1.44	Br	41.6	31.6	26.8	52.0	36.1	12.9
528	1.45	Br	41.6	31.6	26.8	52.0	36.1	12.9
634	1.45	Br	67.3	12.8	19.9	78.0	13.1	8.9
372	1.45	Br	41.6	31.6	26.8	52.0	36.1	12.9
751	1.46	Br	12.8	54.8	32.4	17.3	65.7	17.0
791	1.46	Br	22.6	46.4	31.0	29.8	54.3	15.8

328	1.47	Br	41.6	31.6	26.8	52.0	36.1	12.9
286	1.47	Br	0.0	94.6	5.4	0.0	97.6	2.4
300	1.47	Br	0.0	94.6	5.4	0.0	97.6	2.4
378	1.47	Br	0.0	92.4	7.6	0.0	96.5	3.5
265	1.48	Br	12.8	54.8	32.4	17.3	65.7	17.0
120	1.48	Br	26.5	42.0	31.5	34.9	49.0	16.1
741	1.48	Br	26.5	42.0	31.5	34.9	49.0	16.1
217	1.48	Br	41.6	31.6	26.8	52.0	36.1	12.9
752	1.49	Br	0.0	94.6	5.4	0.0	97.6	2.4
692	1.49	Br	22.6	46.4	31.0	29.8	54.3	15.8
181	1.50	Br	0.0	60.0	40.0	0.0	77.5	22.5
726	1.50	Br	62.6	16.1	21.3	73.5	16.8	9.7
232	1.51	Br	41.6	31.6	26.8	52.0	36.1	12.9
451	1.51	Br	0.0	93.9	6.1	0.0	97.3	2.7
753	1.53	Br	0.0	85.5	14.5	0.0	93.1	6.9
825	1.54	Br	0.0	96.6	3.4	0.0	98.5	1.5
948	1.54	Br	26.5	42.0	31.5	34.9	49.0	16.1
374	1.55	Br	79.6	7.6	12.7	87.2	7.4	5.4
695	1.55	Br	22.6	46.4	31.0	29.8	54.3	15.8
657	1.56	Br	19.3	7.4	73.3	35.6	12.2	52.2
298	1.57	Br	0.0	93.4	6.6	0.0	97.0	3.0
531	1.57	Br	0.0	60.0	40.0	0.0	77.5	22.5
273	1.58	Br	22.6	46.4	31.0	29.8	54.3	15.8
975	1.58	Br	62.6	16.1	21.3	73.5	16.8	9.7
932	1.60	Br	84.1	15.9	0.0	85.6	14.4	0.0
219	1.60	Br	79.9	7.3	12.8	87.5	7.1	5.4
492	1.60	Br	19.3	7.4	73.3	35.6	12.2	52.2
367	1.60	Br	12.8	54.8	32.4	17.3	65.7	17.0
916	1.61	Br	46.2	24.8	29.0	58.2	27.7	14.1
313	1.61	Br	93.4	6.6	0.0	94.1	5.9	0.0
873	1.62	Br	22.6	46.4	31.0	29.8	54.3	15.8
853	1.62	Br	26.5	42.0	31.5	34.9	49.0	16.1
396	1.63	Br	0.0	94.6	5.4	0.0	97.6	2.4
176	1.63	Br	0.0	94.6	5.4	0.0	97.6	2.4
845	1.64	Br	0.0	86.0	14.0	0.0	93.4	6.6
124	1.65	Br	41.6	31.6	26.8	52.0	36.1	12.9
231	1.67	I	22.6	46.4	31.0	29.8	54.3	15.8
233	1.68	I	12.8	54.8	32.4	17.3	65.7	17.0
412	1.68	I	22.6	46.4	31.0	29.8	54.3	15.8
200	1.68	I	93.4	6.6	0.0	94.1	5.9	0.0

943	1.69	I	22.6	46.4	31.0	29.8	54.3	15.8
279	1.70	I	79.9	7.3	12.8	87.5	7.1	5.4
856	1.71	I	67.3	12.8	19.9	78.0	13.1	8.9
672	1.72	I	0.0	15.6	84.4	0.0	29.7	70.3
700	1.72	I	26.5	42.0	31.5	34.9	49.0	16.1
487	1.72	I	0.0	85.5	14.5	0.0	93.1	6.9
197	1.74	I	41.6	31.6	26.8	52.0	36.1	12.9
319	1.74	I	26.5	42.0	31.5	34.9	49.0	16.1
121	1.76	I	12.8	54.8	32.4	17.3	65.7	17.0
852	1.77	I	0.0	34.6	65.4	0.0	54.9	45.1
765	1.79	I	12.8	54.8	32.4	17.3	65.7	17.0
869	1.81	I	9.9	10.3	79.8	19.8	18.3	61.9
321	1.82	I	22.6	46.4	31.0	29.8	54.3	15.8
862	1.85	I	20.1	5.5	74.4	37.5	9.0	53.5
368	1.85	I	12.8	54.8	32.4	17.3	65.7	17.0
354	1.87	I	9.9	10.3	79.8	19.8	18.3	61.9
186	1.89	I	19.3	7.4	73.3	35.6	12.2	52.2
259	1.91	I	41.6	31.6	26.8	52.0	36.1	12.9
537	1.91	I	79.9	7.3	12.8	87.5	7.1	5.4
135	1.95	I	41.6	31.6	26.8	52.0	36.1	12.9
254	1.96	I	62.6	16.1	21.3	73.5	16.8	9.7
658	1.96	I	11.4	9.1	79.5	22.6	16.1	61.3
538	2.00	I	67.3	12.8	19.9	78.0	13.1	8.9
388	2.01	I	19.3	7.4	73.3	35.6	12.2	52.2
839	2.06	I	19.3	7.4	73.3	35.6	12.2	52.2
823	2.09	I	62.6	16.1	21.3	73.5	16.8	9.7
512	2.10	I	5.5	12.0	82.5	11.5	22.1	66.4
297	2.10	I	66.9	13.3	19.8	77.5	13.7	8.8
182	2.12	I	--	--	--	100.0	0.0	0.0
991	2.18	I	79.9	7.3	12.8	87.5	7.1	5.4
645	2.19	I	0.0	93.9	6.1	0.0	97.3	2.7
536	2.23	I	79.9	7.3	12.8	87.5	7.1	5.4
758	2.23	I	22.6	46.4	31.0	29.8	54.3	15.8
735	2.24	I	79.6	7.6	12.7	87.2	7.4	5.4
653	2.26	I	100.0	0.0	0.0	100.0	0.0	0.0
170	2.26	I	93.4	5.6	0.0	94.1	5.9	0.0
196	2.28	I	84.1	15.9	0.0	85.6	14.4	0.0
763	2.30	I	12.8	54.8	32.4	17.3	65.7	17.0
256	2.31	I	84.1	15.9	0.0	85.6	14.4	0.0
518	2.31	I	22.6	46.4	31.0	29.8	54.3	15.8

327	2.33	Bl	26.5	42.0	31.5	34.9	49.0	16.1
369	2.33	Bl	41.6	31.6	26.8	52.0	36.1	12.9
362	2.36	Bl	12.8	54.8	32.4	17.3	65.7	17.0
968	2.36	Bl	100.0	0.0	0.0	100.0	0.0	0.0
168	2.37	Bl	93.4	6.6	0.0	94.1	5.9	0.0
348	2.37	Bl	26.5	42.0	31.5	34.9	49.0	16.1
917	2.39	Bl	22.6	46.4	31.0	29.8	54.3	15.8
678	2.41	Bl	99.6	0.4	0.0	99.6	0.4	0.0
306	2.42	Bl	62.6	16.1	21.3	73.5	16.8	9.7
951	2.43	Bl	93.4	6.6	0.0	94.1	5.9	0.0
187	2.46	Bl	12.8	54.8	32.4	17.3	65.7	17.0
586	2.46	Bl	41.6	31.6	26.8	52.0	36.1	12.9
724	2.48	Bl	41.6	31.6	26.8	52.0	36.1	12.9
893	2.48	Bl	41.6	31.6	26.8	52.0	36.1	12.9
421	2.48	Bl	79.9	7.3	12.8	87.5	7.1	5.4
133	2.49	Bl	97.7	2.3	0.0	97.9	2.1	0.0
847	2.49	Bl	41.6	31.6	26.8	52.0	36.1	12.9
270	2.51	Bl	79.6	7.6	12.7	87.2	7.4	5.4
123	2.51	Bl	79.9	7.3	12.8	87.5	7.1	5.4
149	2.52	Bl	79.9	7.3	12.8	87.5	7.1	5.4
275	2.52	Bl	67.3	12.8	19.9	78.0	13.1	8.9
569	2.52	Bl	79.9	7.3	12.8	87.5	7.1	5.4
746	2.52	Bl	91.1	2.2	6.7	95.3	2.0	2.7
239	2.53	Bl	41.6	31.6	26.8	52.0	36.1	12.9
723	2.53	Bl	100.0	0.0	0.0	100.0	0.0	0.0
652	2.53	Bl	46.2	24.8	29.0	58.2	27.7	14.1
157	2.54	Bl	62.6	16.1	21.3	73.5	16.8	9.7
879	2.55	Bl	22.6	46.4	31.0	29.8	54.3	15.8
574	2.55	Bl	20.1	5.5	74.4	37.5	9.0	53.5
579	2.58	Bl	79.9	7.3	12.8	87.5	7.1	5.4
351	2.58	Bl	66.9	13.3	19.8	77.5	13.7	8.8
749	2.59	Bl	99.1	0.9	0.0	99.2	0.8	0.0
145	2.61	Bl	79.6	7.6	12.7	87.2	7.4	5.4
377	2.61	Bl	84.1	15.9	0.0	85.6	14.4	0.0
857	2.61	Bl	22.6	46.4	31.0	29.8	54.3	15.8
122	2.61	Bl	22.6	46.4	31.0	29.8	54.3	15.8
364	2.62	Bl	95.1	1.1	3.8	97.5	1.0	1.5
234	2.62	Bl	19.3	7.4	73.3	35.6	12.2	52.2
160	2.62	Bl	41.6	31.6	26.8	52.0	36.1	12.9
867	2.63	Bl	79.9	7.3	12.8	87.5	7.1	5.4

539	2.64	Bl	41.6	31.6	26.8	52.0	36.1	12.9
827	2.64	Bl	41.6	31.6	26.8	52.0	36.1	12.9
768	2.64	Bl	35.2	3.5	61.2	56.8	5.1	38.1
268	2.65	Bl	79.6	7.6	12.7	87.2	7.4	5.4
305	2.66	Bl	62.6	16.1	21.3	73.5	16.8	9.7
673	2.66	Bl	35.2	3.4	61.4	56.8	4.8	38.3
278	2.67	Bl	96.6	3.4	0.0	97.0	3.0	0.0
987	2.68	Bl	22.6	46.4	31.0	29.8	54.3	15.8
698	2.69	Bl	12.8	54.8	32.4	17.3	65.7	17.0
453	2.69	Bl	41.6	31.6	26.8	52.0	36.1	12.9
612	2.70	Bl	79.6	7.6	12.7	87.2	7.4	5.4
625	2.70	Bl	22.6	46.4	31.0	29.8	54.3	15.8
947	2.71	Bl	79.9	7.3	12.8	87.5	7.1	5.4
834	2.71	Bl	79.9	7.3	12.8	87.5	7.1	5.4
276	2.73	Bl	41.6	31.6	26.8	52.0	36.1	12.9
457	2.73	Bl	22.6	46.4	31.0	29.8	54.3	15.8
318	2.74	Bl	22.6	46.4	31.0	29.8	54.3	15.8
826	2.75	Bl	100.0	0.0	0.0	100.0	0.0	0.0
128	2.76	Bl	100.0	0.0	0.0	100.0	0.0	0.0
260	2.77	Bl	26.5	42.0	31.5	34.9	49.0	16.1
419	2.78	Bl	22.6	46.4	31.0	29.8	54.3	15.8
986	2.78	Bl	84.1	15.9	0.0	85.6	14.4	0.0
165	2.79	Bl	26.5	42.0	31.5	34.9	49.0	16.1
137	2.80	Bl	79.9	7.3	12.8	87.5	7.1	5.4
172	2.82	Bl	41.6	31.6	26.8	52.0	36.1	12.9
134	2.83	Bl	79.9	7.3	12.8	87.5	7.1	5.4
147	2.84	Bl	93.4	6.6	0.0	94.1	5.9	0.0
285	2.85	Bl	41.6	31.6	26.8	52.0	36.1	12.9
458	2.85	Bl	93.4	6.6	0.0	94.1	5.9	0.0
769	2.90	Bl	84.1	15.9	0.0	85.6	14.4	0.0
927	2.91	Bl	12.8	54.8	32.4	17.3	65.7	17.0
945	2.92	Bl	79.6	7.6	12.7	87.2	7.4	5.4
148	2.95	Bl	99.1	0.9	0.0	99.2	0.8	0.0
169	2.96	Bl	96.6	3.4	0.0	97.0	3.0	0.0
936	2.97	Bl	67.3	12.8	19.9	78.0	13.1	8.9
184	2.99	Bl	79.9	7.3	12.8	87.5	7.1	5.4
851	2.99	Bl	79.9	7.3	12.8	87.5	7.1	5.4
152	3.00	Bl	41.6	31.6	26.8	52.0	36.1	12.9
251	3.02	Bl	79.6	7.6	12.7	87.2	7.4	5.4
796	3.05	Bl	97.7	2.3	0.0	97.9	2.1	0.0

132	3.06	Bl	79.9	7.3	12.8	87.5	7.1	5.4
498	3.10	Bl	99.1	0.9	0.0	99.2	0.8	0.0
250	3.11	Bl	26.5	42.0	31.5	34.9	49.0	16.1
728	3.17	Bl	79.9	7.3	12.8	87.5	7.1	5.4

Appendix D. BN Likelihood Ratios

			Equal Odds			Adjusted Odds		
Sample	**IMI**	**IMI Color**	**Bl**	**Br**	**Int**	**Bl**	**Br**	**Int**
719	1.25	Br	0.0	35.0	0.1	0.0	63.6	0.1
264	1.26	Br	0.3	2.4	1.0	0.3	3.0	1.0
983	1.26	Br	1.4	0.9	0.7	1.4	0.9	0.7
194	1.27	Br	8.0	0.2	0.3	8.9	0.1	0.3
283	1.28	Br	0.0	35.0	0.1	0.0	63.6	0.1
639	1.28	Br	0.0	24.3	0.2	0.0	43.1	0.2
185	1.30	Br	0.7	1.4	0.9	0.7	1.5	0.9
281	1.30	Br	0.7	1.4	0.9	0.7	1.5	0.9
193	1.30	Br	56.8	0.1	0.0	41.2	0.0	0.0
571	1.32	Br	0.6	1.7	0.9	0.5	1.9	0.9
930	1.32	Br	0.6	1.7	0.9	0.5	1.9	0.9
720	1.32	Br	0.6	1.7	0.9	0.5	1.9	0.9
516	1.33	Br	1.4	0.9	0.7	1.4	0.9	0.7
202	1.36	Br	0.0	0.6	7.1	0.0	1.0	7.6
296	1.37	Br	0.0	56.8	0.1	0.0	102.7	0.1
271	1.38	Br	1.4	0.9	0.7	1.4	0.9	0.7
812	1.38	Br	0.0	35.0	0.1	0.0	63.6	0.1
965	1.39	Br	--	0.0	0.0	--	0.0	0.0
785	1.39	Br	0.3	2.4	1.0	0.3	3.0	1.0
957	1.40	Br	0.0	49.3	0.1	0.0	90.4	0.1
125	1.40	Br	0.0	27.4	0.6	0.0	48.9	0.2
578	1.40	Br	0.0	56.8	0.1	0.0	102.7	0.1
163	1.41	Br	0.7	1.4	0.9	0.7	1.5	0.9
519	1.41	Br	10.6	0.4	0.0	7.6	0.3	0.0
756	1.41	Br	0.3	2.4	1.0	0.3	3.0	1.0
161	1.41	Br	0.0	11.8	0.3	0.0	21.1	0.4
529	1.42	Br	0.7	1.4	0.9	0.7	1.5	0.9
742	1.43	Br	1.4	0.9	0.7	1.4	0.9	0.7
143	1.43	Br	0.5	0.2	5.5	0.7	0.2	5.3
584	1.43	Br	0.3	2.4	1.0	0.3	3.0	1.0
269	1.44	Br	1.4	0.9	0.7	1.4	0.9	0.7
634	1.45	Br	4.1	0.3	0.5	4.5	0.2	0.5
528	1.45	Br	1.4	0.9	0.7	1.4	0.9	0.7
372	1.45	Br	1.4	0.9	0.7	1.4	0.9	0.7
751	1.46	Br	0.3	2.4	1.0	0.3	3.0	1.0
791	1.46	Br	0.6	1.7	0.9	0.5	1.9	0.9

328	1.47	Br	1.4	0.9	0.7	1.4	0.9	0.7
286	1.47	Br	0.0	35.0	0.1	0.0	63.6	0.1
300	1.47	Br	0.0	35.0	0.1	0.0	63.6	0.1
378	1.47	Br	0.0	24.3	0.2	0.0	43.1	0.2
265	1.48	Br	0.3	2.4	1.0	0.3	3.0	1.0
120	1.48	Br	0.7	1.4	0.9	0.7	1.5	0.9
741	1.48	Br	0.7	1.4	0.9	0.7	1.5	0.9
217	1.48	Br	1.4	0.9	0.7	1.4	0.9	0.7
752	1.49	Br	0.0	35.0	0.1	0.0	63.6	0.1
692	1.49	Br	0.6	1.7	0.9	0.5	1.9	0.9
181	1.50	Br	0.0	3.0	1.3	0.0	5.4	1.4
726	1.50	Br	3.3	0.4	0.5	3.5	0.3	0.5
232	1.51	Br	1.4	0.9	0.7	1.4	0.9	0.7
451	1.51	Br	0.0	30.8	0.4	0.0	56.4	0.1
753	1.53	Br	0.0	11.8	0.3	0.0	21.1	0.4
825	1.54	Br	0.0	56.8	0.1	0.0	102.7	0.1
948	1.54	Br	0.7	1.4	0.9	0.7	1.5	0.9
374	1.55	Br	7.8	0.2	0.3	8.7	0.1	0.3
695	1.55	Br	0.6	1.7	0.9	0.5	1.9	0.9
657	1.56	Br	0.5	0.2	5.5	0.7	0.2	5.3
531	1.57	Br	0.0	3.0	1.3	0.0	5.4	1.4
298	1.57	Br	0.0	28.3	0.1	0.0	50.6	0.2
975	1.58	Br	3.3	0.4	0.5	3.5	0.3	0.5
273	1.58	Br	0.6	1.7	0.9	0.5	1.9	0.9
932	1.60	Br	10.6	0.4	0.0	7.6	0.3	0.0
219	1.60	Br	8.0	0.2	0.3	8.9	0.1	0.3
492	1.60	Br	0.5	0.2	5.5	0.7	0.2	5.3
367	1.60	Br	0.3	2.4	1.0	0.3	3.0	1.0
916	1.61	Br	1.7	0.7	0.8	1.8	0.6	0.8
313	1.61	Br	28.3	0.1	0.0	20.3	0.1	0.0
873	1.62	Br	0.6	1.7	0.9	0.5	1.9	0.9
853	1.62	Br	0.7	1.4	0.9	0.7	1.5	0.9
396	1.63	Br	0.0	35.0	0.1	0.0	63.6	0.1
176	1.63	Br	0.0	35.0	0.1	0.0	63.6	0.1
845	1.64	Br	0.0	12.3	0.3	0.0	22.1	0.3
124	1.65	Br	1.4	0.9	0.7	1.4	0.9	0.7
231	1.67	I	0.6	1.7	0.9	0.5	1.9	0.9
233	1.68	I	0.3	2.4	1.0	0.3	3.0	1.0
412	1.68	I	0.6	1.7	0.9	0.5	1.9	0.9
200	1.68	I	28.3	0.1	0.0	20.3	0.1	0.0

943	1.69	I	0.6	1.7	0.9	0.5	1.9	0.9
279	1.70	I	8.0	0.2	0.3	8.9	0.1	0.3
856	1.71	I	4.1	0.3	0.5	4.5	0.2	0.5
672	1.72	I	0.0	0.4	10.8	0.0	0.7	11.6
700	1.72	I	0.7	1.4	0.9	0.7	1.5	0.9
487	1.72	I	0.0	11.8	0.3	0.0	21.1	0.4
197	1.74	I	1.4	0.9	0.7	1.4	0.9	0.7
319	1.74	I	0.7	1.4	0.9	0.7	1.5	0.9
121	1.76	I	0.3	2.4	1.0	0.3	3.0	1.0
852	1.77	I	0.0	1.1	3.8	0.0	1.9	4.0
765	1.79	I	0.3	2.4	1.0	0.3	3.0	1.0
869	1.81	I	0.2	0.2	7.9	0.3	0.4	7.9
321	1.82	I	0.6	1.7	0.9	0.5	1.9	0.9
862	1.85	I	0.5	0.1	5.8	0.8	0.2	5.6
368	1.85	I	0.3	2.4	1.0	0.3	3.0	1.0
354	1.87	I	0.2	0.2	7.9	0.3	0.4	7.9
186	1.89	I	0.5	0.2	5.5	0.7	0.2	5.3
259	1.91	I	1.4	0.9	0.7	1.4	0.9	0.7
537	1.91	I	8.0	0.2	0.3	8.9	0.1	0.3
135	1.95	I	1.4	0.9	0.7	1.4	0.9	0.7
254	1.96	I	3.3	0.4	0.5	3.5	0.3	0.5
658	1.96	I	0.3	0.2	7.8	0.4	0.3	7.7
538	2.00	I	4.1	0.3	0.5	4.5	0.2	0.5
388	2.01	I	0.5	0.2	5.5	0.7	0.2	5.3
839	2.06	I	0.5	0.2	5.5	0.7	0.2	5.3
823	2.09	I	3.3	0.4	0.5	3.5	0.3	0.5
512	2.10	I	0.1	0.3	9.4	0.2	0.4	9.6
297	2.10	I	4.0	0.3	0.5	4.4	0.2	0.5
182	2.12	I	--	0.0	0.0	--	0.0	0.0
991	2.18	I	8.0	0.2	0.3	8.9	0.1	0.3
645	2.19	I	0.0	30.8	0.4	0.0	56.4	0.1
536	2.23	I	8.0	0.2	0.3	8.9	0.1	0.3
758	2.23	I	0.6	1.7	0.9	0.5	1.9	0.9
735	2.24	I	7.8	0.2	0.3	8.7	0.1	0.3
653	2.26	I	--	0.0	0.0	--	0.0	0.0
170	2.26	I	28.3	0.1	0.0	20.4	0.1	0.0
196	2.28	I	10.6	0.4	0.0	7.6	0.3	0.0
763	2.30	I	0.3	2.4	1.0	0.3	3.0	1.0
518	2.31	I	0.6	1.7	0.9	0.5	1.9	0.9
256	2.31	I	10.6	0.4	0.0	7.6	0.3	0.0

327	2.33	Bl	0.7	1.4	0.9	0.7	1.5	0.9
369	2.33	Bl	1.4	0.9	0.7	1.4	0.9	0.7
362	2.36	Bl	0.3	2.4	1.0	0.3	3.0	1.0
968	2.36	Bl	--	0.0	0.0	--	0.0	0.0
168	2.37	Bl	28.3	0.1	0.0	20.3	0.1	0.0
348	2.37	Bl	0.7	1.4	0.9	0.7	1.5	0.9
917	2.39	Bl	0.6	1.7	0.9	0.5	1.9	0.9
678	2.41	Bl	498.0	0.01	0.0	316.9	0.0	0.0
306	2.42	Bl	3.3	0.4	0.5	3.5	0.3	0.5
951	2.43	Bl	28.3	0.1	0.0	20.3	0.1	0.0
187	2.46	Bl	0.3	2.4	1.0	0.3	3.0	1.0
586	2.46	Bl	1.4	0.9	0.7	1.4	0.9	0.7
724	2.48	I	1.4	0.9	0.7	1.4	0.9	0.7
893	2.48	Bl	1.4	0.9	0.7	1.4	0.9	0.7
421	2.48	Bl	8.0	0.2	0.3	8.9	0.1	0.3
133	2.49	Bl	85.0	0.05	0.0	59.3	0.0	0.0
847	2.49	Bl	1.4	0.9	0.7	1.4	0.9	0.7
270	2.51	Bl	7.8	0.2	0.3	8.7	0.1	0.3
123	2.51	Bl	8.0	0.2	0.3	8.9	0.1	0.3
275	2.52	Bl	4.1	0.3	0.5	4.5	0.2	0.5
149	2.52	Bl	8.0	0.2	0.3	8.9	0.1	0.3
569	2.52	Bl	8.0	0.2	0.3	8.9	0.1	0.3
746	2.52	Bl	20.5	0.0	0.1	25.8	0.0	0.1
239	2.53	Bl	1.4	0.9	0.7	1.4	0.9	0.7
723	2.53	Bl	--	0.0	0.0	--	0.0	0.0
652	2.53	Bl	1.7	0.7	0.8	1.8	0.6	0.8
157	2.54	Bl	3.3	0.4	0.5	3.5	0.3	0.5
879	2.55	Bl	0.6	1.7	0.9	0.5	1.9	0.9
574	2.55	Bl	0.5	0.1	5.8	0.8	0.2	5.6
579	2.58	Bl	8.0	0.2	0.3	8.9	0.1	0.3
351	2.58	Bl	4.0	0.3	0.5	4.4	0.2	0.5
749	2.59	Bl	220.2	0.02	0.0	157.8	0.0	0.0
145	2.61	Bl	7.8	0.2	0.3	8.7	0.1	0.3
377	2.61	Bl	10.6	0.4	0.0	7.6	0.3	0.0
857	2.61	Bl	0.6	1.7	0.9	0.5	1.9	0.9
122	2.61	Bl	0.6	1.7	0.9	0.5	1.9	0.9
364	2.62	Bl	38.8	0.0	0.1	49.6	0.0	0.1
234	2.62	Bl	0.5	0.2	5.5	0.7	0.2	5.3
160	2.62	Bl	1.4	0.9	0.7	1.4	0.9	0.7
867	2.63	Bl	8.0	0.2	0.3	8.9	0.1	0.3

539	2.64	Bl	1.4	0.9	0.7	1.4	0.9	0.7
827	2.64	Bl	1.4	0.9	0.7	1.4	0.9	0.7
768	2.64	Bl	1.1	0.1	3.2	1.7	0.1	3.0
268	2.65	Bl	7.8	0.2	0.3	8.7	0.1	0.3
305	2.66	Bl	3.3	0.4	0.5	3.5	0.3	0.5
673	2.66	Bl	1.1	0.1	3.2	1.7	0.1	3.0
278	2.67	Bl	56.8	0.1	0.0	41.2	0.0	0.0
987	2.68	Bl	0.6	1.7	0.9	0.5	1.9	0.9
698	2.69	Bl	0.3	2.4	1.0	0.3	3.0	1.0
453	2.69	Bl	1.4	0.9	0.7	1.4	0.9	0.7
625	2.70	Bl	0.6	1.7	0.9	0.5	1.9	0.9
612	2.70	Bl	7.8	0.2	0.3	8.7	0.1	0.3
947	2.71	Bl	8.0	0.2	0.3	8.9	0.1	0.3
834	2.71	Bl	8.0	0.2	0.3	8.9	0.1	0.3
457	2.73	Bl	0.6	1.7	0.9	0.5	1.9	0.9
276	*2.73*	Bl	1.4	0.9	0.7	1.4	0.9	0.7
318	2.74	Bl	0.6	1.7	0.9	0.5	1.9	0.9
826	2.75	Bl	--	0.0	0.0	--	0.0	0.0
128	2.76	Bl	--	0.0	0.0	--	0.0	0.0
260	2.77	Bl	0.7	1.4	0.9	0.7	1.5	0.9
419	2.78	*Bl*	0.6	1.7	0.9	0.5	1.9	0.9
986	2.78	Bl	10.6	0.4	0.0	7.6	0.3	0.0
165	2.79	Bl	0.7	1.4	0.9	0.7	1.5	0.9
137	2.80	Bl	8.0	0.2	0.3	8.9	0.1	0.3
172	2.82	Bl	1.4	0.9	0.7	1.4	0.9	0.7
134	2.83	Bl	8.0	0.2	0.3	8.9	0.1	0.3
147	2.84	Bl	28.3	0.1	0.0	20.3	0.1	0.0
285	*2.85*	Bl	1.4	0.9	0.7	1.4	0.9	0.7
458	2.85	Bl	28.3	0.1	0.0	20.3	0.1	0.0
769	2.90	Bl	10.6	0.4	0.0	7.6	0.3	0.0
927	2.91	Bl	0.3	2.4	1.0	0.3	3.0	1.0
945	2.92	Bl	7.8	0.2	0.3	8.7	0.1	0.3
148	2.95	Bl	220.2	0.02	0.0	157.8	0.0	0.0
169	2.96	Bl	56.8	0.1	0.0	41.2	0.0	0.0
936	2.97	Bl	4.1	0.3	0.5	4.5	0.2	0.5
184	2.99	Bl	8.0	0.2	0.3	8.9	0.1	0.3
851	2.99	Bl	8.0	0.2	0.3	8.9	0.1	0.3
152	3.00	Bl	1.4	0.9	0.7	1.4	0.9	0.7
251	3.02	Bl	7.8	0.2	0.3	8.7	0.1	0.3
796	3.05	Bl	85.0	0.05	0.0	59.3	0.0	0.0

132	3.06	Bl	8.0	0.2	0.3	8.9	0.1	0.3
498	3.10	Bl	220.2	0.02	0.0	157.8	0.0	0.0
250	3.11	Bl	0.7	1.4	0.9	0.7	1.5	0.9
728	3.17	Bl	8.0	0.2	0.3	8.9	0.1	0.3

Appendix E. Digital Photo Collection

120.jpg 121.jpg 122.jpg 123.jpg 124.jpg

125.jpg 128.jpg 132.jpg 133.jpg 134.jpg

135.jpg 137.jpg 143.jpg 145.jpg 147.jpg

148.jpg 149.jpg 152.jpg 157.jpg 160.jpg

161.jpg 163.jpg 165.jpg 168.jpg 169.jpg

170.jpg 172.jpg 176.jpg 181.jpg 182.jpg

184.jpg 185.jpg 186.jpg 187.jpg 193.jpg

194.jpg 196.jpg 197.jpg 200.jpg 202.jpg

217.jpg 219.jpg 231.jpg 232.jpg 233.jpg

234.jpg 239.jpg 250.jpg 251.jpg 254.jpg

256.jpg 259.jpg 260.jpg 264.jpg 265.jpg

268.jpg 269.jpg 270.jpg 271.jpg 273.jpg

275.jpg 276.jpg 278.jpg 279.jpg 281.jpg

283.jpg 285.jpg 286.jpg 296.jpg 297.jpg

298.jpg 300.jpg 305.jpg 306.jpg 313.jpg

318.jpg 319.jpg 321.jpg 327.jpg 328.jpg

348.jpg 351.jpg 354.jpg 362.jpg 364.jpg

367.jpg 368.jpg 369.jpg 372.jpg 374.jpg

377.jpg 378.jpg 388.jpg 396.jpg 412.jpg

419.jpg 421.jpg 451.jpg 453.jpg 457.jpg

458.jpg 487.jpg 492.jpg 498.jpg 512.jpg

516.jpg 518.jpg 519.jpg 528.jpg 529.jpg

531.jpg 536.jpg 537.jpg 538.jpg 539.jpg

569.jpg 571.jpg 574.jpg 578.jpg 579.jpg

584.jpg 586.jpg 612.jpg 625.jpg 634.jpg

639.jpg 645.jpg 652.jpg 653.jpg 657.jpg

658.jpg 672.jpg 673.jpg 678.jpg 692.jpg

695.jpg 698.jpg 700.jpg 719.jpg 720.jpg

723.jpg 724.jpg 726.jpg 728.jpg 735.jpg

741.jpg 742.jpg 746.jpg 749.jpg 751.jpg

752.jpg 753.jpg 756.jpg 758.jpg 763.jpg

765.jpg 768.jpg 769.jpg 785.jpg 791.jpg

796.jpg 812.jpg 823.jpg 825.jpg 826.jpg

827.jpg 834.jpg 839.jpg 845.jpg 847.jpg

851.jpg 852.jpg 853.jpg 856.jpg 857.jpg

862.jpg 867.jpg 869.jpg 873.jpg 879.jpg

893.jpg 916.jpg 917.jpg 927.jpg 930.jpg

932.jpg 936.jpg 943.jpg 945.jpg 947.jpg

948.jpg 951.jpg 957.jpg 965.jpg 968.jpg

975.jpg 983.jpg 986.jpg 987.jpg 991.jpg

Appendix F. SNP Profile Electropherograms

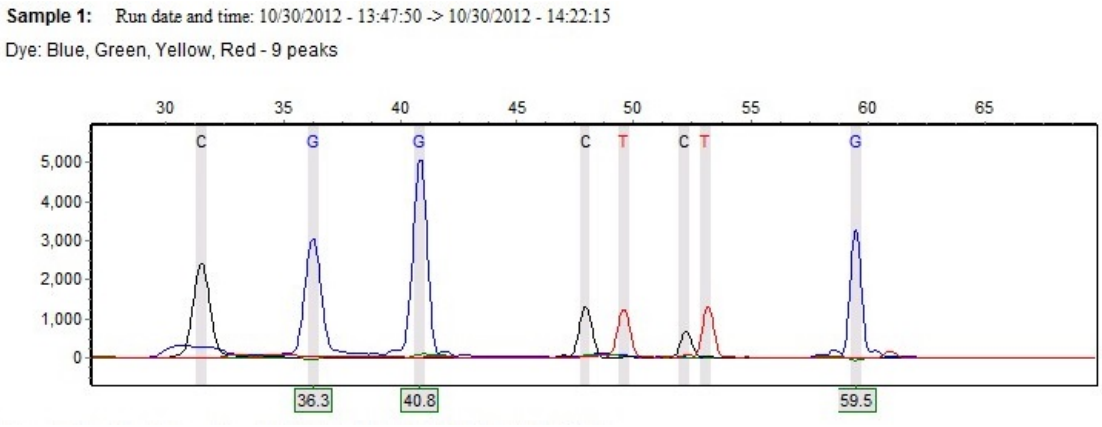

Figure F1. Sample 120

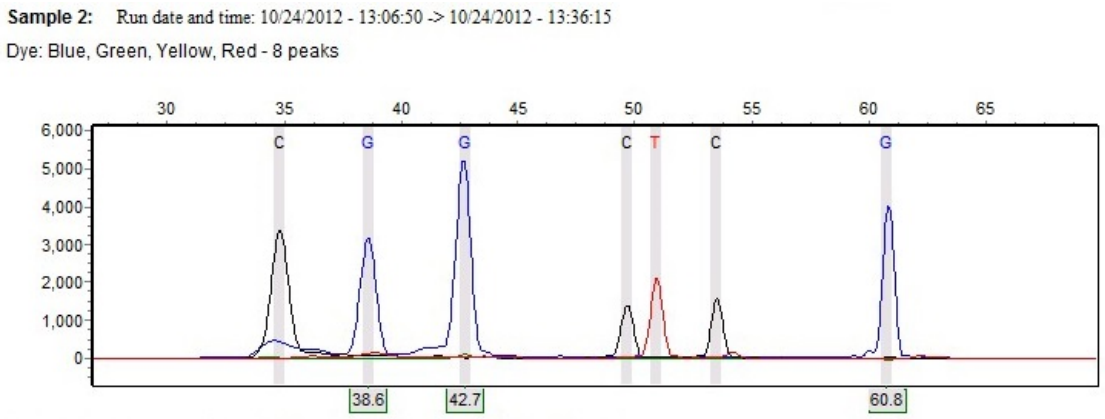

Figure F2. Sample 121

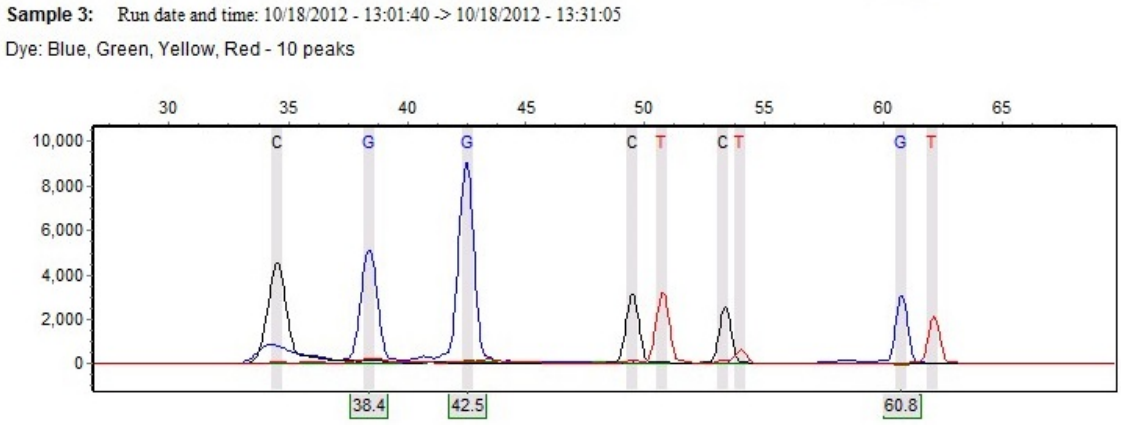

Figure F3. Sample 122

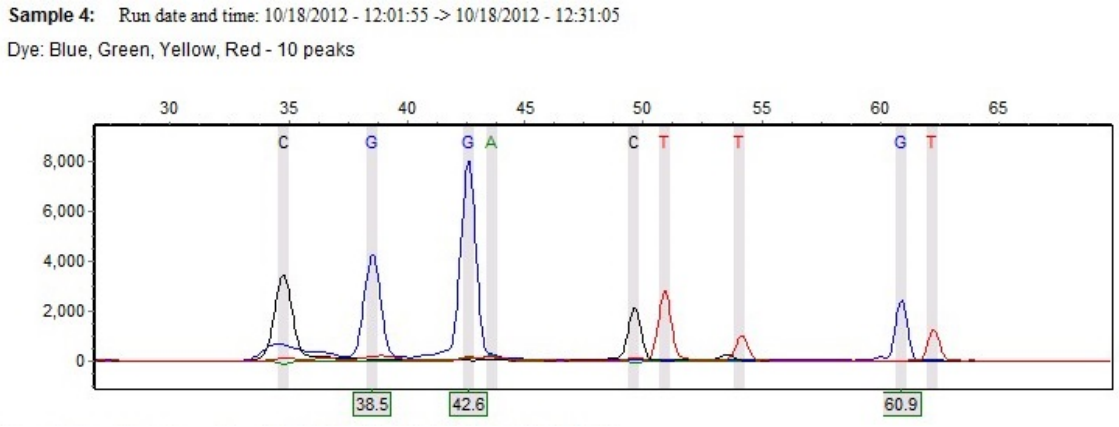

Figure F4. Sample 123

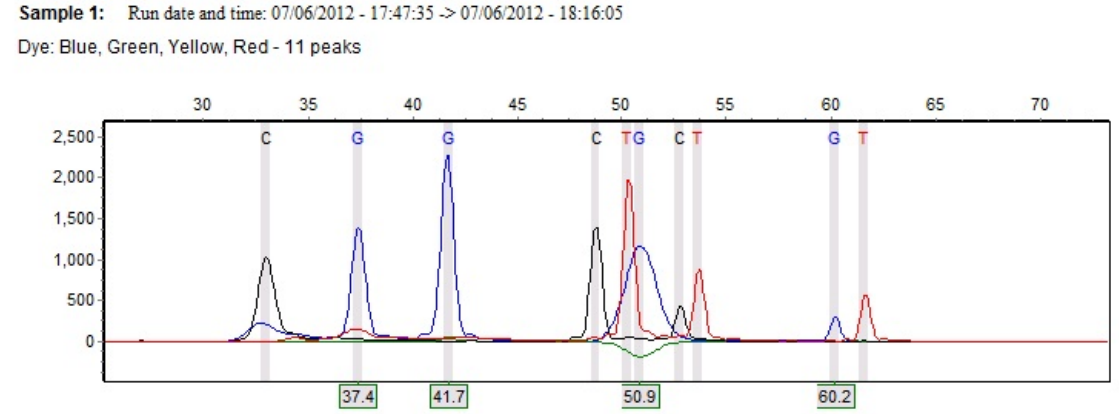

Figure F5. Sample 124

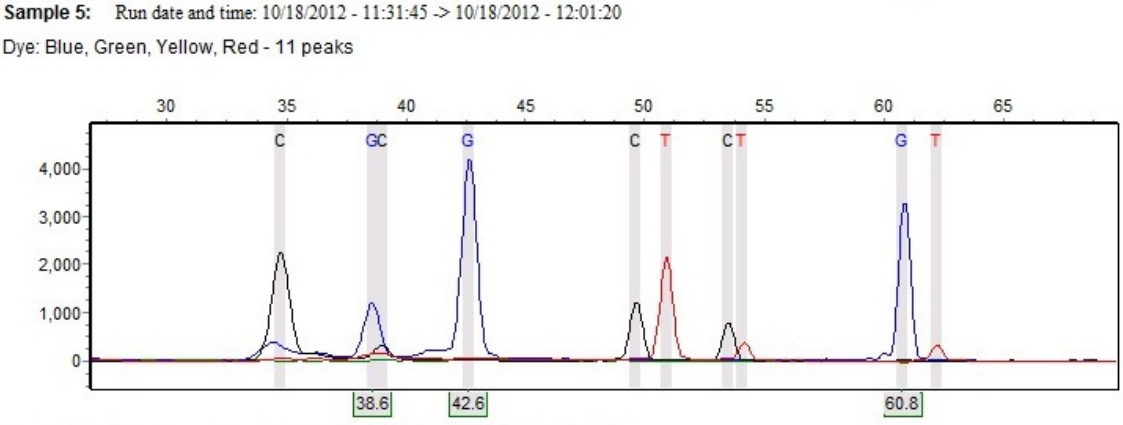

Figure F6. Sample 125

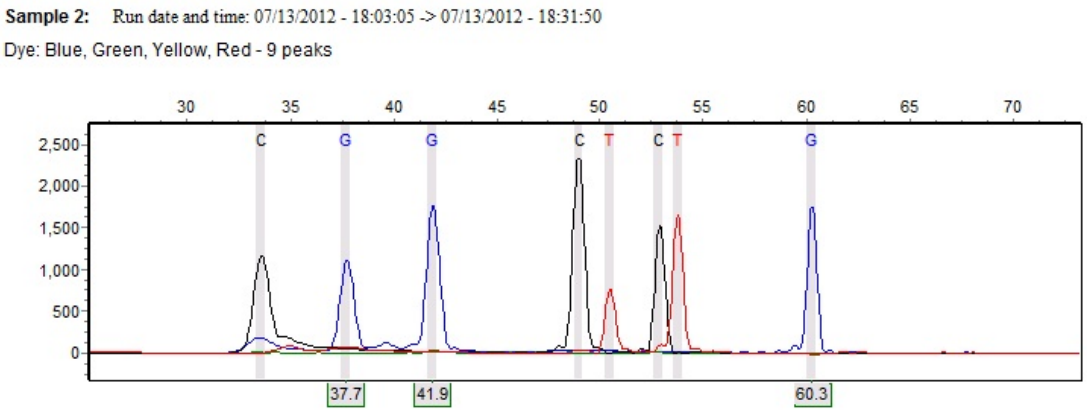

Figure F7. Sample 128

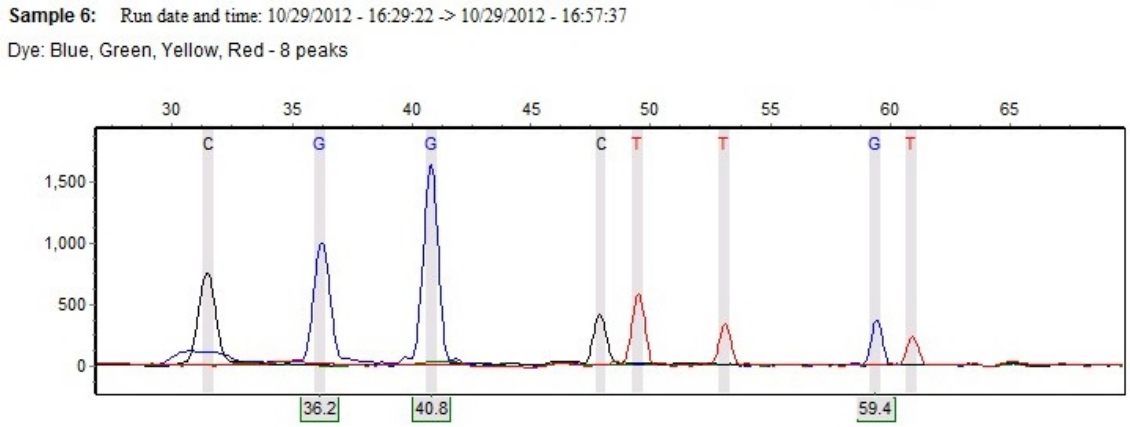

Figure F8. Sample 132

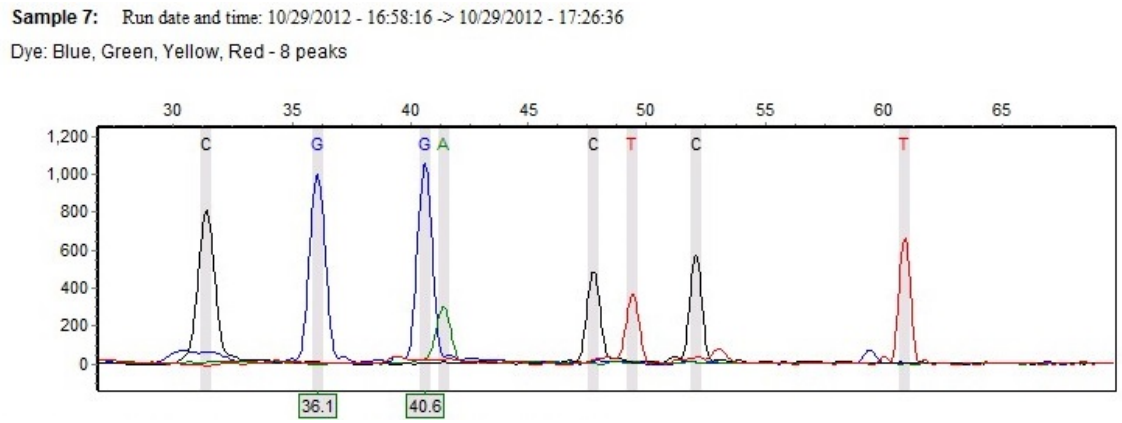

Figure F9. Sample 133

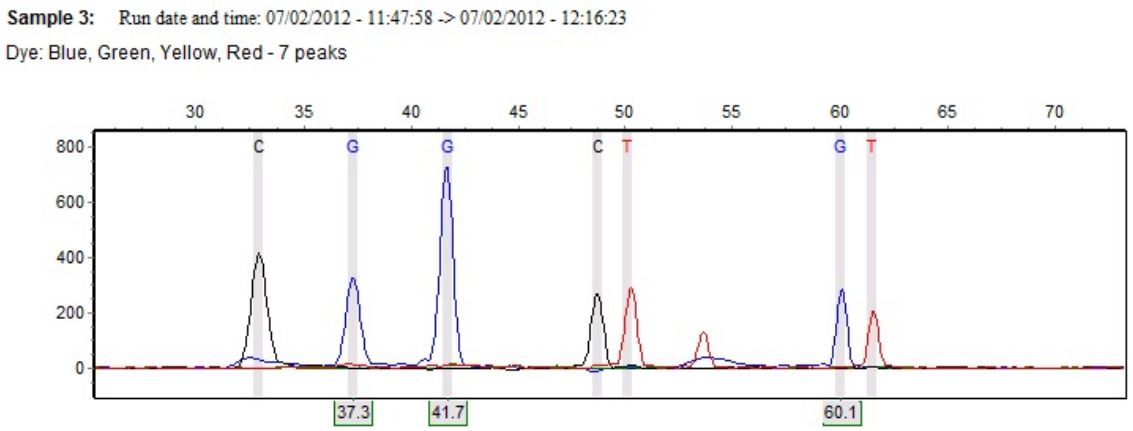

Figure F10. Sample 134

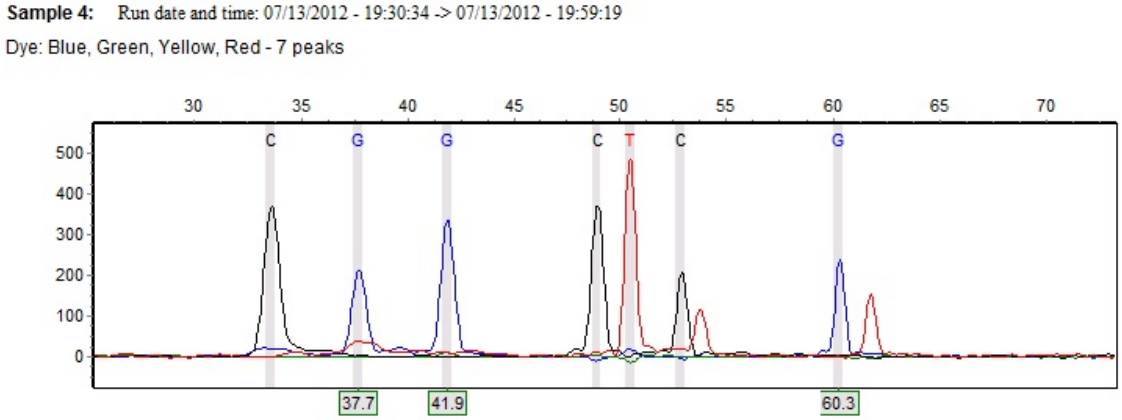

Figure F11. Sample 135

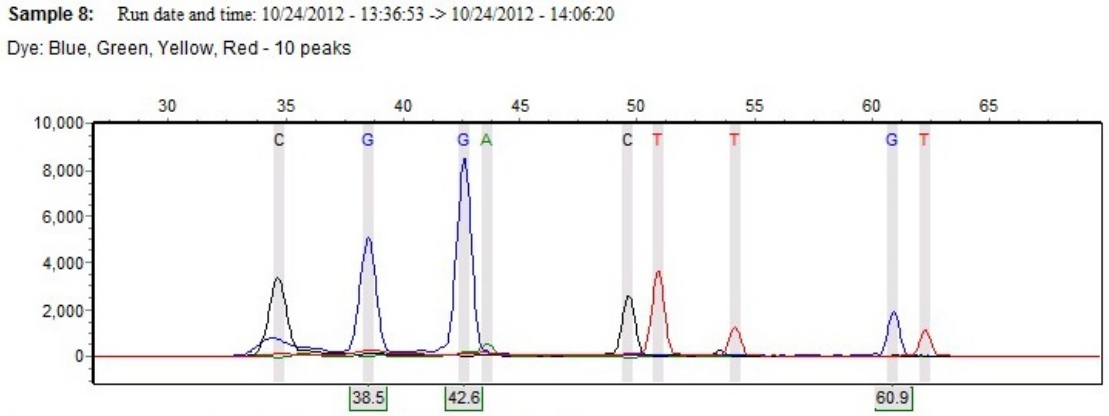

Figure F12. Sample 137

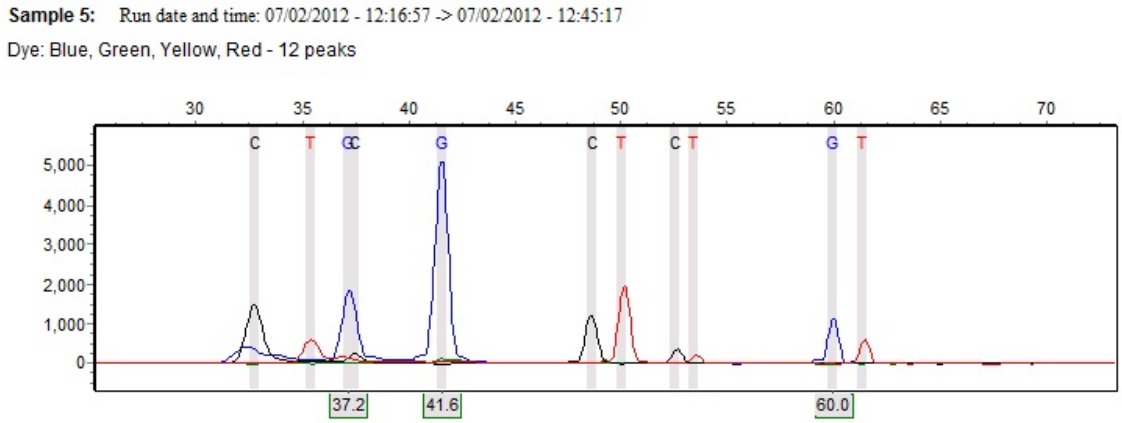

Figure F13. Sample 143

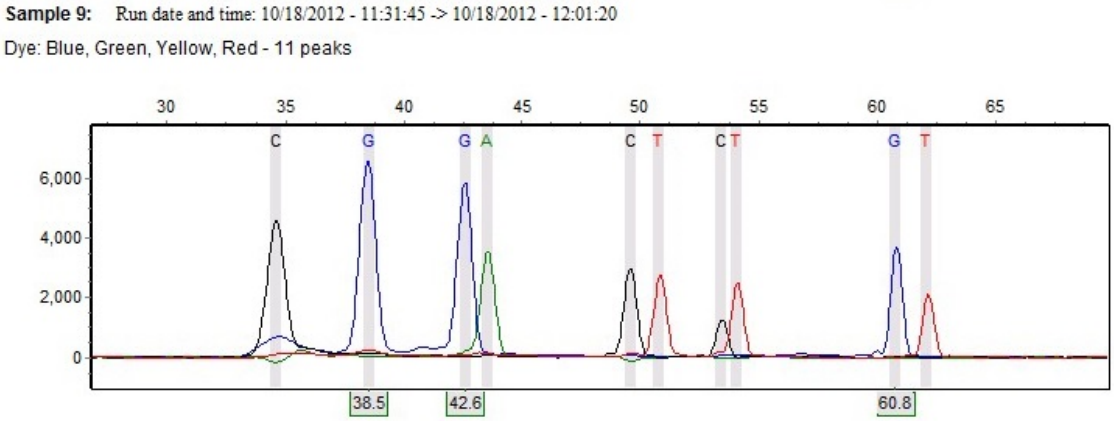

Figure F14. Sample 145

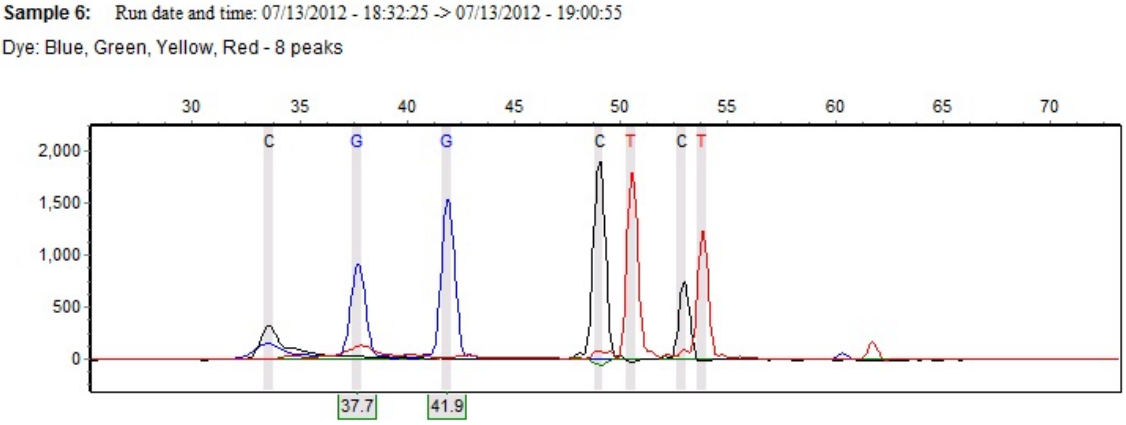

Figure F15. Sample 147

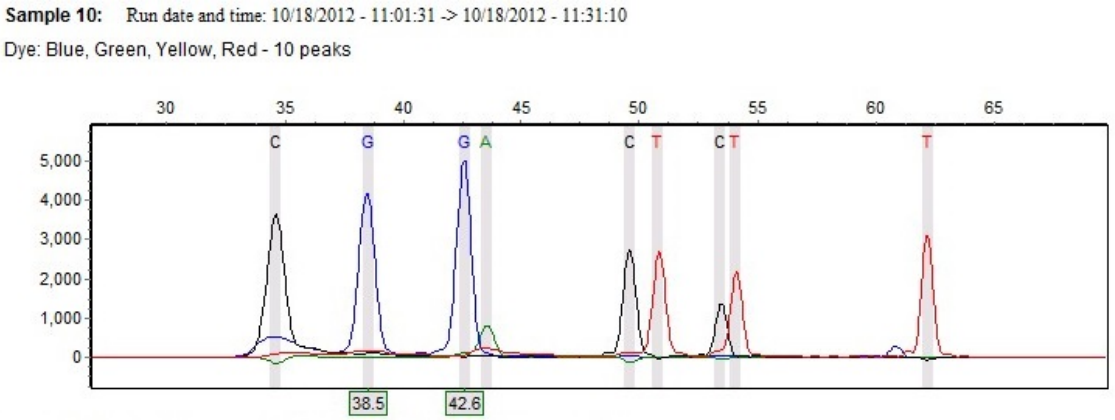

Figure F16. Sample 148

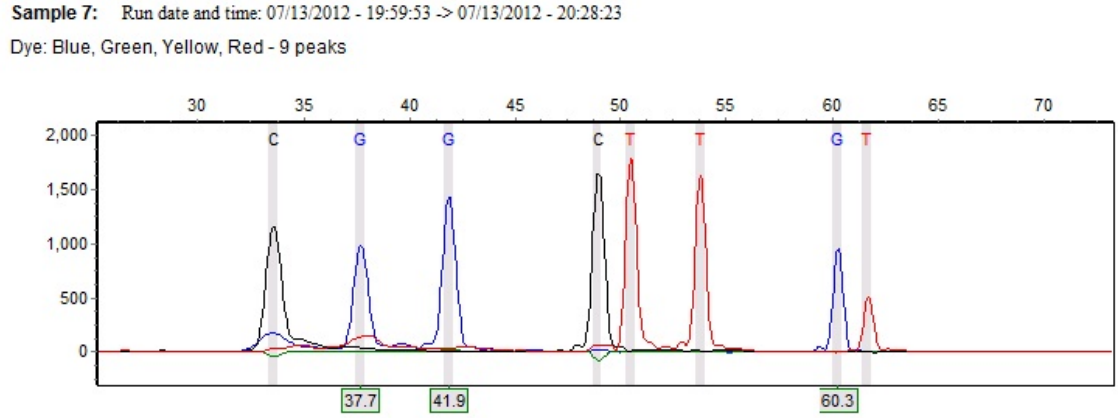

Figure F17. Sample 149

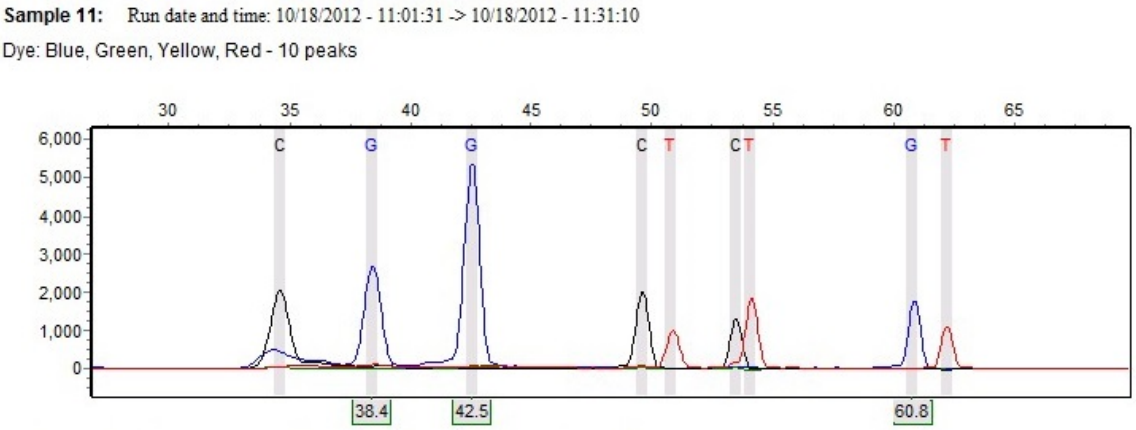

Figure F18. Sample 152

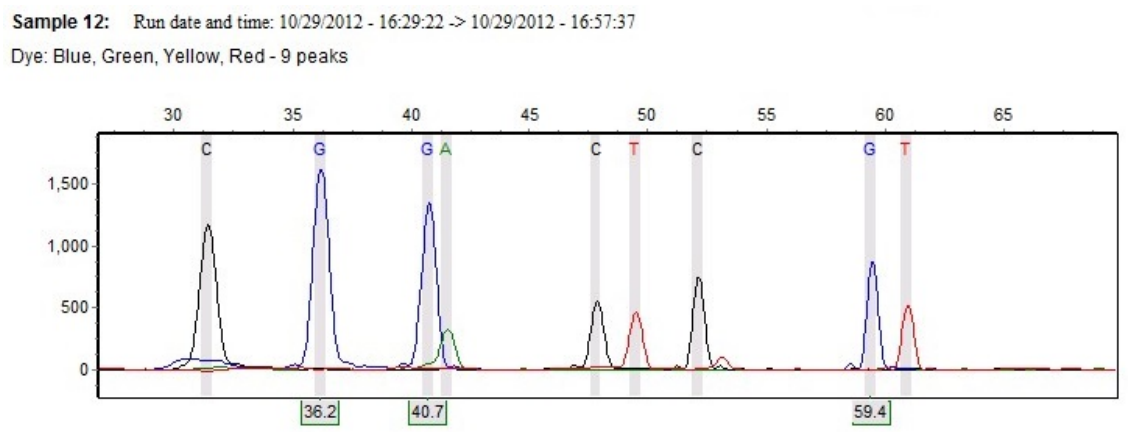

Figure F19. Sample 157

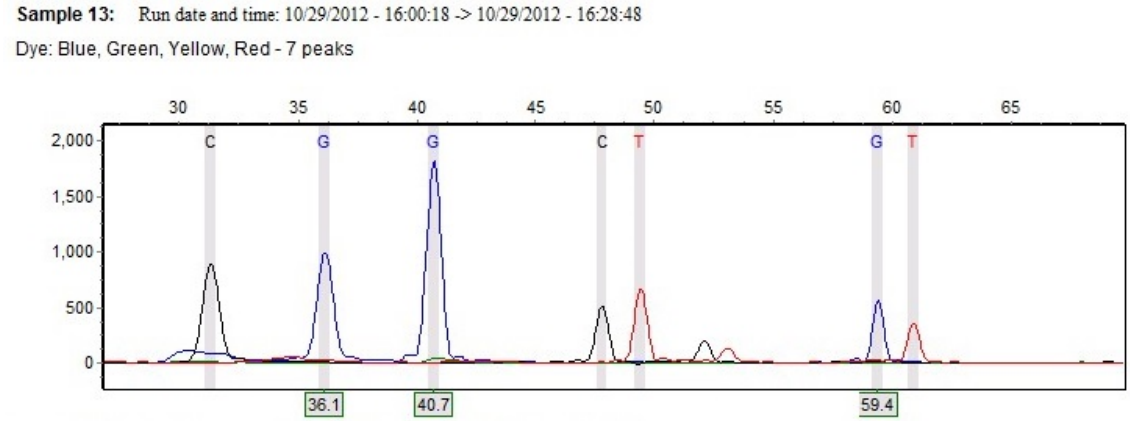

Figure F20. Sample 160

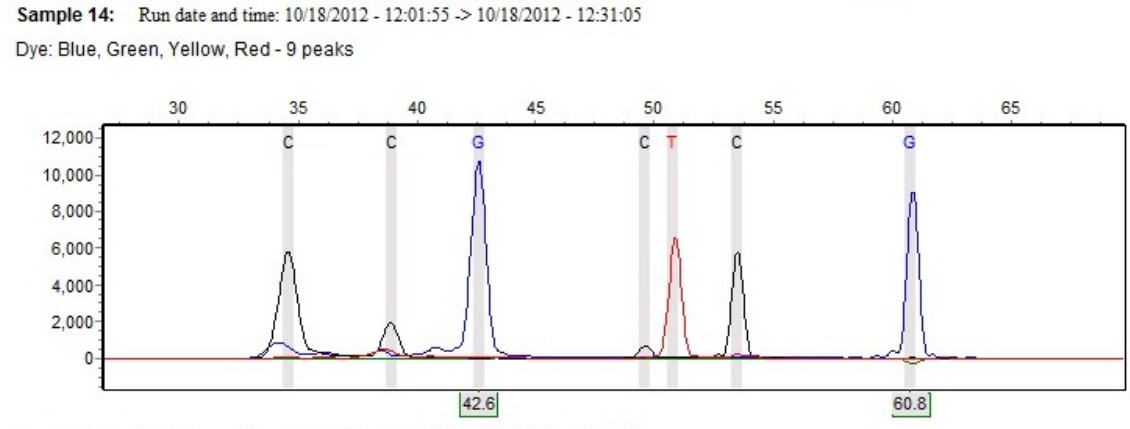

Figure F21. Sample 161

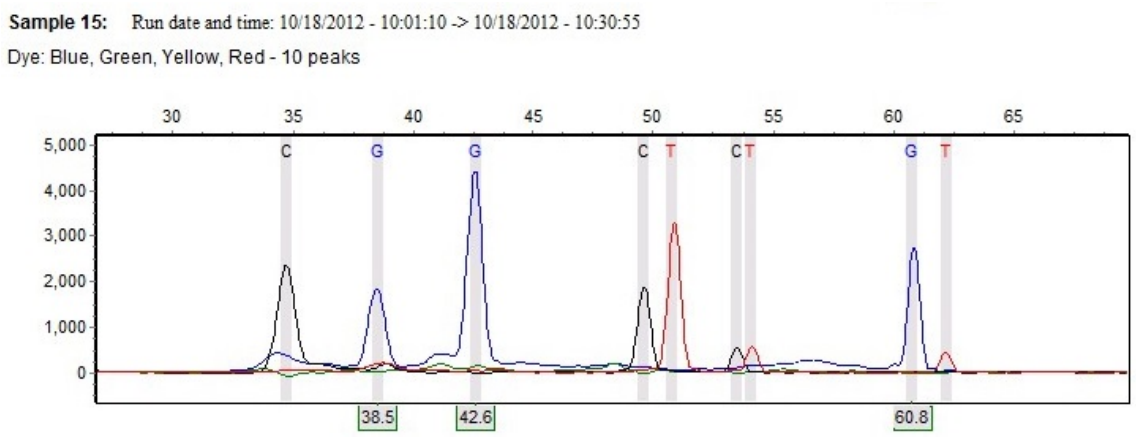

Figure F22. Sample 163

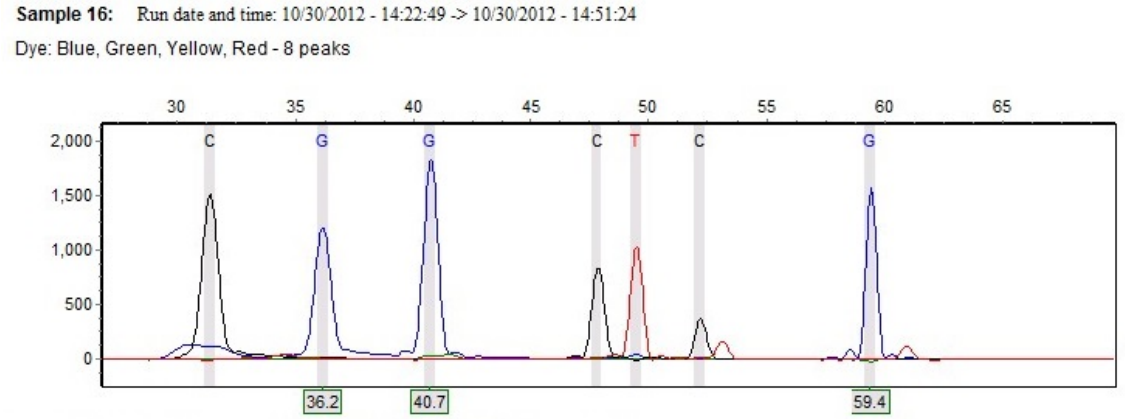

Figure F23. Sample 165

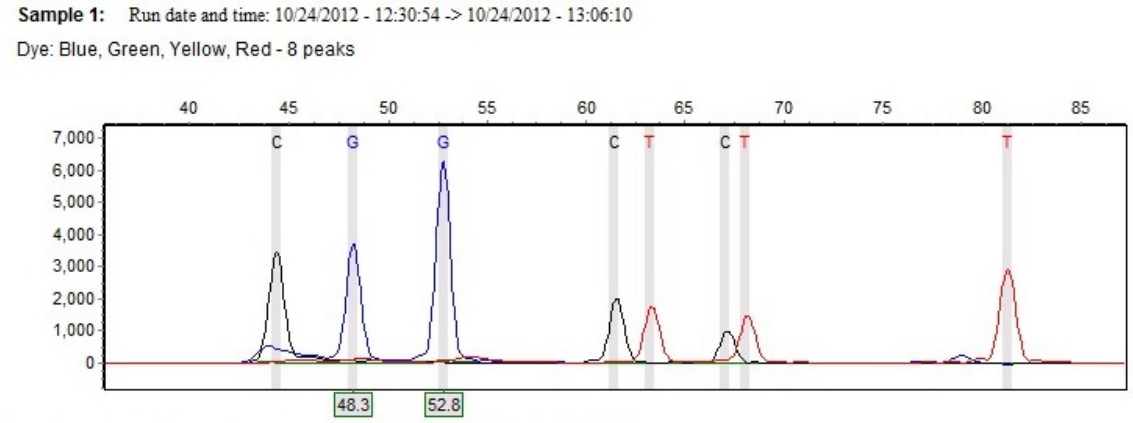

Figure F24. Sample 168

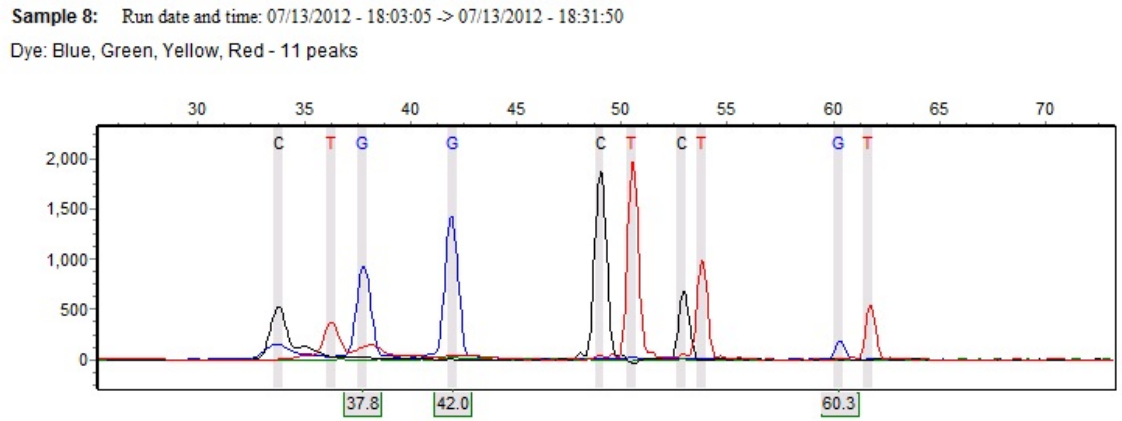

Figure F25. Sample 169

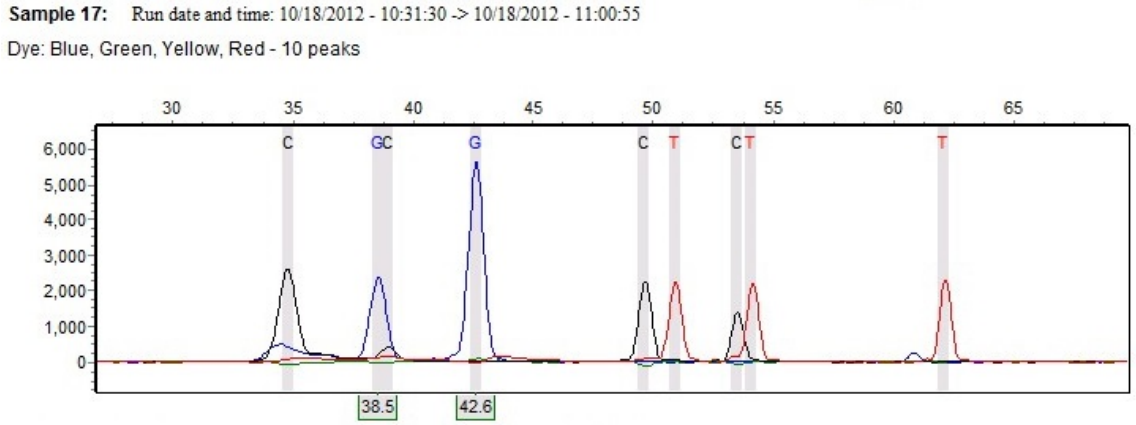

Figure F26. Sample 170

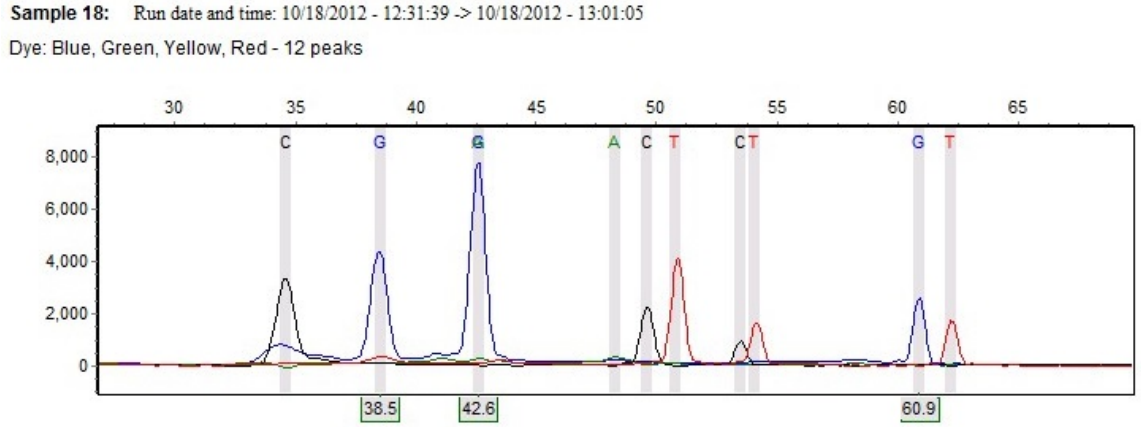

Figure F27. Sample 172

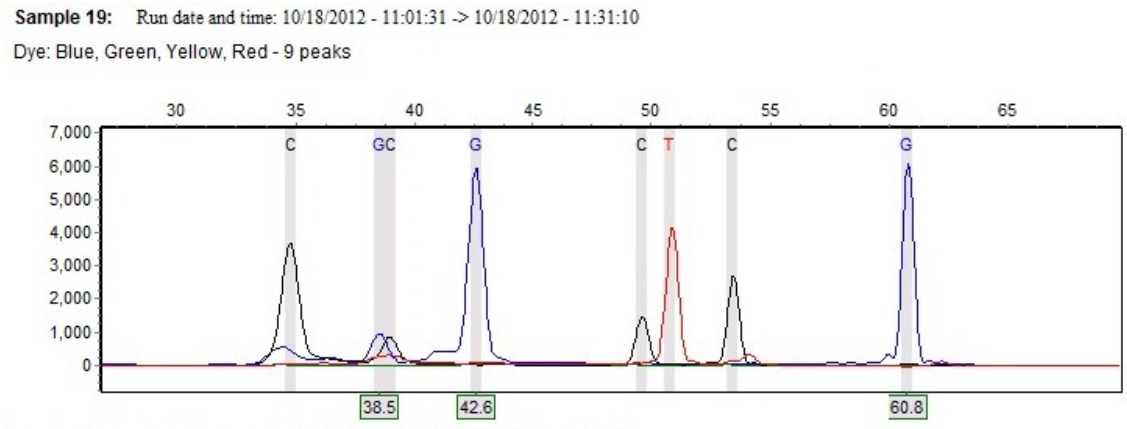

Figure F28. Sample 176

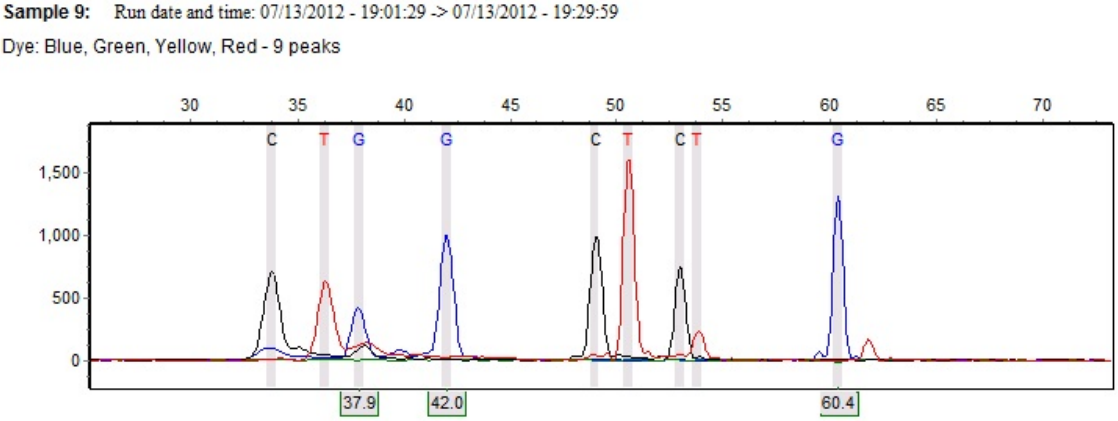

Figure F29. Sample 181

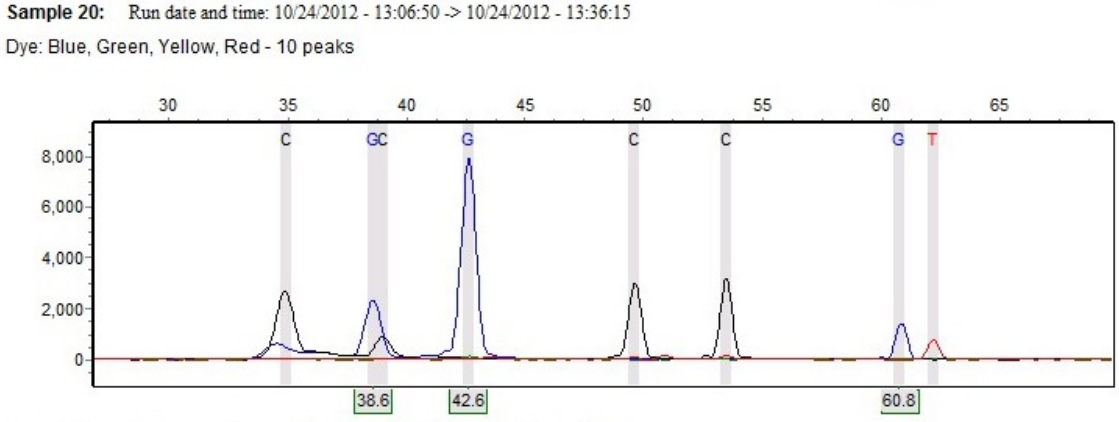

Figure F30. Sample 182

Sample 10: Run date and time: 07/13/2012 - 19:01:29 -> 07/13/2012 - 19:29:59

Dye: Blue, Green, Yellow, Red - 10 peaks

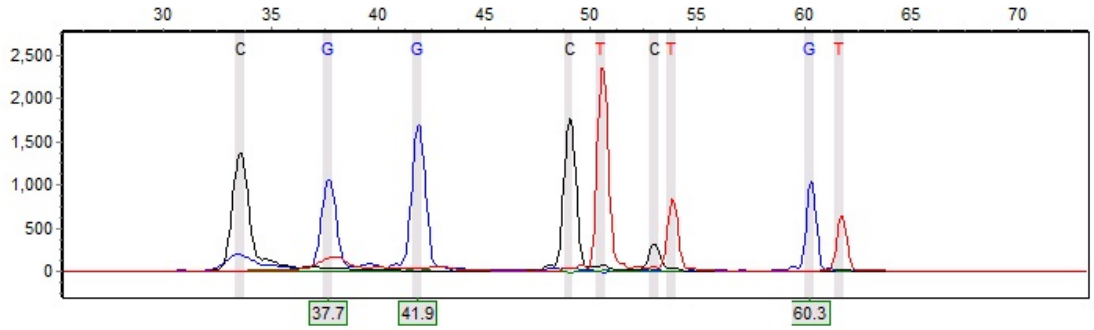

Figure F31. Sample 184

Sample 21: Run date and time: 10/30/2012 - 14:22:49 -> 10/30/2012 - 14:51:24

Dye: Blue, Green, Yellow, Red - 9 peaks

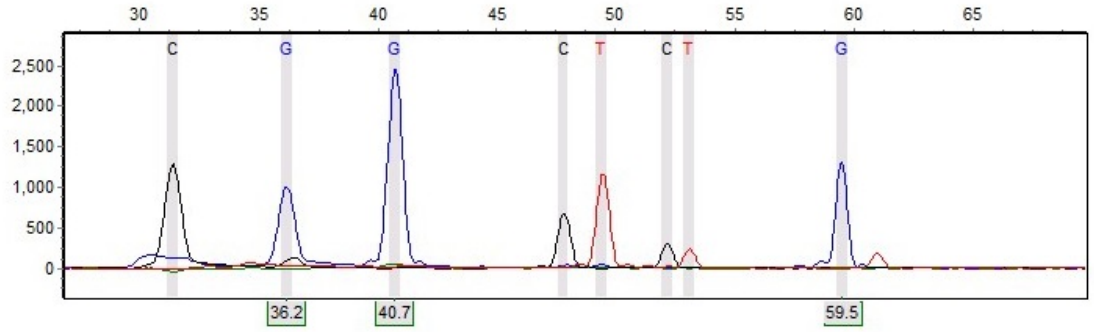

Figure F32. Sample 185

Sample 11: Run date and time: 07/09/2012 - 10:55:20 -> 07/09/2012 - 11:33:00

Dye: Blue, Green, Yellow, Red - 10 peaks

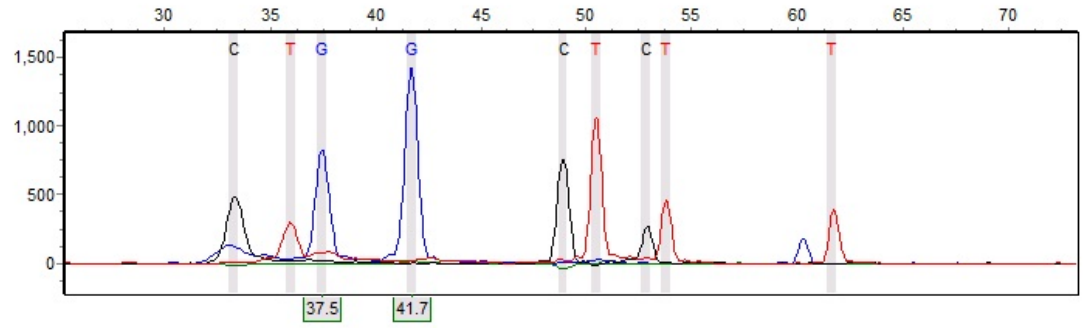

Figure F33. Sample 186

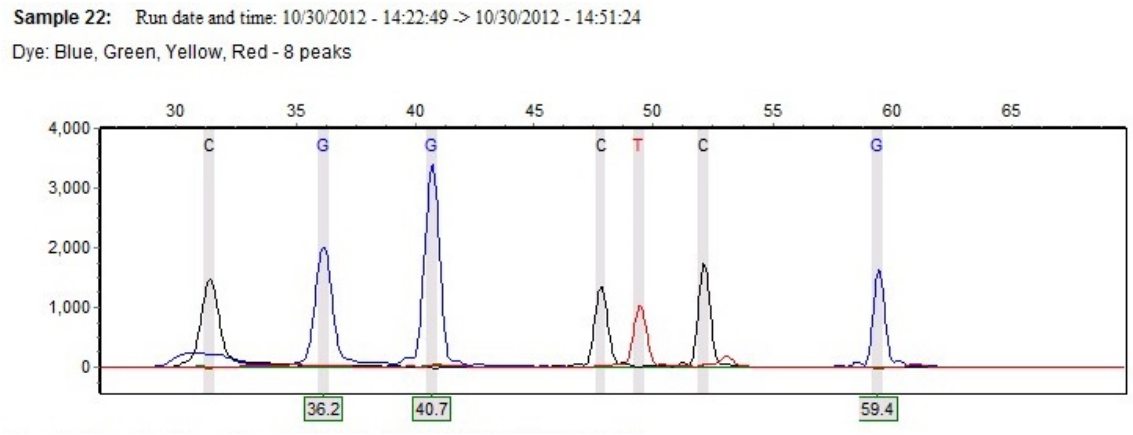

Figure F34. Sample 187

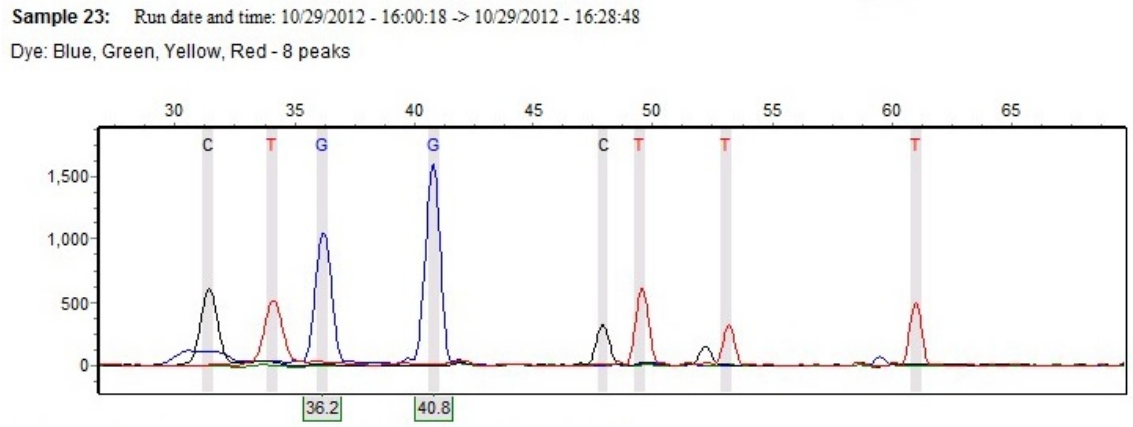

Figure F35. Sample 193

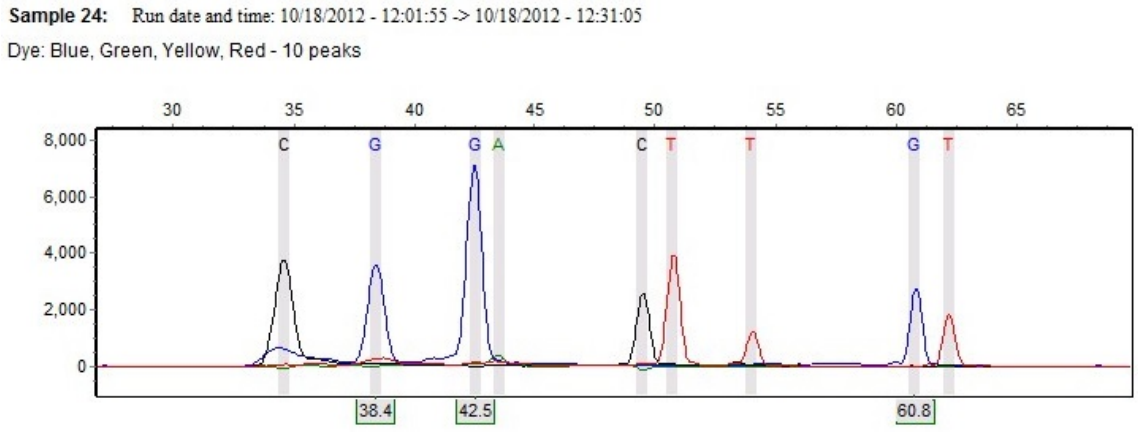

Figure F36. Sample 194

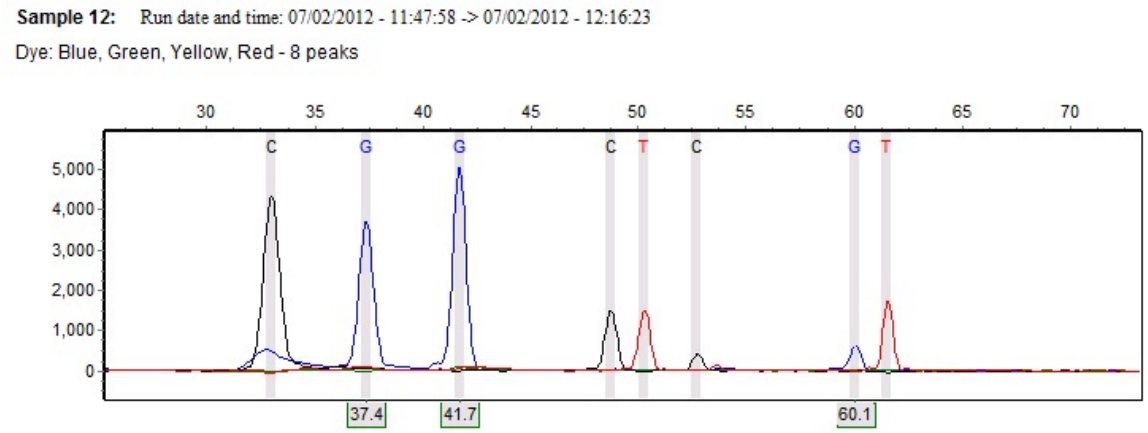

Figure F37. Sample 196

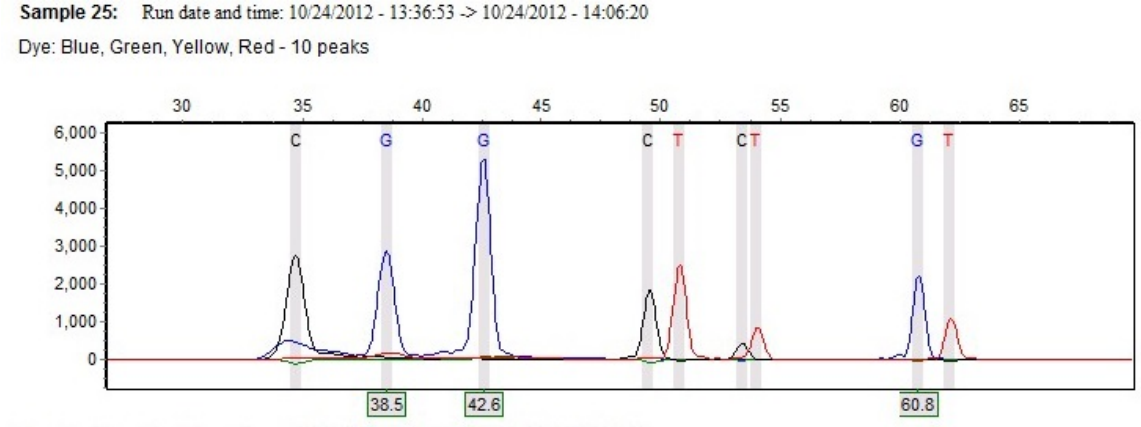

Figure F38. Sample 197

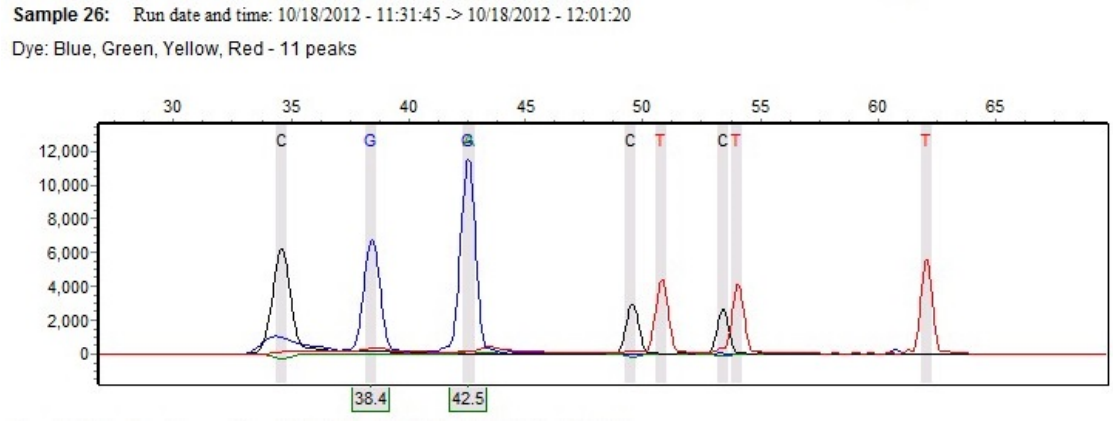

Figure F39. Sample 200

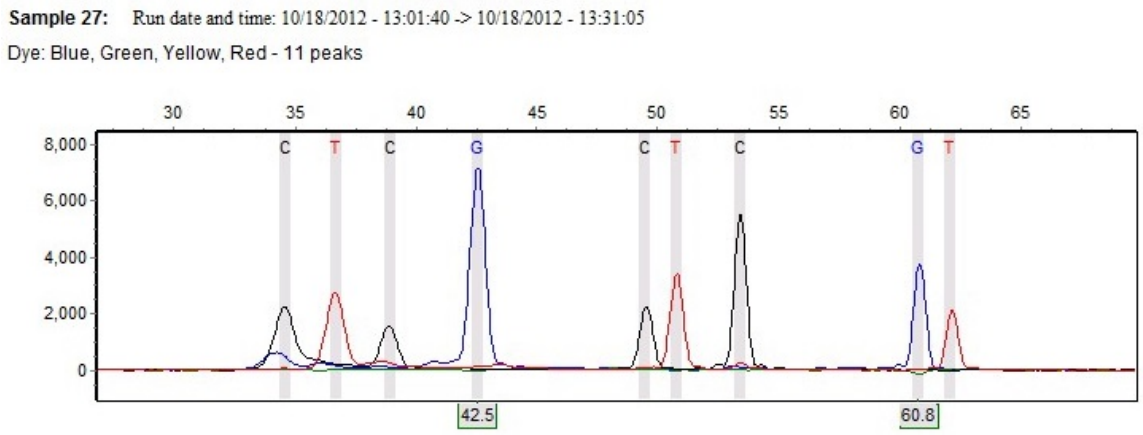

Figure F40. Sample 202

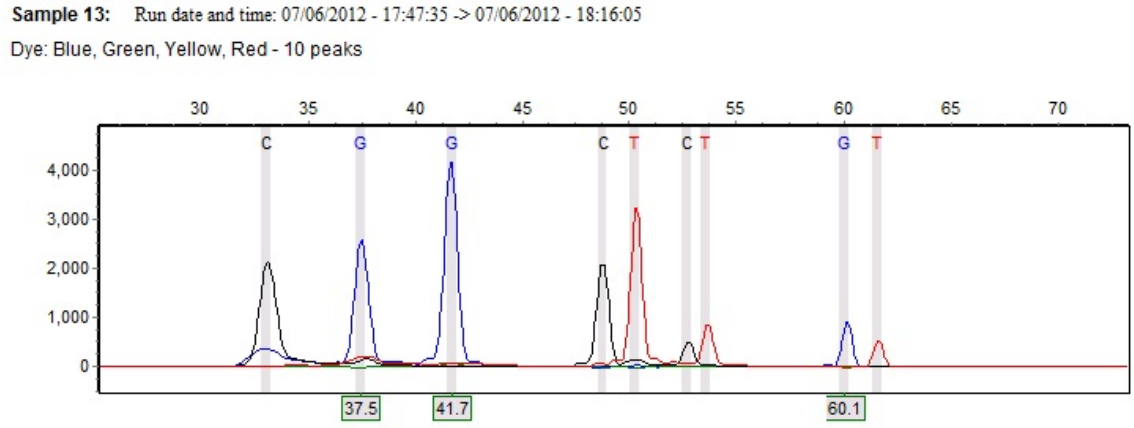

Figure F41. Sample 217

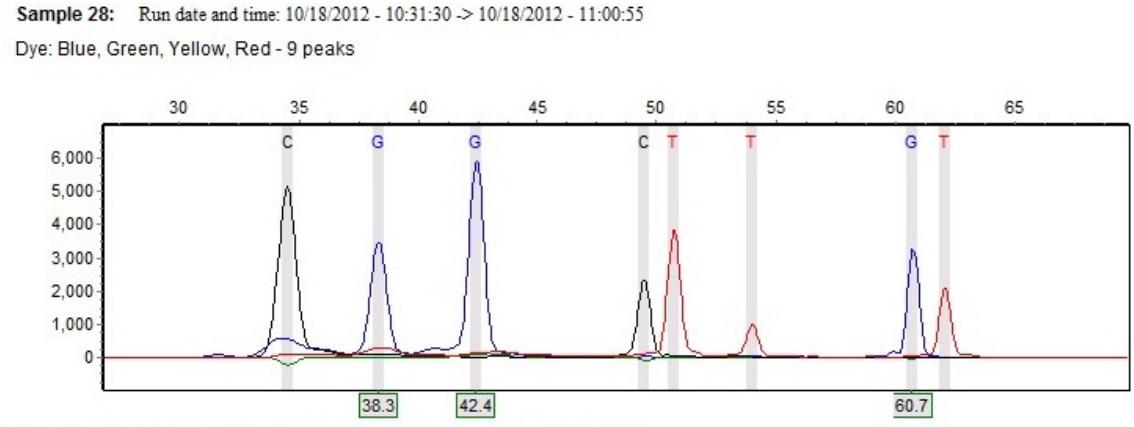

Figure F42. Sample 219

Sample 14: Run date and time: 07/13/2012 - 19:59:53 -> 07/13/2012 - 20:28:23

Dye: Blue, Green, Yellow, Red - 8 peaks

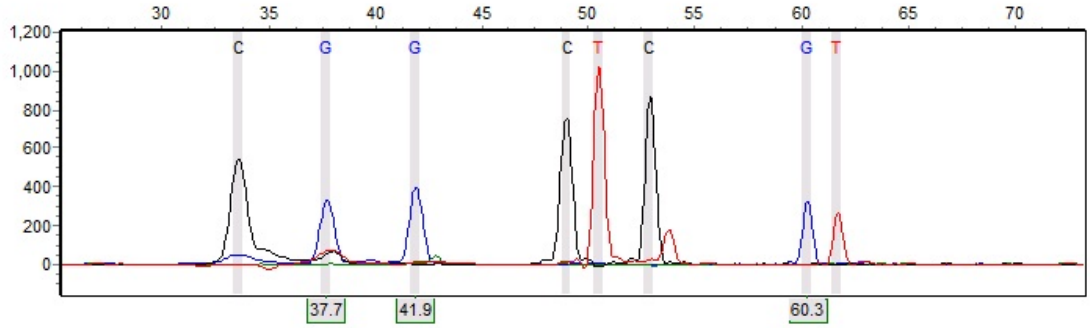

Figure F43. Sample 231

Sample 15: Run date and time: 07/13/2012 - 19:30:34 -> 07/13/2012 - 19:59:19

Dye: Blue, Green, Yellow, Red - 10 peaks

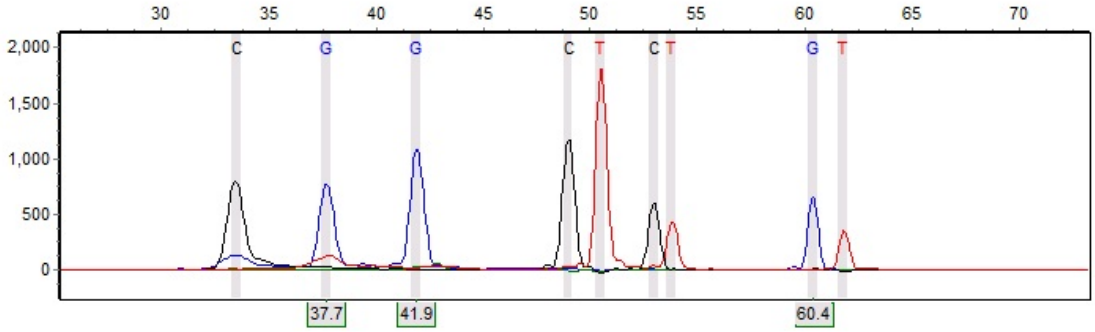

Figure F44. Sample 232

Sample 16: Run date and time: 07/13/2012 - 19:59:53 -> 07/13/2012 - 20:28:23

Dye: Blue, Green, Yellow, Red - 7 peaks

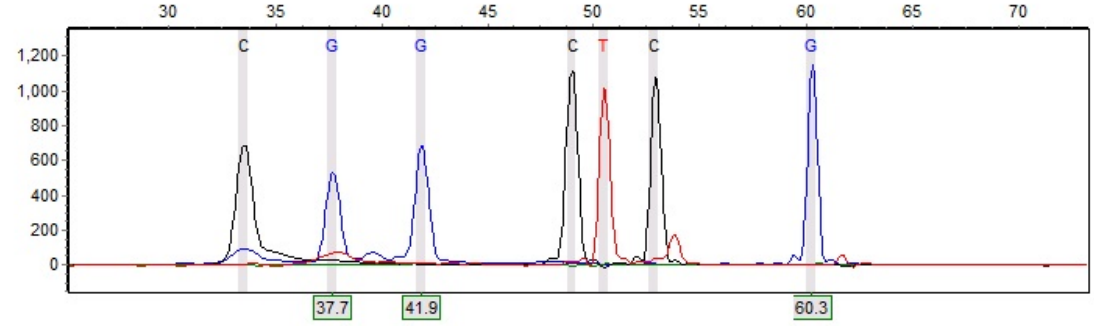

Figure F45. Sample 233

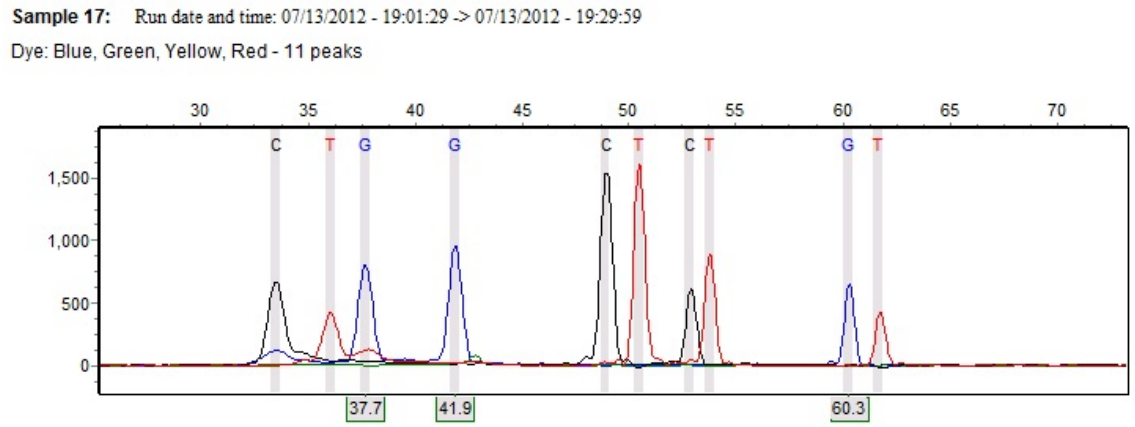

Figure F46. Sample 234

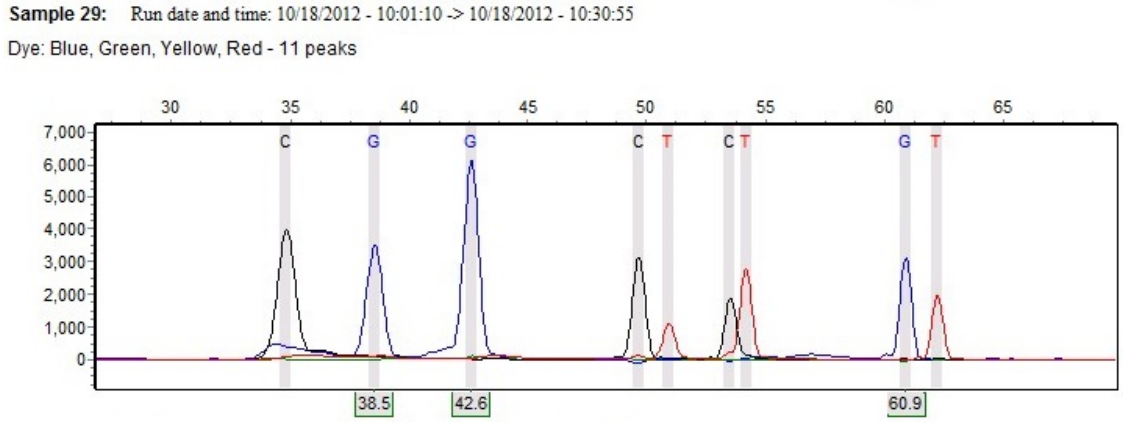

Figure F47. Sample 239

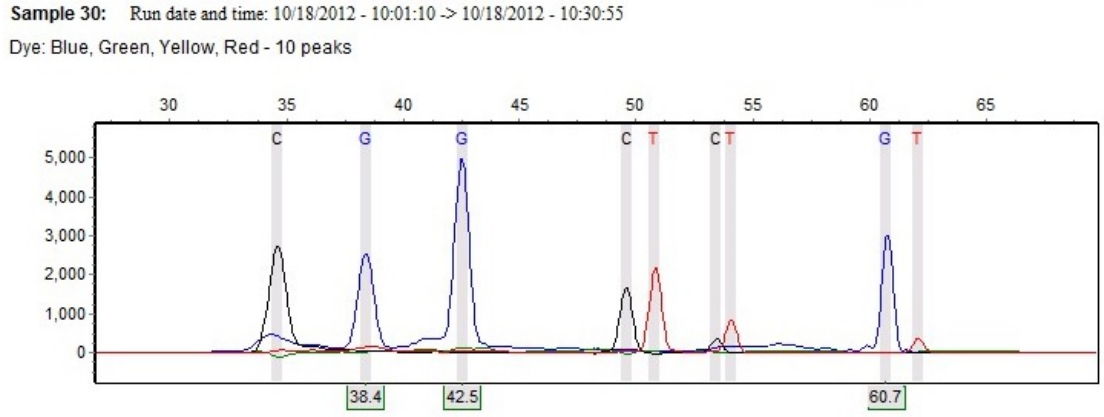

Figure F48. Sample 250

Sample 18: Run date and time: 07/06/2012 - 17:18:36 -> 07/06/2012 - 17:47:01

Dye: Blue, Green, Yellow, Red - 11 peaks

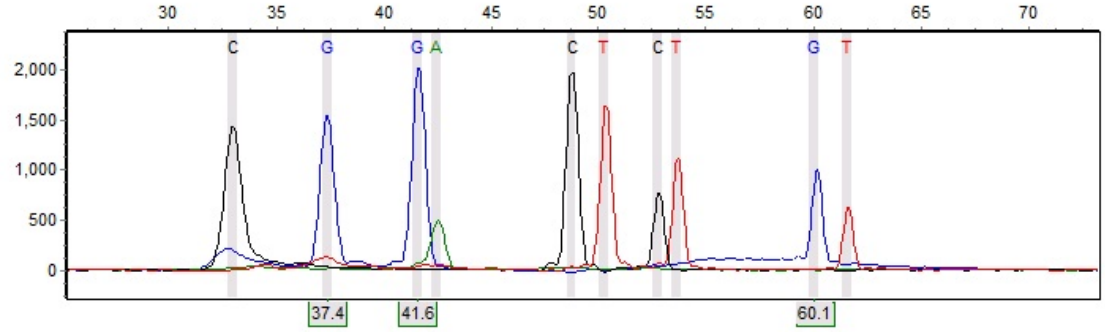

Figure F49. Sample 251

Sample 19: Run date and time: 07/06/2012 - 16:45:31 -> 07/06/2012 - 17:18:01

Dye: Blue, Green, Yellow, Red - 10 peaks

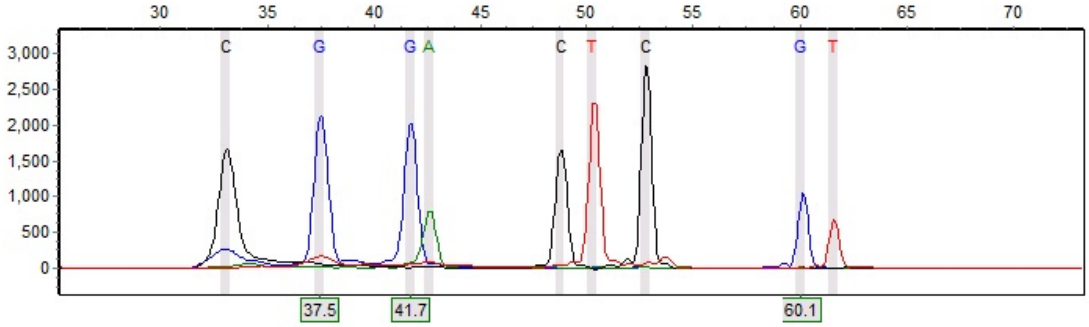

Figure F50. Sample 254

Sample 31: Run date and time: 10/18/2012 - 10:01:10 -> 10/18/2012 - 10:30:55

Dye: Blue, Green, Yellow, Red - 9 peaks

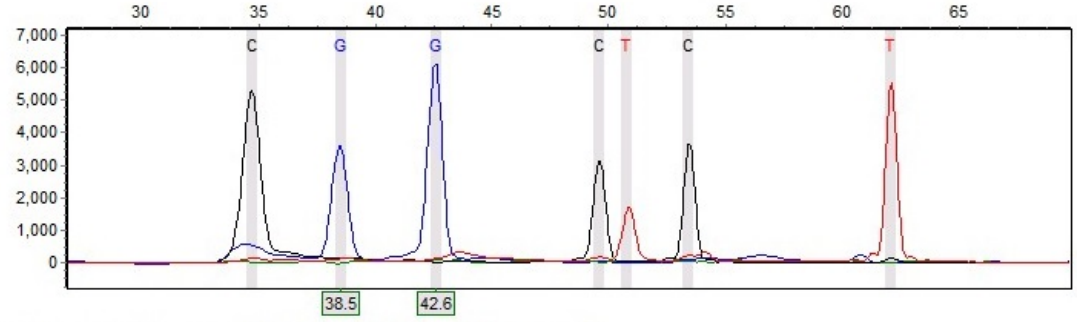

Figure F51. Sample 256

Sample 20: Run date and time: 07/13/2012 - 19:30:34 -> 07/13/2012 - 19:59:19

Dye: Blue, Green, Yellow, Red - 9 peaks

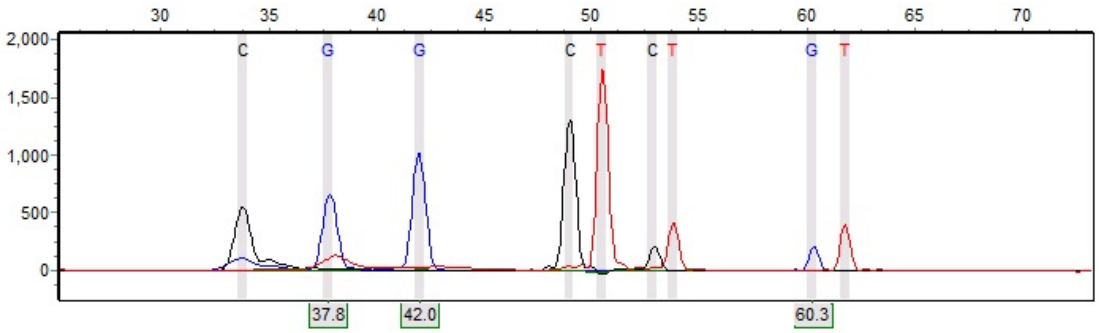

Figure F52. Sample 259

Sample 32: Run date and time: 10/29/2012 - 16:00:18 -> 10/29/2012 - 16:28:48

Dye: Blue, Green, Yellow, Red - 8 peaks

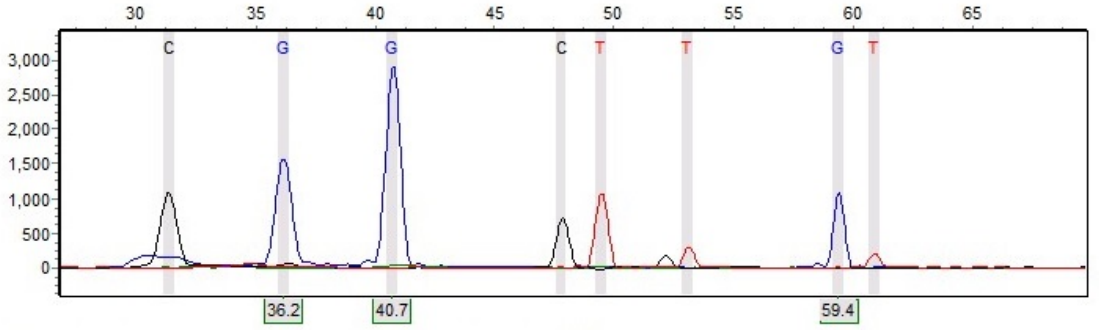

Figure F53. Sample 260

Sample 21: Run date and time: 07/13/2012 - 17:30:21 -> 07/13/2012 - 18:02:31

Dye: Blue, Green, Yellow, Red - 7 peaks

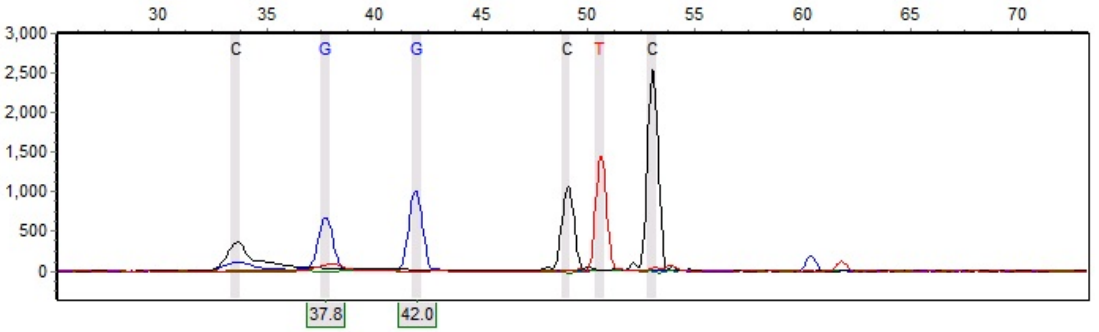

Figure F54. Sample 264

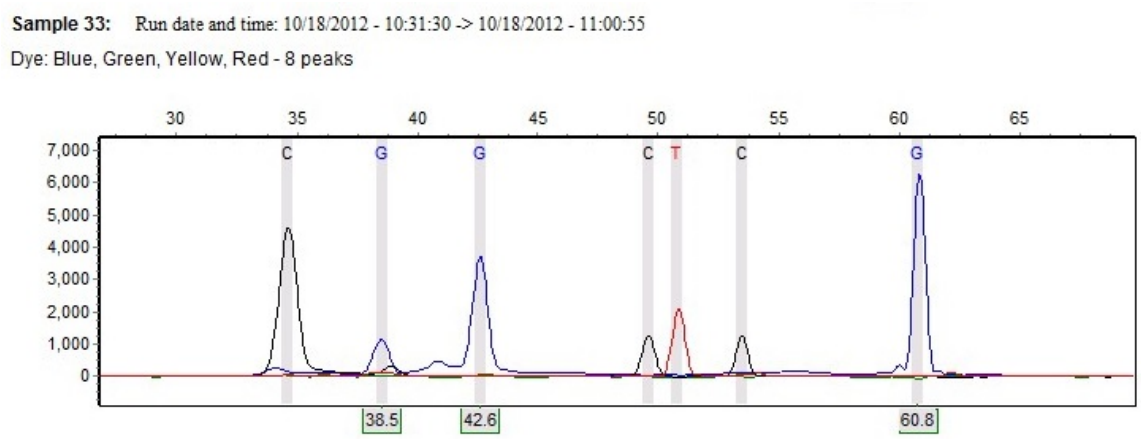

Figure F55. Sample 265

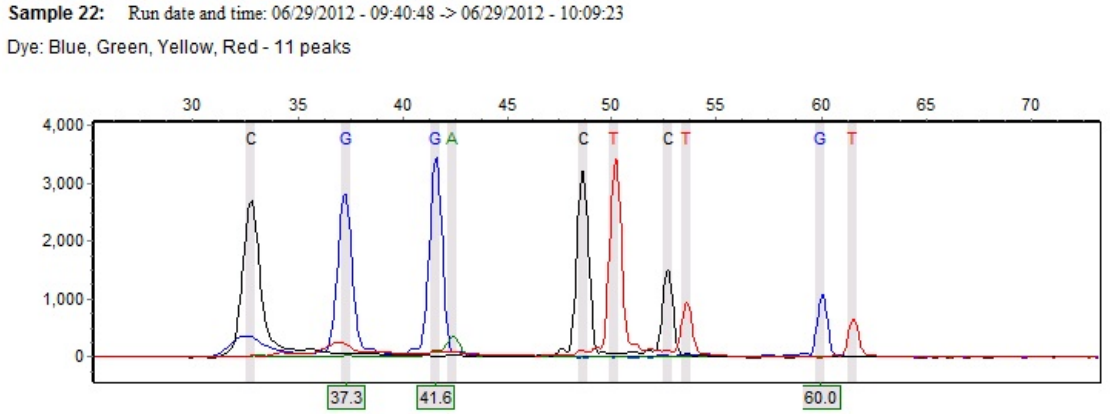

Figure F56. Sample 268

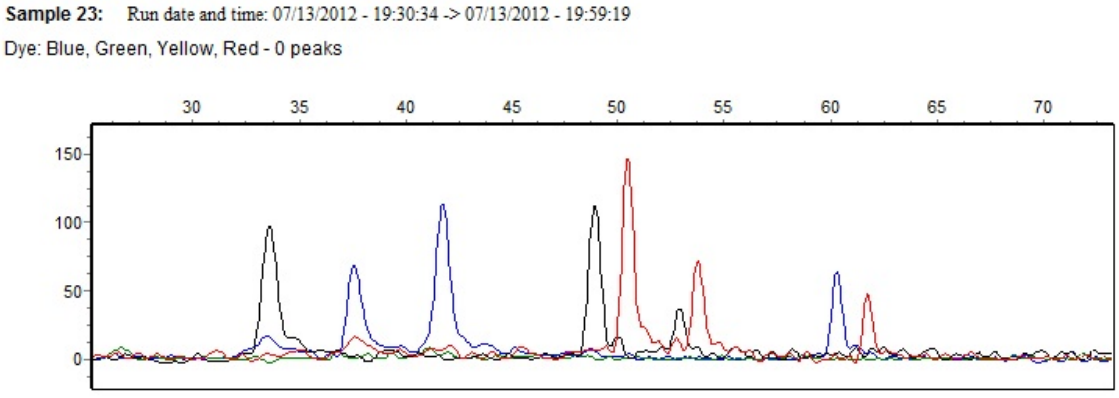

Figure F57. Sample 269

Sample 34: Run date and time: 10/18/2012 - 08:57:12 -> 10/18/2012 - 09:29:55

Dye: Blue, Green, Yellow, Red - 11 peaks

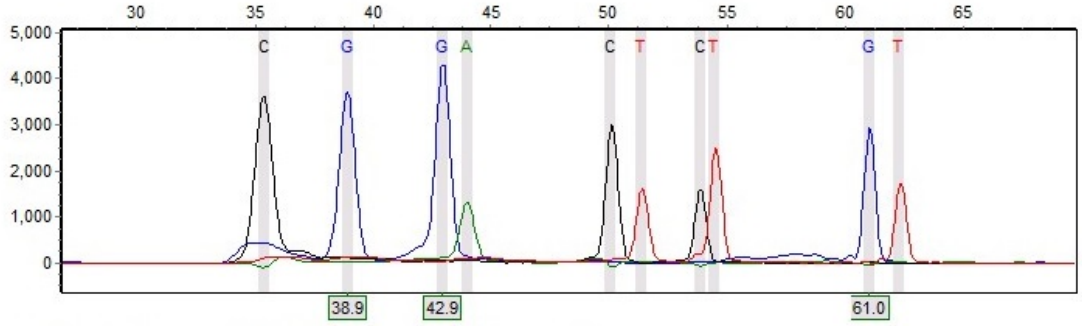

Figure F58. Sample 270

Sample 35: Run date and time: 10/29/2012 - 15:30:58 -> 10/29/2012 - 15:59:44

Dye: Blue, Green, Yellow, Red - 8 peaks

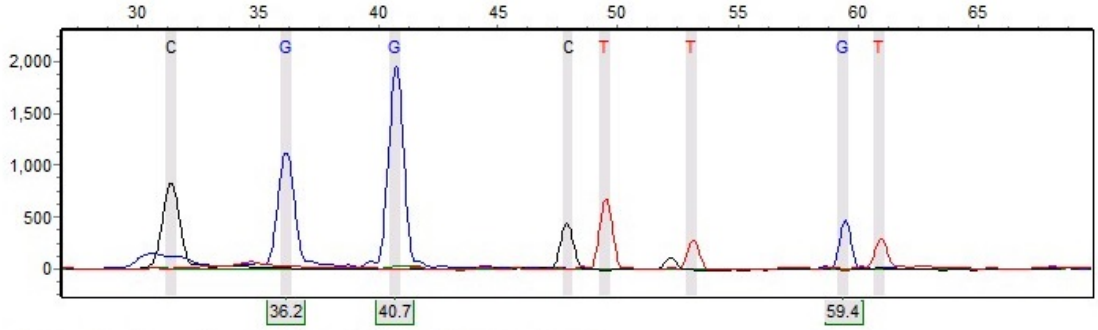

Figure F59. Sample 271

Sample 24: Run date and time: 07/06/2012 - 17:18:36 -> 07/06/2012 - 17:47:01

Dye: Blue, Green, Yellow, Red - 9 peaks

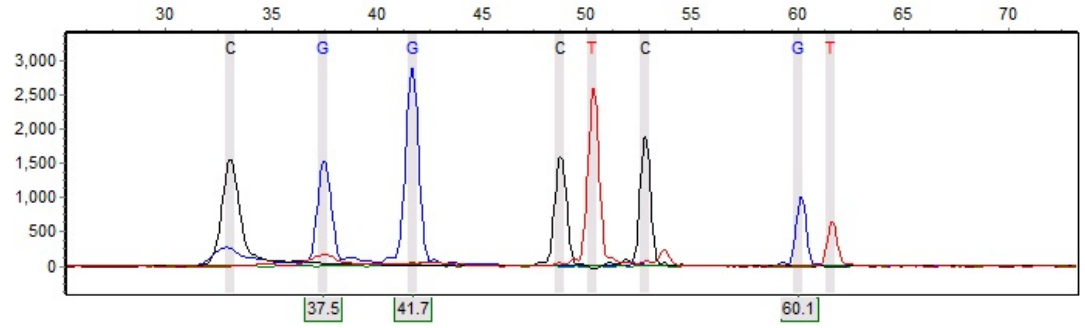

Figure F60. Sample 273

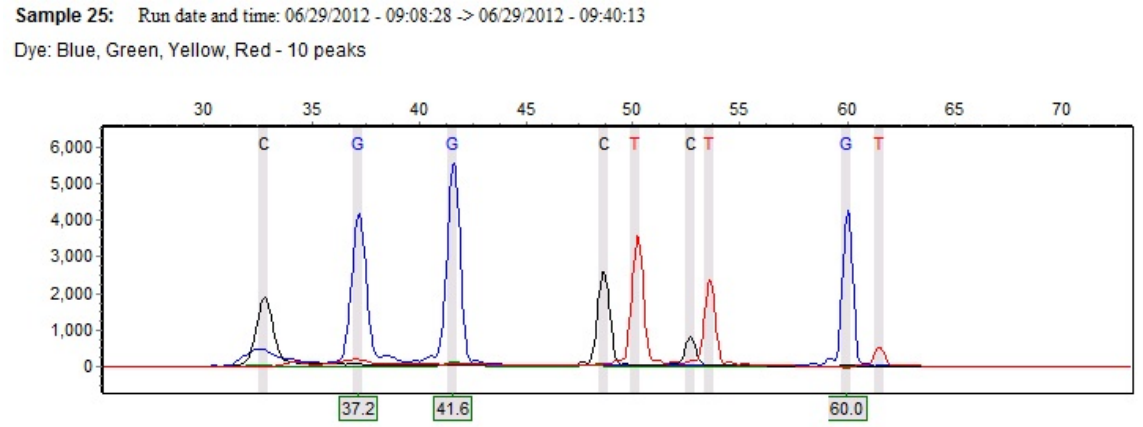

Figure F61. Sample 275

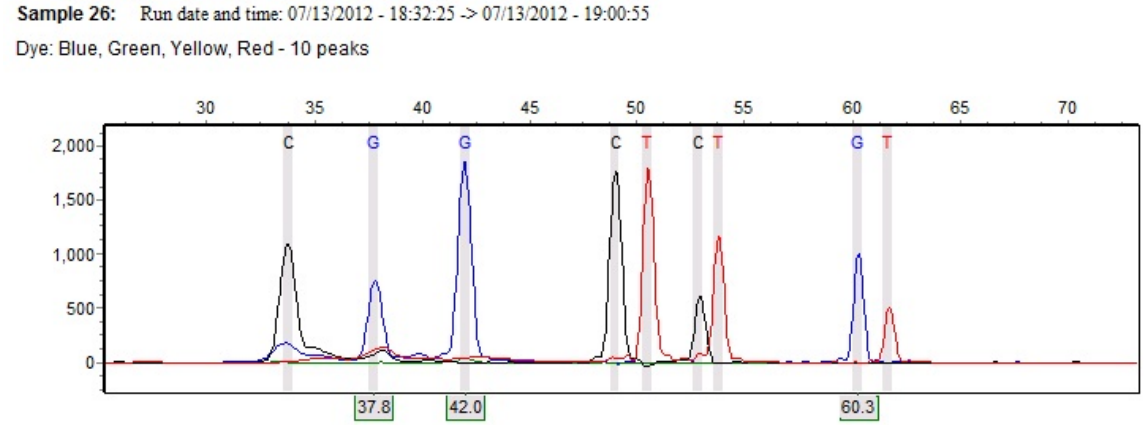

Figure F62. Sample 276

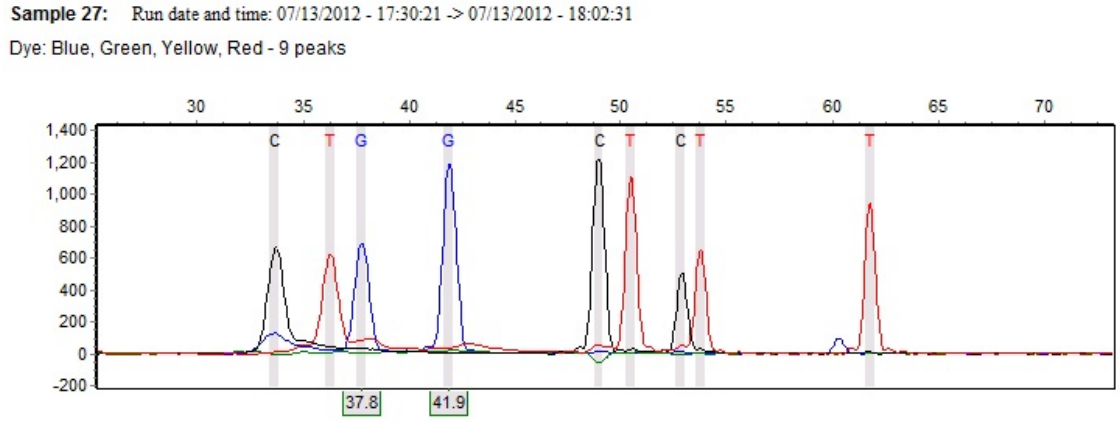

Figure F63. Sample 278

Sample 28: Run date and time: 07/09/2012 - 10:55:20 -> 07/09/2012 - 11:33:00

Dye: Blue, Green, Yellow, Red - 10 peaks

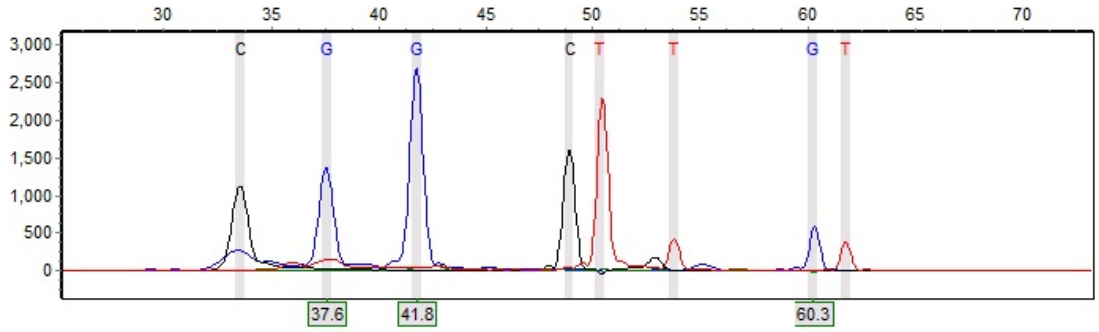

Figure F64. Sample 279

Sample 29: Run date and time: 07/13/2012 - 17:30:21 -> 07/13/2012 - 18:02:31

Dye: Blue, Green, Yellow, Red - 9 peaks

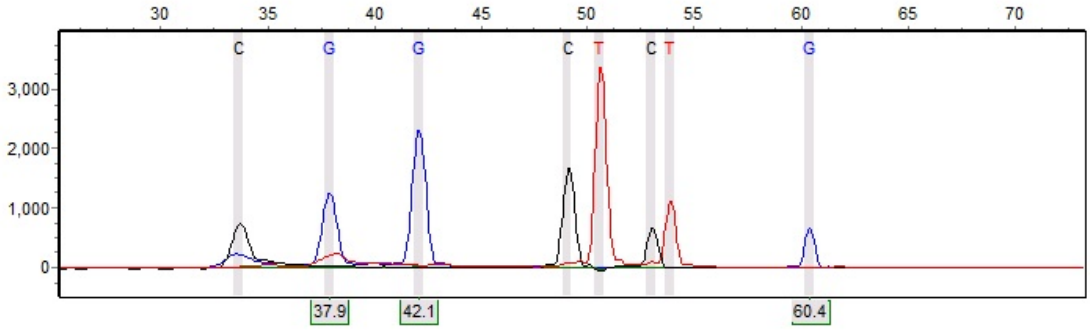

Figure F65. Sample 281

Sample 30: Run date and time: 07/13/2012 - 19:59:53 -> 07/13/2012 - 20:28:23

Dye: Blue, Green, Yellow, Red - 1 peaks

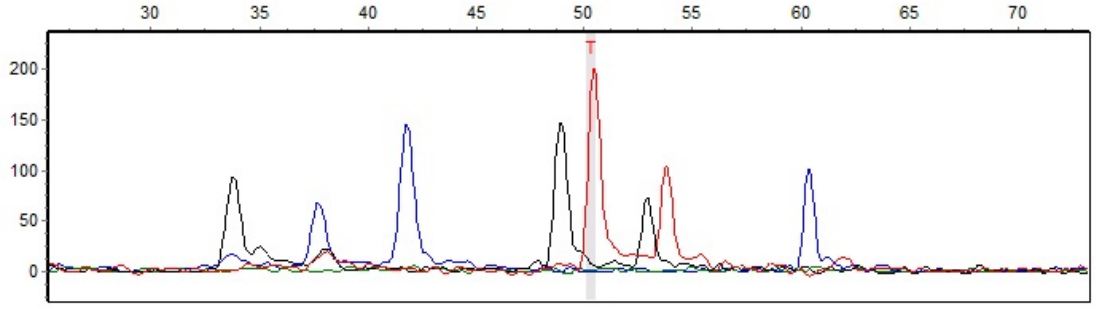

Figure F66. Sample 283

Sample 31: Run date and time: 07/13/2012 - 18:32:25 -> 07/13/2012 - 19:00:55

Dye: Blue, Green, Yellow, Red - 10 peaks

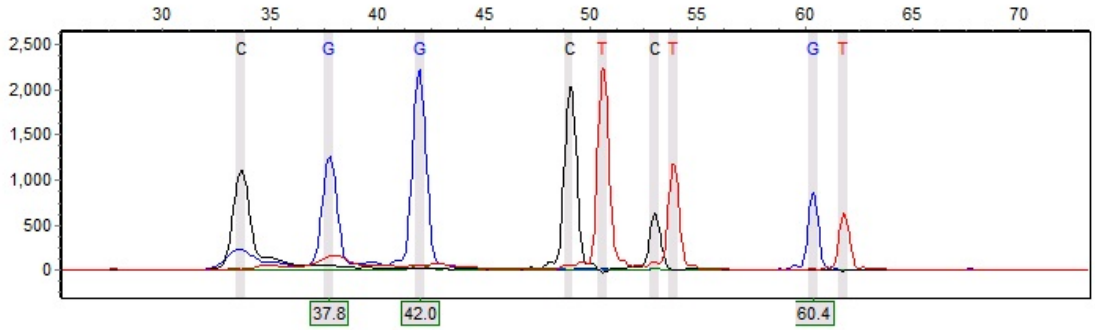

Figure F67. Sample 285

Sample 32: Run date and time: 07/09/2012 - 15:05:07 -> 07/09/2012 - 15:36:37

Dye: Blue, Green, Yellow, Red - 11 peaks

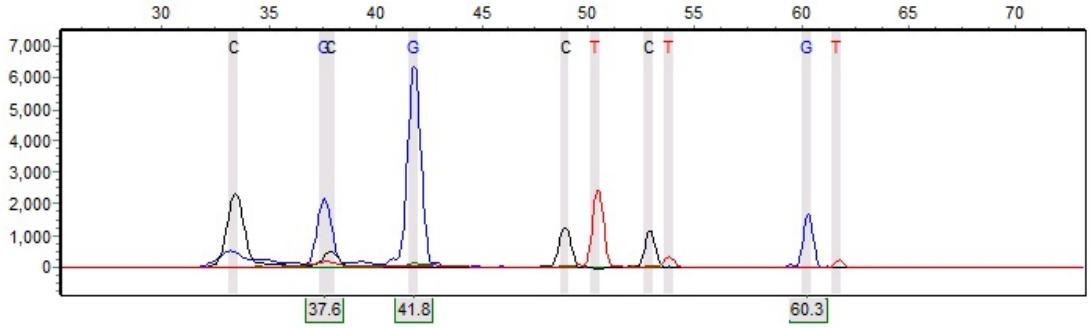

Figure F68. Sample 286

Sample 36: Run date and time: 10/30/2012 - 13:47:50 -> 10/30/2012 - 14:22:15

Dye: Blue, Green, Yellow, Red - 9 peaks

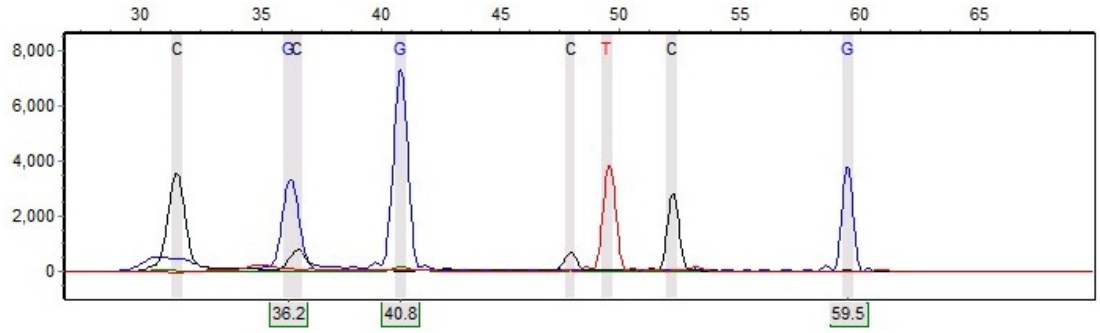

Figure F69. Sample 296

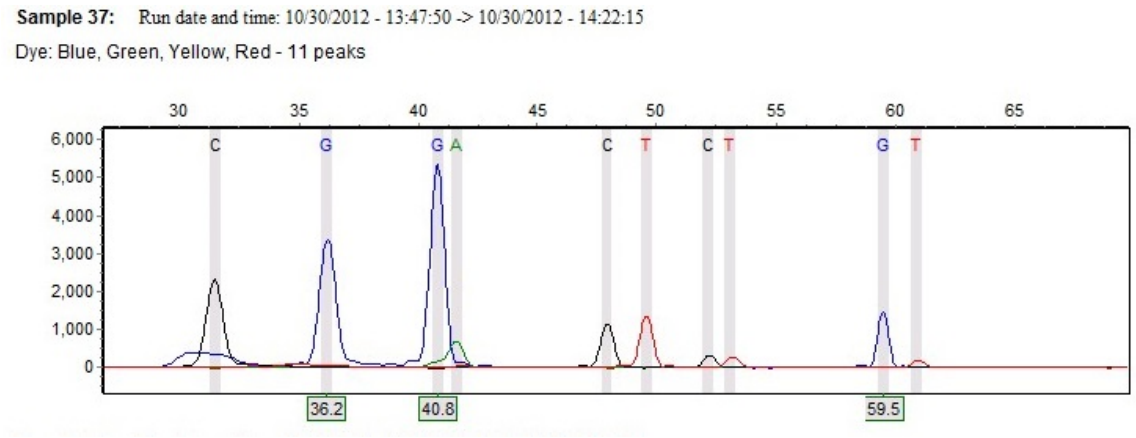

Figure F70. Sample 297

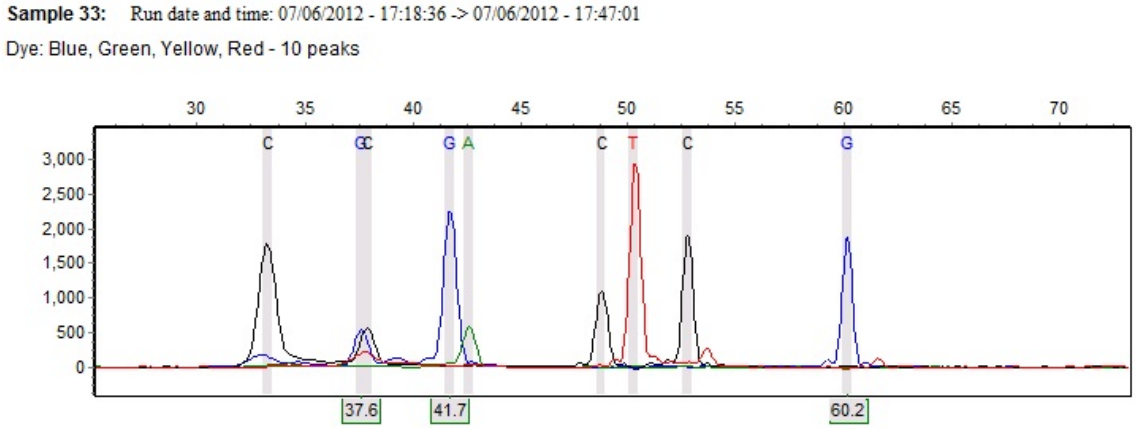

Figure F71. Sample 298

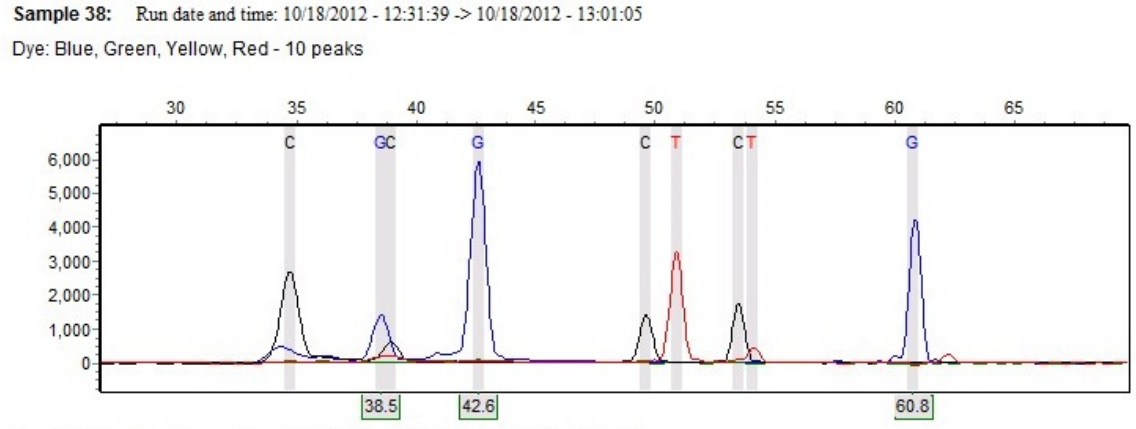

Figure F72. Sample 300

Sample 39: Run date and time: 10/18/2012 - 08:57:12 -> 10/18/2012 - 09:29:55

Dye: Blue, Green, Yellow, Red - 13 peaks

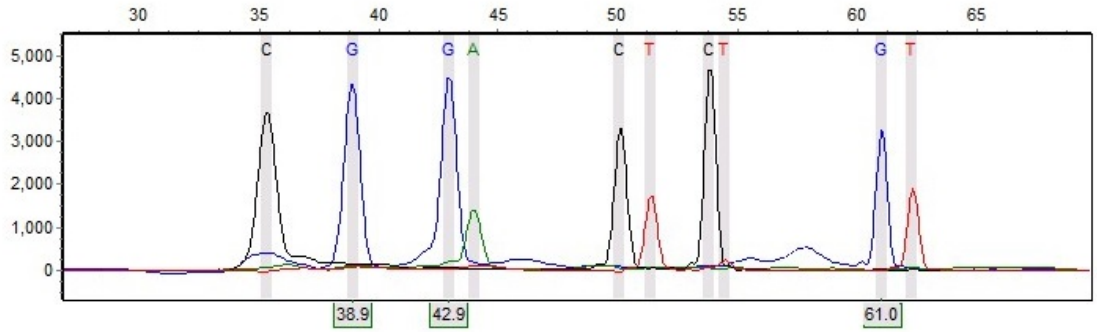

Figure F73. Sample 305

Sample 40: Run date and time: 10/18/2012 - 12:31:39 -> 10/18/2012 - 13:01:05

Dye: Blue, Green, Yellow, Red - 11 peaks

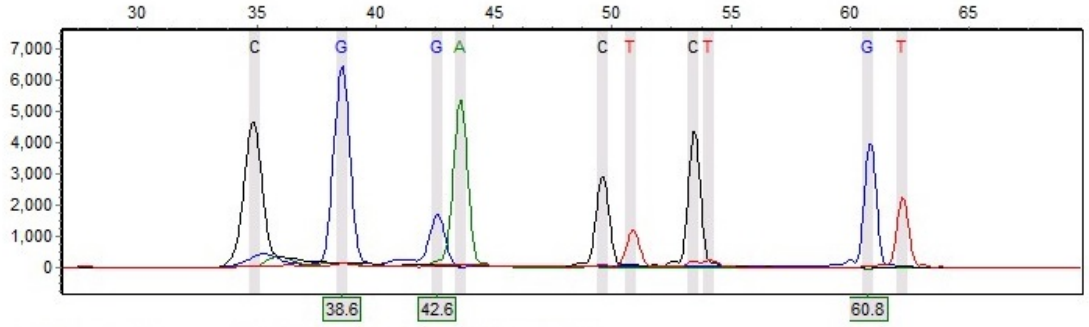

Figure F74. Sample 306

Sample 34: Run date and time: 07/13/2012 - 18:32:25 -> 07/13/2012 - 19:00:55

Dye: Blue, Green, Yellow, Red - 9 peaks

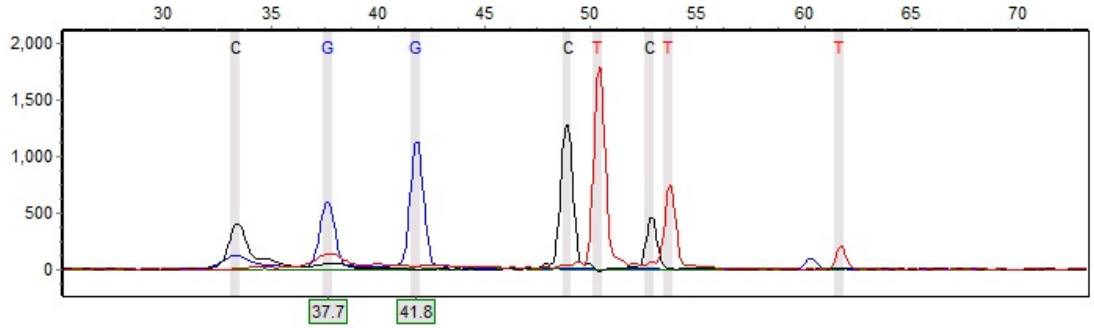

Figure F75. Sample 313

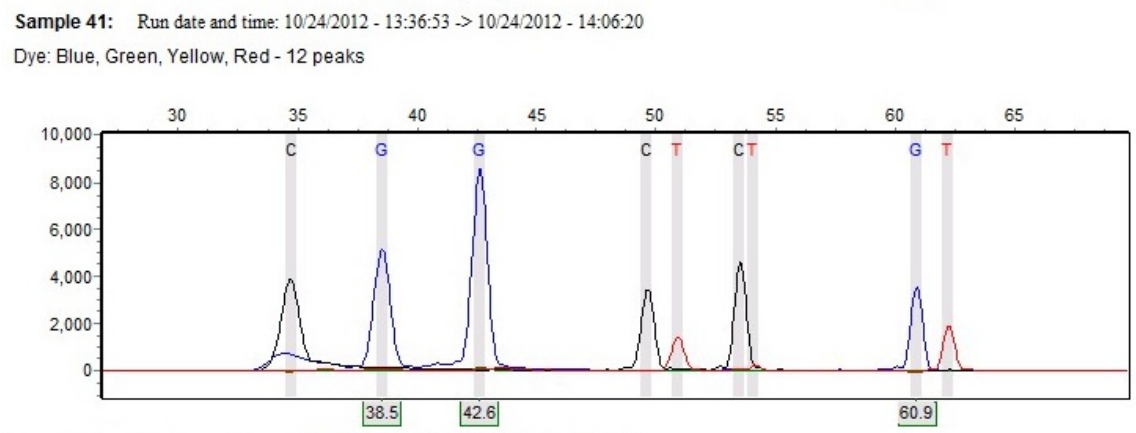

Figure F76. Sample 318

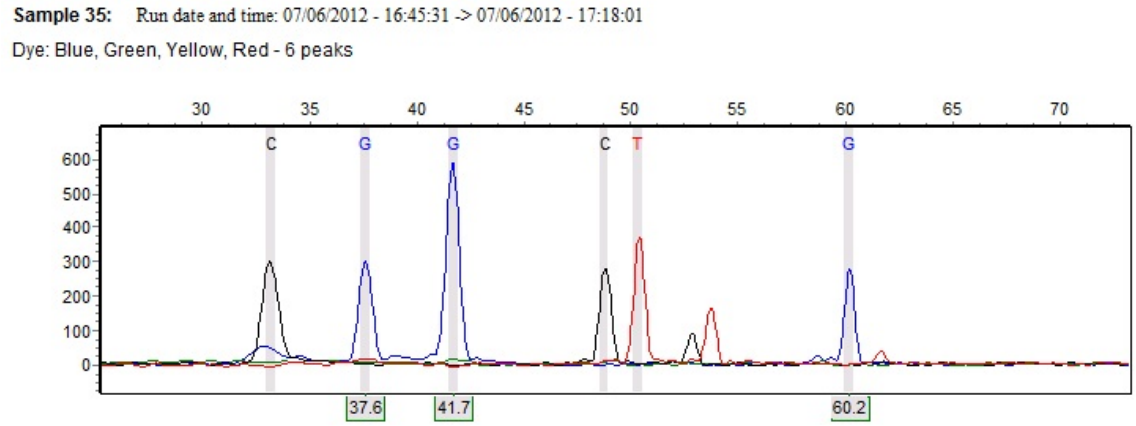

Figure F77. Sample 319

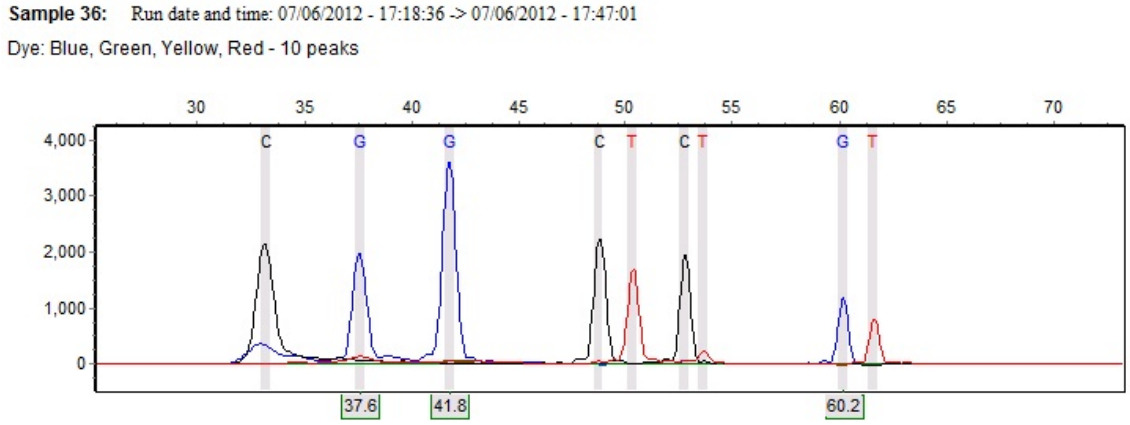

Figure F78. Sample 321

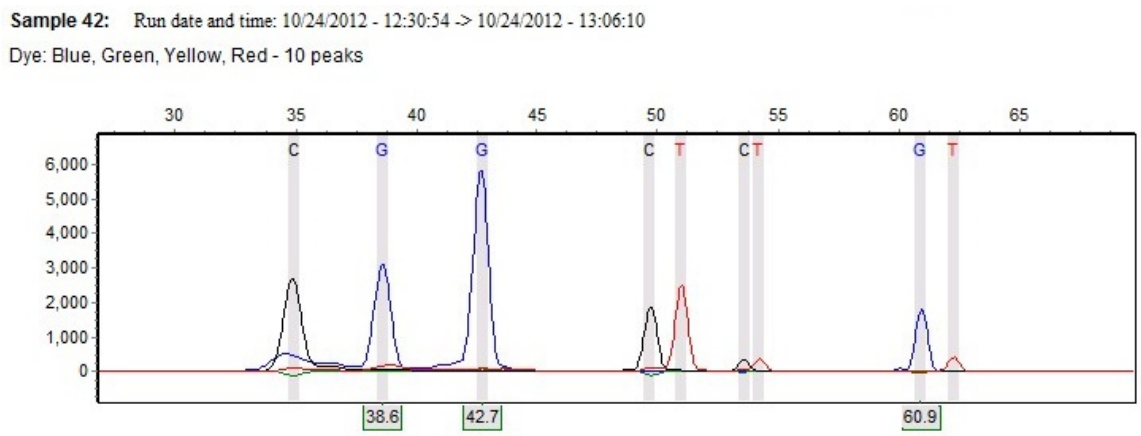

Figure F79. Sample 327

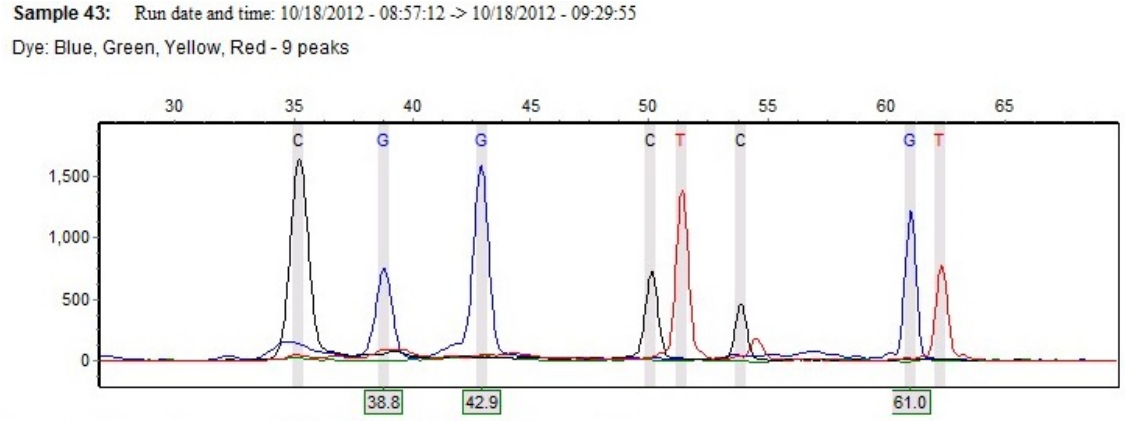

Figure F80. Sample 328

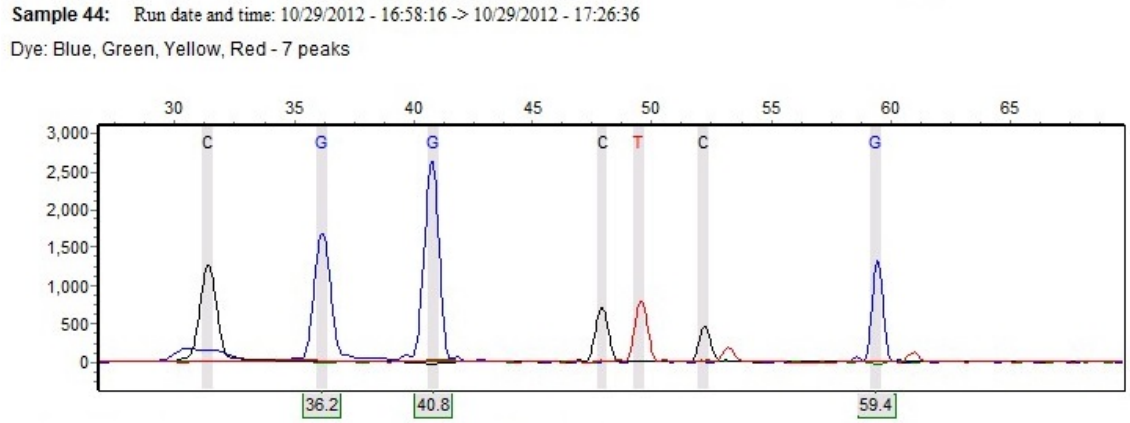

Figure F81. Sample 348

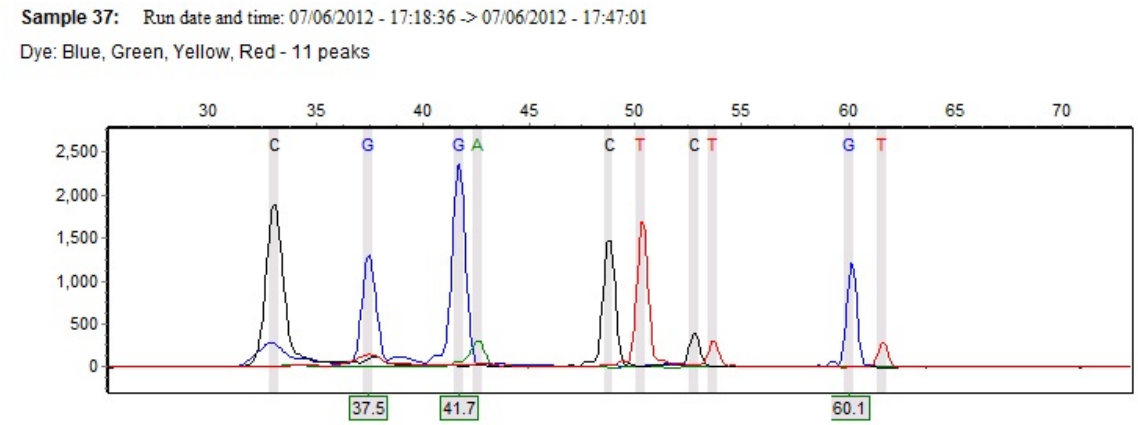

Figure F82. Sample 351

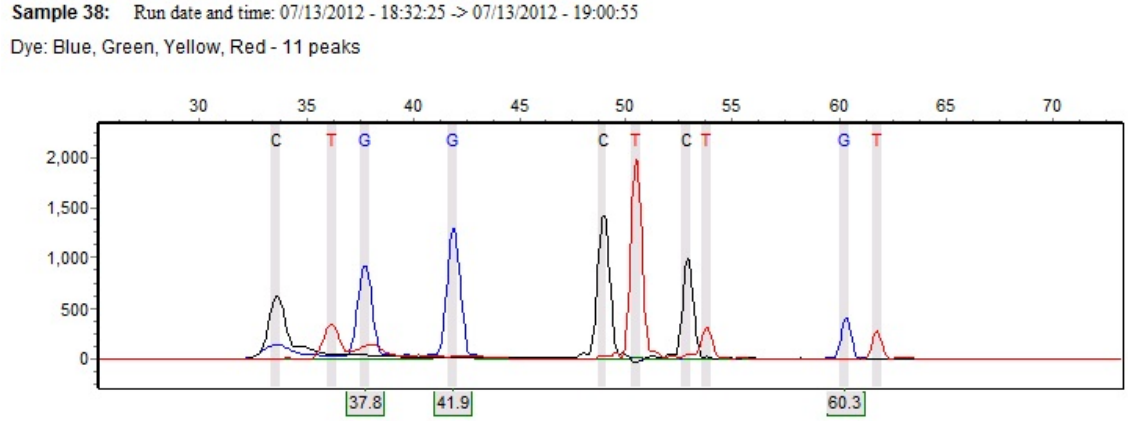

Figure F83. Sample 354

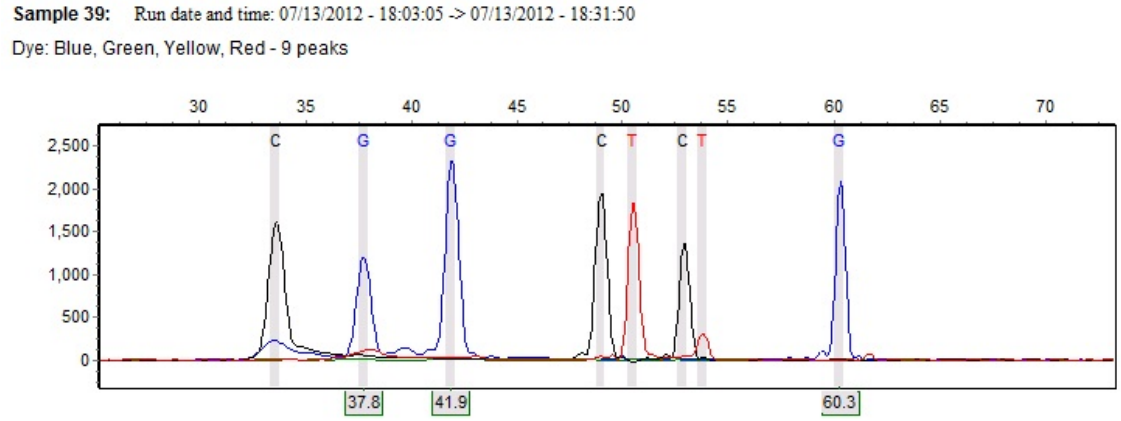

Figure F84. Sample 362

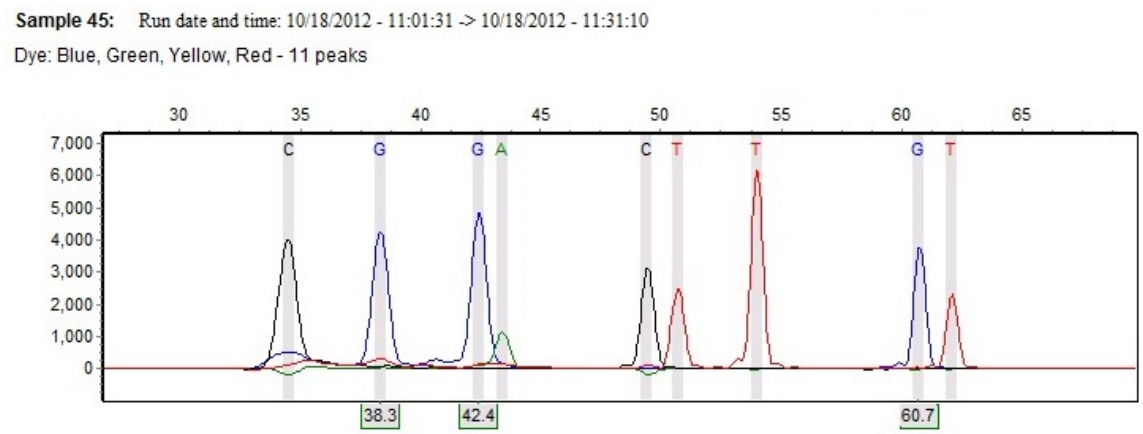

Figure F85. Sample 364

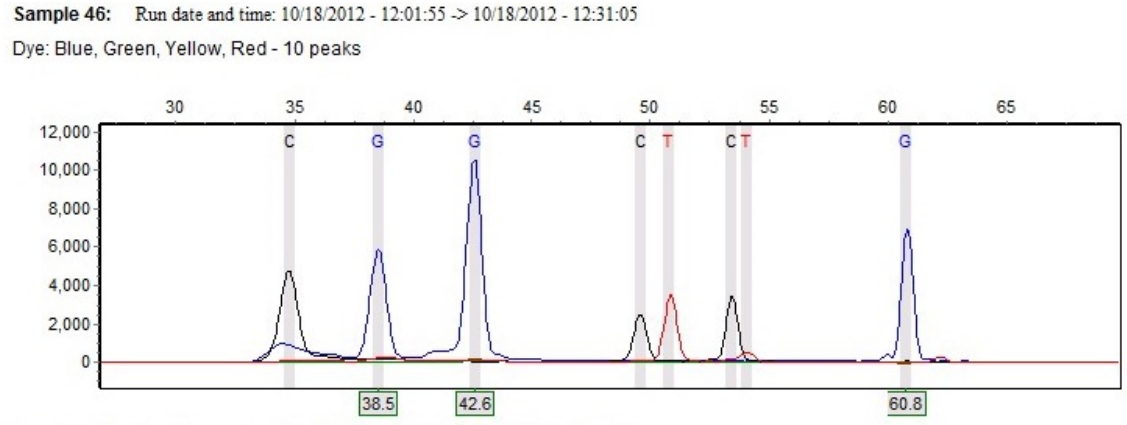

Figure F86. Sample 367

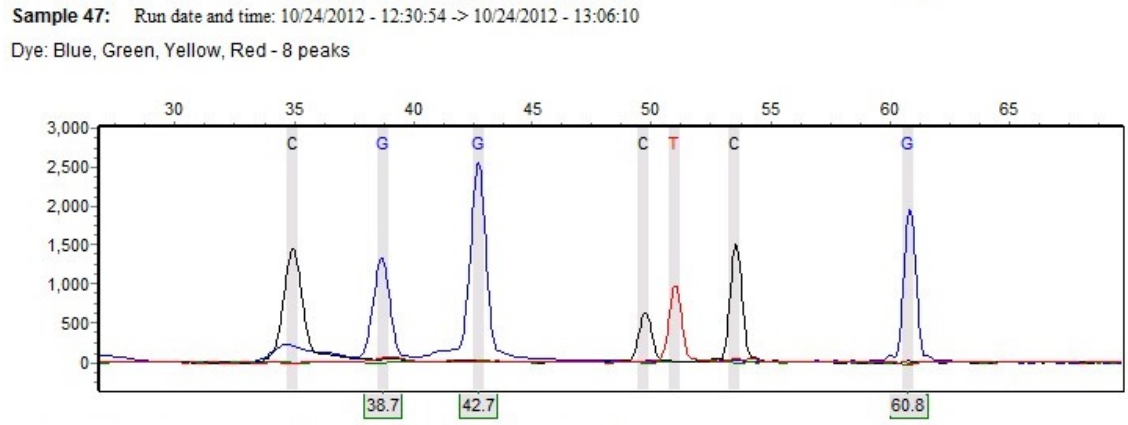

Figure F87. Sample 368

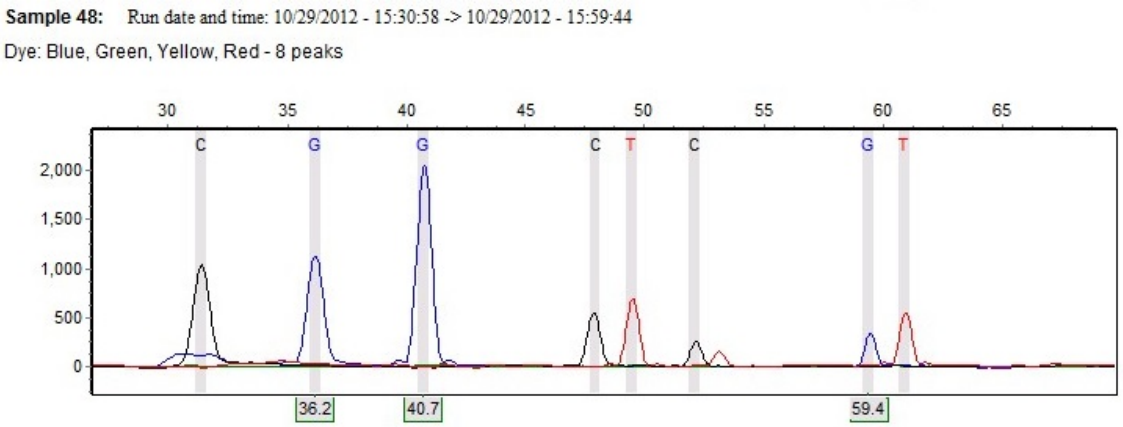

Figure F88. Sample 369

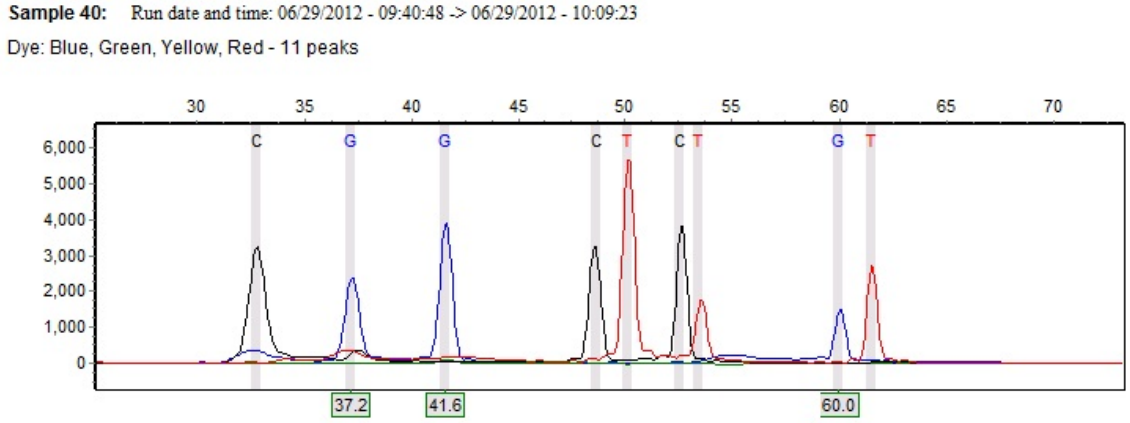

Figure F89. Sample 372

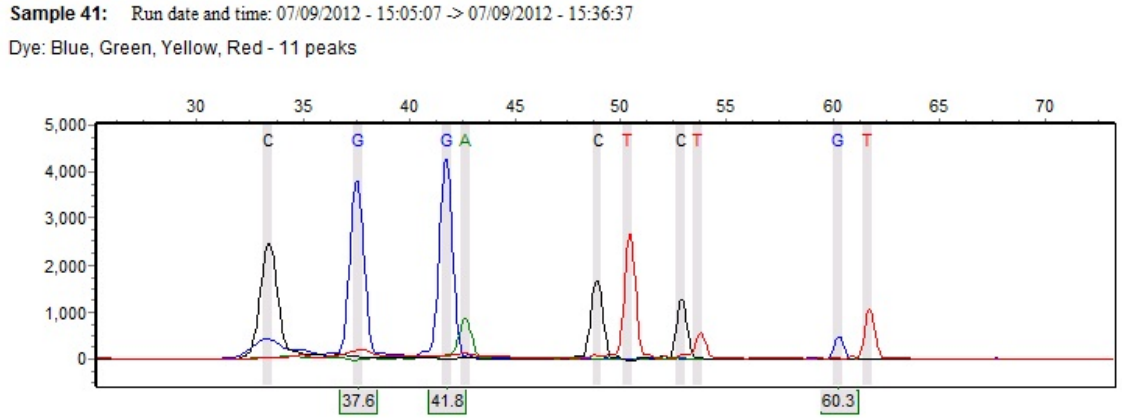

Figure F90. Sample 374

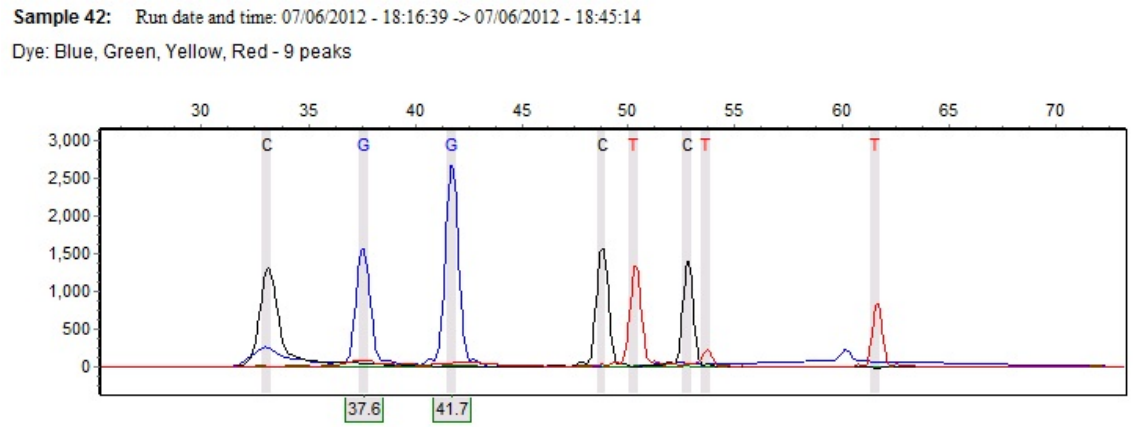

Figure F91. Sample 377

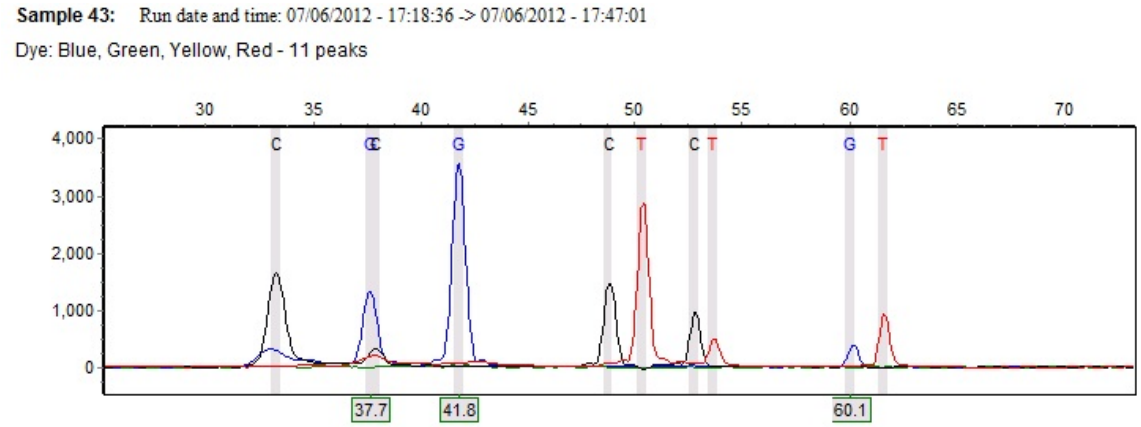

Figure F92. Sample 378

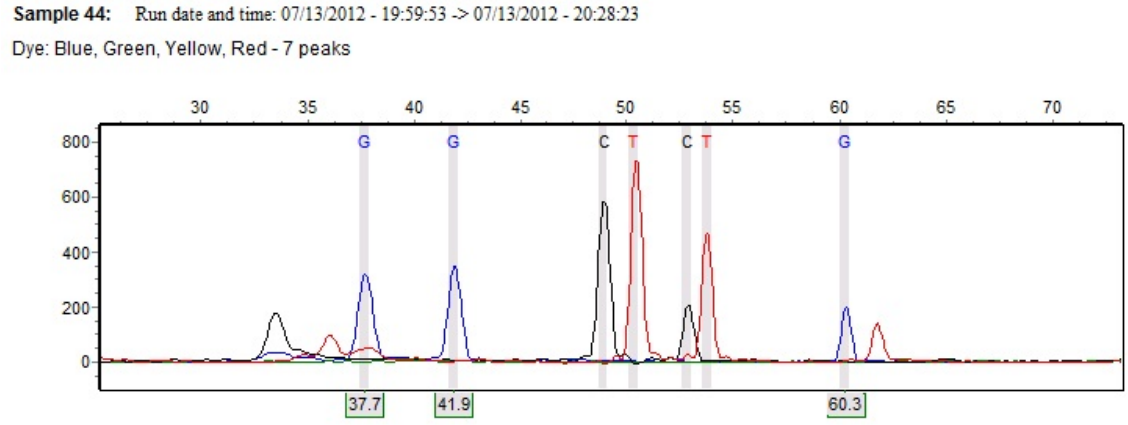

Figure F93. Sample 388

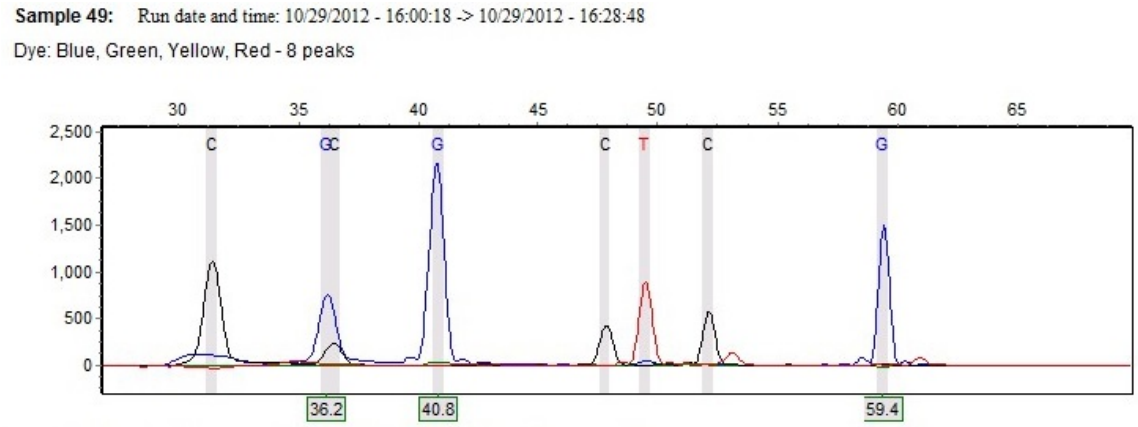

Figure F94. Sample 396

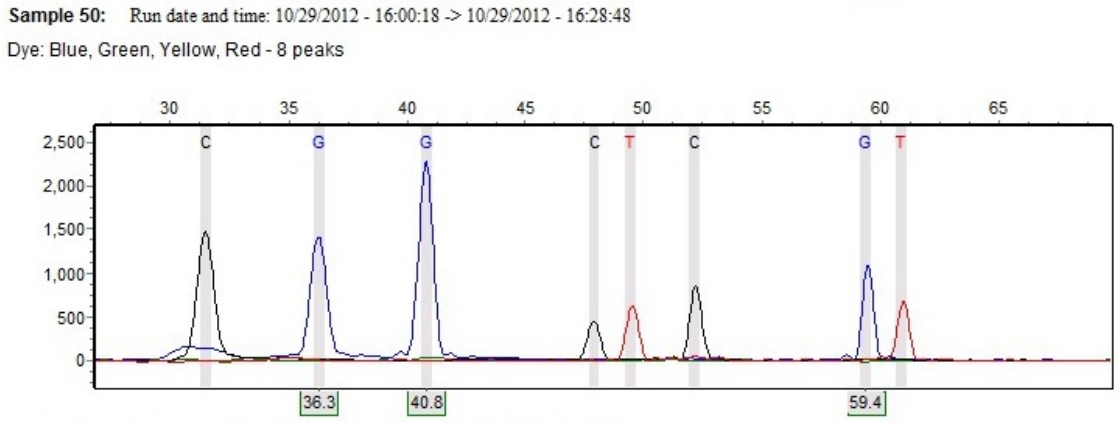

Figure F95. Sample 412

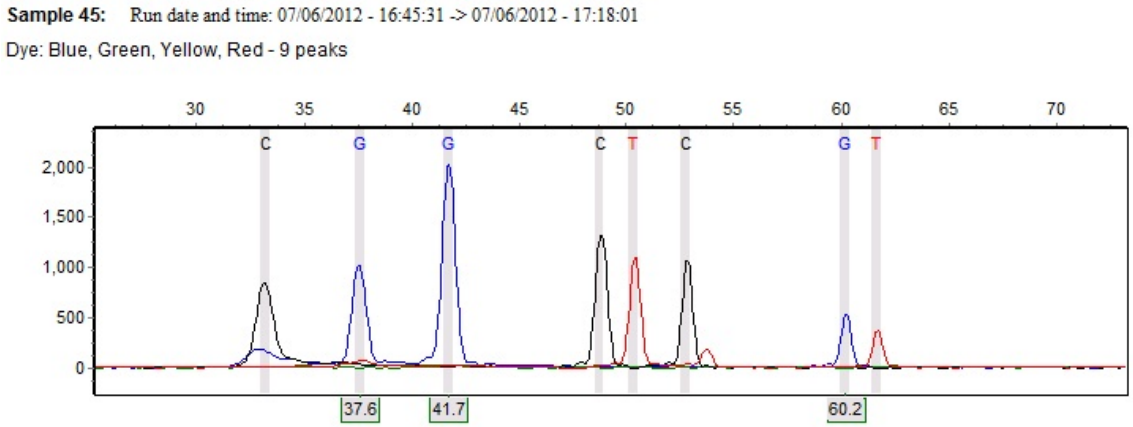

Figure F96. Sample 419

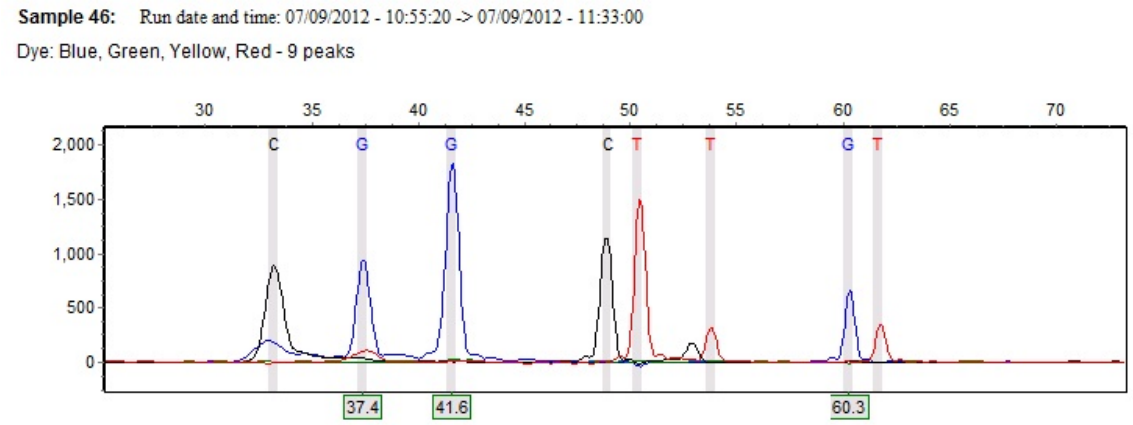

Figure F97. Sample 421

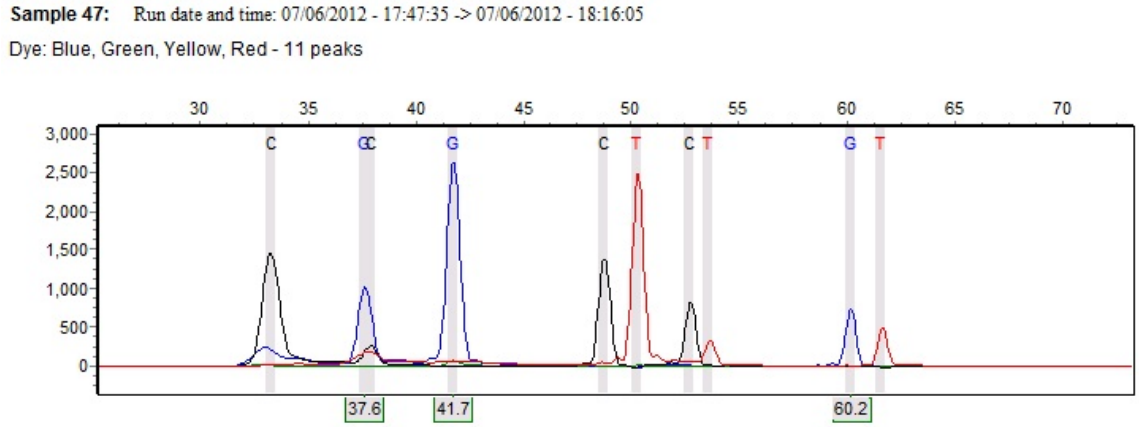

Figure F98. Sample 451

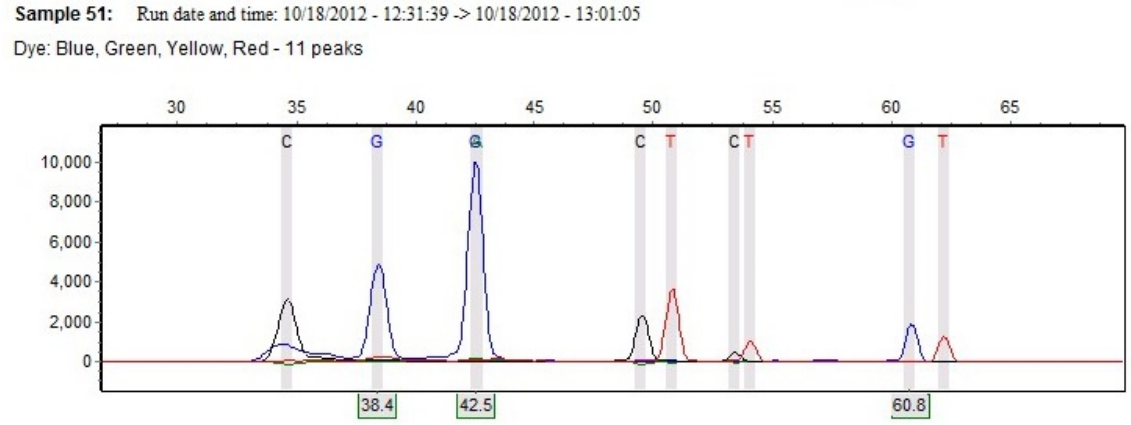

Figure F99. Sample 453

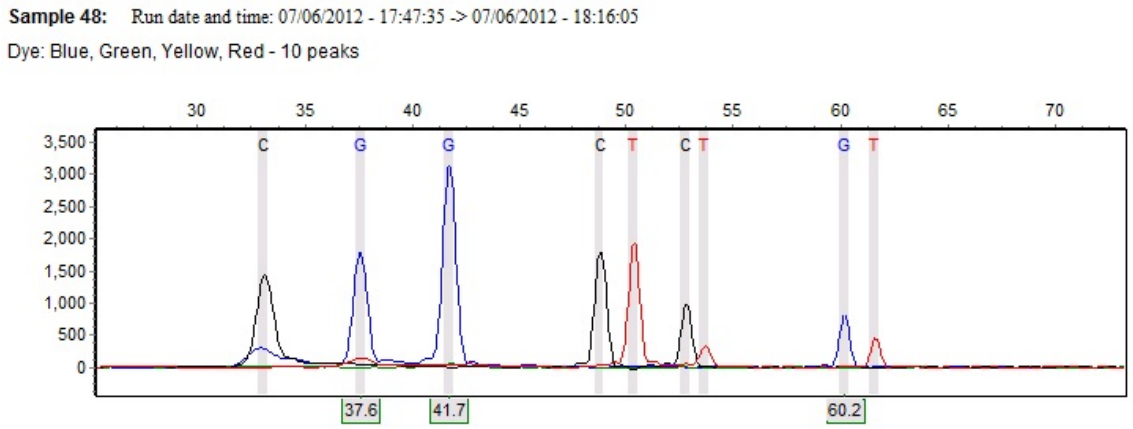

Figure F100. Sample 457

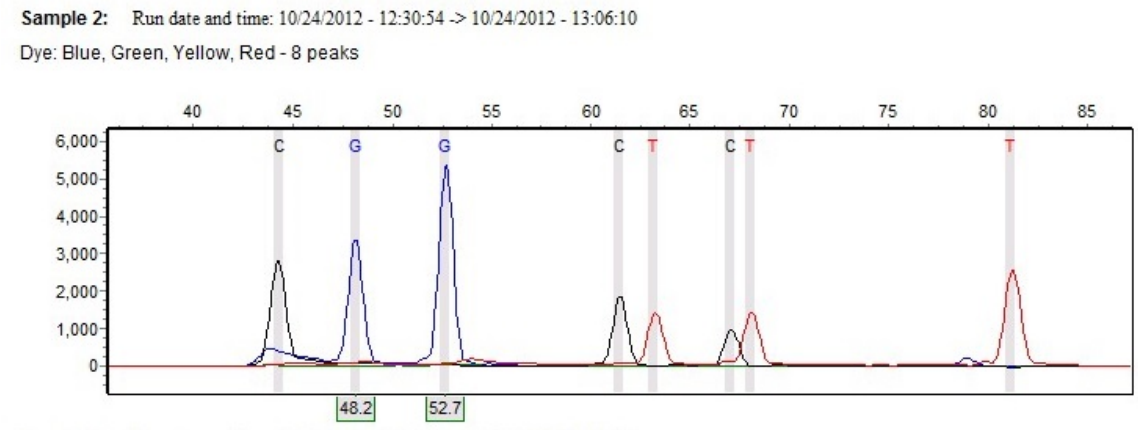

Figure F101. Sample 458

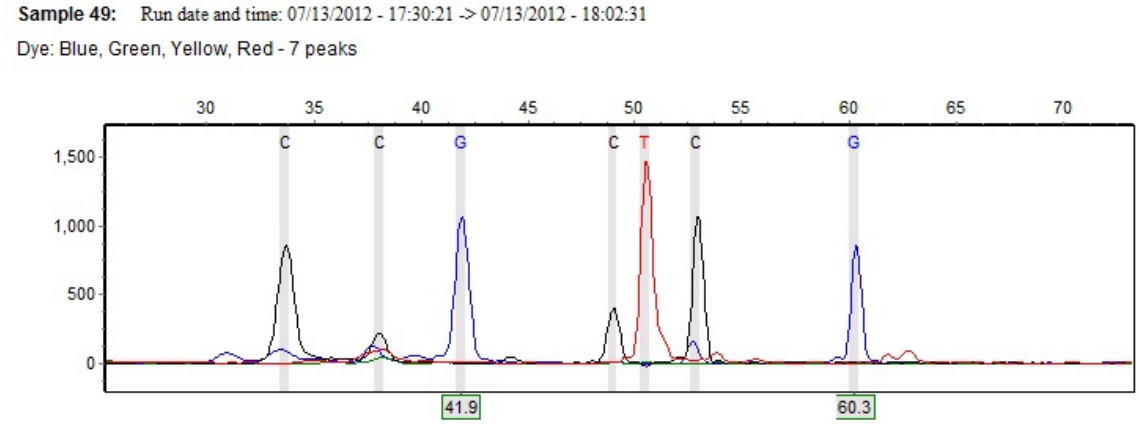

Figure F102. Sample 487

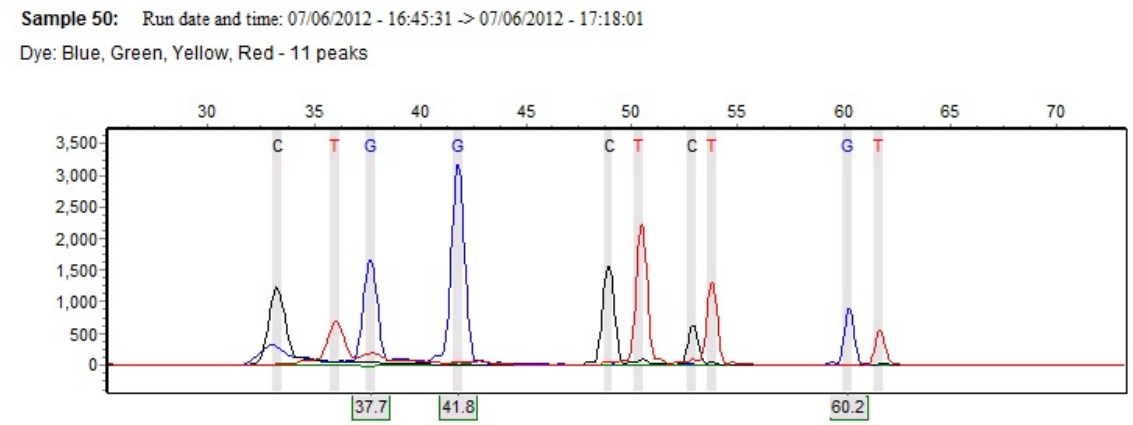

Figure F103. Sample 492

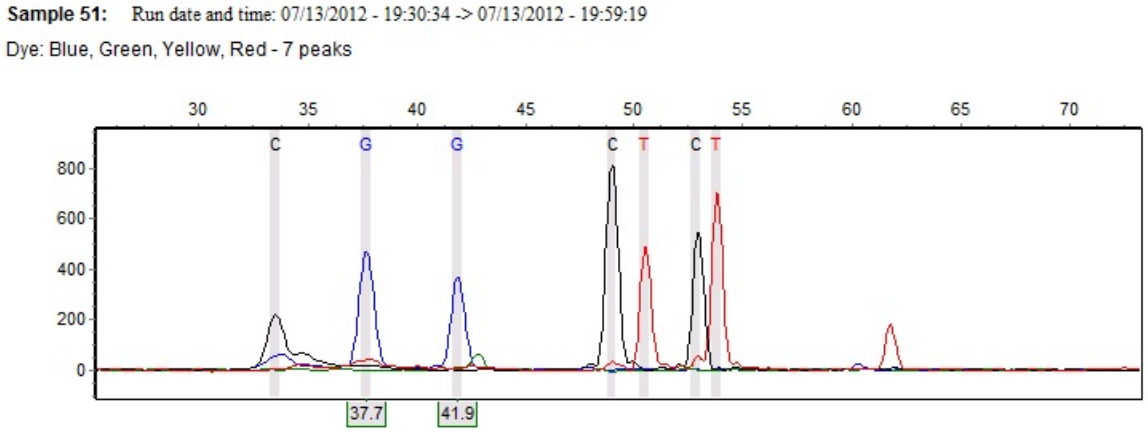

Figure F104. Sample 498

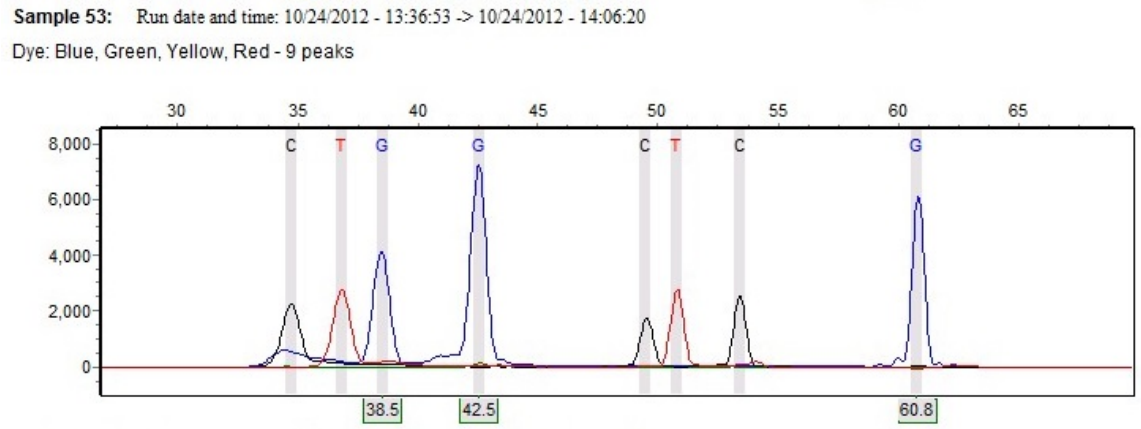

Figure F105. Sample 512

Sample 54: Run date and time: 10/29/2012 - 16:29:22 -> 10/29/2012 - 16:57:37

Dye: Blue, Green, Yellow, Red - 9 peaks

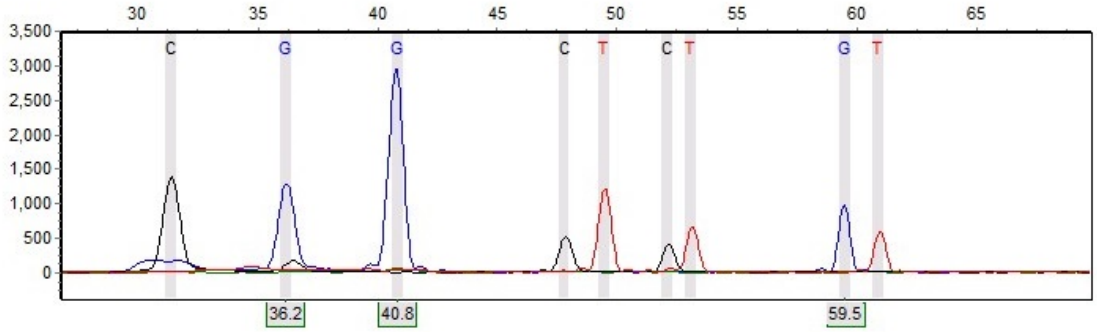

Figure F106. Sample 516

Sample 52: Run date and time: 07/09/2012 - 10:55:20 -> 07/09/2012 - 11:33:00

Dye: Blue, Green, Yellow, Red - 10 peaks

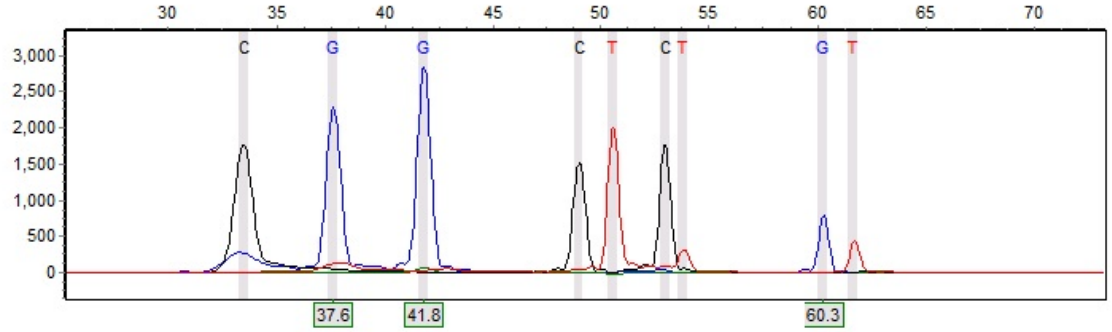

Figure F107. Sample 518

Sample 55: Run date and time: 10/30/2012 - 14:22:49 -> 10/30/2012 - 14:51:24

Dye: Blue, Green, Yellow, Red - 12 peaks

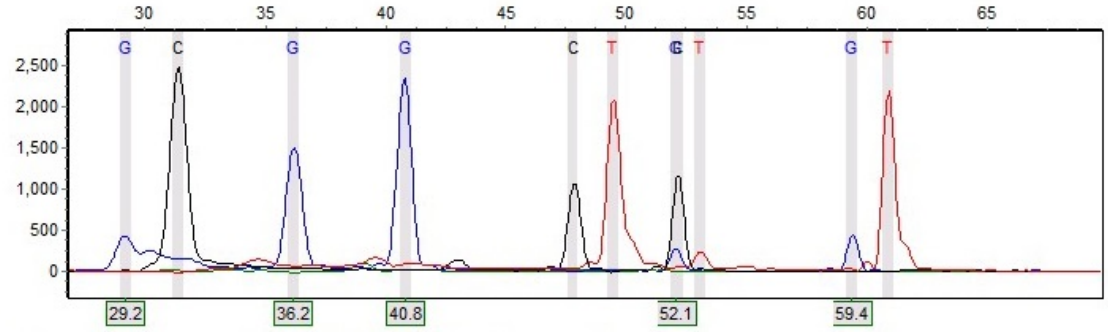

Figure F108. Sample 519

Sample 53: Run date and time: 07/06/2012 - 17:47:35 -> 07/06/2012 - 18:16:05

Dye: Blue, Green, Yellow, Red - 10 peaks

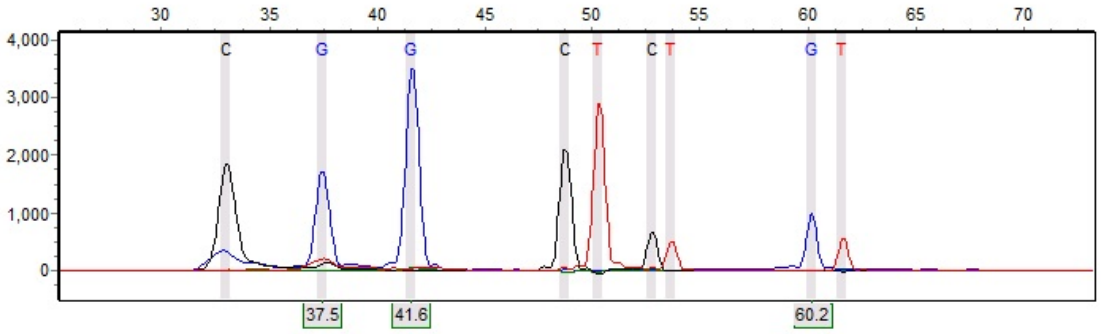

Figure F109. Sample 528

Sample 56: Run date and time: 10/29/2012 - 16:00:18 -> 10/29/2012 - 16:28:48

Dye: Blue, Green, Yellow, Red - 9 peaks

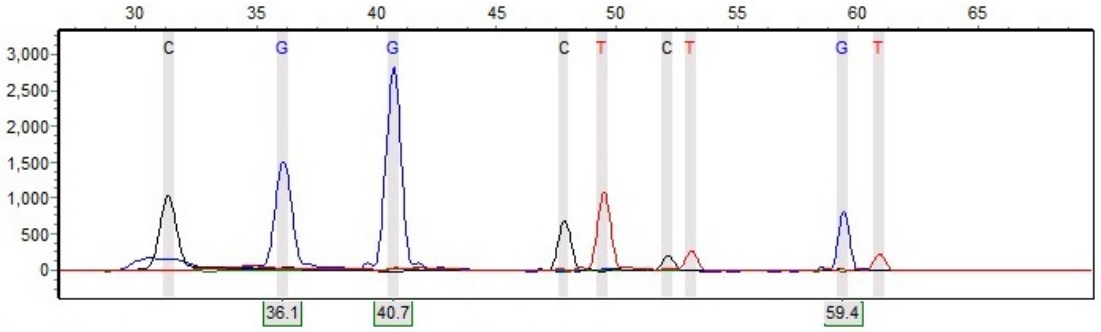

Figure F110. Sample 529

Sample 54: Run date and time: 07/13/2012 - 17:30:21 -> 07/13/2012 - 18:02:31

Dye: Blue, Green, Yellow, Red - 7 peaks

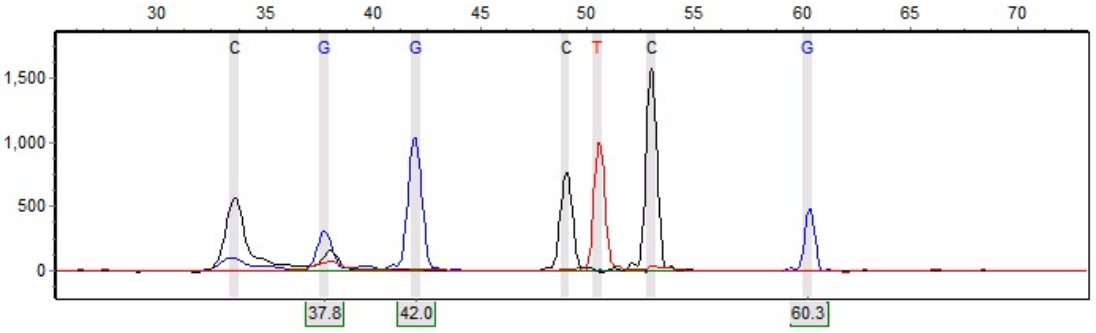

Figure F111. Sample 531

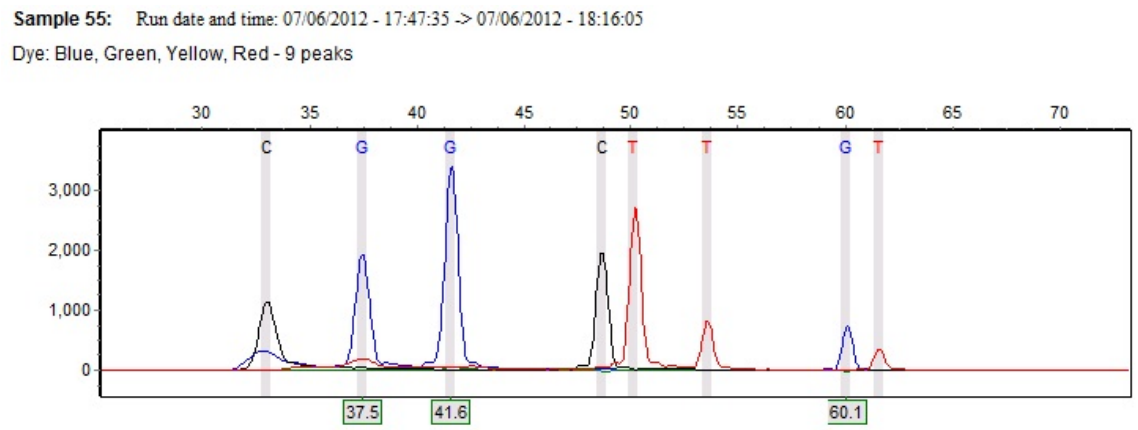

Figure F112. Sample 536

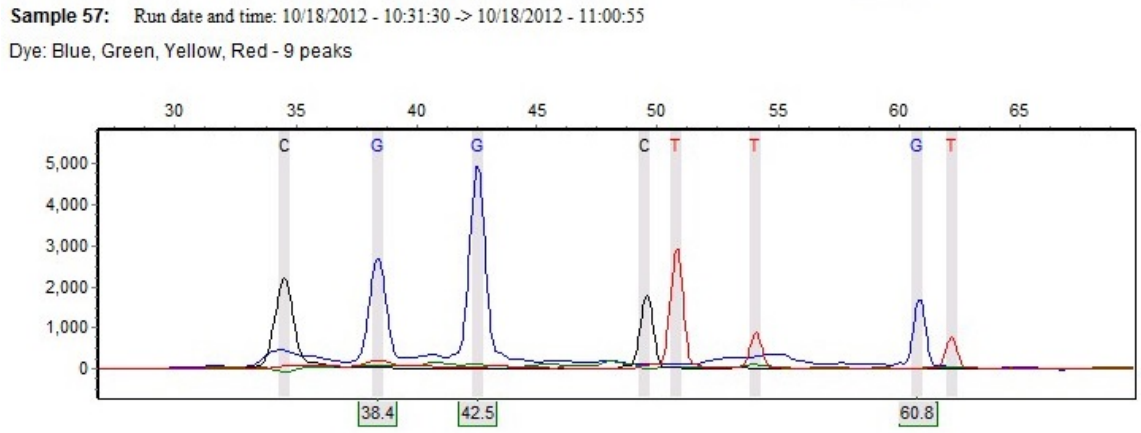

Figure F113. Sample 537

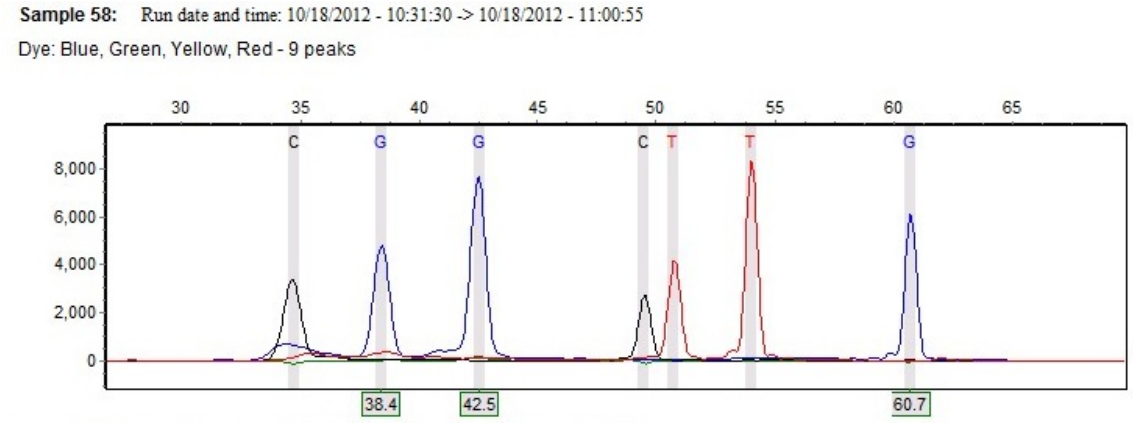

Figure F114. Sample 538

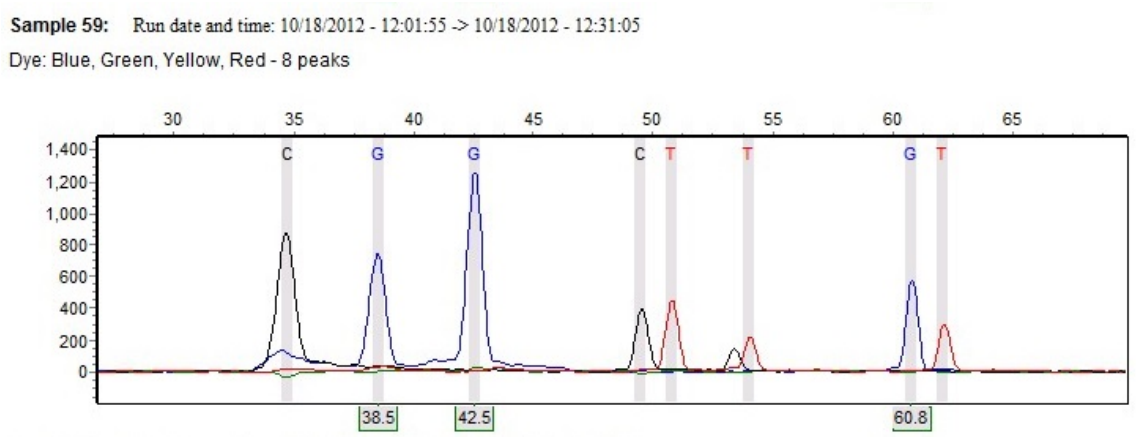

Figure F115. Sample 539

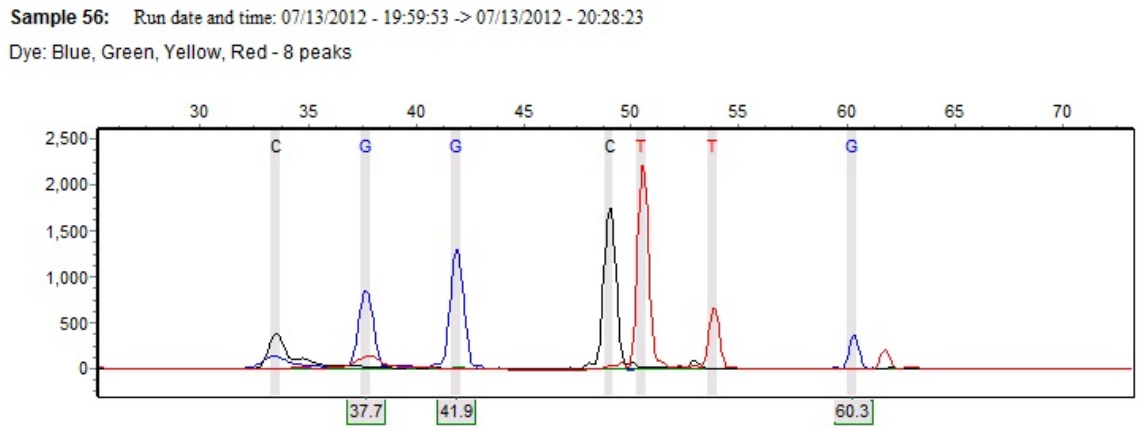

Figure F116. Sample 569

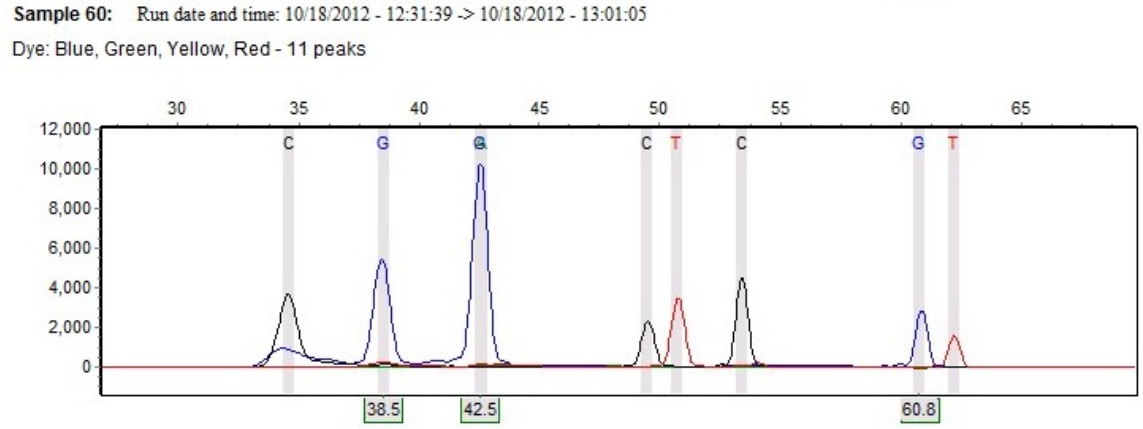

Figure F117. Sample 571

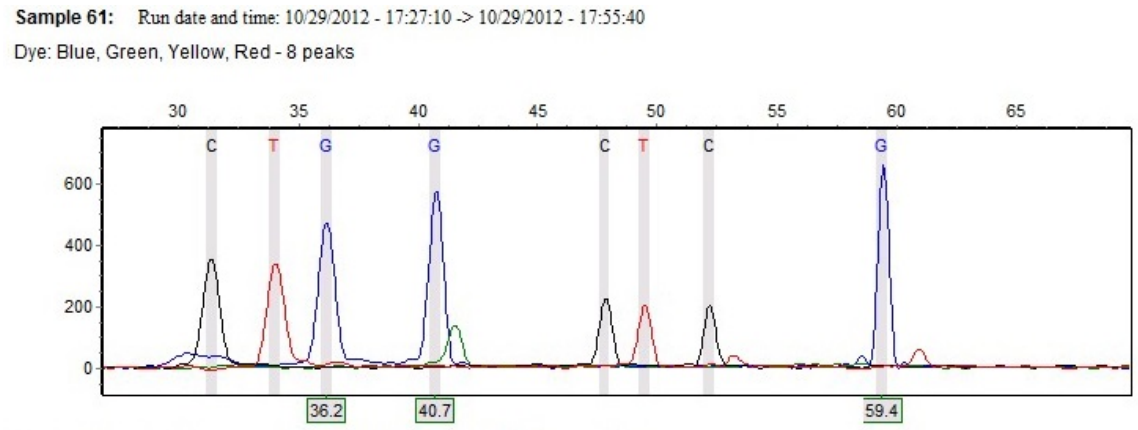

Figure F118. Sample 574

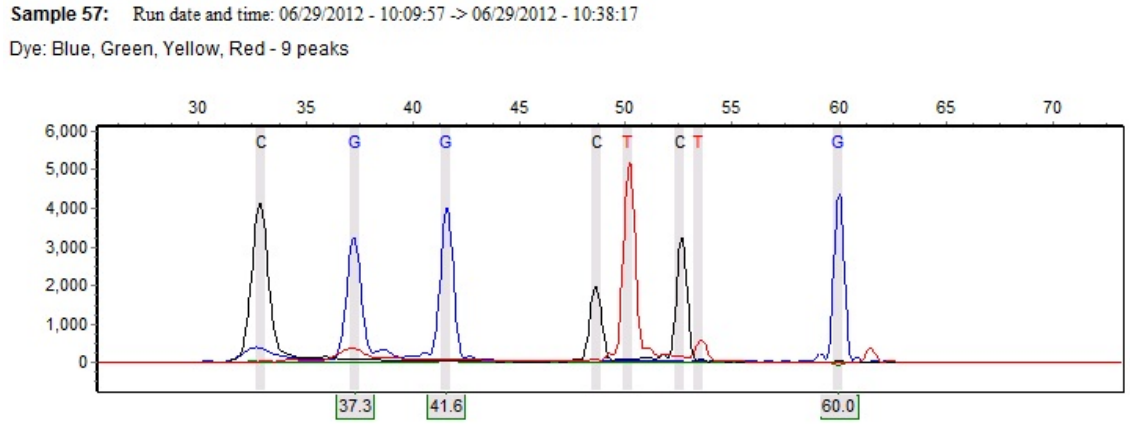

Figure F119. Sample 578

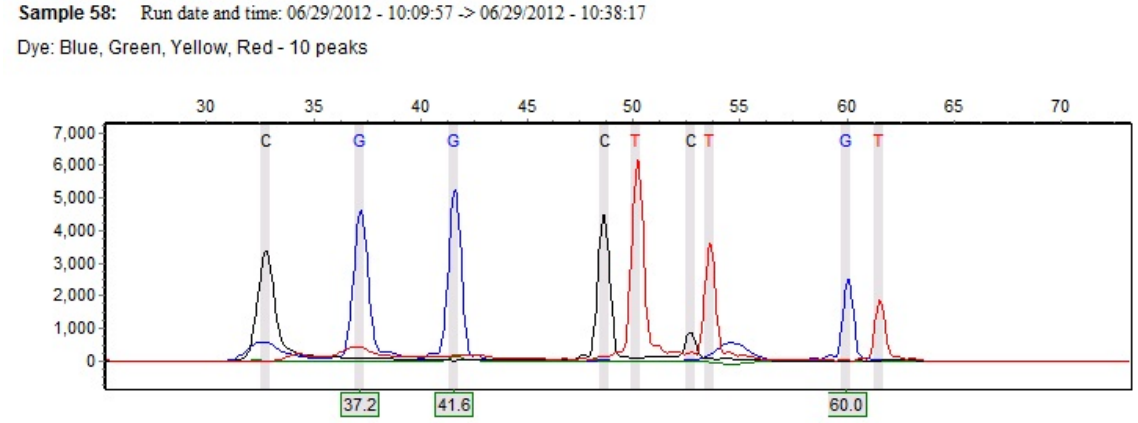

Figure F120. Sample 579

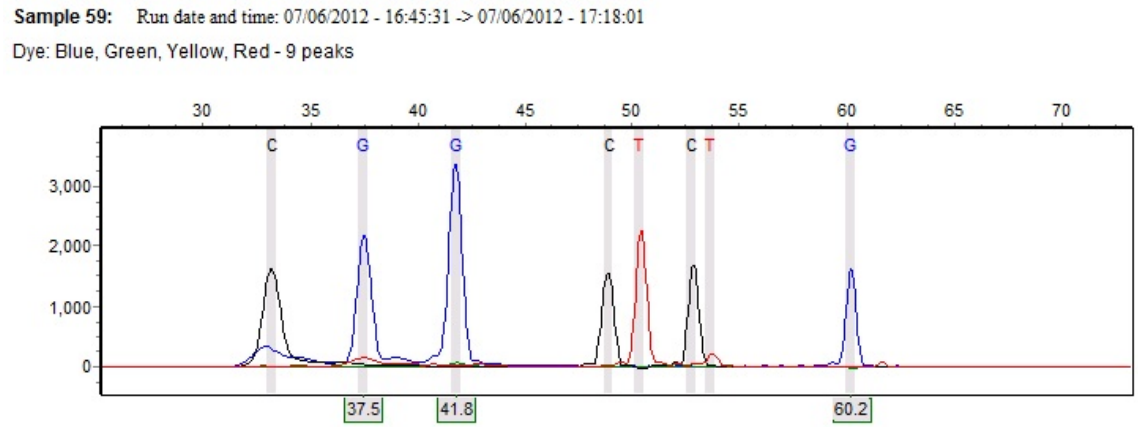

Figure F121. Sample 584

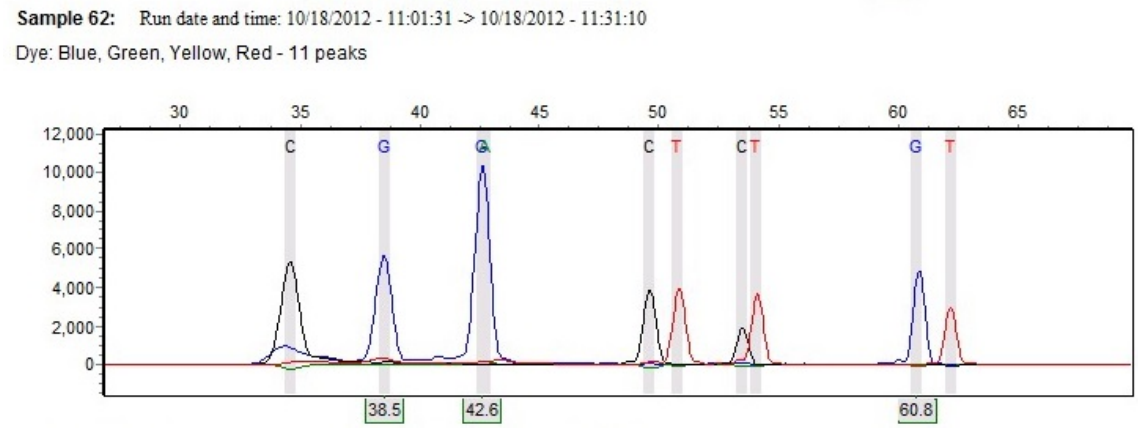

Figure F122. Sample 586

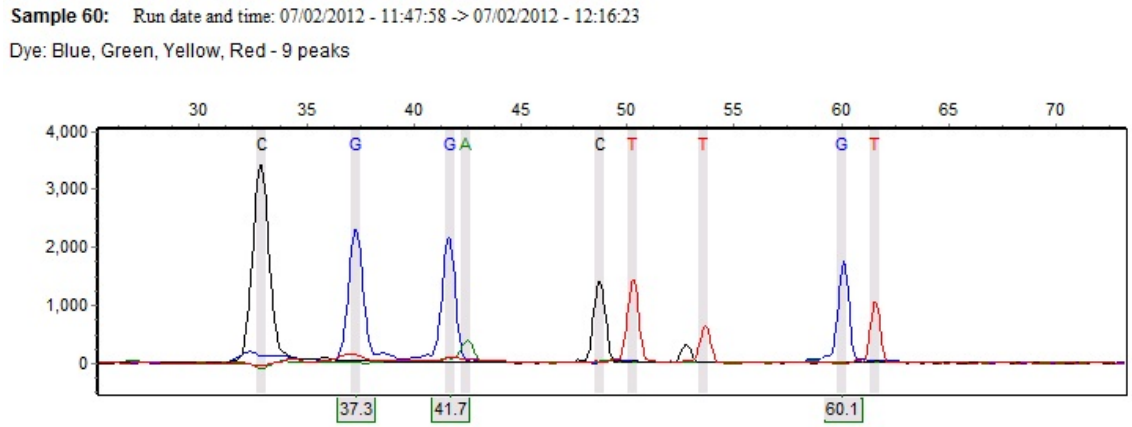

Figure F123. Sample 612

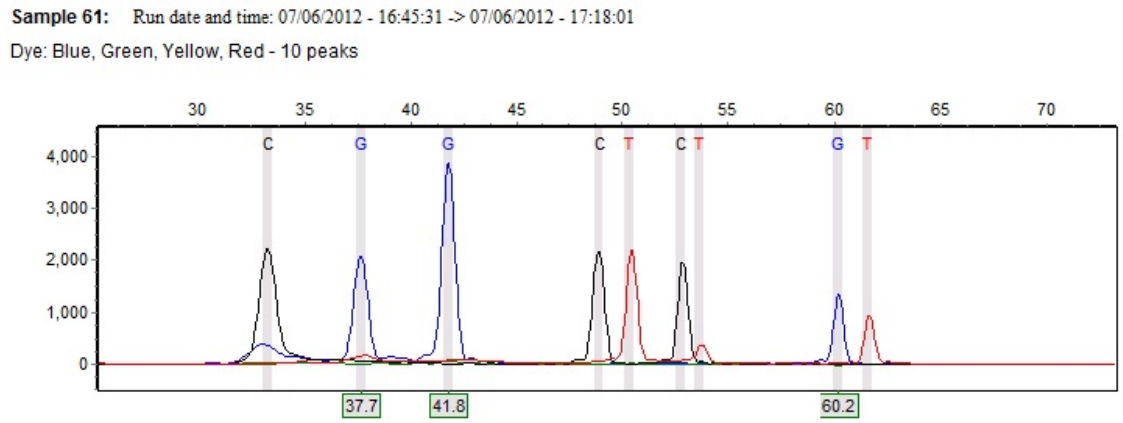

Figure F124. Sample 625

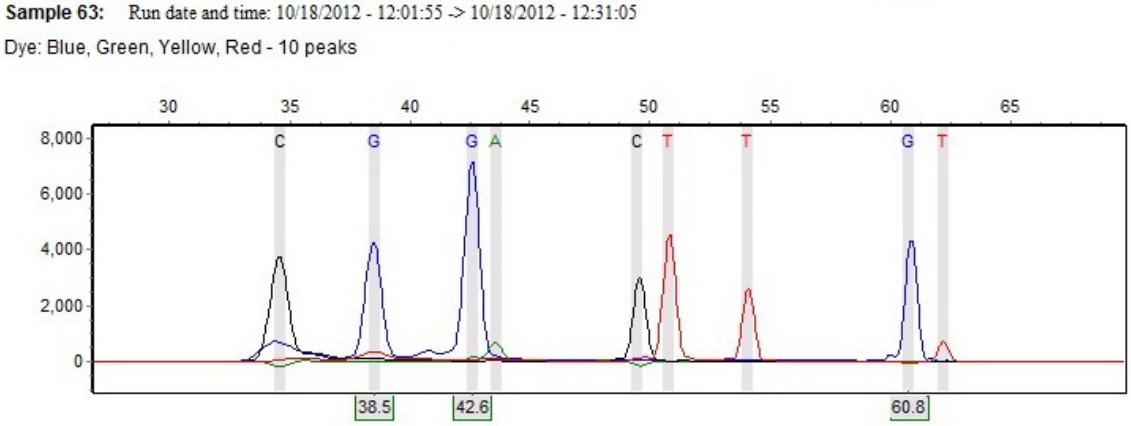

Figure F125. Sample 634

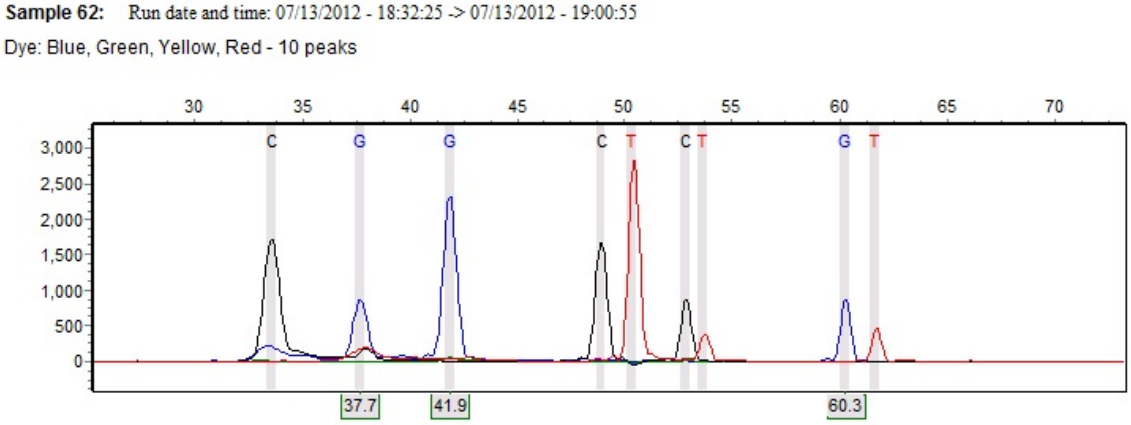

Figure F126. Sample 639

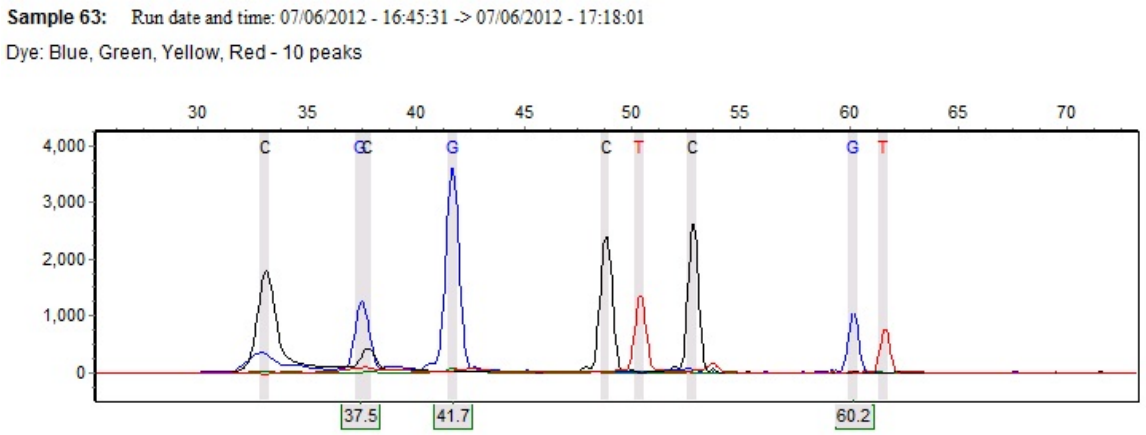

Figure F127. Sample 645

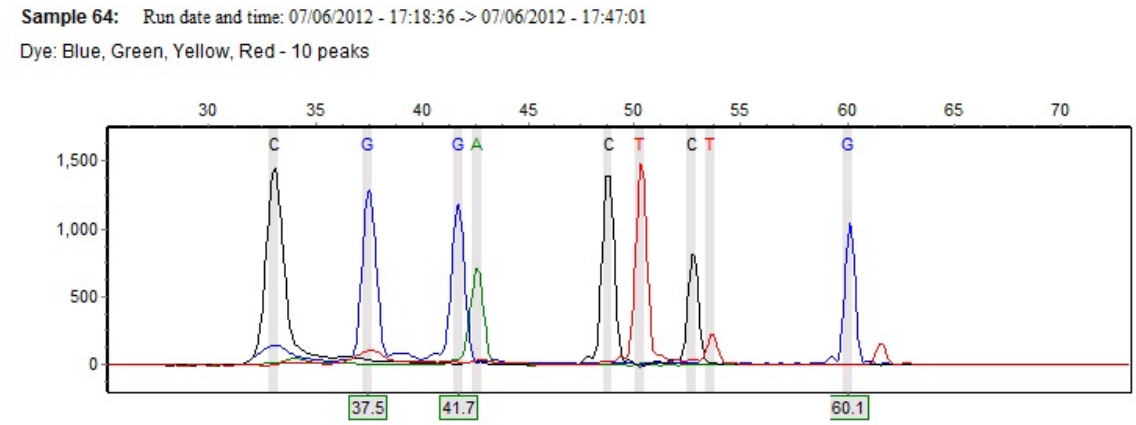

Figure F128. Sample 652

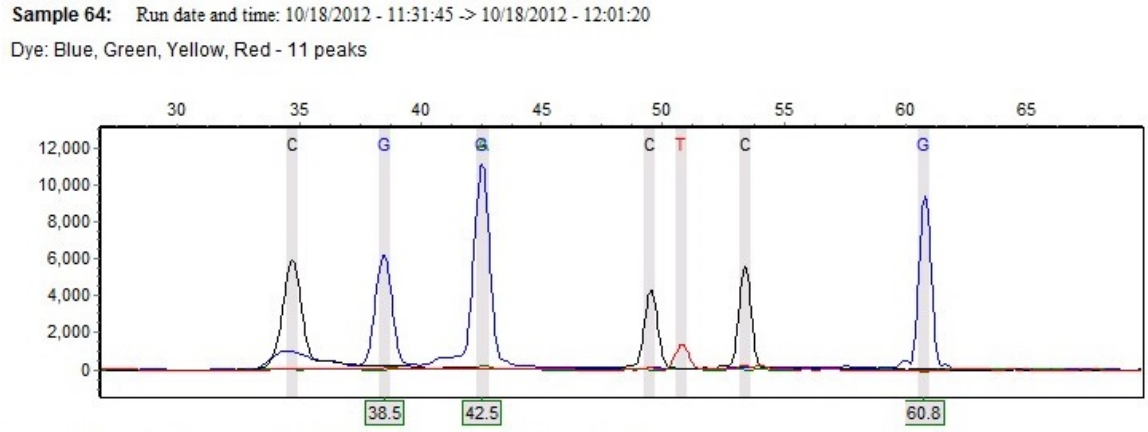

Figure F129. Sample 653

Sample 65: Run date and time: 07/13/2012 - 19:01:29 -> 07/13/2012 - 19:29:59

Dye: Blue, Green, Yellow, Red - 11 peaks

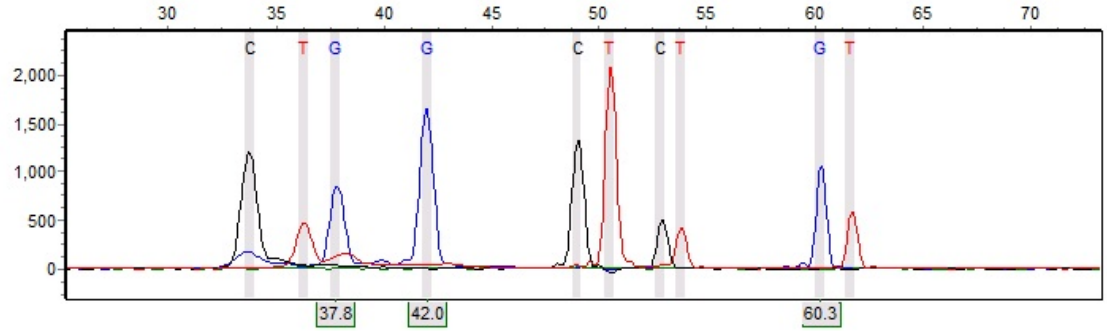

Figure F130. Sample 657

Sample 66: Run date and time: 07/13/2012 - 19:01:29 -> 07/13/2012 - 19:29:59

Dye: Blue, Green, Yellow, Red - 10 peaks

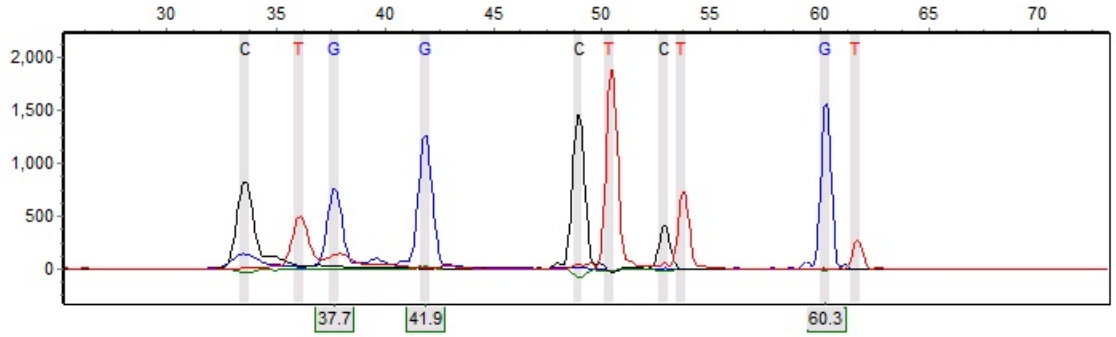

Figure F131. Sample 658

Sample 67: Run date and time: 06/29/2012 - 09:08:28 -> 06/29/2012 - 09:40:13

Dye: Blue, Green, Yellow, Red - 11 peaks

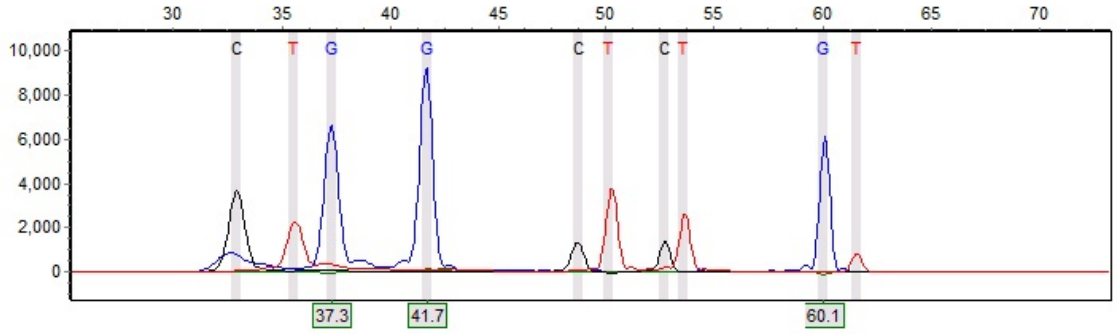

Figure F132. Sample 672

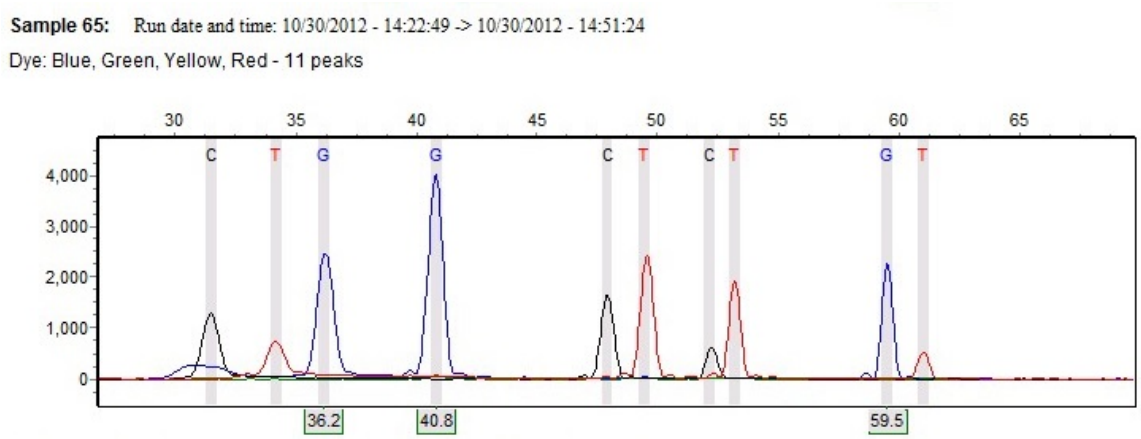

Figure F133. Sample 673

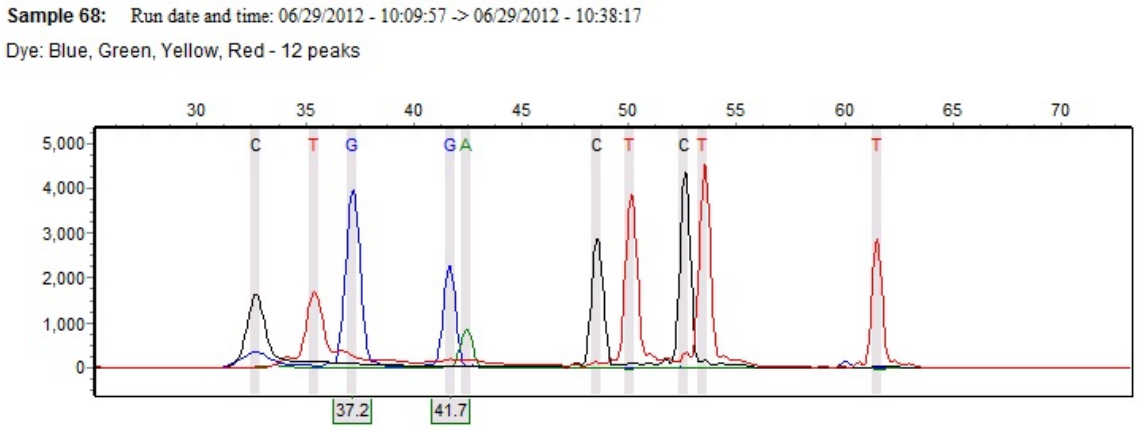

Figure F134. Sample 678

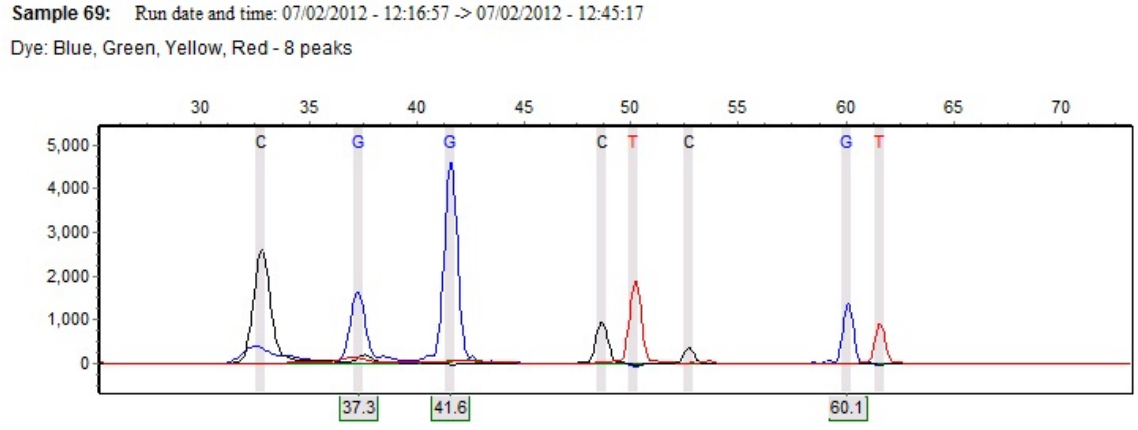

Figure F135. Sample 692

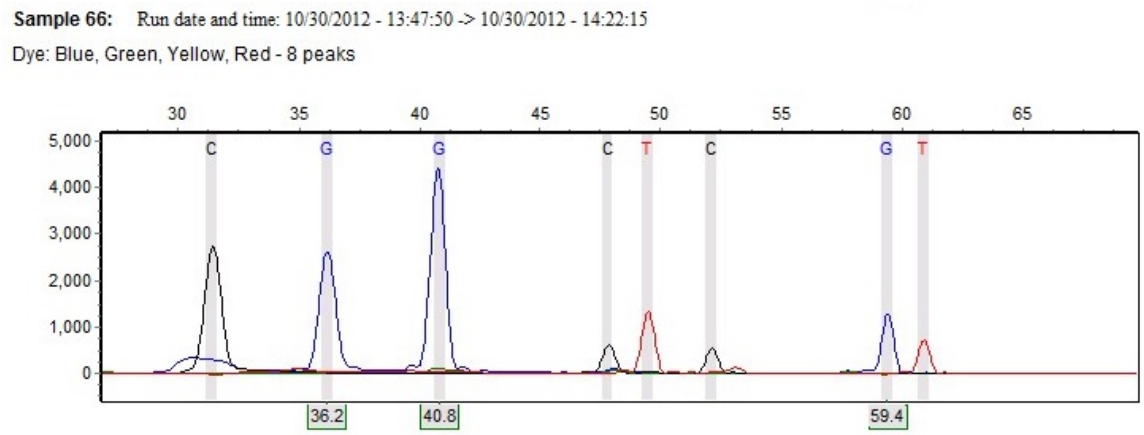

Figure F136. Sample 695

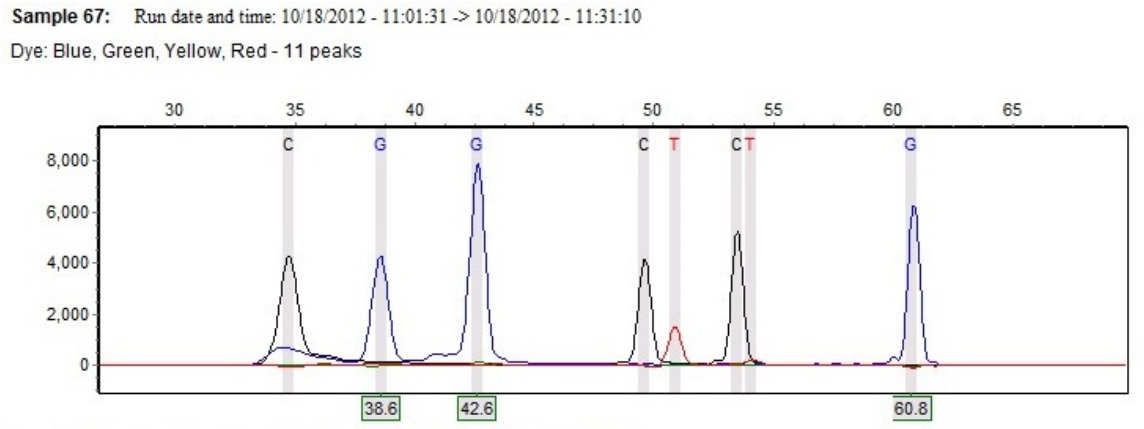

Figure F137. Sample 698

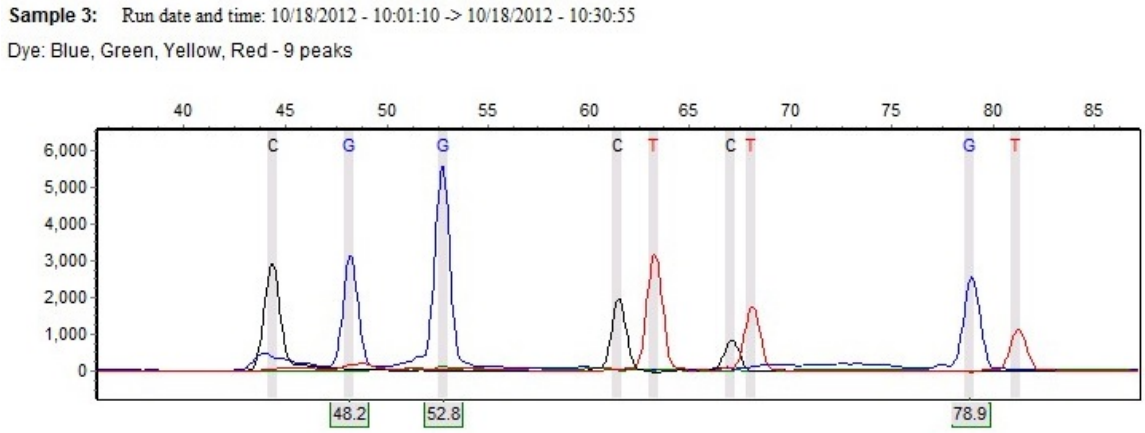

Figure F138. Sample 700

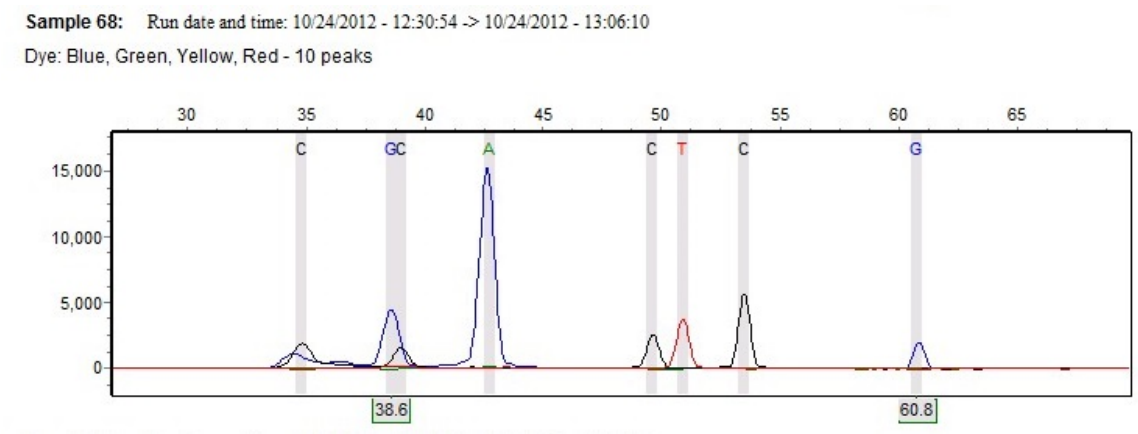

Figure F139. Sample 719

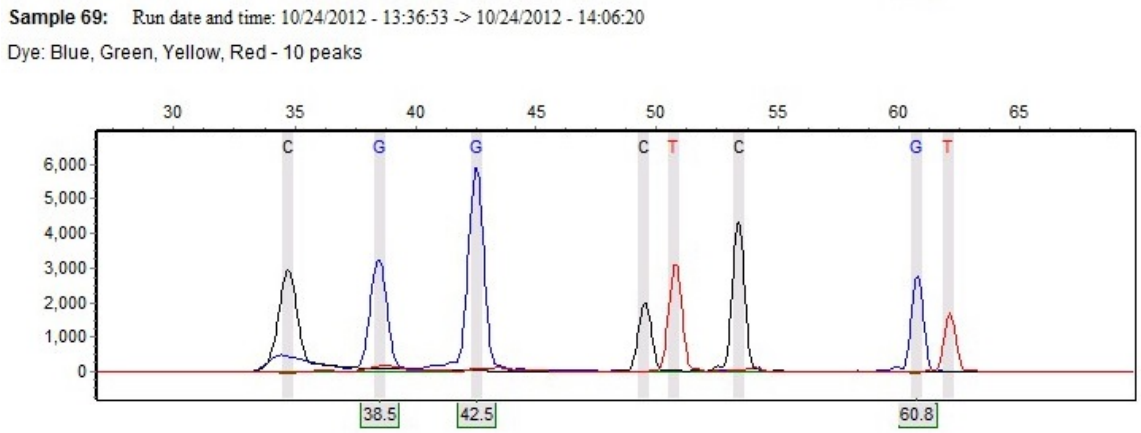

Figure F140. Sample 720

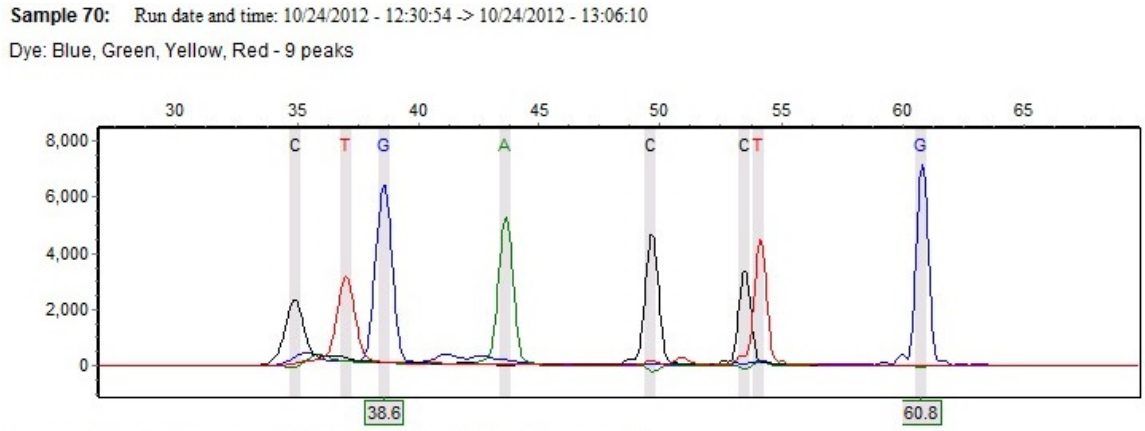

Figure F141. Sample 723

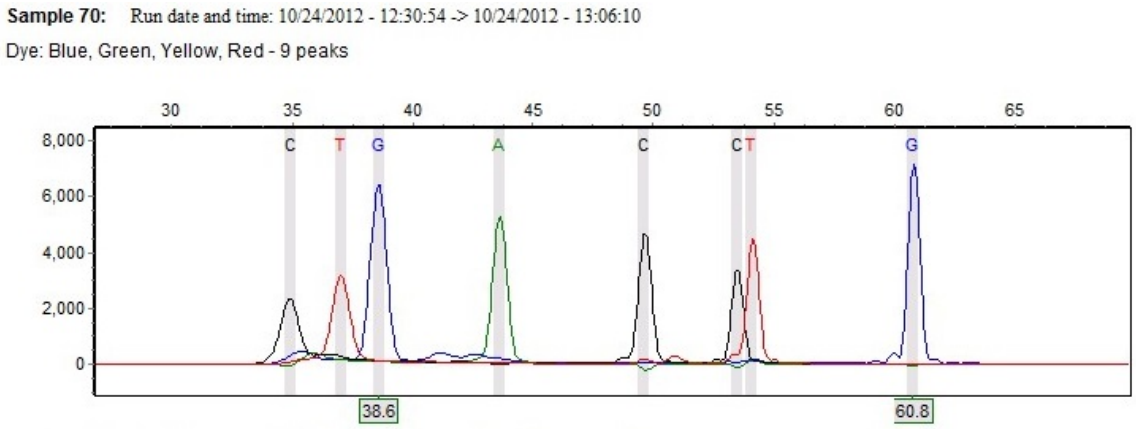

Figure F142. Sample 724

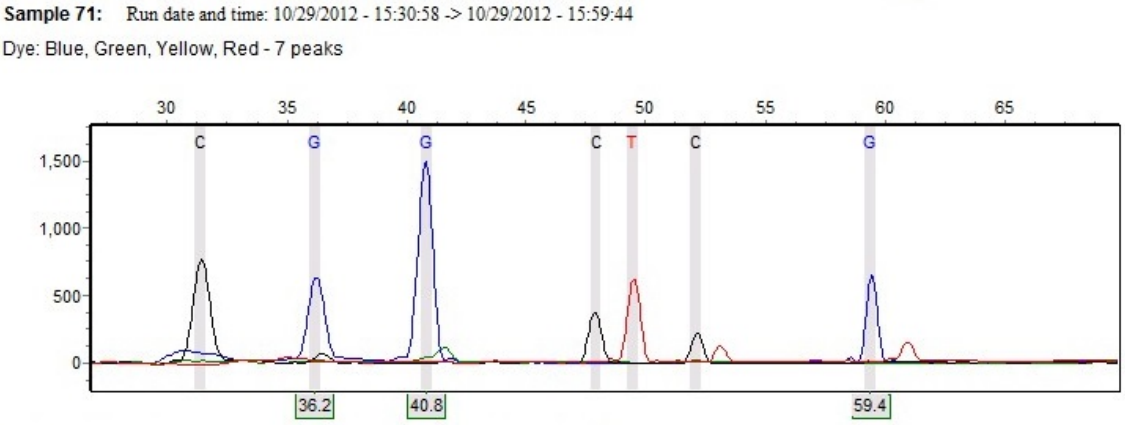

Figure F143. Sample 726

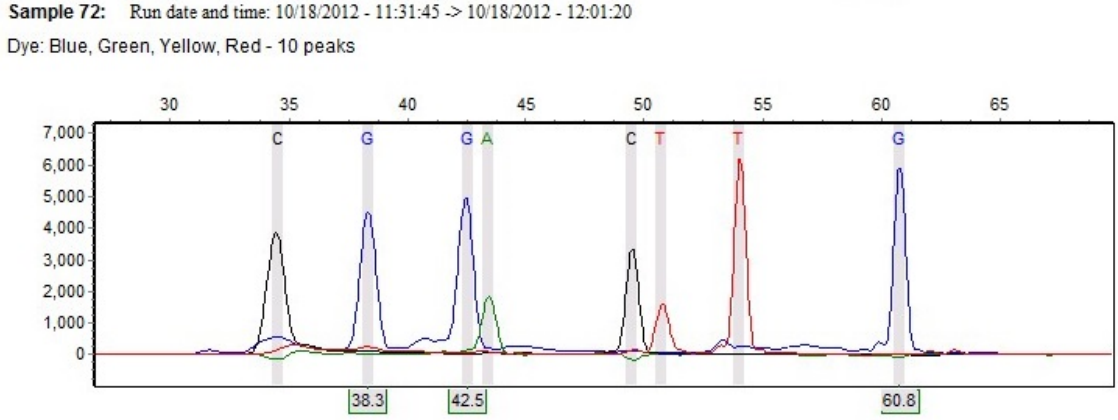

Figure F144. Sample 728

Sample 73: Run date and time: 07/06/2012 - 18:16:39 -> 07/06/2012 - 18:45:14

Dye: Blue, Green, Yellow, Red - 11 peaks

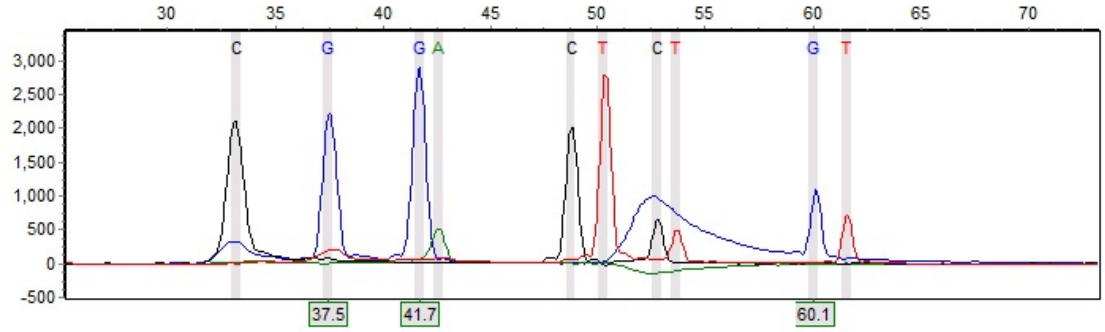

Figure F145. Sample 735

Sample 71: Run date and time: 10/29/2012 - 15:30:58 -> 10/29/2012 - 15:59:44

Dye: Blue, Green, Yellow, Red - 7 peaks

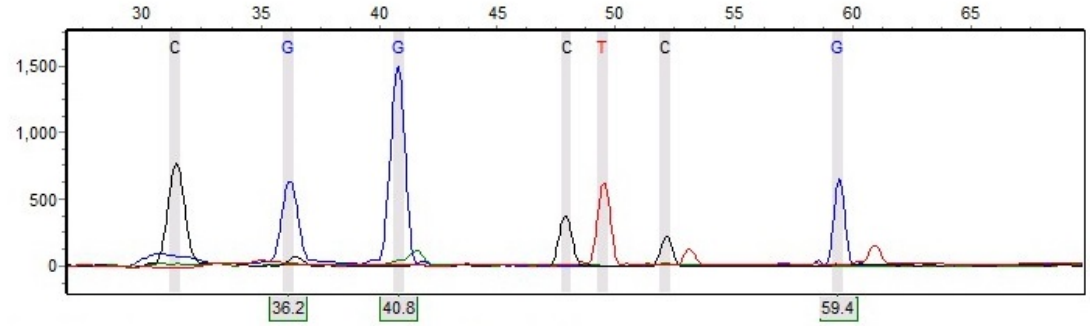

Figure F146. Sample 741

Sample 74: Run date and time: 07/13/2012 - 18:03:05 -> 07/13/2012 - 18:31:50

Dye: Blue, Green, Yellow, Red - 9 peaks

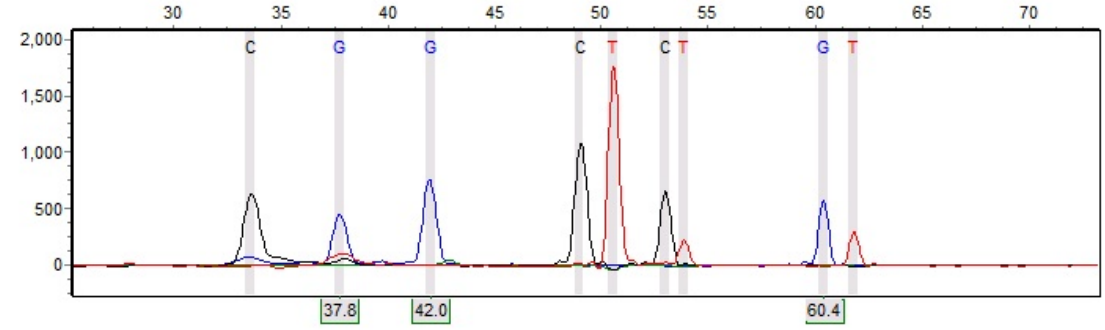

Figure F147. Sample 742

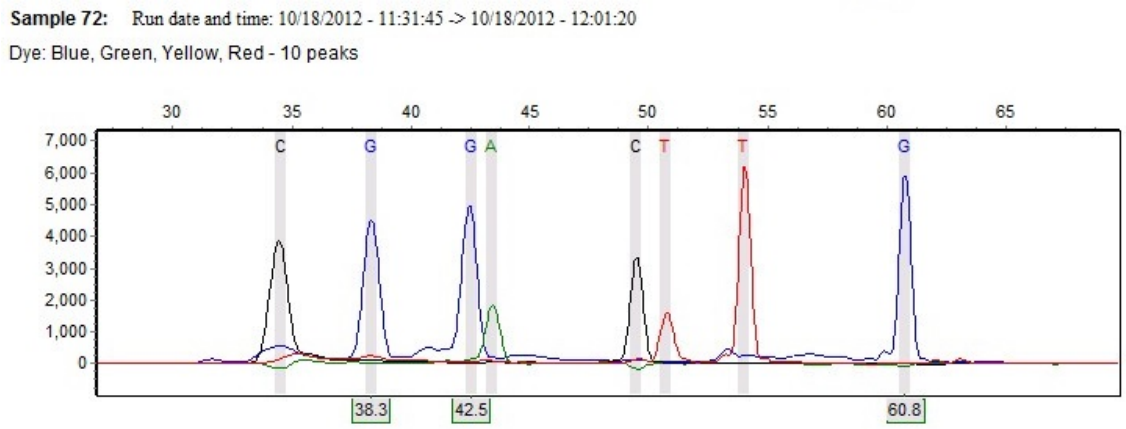

Figure F148. Sample 746

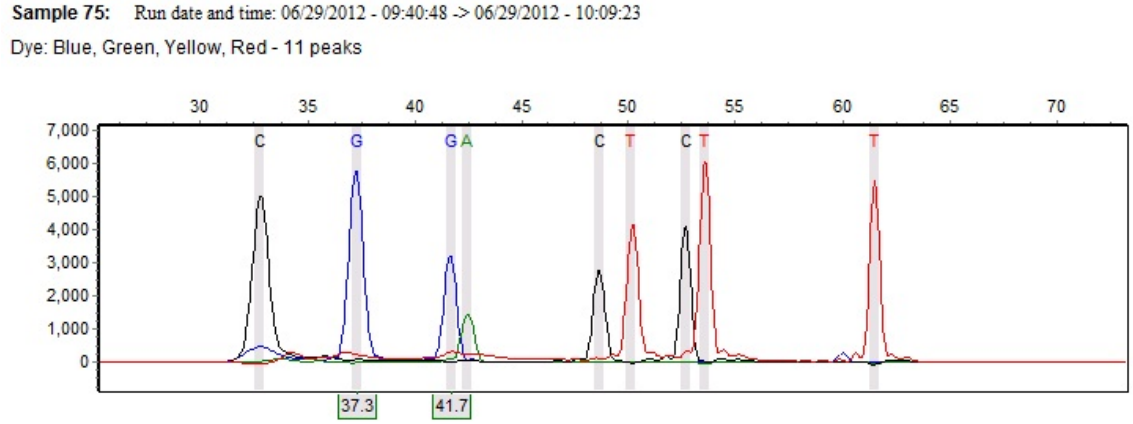

Figure F149. Sample 749

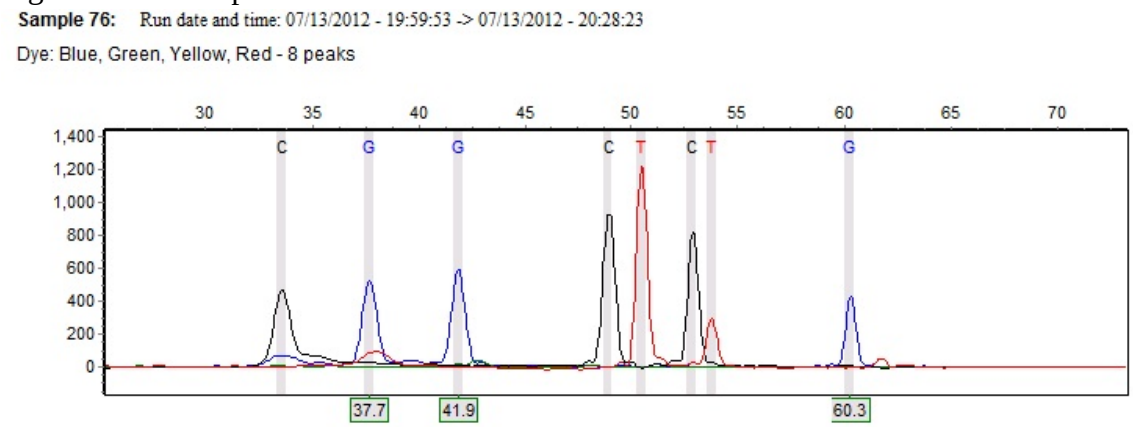

Figure F150. Sample 751

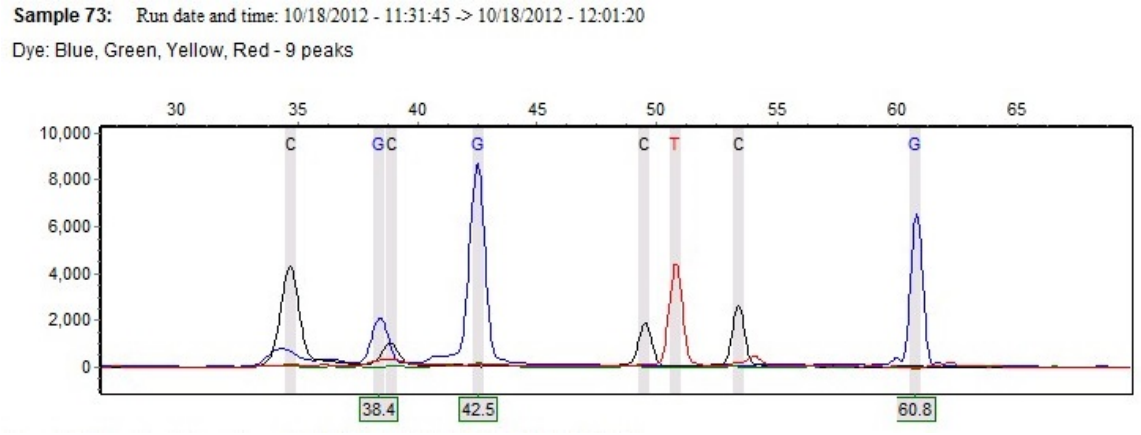

Figure F151. Sample 752

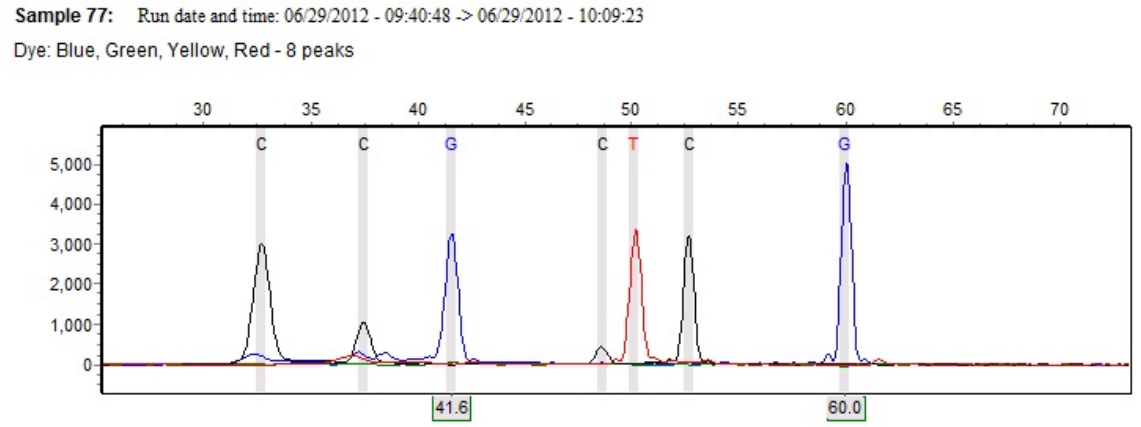

Figure F152. Sample 753

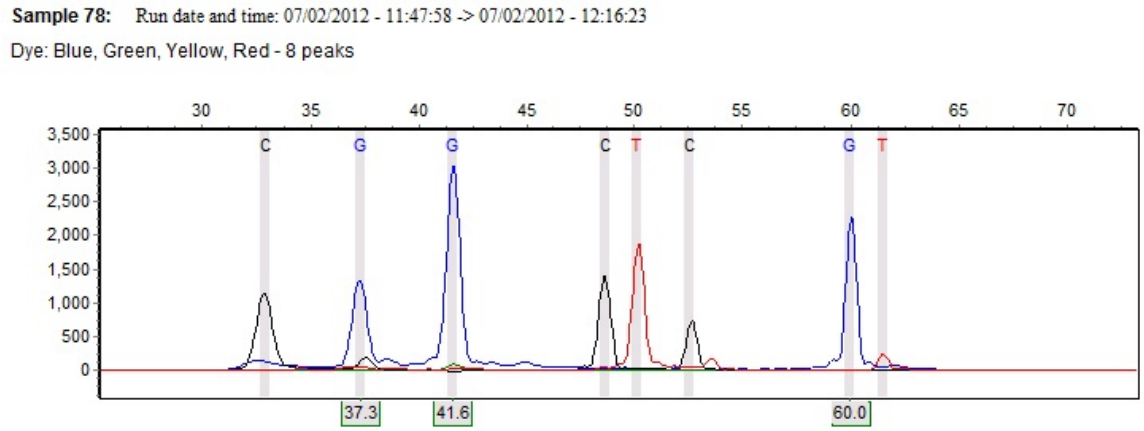

Figure F153. Sample 756

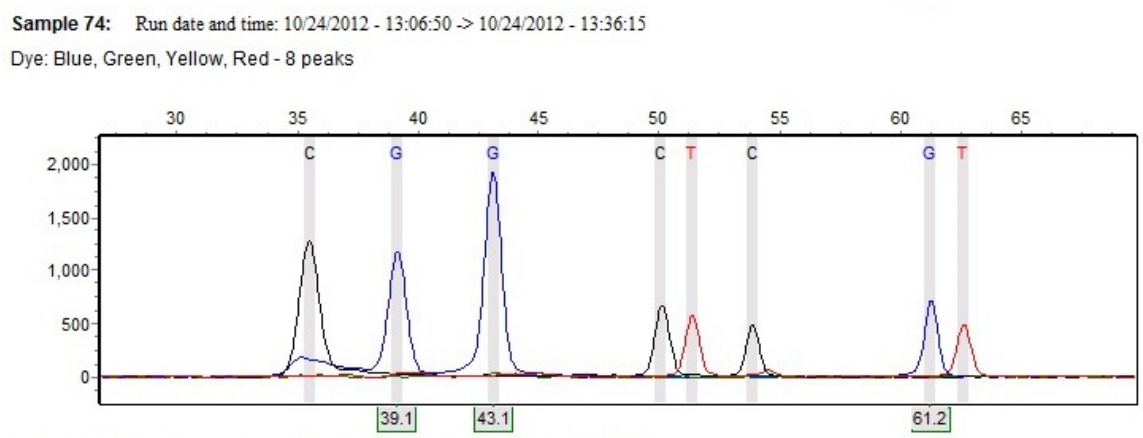

Figure F154. Sample 758

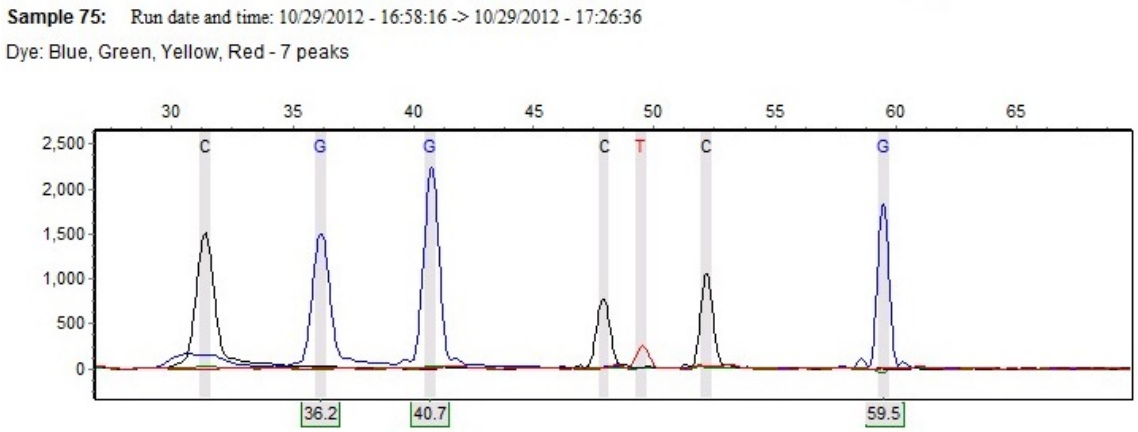

Figure F155. Sample 763

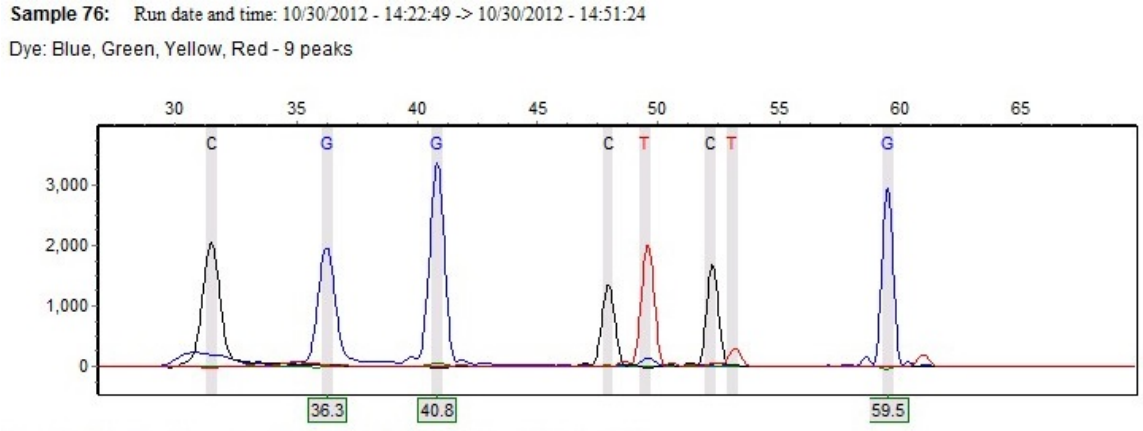

Figure F156. Sample 765

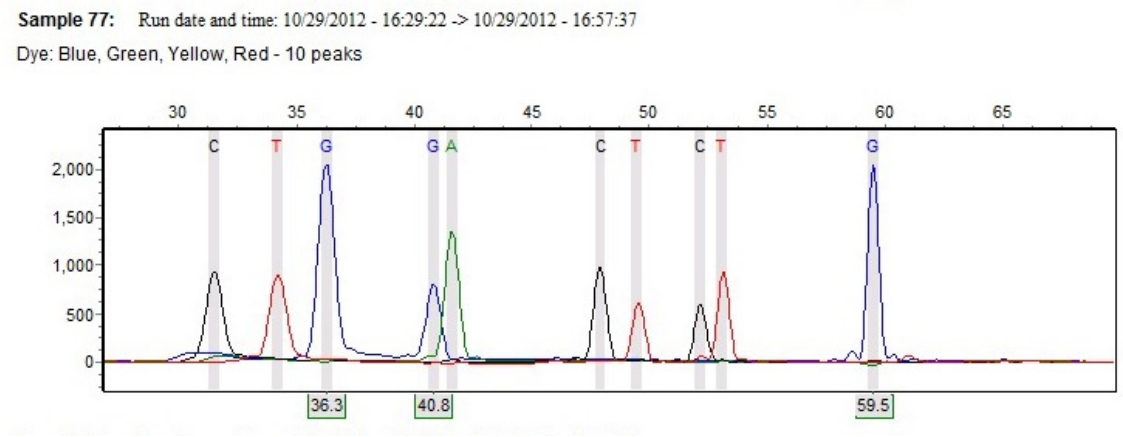

Figure F157. Sample 768

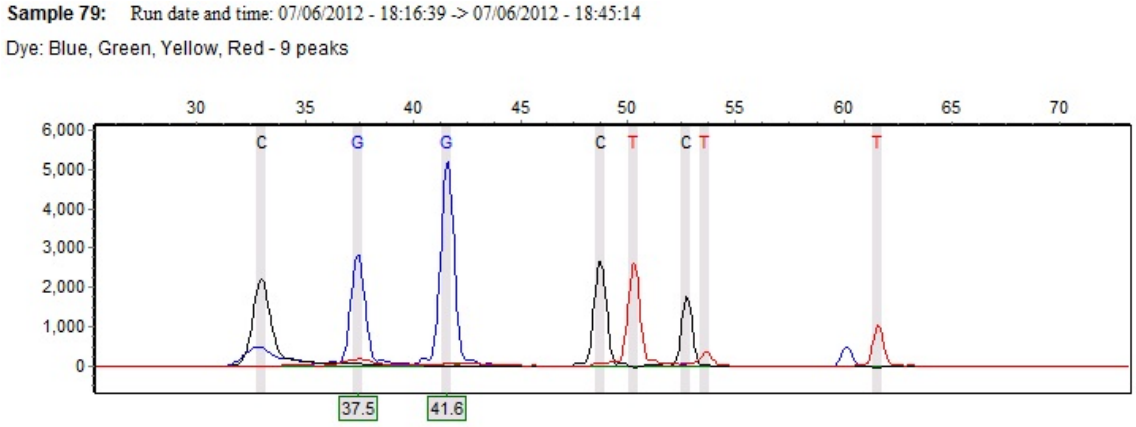

Figure F158. Sample 769

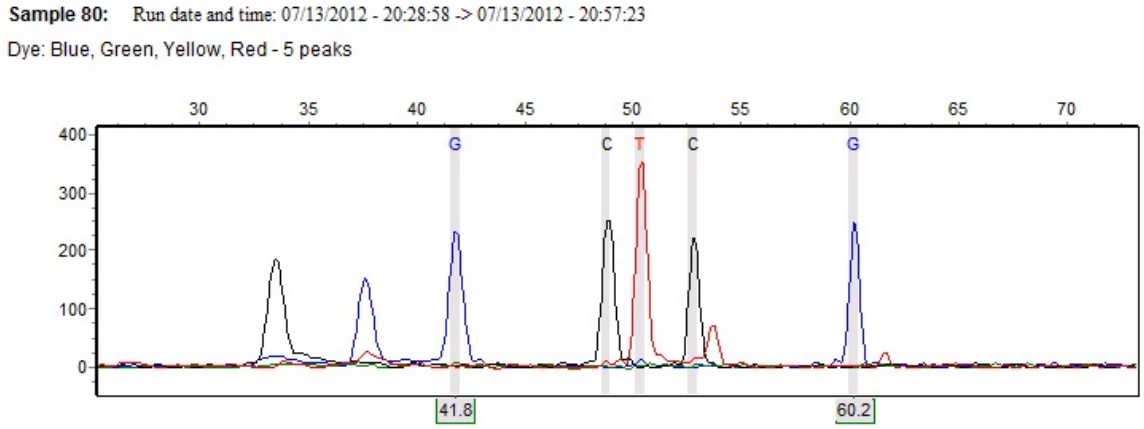

Figure F159. Sample 785

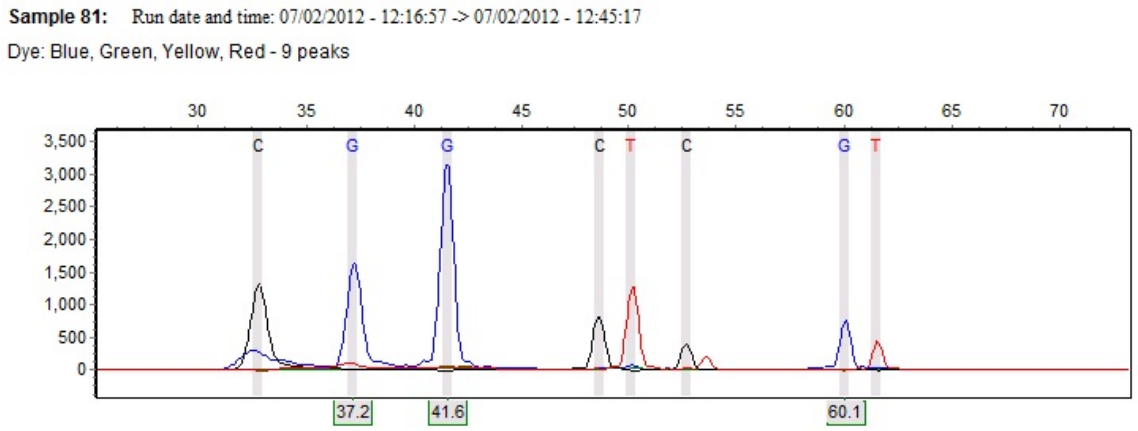

Figure F160. Sample 791

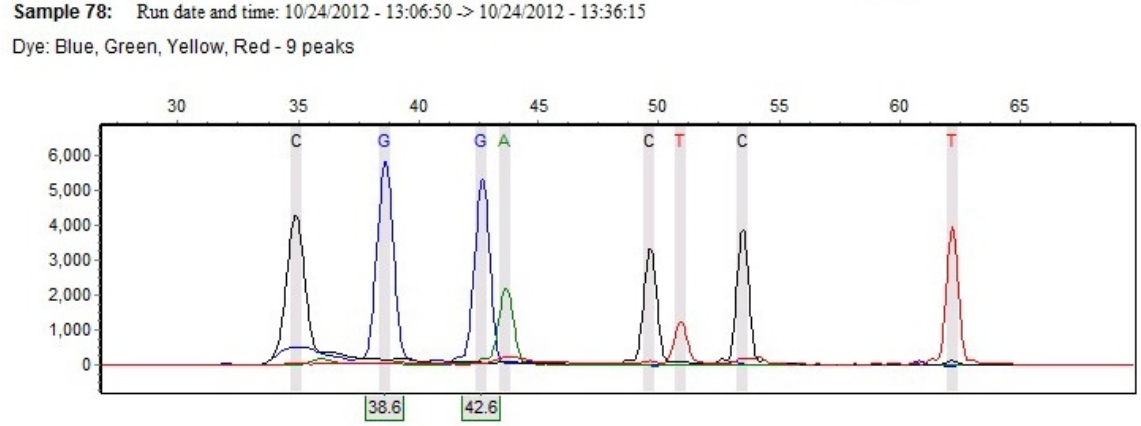

Figure F161. Sample 796

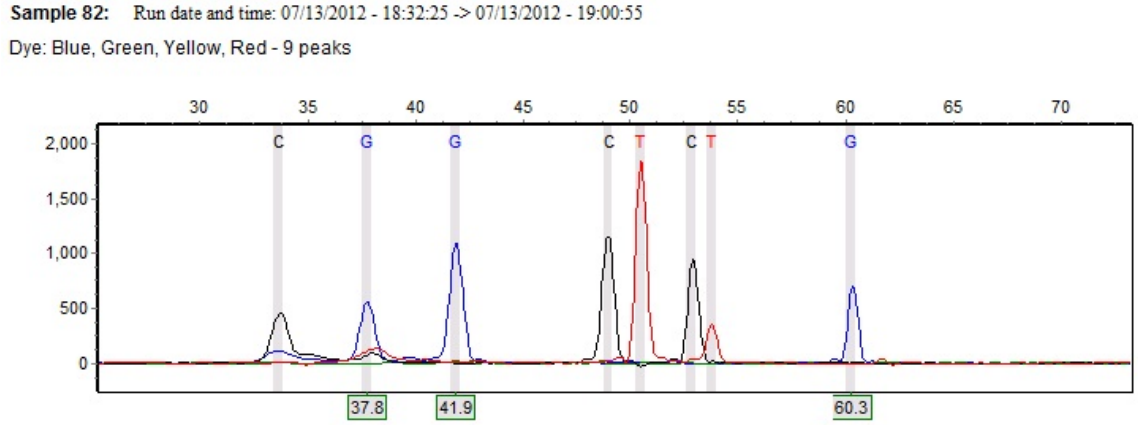

Figure F162. Sample 812

Sample 83: Run date and time: 07/06/2012 - 18:45:48 -> 07/06/2012 - 19:14:13

Dye: Blue, Green, Yellow, Red - 10 peaks

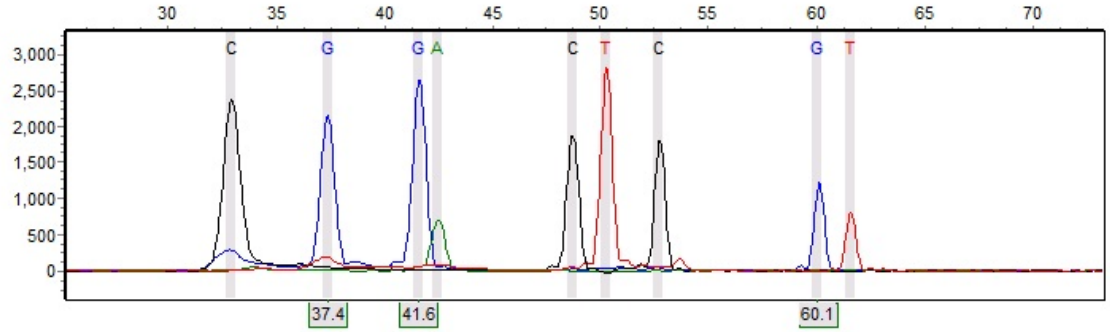

Figure F163. Sample 823

Sample 84: Run date and time: 07/06/2012 - 18:45:48 -> 07/06/2012 - 19:14:13

Dye: Blue, Green, Yellow, Red - 8 peaks

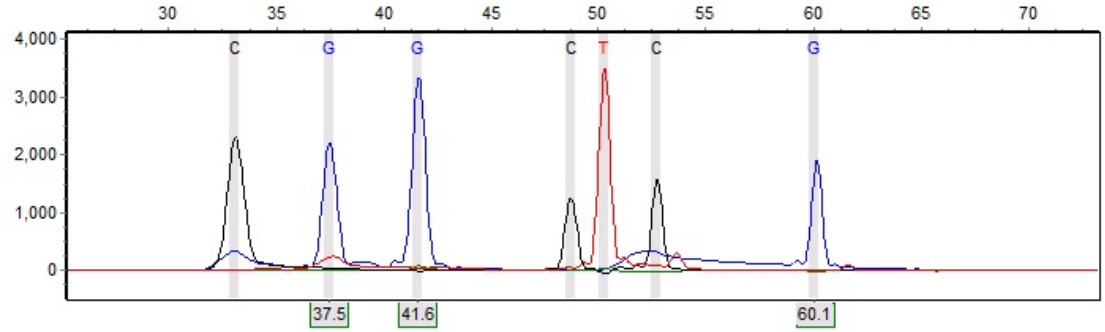

Figure F164. Sample 825

Sample 85: Run date and time: 07/06/2012 - 18:16:39 -> 07/06/2012 - 18:45:14

Dye: Blue, Green, Yellow, Red - 11 peaks

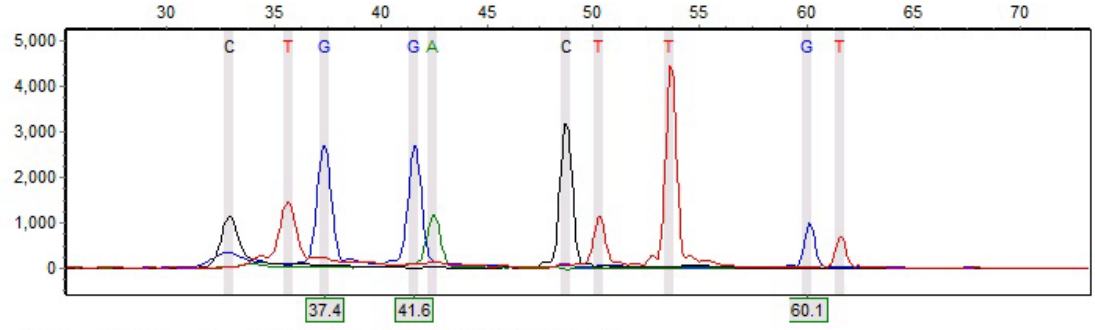

Figure F165. Sample 826

Sample 86: Run date and time: 07/06/2012 - 18:45:48 -> 07/06/2012 - 19:14:13

Dye: Blue, Green, Yellow, Red - 10 peaks

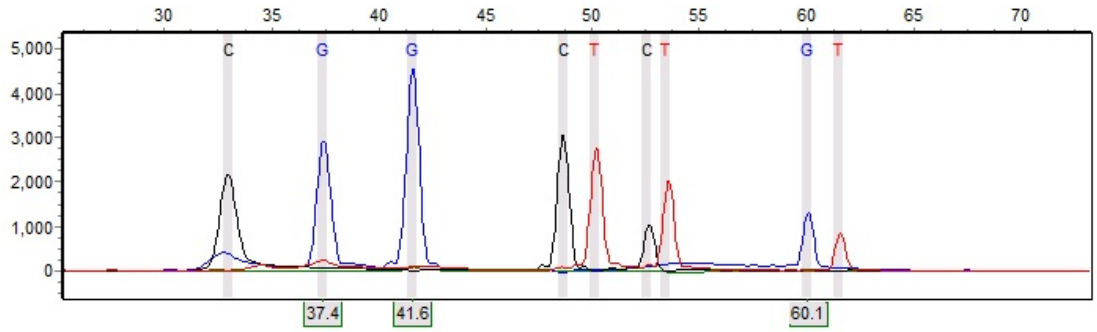

Figure F166. Sample 827

Sample 87: Run date and time: 07/13/2012 - 17:30:21 -> 07/13/2012 - 18:02:31

Dye: Blue, Green, Yellow, Red - 8 peaks

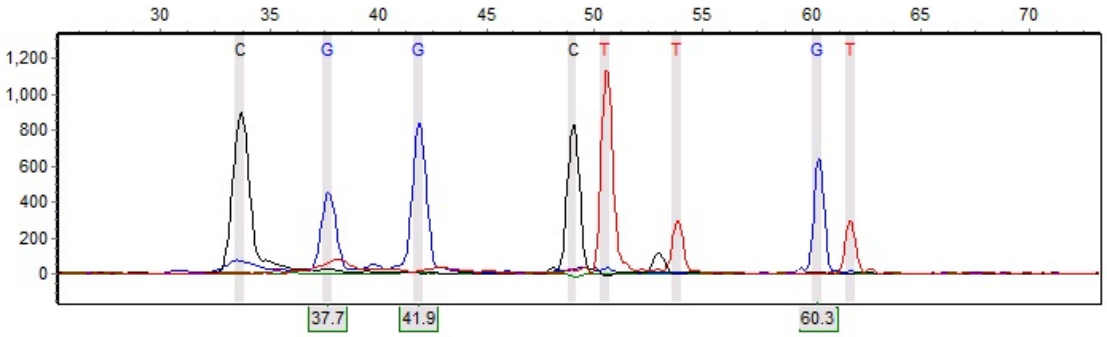

Figure F167. Sample 834

Sample 88: Run date and time: 07/02/2012 - 11:47:58 -> 07/02/2012 - 12:16:23

Dye: Blue, Green, Yellow, Red - 10 peaks

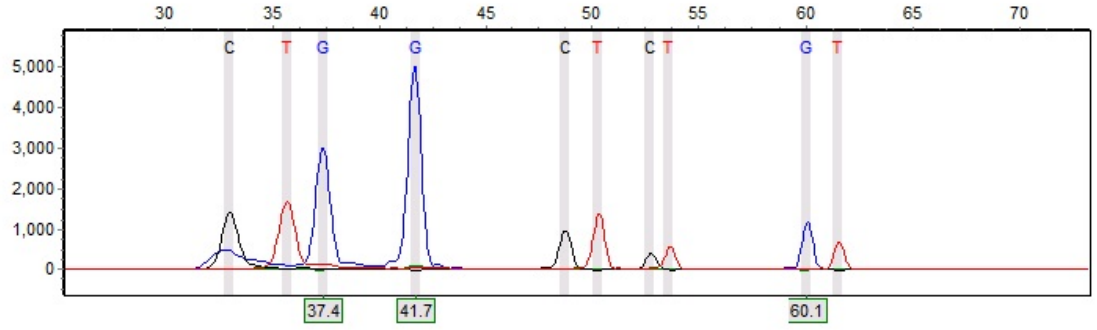

Figure F168. Sample 839

Sample 89: Run date and time: 06/29/2012 - 10:09:57 -> 06/29/2012 - 10:38:17

Dye: Blue, Green, Yellow, Red - 11 peaks

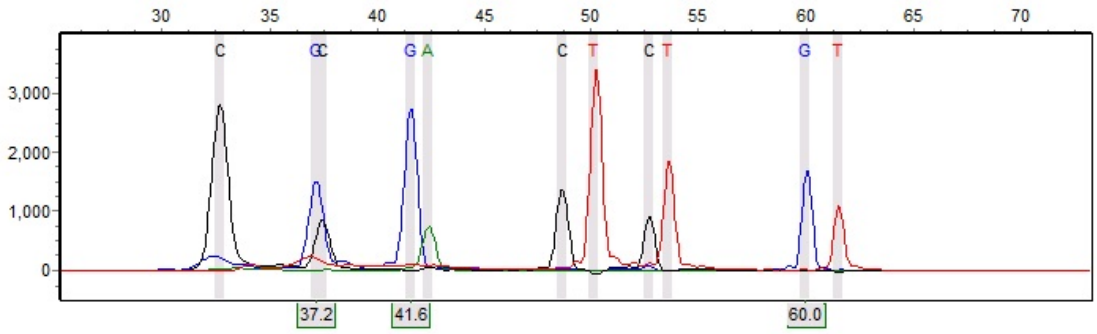

Figure F169. Sample 845

Sample 90: Run date and time: 07/13/2012 - 19:30:34 -> 07/13/2012 - 19:59:19

Dye: Blue, Green, Yellow, Red - 9 peaks

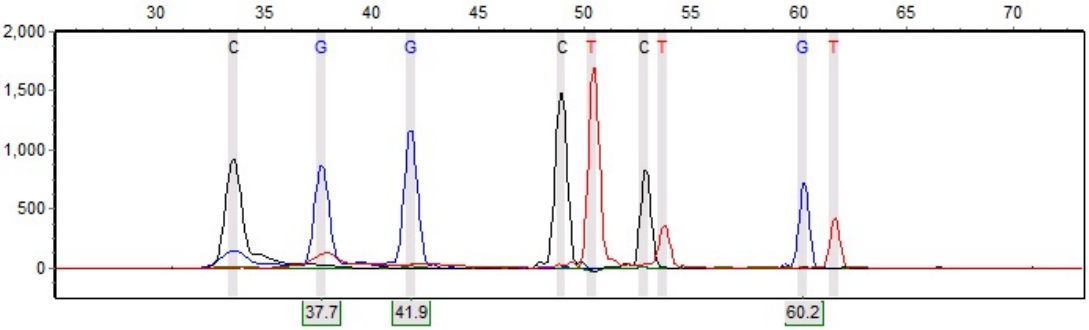

Figure F170. Sample 847

Sample 91: Run date and time: 07/06/2012 - 18:16:39 -> 07/06/2012 - 18:45:14

Dye: Blue, Green, Yellow, Red - 9 peaks

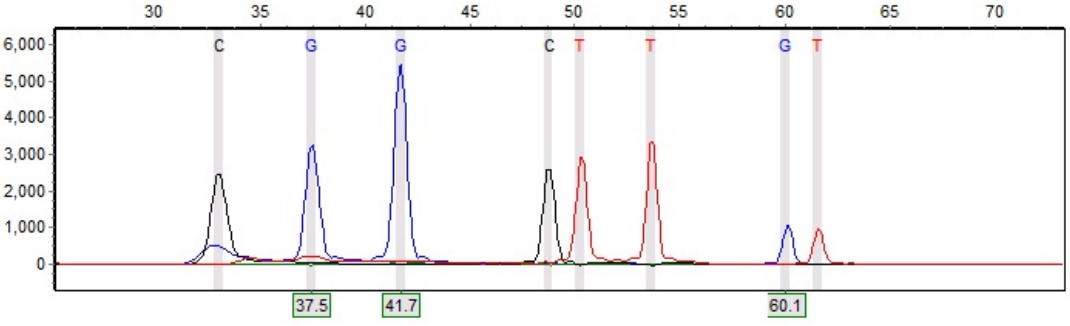

Figure F171. Sample 851

Sample 92: Run date and time: 07/06/2012 - 18:45:48 -> 07/06/2012 - 19:14:13

Dye: Blue, Green, Yellow, Red - 13 peaks

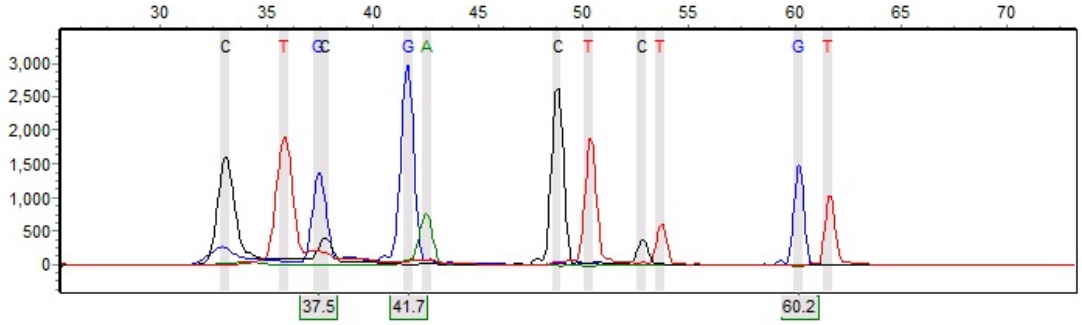

Figure F172. Sample 852

Sample 93: Run date and time: 07/13/2012 - 17:30:21 -> 07/13/2012 - 18:02:31

Dye: Blue, Green, Yellow, Red - 9 peaks

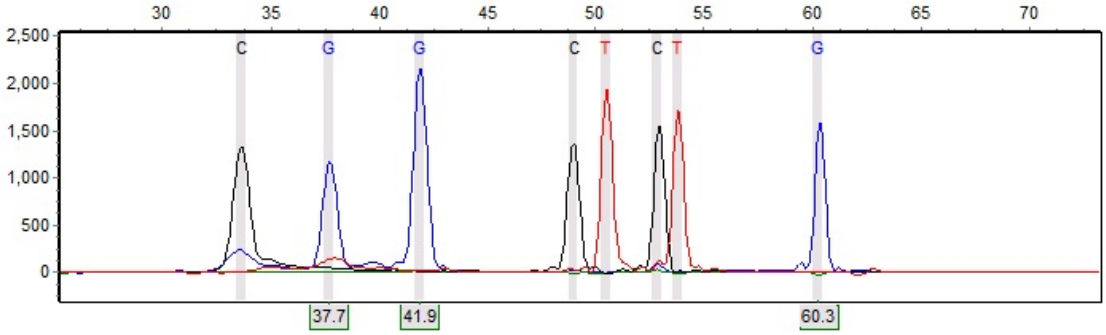

Figure F173. Sample 853

Sample 79: Run date and time: 10/29/2012 - 16:29:22 -> 10/29/2012 - 16:57:37

Dye: Blue, Green, Yellow, Red - 7 peaks

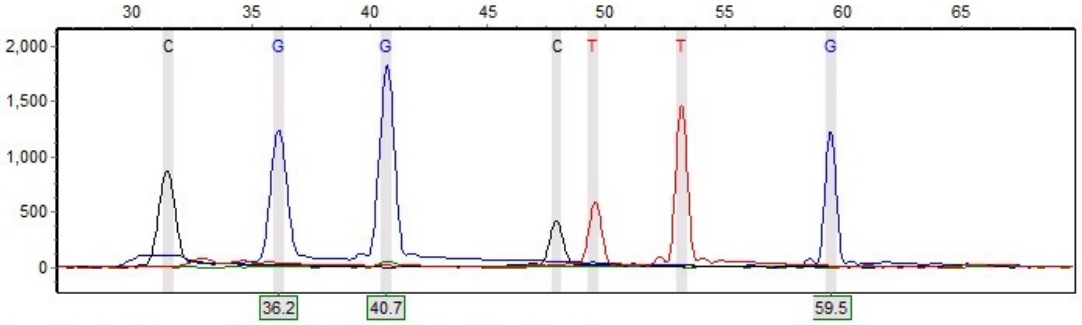

Figure F174. Sample 856

Sample 94: Run date and time: 07/13/2012 - 19:01:29 -> 07/13/2012 - 19:29:59

Dye: Blue, Green, Yellow, Red - 9 peaks

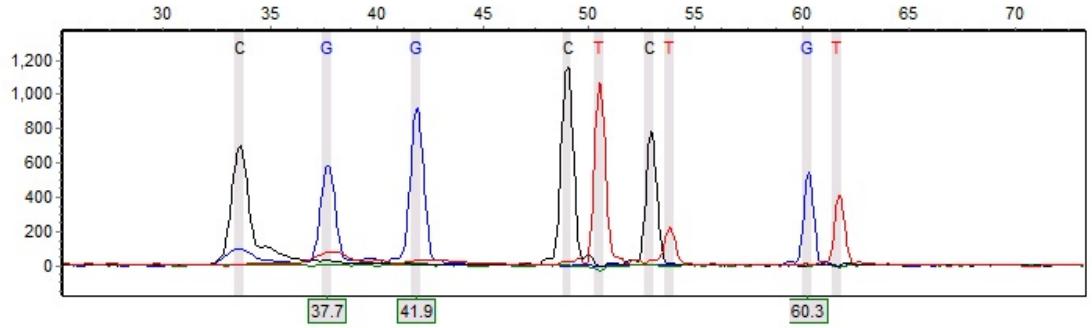

Figure F175. Sample 857

Sample 95: Run date and time: 07/13/2012 - 19:01:29 -> 07/13/2012 - 19:29:59

Dye: Blue, Green, Yellow, Red - 11 peaks

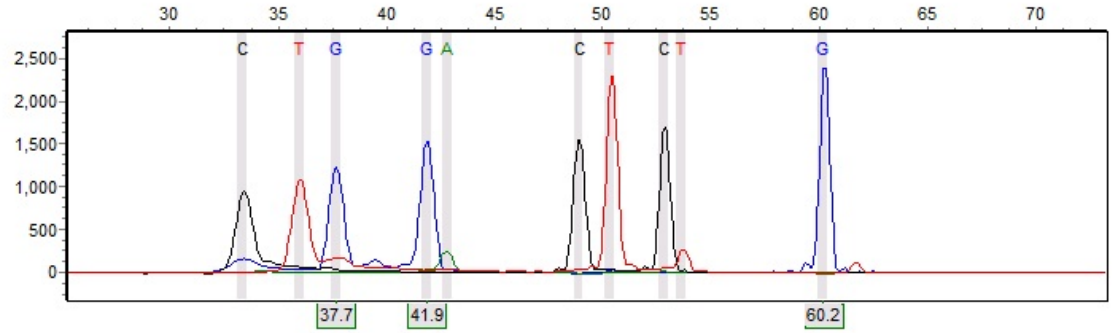

Figure F176. Sample 862

Sample 96: Run date and time: 07/02/2012 - 11:47:58 -> 07/02/2012 - 12:16:23

Dye: Blue, Green, Yellow, Red - 8 peaks

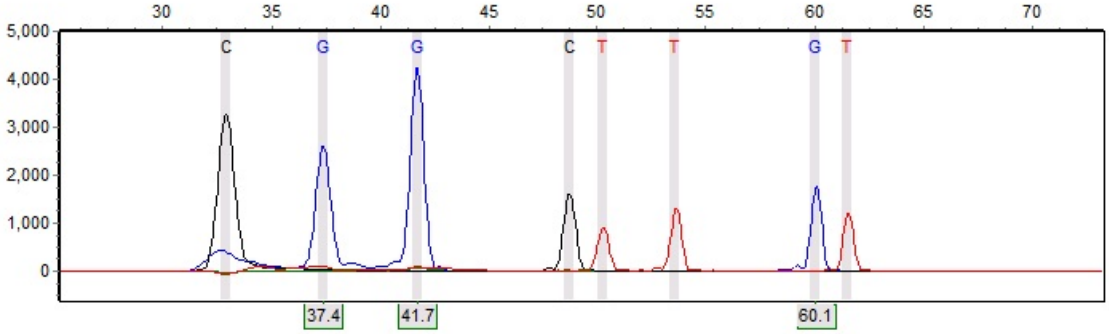

Figure F177. Sample 867

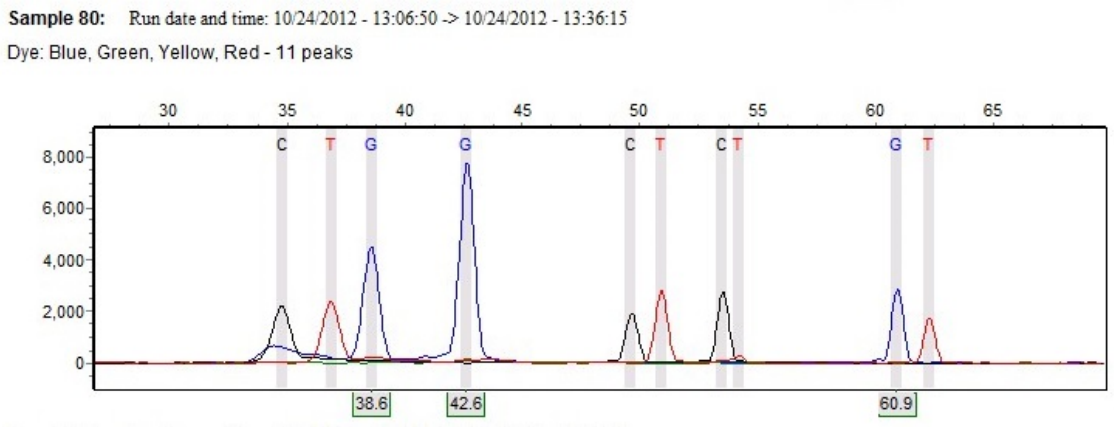

Figure F178. Sample 869

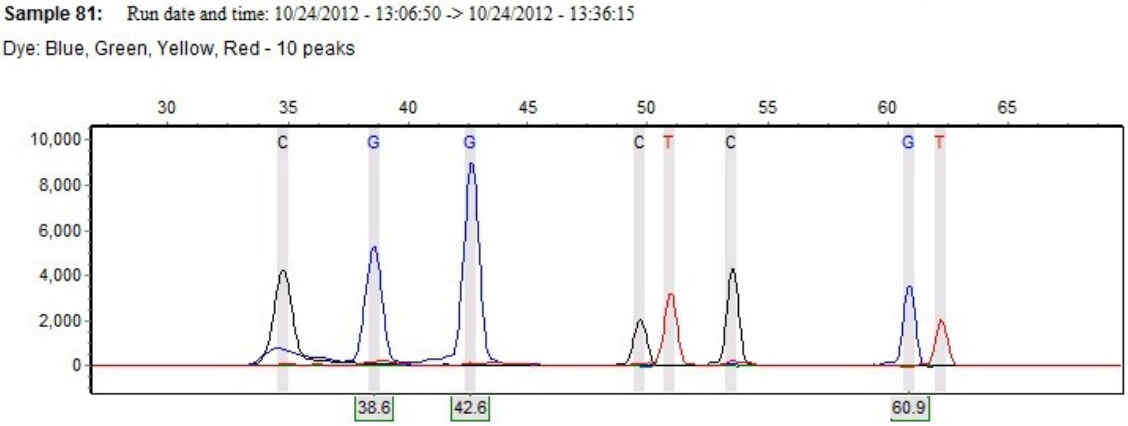

Figure F179. Sample 873

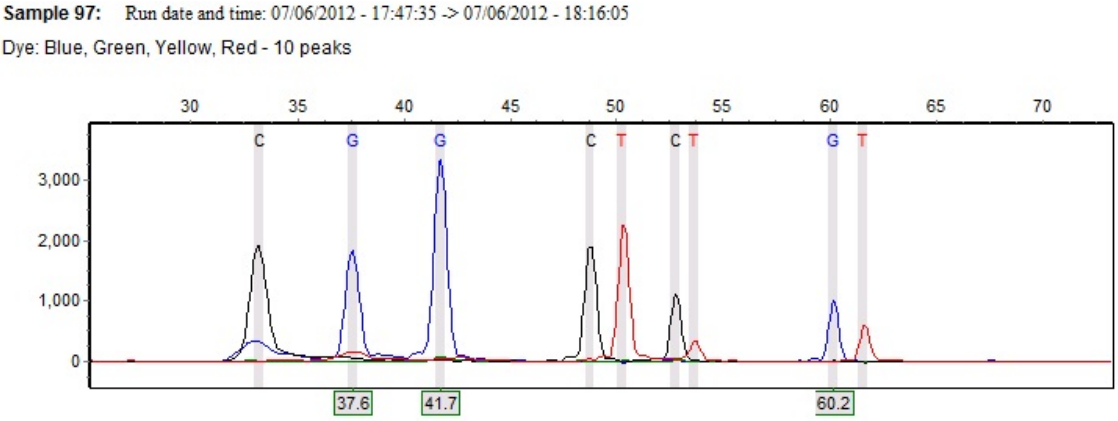

Figure F180. Sample 879

Sample 82: Run date and time: 10/29/2012 - 17:27:10 -> 10/29/2012 - 17:55:40

Dye: Blue, Green, Yellow, Red - 9 peaks

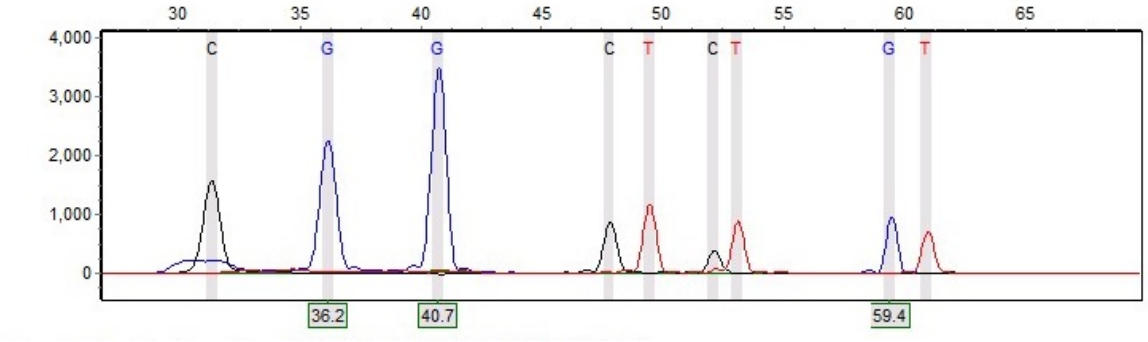

Figure F181. Sample 893

Sample 83: Run date and time: 10/18/2012 - 11:31:45 -> 10/18/2012 - 12:01:20

Dye: Blue, Green, Yellow, Red - 9 peaks

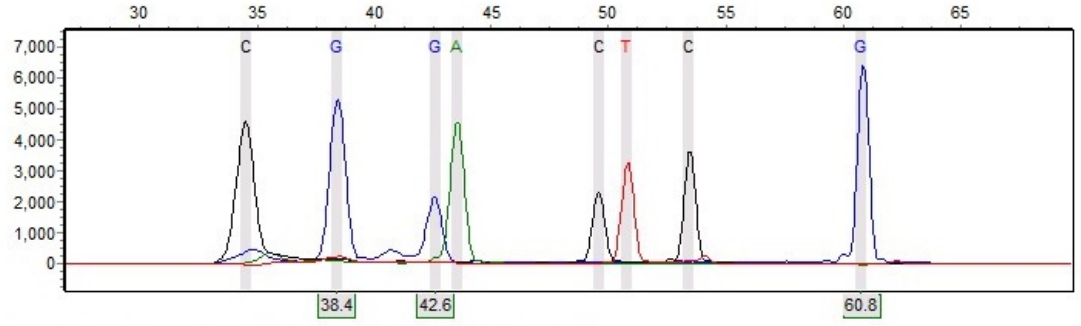

Figure F182. Sample 916

Sample 98: Run date and time: 07/02/2012 - 11:47:58 -> 07/02/2012 - 12:16:23

Dye: Blue, Green, Yellow, Red - 8 peaks

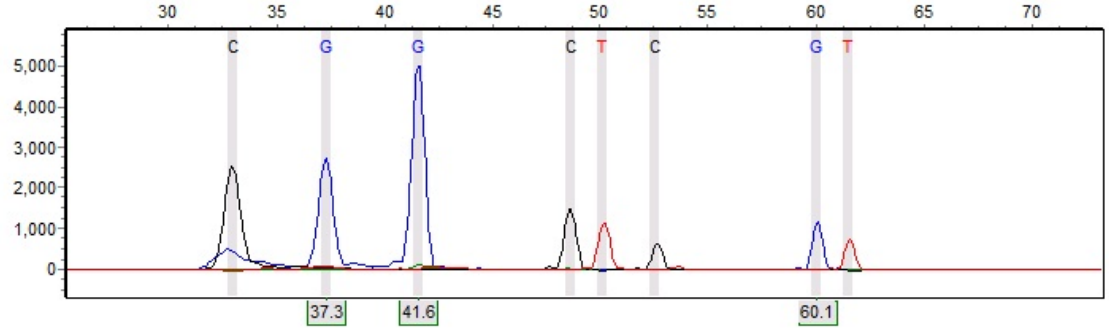

Figure F183. Sample 917

Sample 84: Run date and time: 10/29/2012 - 16:29:22 -> 10/29/2012 - 16:57:37

Dye: Blue, Green, Yellow, Red - 7 peaks

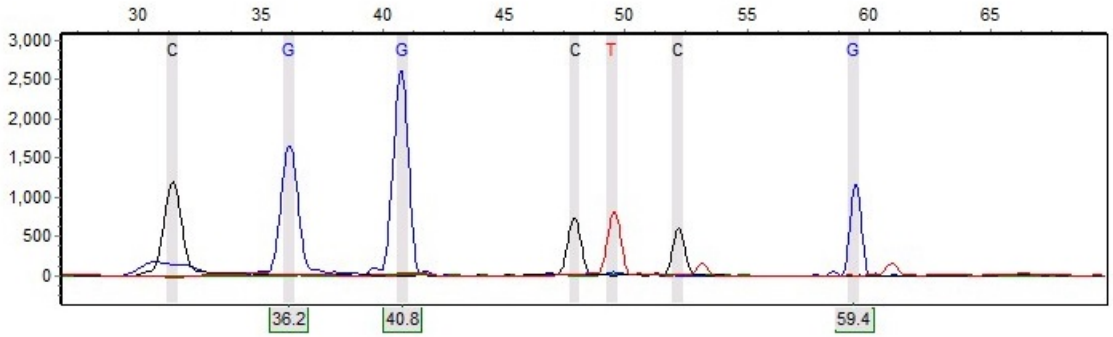

Figure F184. Sample 927

Sample 85: Run date and time: 10/29/2012 - 15:30:58 -> 10/29/2012 - 15:59:44

Dye: Blue, Green, Yellow, Red - 8 peaks

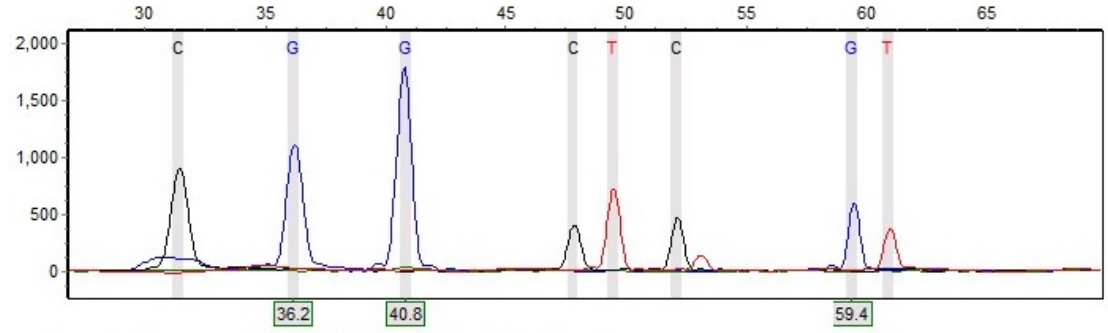

Figure F185. Sample 930

Sample 99: Run date and time: 06/29/2012 - 09:40:48 -> 06/29/2012 - 10:09:23

Dye: Blue, Green, Yellow, Red - 11 peaks

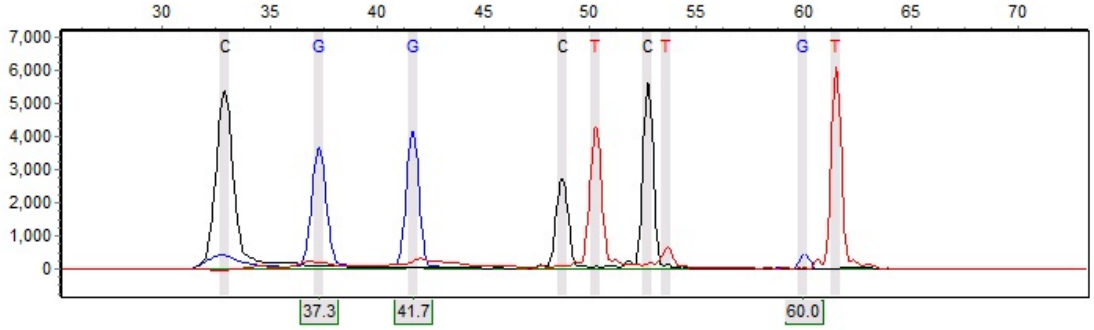

Figure F186. Sample 932

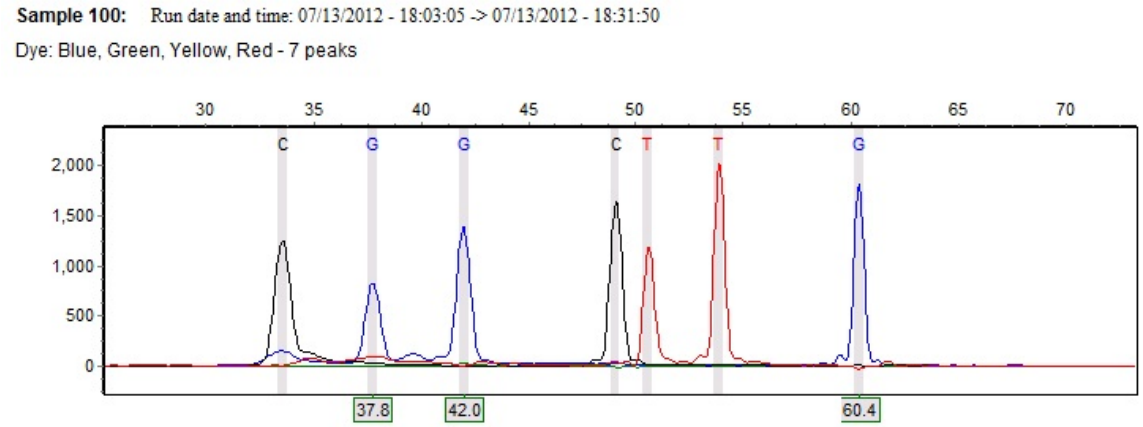

Figure F187. Sample 936

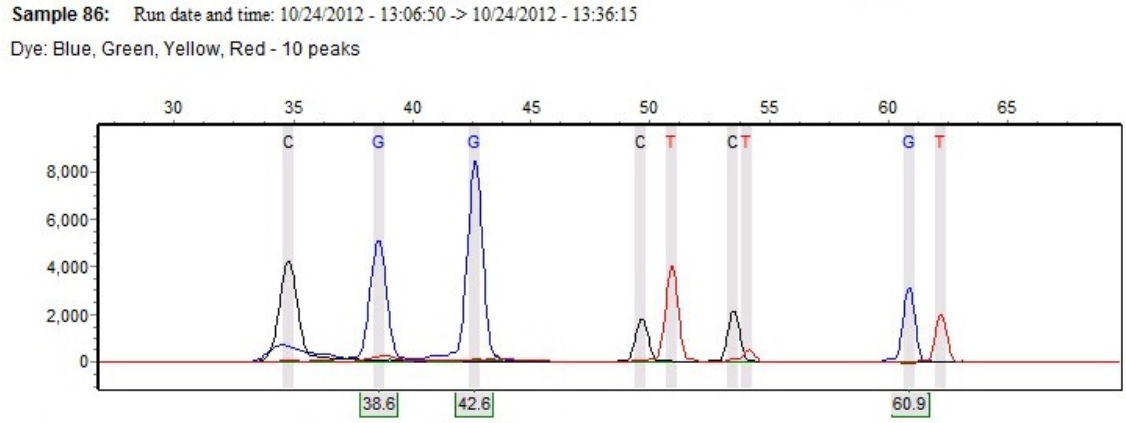

Figure F188. Sample 943

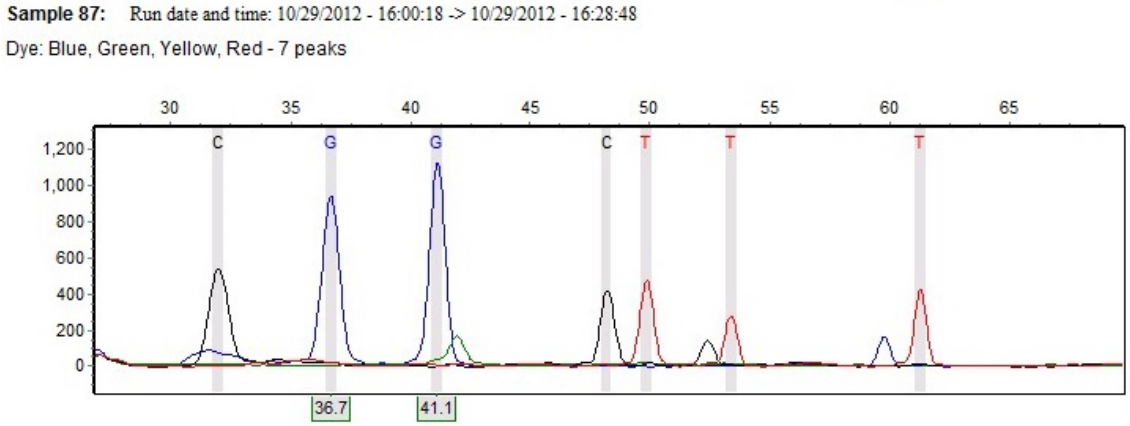

Figure F189. Sample 945

Sample 101: Run date and time: 07/09/2012 - 10:55:20 -> 07/09/2012 - 11:33:00

Dye: Blue, Green, Yellow, Red - 9 peaks

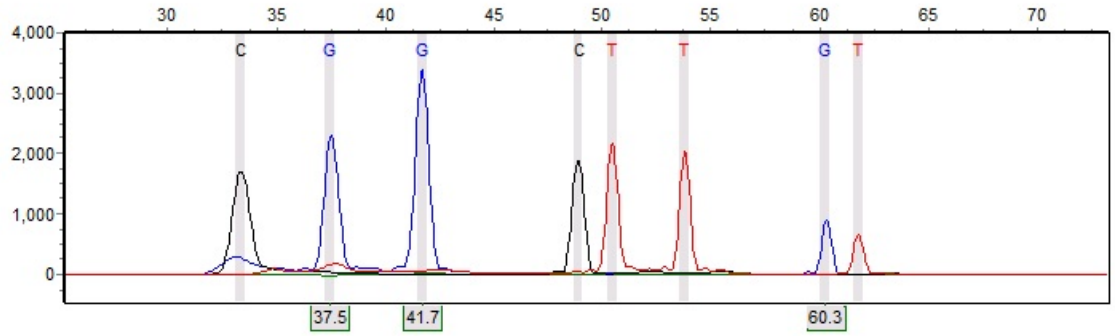

Figure F190. Sample 947

Sample 88: Run date and time: 10/29/2012 - 16:29:22 -> 10/29/2012 - 16:57:37

Dye: Blue, Green, Yellow, Red - 8 peaks

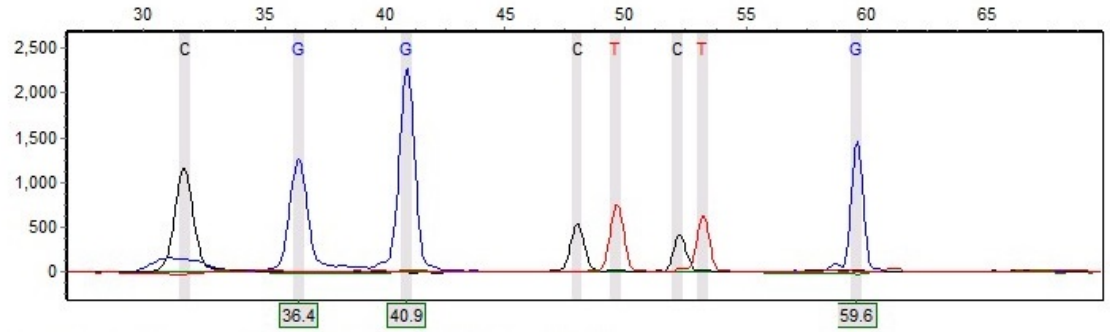

Figure F191. Sample 948

Sample 102: Run date and time: 06/29/2012 - 09:40:48 -> 06/29/2012 - 10:09:23

Dye: Blue, Green, Yellow, Red - 9 peaks

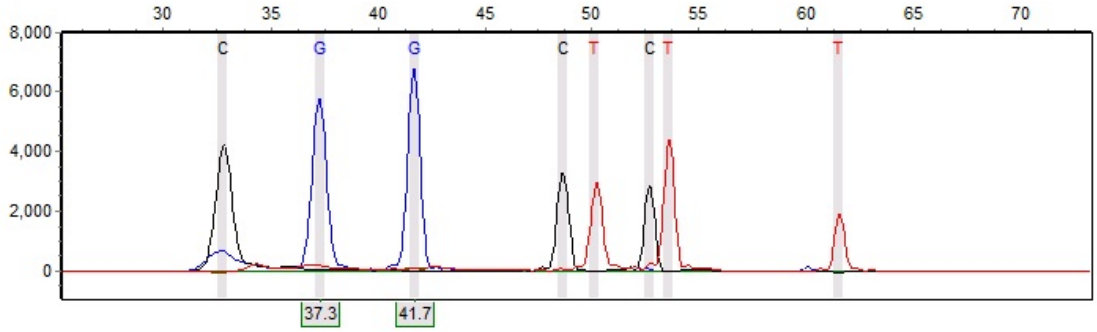

Figure F192. Sample 951

Sample 89: Run date and time: 10/18/2012 - 12:31:39 -> 10/18/2012 - 13:01:05

Dye: Blue, Green, Yellow, Red - 12 peaks

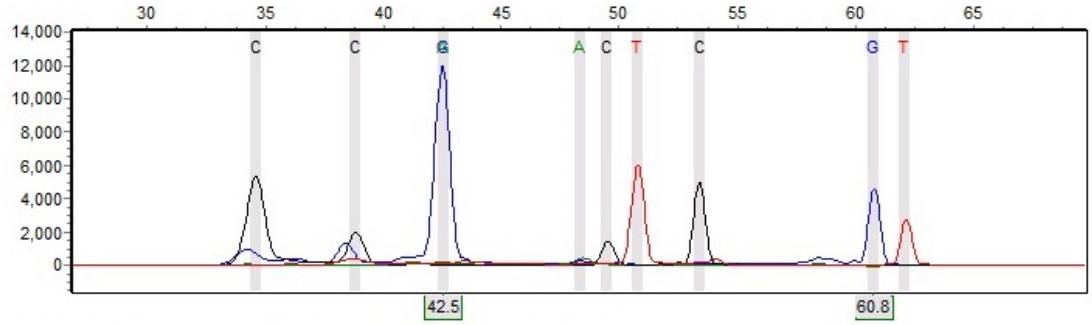

Figure F193. Sample 957

Sample 90: Run date and time: 10/29/2012 - 15:30:58 -> 10/29/2012 - 15:59:44

Dye: Blue, Green, Yellow, Red - 7 peaks

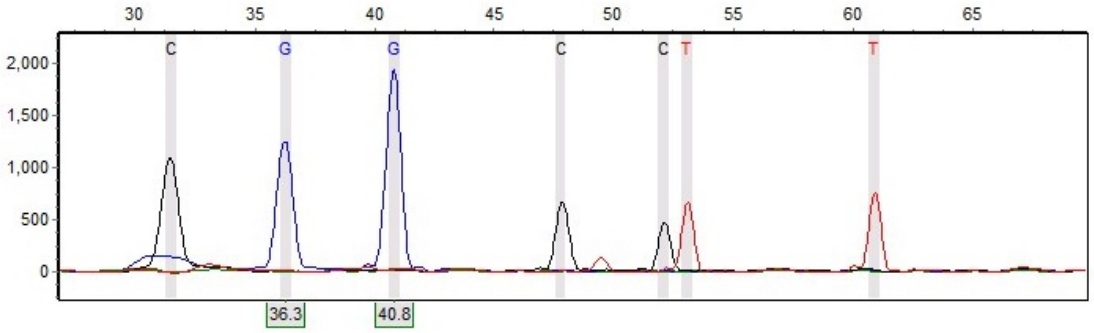

Figure F194. Sample 965

Sample 91: Run date and time: 10/29/2012 - 16:58:16 -> 10/29/2012 - 17:26:36

Dye: Blue, Green, Yellow, Red - 6 peaks

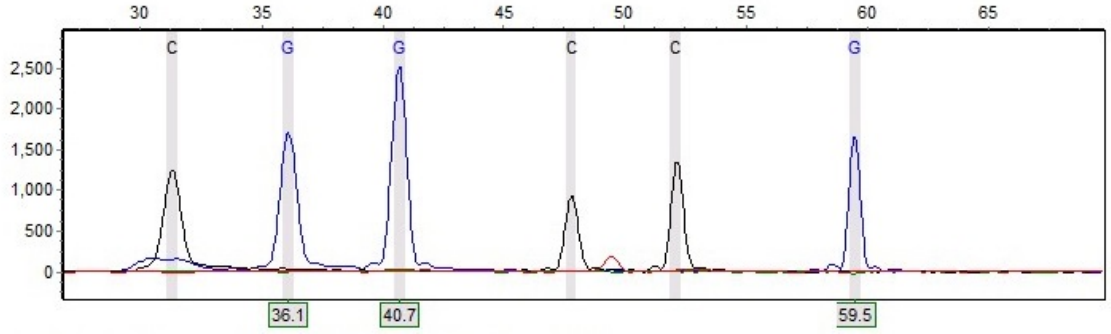

Figure F195. Sample 968

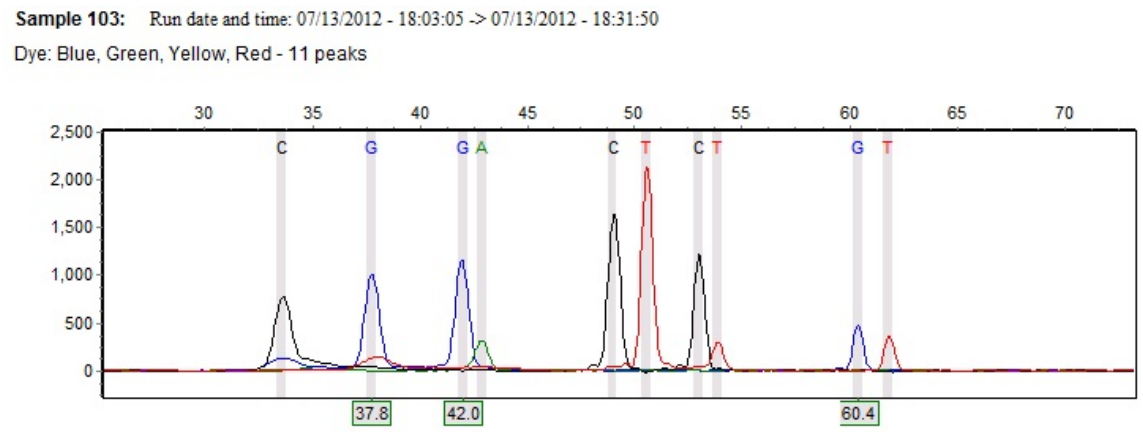

Figure F196. Sample 975

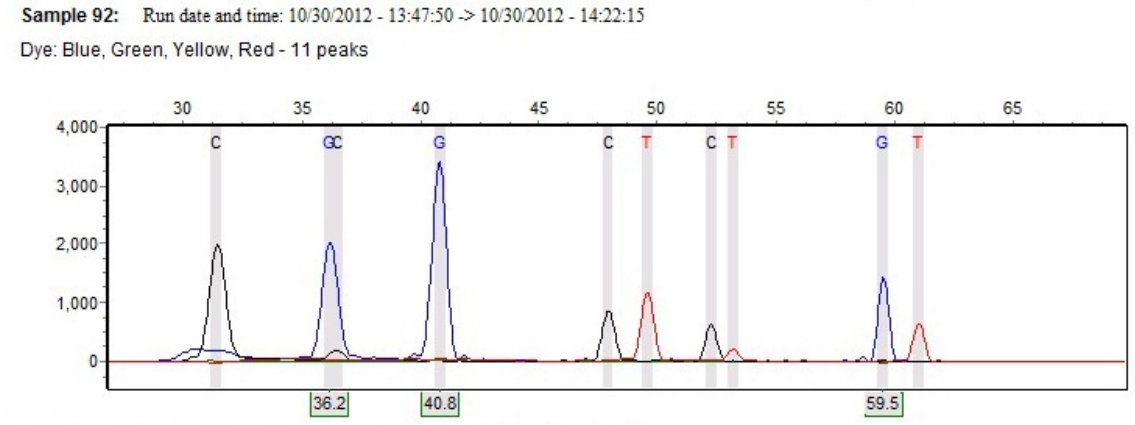

Figure F197. Sample 983

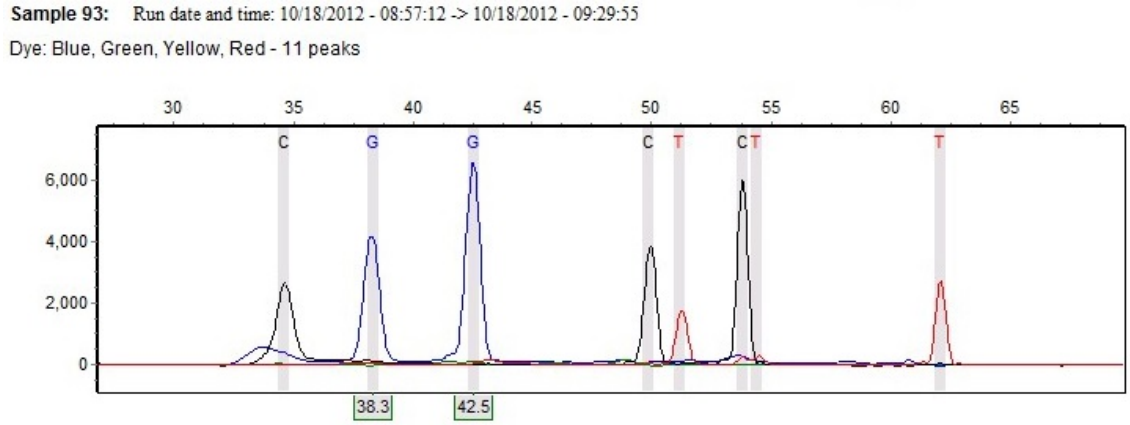

Figure F198. Sample 986

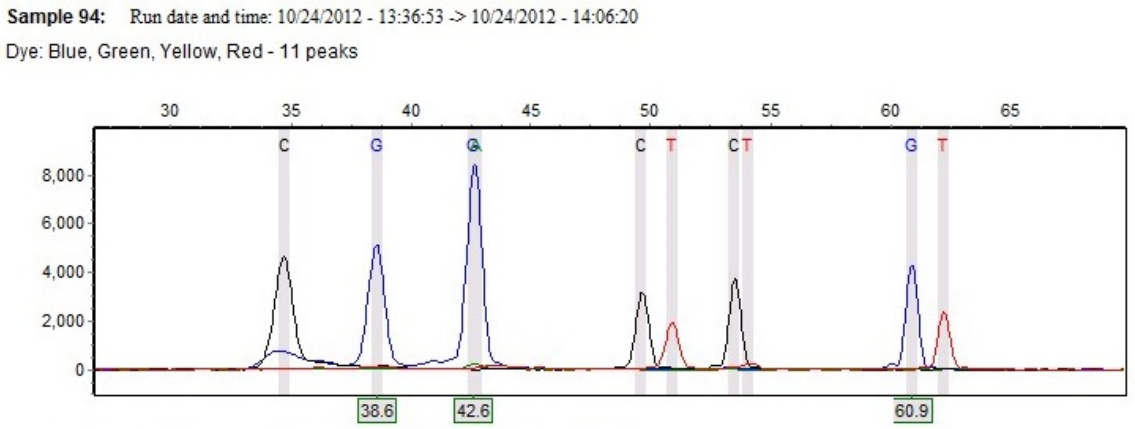

Figure F199. Sample 987

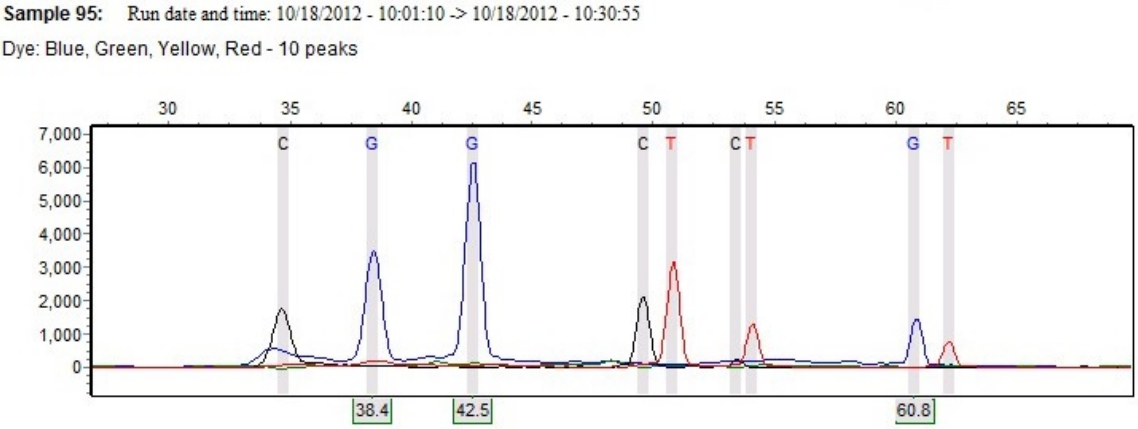

Figure F200. Sample 991